UNIVERSITY OF THE WITWATERSRAND
JOHANNESBURG

SCHOOL OF MECHANICAL ENGINEERING

AN INVESTIGATION INTO PRACTICAL ASPECTS OF TRANSPIRATION FLOWS

M KRIEG

A dissertation presented in fulfilment of the requirements for the Degree of Master of Science in Engineering

MARCH 1978

To my Mother and Father .....
and Summertime

DECLARATION

I, MARK HANS ROBERT FRIEDRICH KRIEG, hereby declare that the dissertation is my own work and has not been submitted by me for a degree at any other University.

M.H.R.F. KRIEG

ABSTRACT

It was felt that by attaching a porous matrix to a rigid base with metering holes or slots, these materials would become more viable in transpiration cooling. Such an alteration was expected to affect the mean velocity profile of the injected turbulent boundary layer. This, and the more basic study of turbulent transport, required attention. An investigation of the literature showed that although a great deal of work had been done, there was little to compare with the present problem.

A wind tunnel was designed and constructed which produced a 2-D incompressible turbulent shear layer on a porous plate, through which a secondary stream was injected. A flow situation with a step change in injection was thus modelled. A main stream velocity of 21 m/s (corresponding to $Re_x = 1{,}178 \times 10^6$), and an average injection ratio (v_w/U_∞) of 0,017, was attained. Results indicated that blockage below the porous surface resulted in an apparently higher injection ratio for the same total flow rate.

To further the understanding of turbulent transport, a programme was written which solved the momentum equation. The eddy-viscosity formulation suggested by Cebeci was tested in this solution. It could be used to calculate the velocity profiles, with varying injection and pressure gradients, of either laminar or turbulent external boundary layers.

A numerically calculated profile and the experimental results of another researcher compared very well. The trend for the 'transition' region from flat plate turbulent flow to the injected turbulent boundary layer was established experimentally, and reflected in the computer

generated profiles. Exact comparison was not possible, owing to lack of time to rewrite part of the programme.

Experimental results were cross-plotted, and this indicated the possibility of a short-cut method for deriving velocity profiles with injection. Skin friction was not measured in the tests, and was found to be very inadequately documented in previous work. This must be a very important aspect of the injected turbulent shear layer, and requires further work.

A preliminary investigation of the flow in the porous matrix, especially the spread of an axisymmetric jet, was done. Initially experiment was expected to precede analysis, and a rig was built for future research.

ACKNOWLEDGEMENTS

I wish to express my sincere appreciation and gratitude to the following :-

* Mrs B.A. Rotteveel, whose work guided me to this project, and who assisted me in the initial planning and analytical stage.

* Professor B.W. Skews, for his invaluable suggestions, encouragement and patience, and without whom this project could not have been completed.

* Dr D. van der Merwe, for his interest, and the loan of the spectrum analyser.

* Mr E.A. Moss, who assisted in the understanding of turbulent flows.

* Mr F.A.S. Bezuidenhout and the staff of the Mechanical Engineering Laboratory, who constructed the wind tunnel.

* Mr D. Hutson, formerly of DCE Vokes, for arranging the loan of a fan.

* Mr J. de Jager, for his helpful suggestions in computer programming.

* Jenny Marcus, for typing this dissertation.

Financial support was received in the form of :-

A University of the Witwatersrand Senior Bursary
A C.S.I.R. bursary
An Adolph Wagner scholarship.

CONTENTS

		Page
DECLARATION		iii
ABSTRACT		iv
ACKNOWLEDGEMENTS		vi
CONTENTS		vii
NOTATION		x
CHAPTER		
1	INTRODUCTION	1
2	OBJECT	3
3	REVIEW OF LITERATURE ON THE TURBULENT BOUNDARY LAYER WITH INJECTION	
3.1	Introduction	5
3.2	Experimental Work	6
3.3	Analytical Developments	8
4	A THEORETICAL APPROACH TO THE TURBULENT BOUNDARY LAYER WITH TRANSPIRATION	
4.1	Introduction	18
4.2	The Continuity and Momentum Equations	20
4.3	Formulation for the Reynolds Stress	20
4.4	Eddy Viscosity Formulation for the Fully Turbulent Region	22
4.5	Boundary Conditions	24
4.6	The Transformed Momentum and Related Equations : A Summary	25
5	COMPUTER SOLUTION OF THE MOMENTUM EQUATION	
5.1	Introduction	26
5.2	Linearisation of the Momentum Equation	26
5.3	The Finite Difference Grid	27

		Page
5.4	The Momentum Equation in Finite Difference Form	28
5.5	The Finite Difference Molecule	32
5.6	Flow Chart	34
5.7	Discussion of Various Features of the Programme	35
6	EXPERIMENTAL APPARATUS AND PROCEDURE	
6.1	Introduction	42
6.2	The Wind Tunnel	42
6.3	Hot Wire Anemometry	48
6.4	The Energy Spectrum	49
6.5	Experimental Procedure	50
7	PRESENTATION AND DISCUSSION OF RESULTS	
7.1	Introduction	52
7.2	Initial Tests	53
7.3	Experimental Work	61
7.4	Computer Programme Results	98
8	CONCLUSIONS	117
9	SUGGESTIONS FOR FURTHER WORK	118
APPENDIX		
A1	Transformation of the Momentum Equation	120
A2	The Finite Difference Approximations	122
A3	Flow in Porous Media	127
A4	Tests on the Porous Matrix	131
B1	Design of the Wind Tunnel, Fan and Contraction	137
B2	The Working Section	142
B3	Engineering Drawing	142
C1	Calibration of the Orifice Plate	144
C2	Calibration of Thermocouple	144

		Page
C3	The Calibration of the Hot Wire	145
C4	Temperature Correction for the Anemometer Output	146
C5	Correction for Proximity of the Wall	147
D1	The Experimental Results	148
E1	Accuracy of Experimental Equipment	174
F1	Some Details Pertaining to the Programme	177
F2	Initial Computer Runs	178
F3	Results of Main Computer Runs	182
F4	Input Data for the Programme	186
LIST OF REFERENCES		198

NOTATION

ROMAN

a	Pipe diameter
A	Van Driest damping length
A^+	Van Driest damping constant
$[A]$	Coefficient matrix in $[A]\{X\} = \{B\}$
$\{B\}$	Vector of constants
c_f	Skin friction coefficient
d	Orifice diameter
D	Pipe diameter
D_o	Particle diameter
E	Voltage drop across hot-wire
E_o	Voltage drop across hot-wire for zero velocity
E_n	Voltage drop, corrected for temperature
$E_1(n)$	Contribution to energy of fluctuation for frequency $n + dn$
$\underline{f}$	Force vector (per unit volume)
f	Dimensionless stream function, general function
F	Local injection ratio, v_w/U_∞
F_{av}	Average injection ratio, v_w/U_{Cl}
g	General function
G	Main stream mass flux, $G = \rho_\infty U_\infty$
h	First step in η grid
H	Shape factor
k	Roughness height
k^+	Non-dimensionalised roughness height, $k^+ = ku_w^*/\nu$

K	Ratio of adjacent η intervals
l	Mixing length
L	Length scale, porous matrix thickness in direction of flow
m''	Injection mass flux
n	Frequency
$N-4$	Number of equations in system $[A]\{X\} = \{B\}$
p	Pressure
p^+	Pressure gradient term, $-dp/dx.\nu/\rho(u_\omega{}^*)^3$
Re_L	Reynolds number, $Re_L = U_\infty L/\nu$
t,	Temperature
T	Turbulence intensity
u	Axial velocity, $u^+ = u/u_\omega{}^*$
$u_\omega{}^*, u_\tau$	Wall shear velocity
$\underline{v}$	Velocity vector
v	Velocity normal to wall
v_ω	Injection velocity, $v_\omega{}^+ = v_\omega/u_\omega{}^*$
x	Co-ordinate parallel to flow
$\{X\}$	Vector of unknowns
XTR	Start of porous plate, measured from origin
y	Co-ordinate normal to flow, $y^+ = yu_\omega{}^*/\nu$

GREEK

α	Constant in outer eddy-viscosity formulation
β	Pressure gradient parameter, $\beta = (2\xi).(du_e/d\xi)/u_e$
γ	Intermittency term
δ	Boundary layer thickness

δ^*	Displacement thickness
Δ	Differential, e.g. $\Delta p = p_2 - p_1$
ε	Eddy viscosity, $\varepsilon^+ = \varepsilon/\nu$
η	Transformed y-co-ordinate
θ	Momentum thickness
κ	Universal constant in logarithmic portion of turbulent profile
μ	Dynamic viscosity
ν	Kinematic viscosity
ξ	Transformed x-co-ordinate
ρ	Density
τ	Shear stress
ϕ	Translated stream function
ψ	Stream function

SUBSCRIPTS

CL	Centre line at Working Section inlet
e	Edge of boundary layer
i	Inner region
o	Outer region, unblown condition
s	Static, laminar sub-layer
w	Wall condition
$\_$	Vector
$=$	Second order tensor

SUPERSCRIPTS

+	Non-dimensional
'	Derivative with respect to η, fluctuating quantity
—	Integral averaged quantity (time based, unless otherwise stated)

MATHEMATICAL OPERATORS

grad, ∇	$(\delta/\delta x \ \delta/\delta y \ \delta/\delta z)$
div $\underline{v}$, $\nabla . \underline{v}$	$\delta u/\delta x + \delta v/\delta y + \delta w/\delta z$
∇^2	$\delta^2/\delta x^2 + \delta^2/\delta y^2 + \delta^2/\delta z^2$

CHAPTER 1

INTRODUCTION

The need for cooling engineering components becomes necessary when the components are in a high temperature environment. This problem frequently arises in flow situations. Important examples are :- turbine blades and combustion chambers in jet engines, exposed surfaces of supersonic vehicles such as aircraft, missiles and space craft. A further example is the lining of nuclear reactors. At present, turbine vanes and blades are film cooled by blowing cool air through discrete holes near the leading and trailing edge of the blades. This is a very important application, because the efficiency of the engine increases with cycle temperature.

An improvement in efficiency can have a dramatic effect in increasing the range of aircraft. Suciu (1970) showed that an aircraft with constant gross weight can transport a payload some 40% further if the cycle turbine inlet temperature is increased from 950°C to 1260°C. Metallurgical developments have resulted in much higher allowable metal temperatures, and film cooling has also made a significant contribution.

The coolant which is injected through the porous surface will certainly affect the boundary layer, skin friction, aerodynamic characteristics of an aerofoil (lift, drag) as well as the heat transfer coefficient. It was therefore decided that the mass transfer problem had to be investigated first. A great deal of work, both experimental and semi-analytic, has been done in this field. Unfortunately, because of the magnitude of the problem, and the large number of variables, tests have not been very systematic. Considerable thought was devoted to film cooling, and the possibility of using porous materials for the manufacture of turbine blades. As a result, an experimental research programme was embarked on.

In particular, a turbulent boundary layer was established on a smooth flat plate before it reached a porous plate, where the flow encountered injection. A computer programme was written to simulate this situation. A deeper understanding of turbulent flow thus became possible, which is necessary not only for the abovementioned applications. In the design of air intake ducts for aircraft, turbulence and intermittency must be accounted for to ensure the required flow rate. Further applications are boundary layer control on aircraft wings, using suction or injection, and hence drag reduction.

The work of various authors is discussed. It was found that there were fundamental differences between this work and that of other researchers. This made comparison very difficult. A new approach to the use of porous materials in the manufacture of turbine blades is shown. A stable computational technique was developed and the existence of a new two-parameter family of curves for the injected turbulent boundary layer is presented.

CHAPTER 2

OBJECT

Investigation of existing turbine blades in aircraft gas turbines, e.g. Pratt and Whitney JT9, General Electric CF6 and Rolls Royce RB211, showed that film cooling has become an integral part in the design of first stage stator vanes and rotor blades. Impingement cooling is used in the second stage. Clearly, the technology for manufacturing these blades with internal ducting is fully developed. Welding a porous envelope onto a blade was suggested by Grootenhuis (1959).

Because the pressure distribution on an aerofoil would result in minimum transpiration at the leading edge, a complete envelope would be unsatisfactory. This could be overcome by having porous inserts at the leading edge and mid-chord positions. A configuration of solid wall, followed by porous wall thus arose. Furthermore, the porous wall is notoriously weak, and would require to be bonded to a solid wall at the inner surface to maintain the aerodynamic loads.

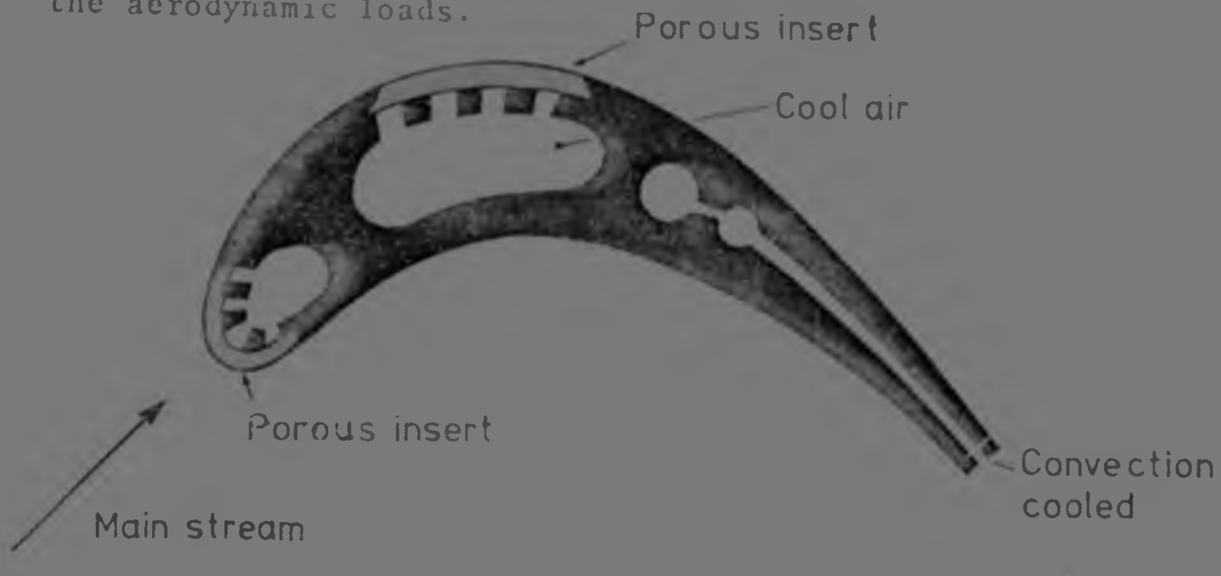

FIG 2.1 : CROSS SECTION OF BLADE WITH POROUS INSERTS

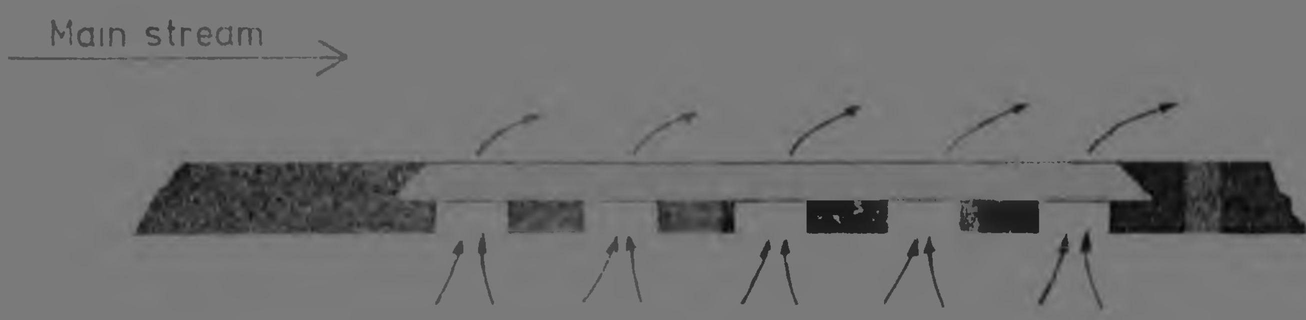

FIG 2.2 : BOUNDARY LAYER WITH STEP CHANGE IN ROUGHNESS AND INJECTION

It may be expected that the heat transfer from the metal to the coolant would be improved because the surface area is greatly increased in the porous medium. Furthermore, the webs between discrete holes in film cooling are very thin and hence prone to melting or combustion.

A great deal of research has been done in the field of transpiration cooling. However, the effect of a short porous insert with blockage below the porous matrix still remained to be explored.

To achieve this, an experimental rig, shown in Fig 6.3, was designed. This enabled tests on a flat plate in 2-D flow to be carried out. A [illegible] of data for uniform blowing was to be established, with which results for non-uniform injection could be compared.

The first stage was to consider only the effect of sudden mass transfer into an established turbulent boundary layer, without heat transfer.

The spread of the jet of coolant from the restricted inner porous surface to the open exposed surface clearly is an important consideration.

CHAPTER 3

REVIEW OF LITERATURE ON THE TURBULENT BOUNDARY LAYER WITH INJECTION

3.1 Introduction

One of the earliest papers to appear on transpiration cooling was published by Duwez and Wheeler (1948). The authors concentrated on a porous tube with high temperature axial flow and cold air injection through the walls. Their results compared well with that of Krieg (1975). In 1956 Mickley and Davis followed with an extensive experimental investigation which is still used for qualifying rigs, and for comparison with analytical or computer profiles. Chemical engineers have shown great interest in fluidized beds, ie. the flow inside a porous matrix. This latter line of investigation was considered relevant to the present work (see Appendix A3). The research may be categorised as follows :

(i) Fluidized beds;

(ii) Turbulent boundary layers with suction or injection at the wall :

- a) in channels
- b) in tubes
- c) on a flat plate.

Each of these may be further subdivided into experimental, analytic and numerical results, with or without heat transfer, and into compressible or incompressible flow.

Note that injection through discrete holes or slots has enjoyed much attention (e.g. Hartnett *et al* 1961), but is not reported on here.

3.2 Experimental Work

As mentioned above, the first thorough experimental investigation was that of Mickley and Davis (1956). Free stream velocities ranged from 5,2 m/s to 18,3 m/s, Re_x from 4 x 10^4 to 3 x 10^6 and v_w/U_∞ values of 0; 0,001; 0,002; 0,003; 0,005 and 0,010. They found that the boundary layer decreased in thickness near the outlet of the tunnel. This latter problem was overcome by adding a flow divider to the outlet of the tunnel. The estimated values of $c_f/2$ were shown plotted against Re_x. Where c_f tended to 0 or to negative values, the results were not reported. This occurred at values of F = 5 x 10^{-3} and above. Negative c_f would indicate reverse flow, however, as will be discussed later, this need not be the case. Up to F = 3 x 10^{-3}, the values of c_f compare with those predicted by McQuaid (1967), if these curves are extrapolated. Their plot of u^+ vs log y^+ fitted the universal turbulent boundary layer profile acceptably. Graphs of u/U_∞ vs y/δ were shown for F = 0,003 and F = 0,005. To predict these profiles, it was necessary to allow κ, the mixing length constant, to vary. κ increased with F. The trend today is to assume κ constant, and to introduce a function in v_w.

Grootenhuis (1959) concentrated on heat transfer, as did most early investigators. Appart from the experimental results and correlation, this paper points out numerous applications of effusion cooling, discusses types of porous materials, shows thermal conductivity vs porosity for sintered bronze and stainless steel, and the internal heat transfer correlation for porous bronze. A list is given of manufacturers of porous materials, both sintered and woven, the various grades, their porosity and U.T.S. Blade designs were suggested, but required a complete porous envelope, spot welded to a hollow stem (see Fig 3.1).

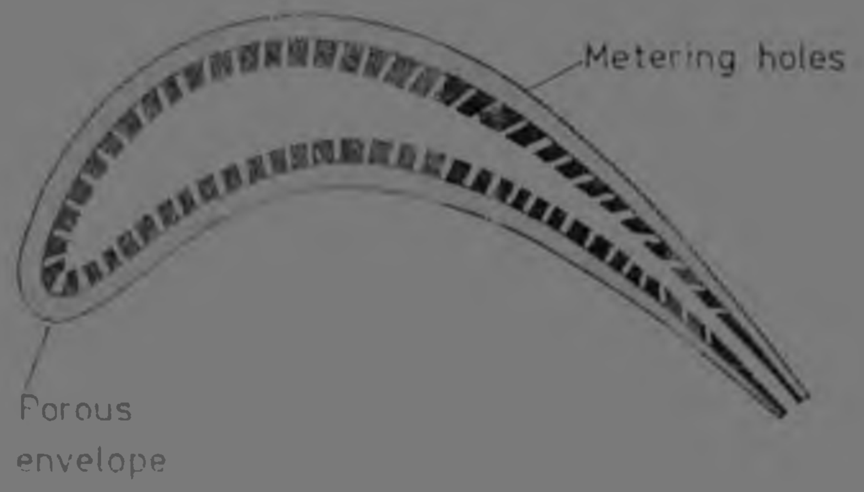

FIG 3.1 : PROPOSED DESIGN FOR A POROUS TURBINE BLADE OR VANE

A new wind tunnel was described by Moffat and Kays (1969). Their research was to establish a basis of experimental data for skin friction and heat transfer. Reynolds number, blowing fraction and Stanton number were varied systematically on a flat, porous plate. This floor was supported on 24 plenum chambers which allowed F to be controlled as a function of x. Electric heaters were installed below the porous plates, so that the transpiration flow could be heated. This unfortunately results, for an injected boundary layer, in an incorrect temperature profile. Results were presented for Stanton number varying with blowing fraction; these values showed good correlation.

The second part of this work was reported by Simpson *et al* (1969). Skin friction results were presented for v_w constant, $v_w \propto x$, $v_w \propto x^{-[illegible]}$ and $v_w \propto x^{-0.5}$. c_f was presented as a function of $\dot{m}''/G(c_{fo}/2)$. Various techniques for calculating c_f from profile data were suggested. These included a momentum integral equation method, viscous sublayer model method and the heat transfer analogue method, which was the only method to yield results for blowing fractions above 0,0078. Indications were that for $b[-\dot{m}''/G(c_{fo}/2)]$ greater than 4, c_f tended to zero. Surface roughness was not included in the skin friction calculations.

Schetz and Nerney (1977) performed tests on an axisymmetric model. A skin friction balance was built into the porous wall : the floating element had its own transpiration supply. A crystal strain gauge was attached to the floating element support. The velocity profiles were obtained with a pitot rake. It was mentioned that the effect of roughness should first be ascertained for the porous wall without injection or suction. Note that the floating element is one of the more attractive techniques for measuring skin friction. Once true values are established, semi-analytic methods may be tested against these. It was found that blowing through the porous floating element made no difference to the results. The porous wall without injection showed significantly higher values of c_f than the equivalent smooth wall. The roughness increased the turbulence intensity in the boundary layer. With the new skin friction results, the laws of the wall, one by Simpson, one by Stevenson, could be tested. It was shown clearly that these laws are inadequate. The "deductive" approach of Van Driest (1956) could not be extended as had been suggested, but a new formulation using the Reichardt model $\{\rho\varepsilon = \kappa\rho\nu[y^+ - y^+_a \tanh(y^+/y^+_a)]$ was presented. This new approach should yield significantly better results.

3.3 Analytical Developments

Before commencing this subsection, it should be noted that turbulent flow is of such a random nature that any analysis must contain empirical or experimentally determined constants. When considering quantities such as velocity, a time based average value is implied.

Mickley and Davis (1956) concentrated on experimental work, and the determination of c_f. This was done by evaluating $d\theta/dx$, and solving for c_f from :

$$\frac{d\theta}{dx} - \frac{v_w}{U_\infty} + \left(2 + \frac{\delta^*}{\theta}\right) \frac{\theta}{U_\infty} \frac{dU_\infty}{dx} = \frac{\tau_w}{\rho_\infty U_\infty^2} = \frac{c_f}{2} \qquad \text{..... [3.3.1(a)]}$$

For neglible pressure gradient, this reduces to :-

$$\frac{d\theta}{dx} - \frac{v_w}{U_\infty} = \frac{\tau_w}{\rho_\infty U_\infty^2} = \frac{c_f}{2} \qquad \text{....... [3.3.1(b)]}$$

The difficulty unfortunately lies in determining $\frac{d\theta}{dx}$.

The remainder of the analysis attempted to extend the mixing length theory for flow with $v_w \neq 0$. Reasonable correlation was obtained up to $F = 0{,}005$, but κ was no longer constant, but increased with F. To plot experimental data non-dimensionalized with respect to u_w^*, when this quantity is calculated from semi-analytic considerations, seems very unsatisfactory. Only if τ_w is measured directly can an estimate of the reliability of the analysis be made.

It was assumed that there was only a laminar sublayer and a turbulent region (ie. no buffer layer), with a transition point at y_a. As do most researchers, they assumed the predominance of the $v_w \delta u/\delta y$ term in the equation

$$u\frac{\delta u}{\delta x} + v\frac{\delta u}{\delta y} = \frac{1}{\rho}\left(\frac{\delta \tau}{y} - \frac{dp}{dx}\right) \qquad \text{....... [3.3.2]}$$

For an incompressible layer, the following expressions were obtained :

$$\text{Sublayer} \quad \frac{u_\tau y}{\nu} = 2\frac{u_\tau}{v_w} \ln\left(1 + \frac{v_w u}{u_\tau^2}\right) \qquad \text{....... [3.3.3]}$$

$$\text{Turbulent region} \quad \ln \frac{u_\tau y}{\nu} - \ln \frac{u_\tau y_a}{\nu} = 2\kappa\frac{u_\tau}{v_w} \left[\left(1 + \frac{v_w u}{u_\tau^2}\right)^{\frac{1}{2}} - \left(1 + \frac{v_w u_a}{u_\tau^2}\right)^{\frac{1}{2}}\right] \qquad \text{.... [3.3.4]}$$

Black and Sarnecki (1958) approached the problem in a very similar manner. The mixing length was considered proportional to distance from the wall,

$$l = \kappa y \qquad \text{....... [3.3.5]}$$

Assuming incompressible, two dimensional flow, Prandtl's boundary layer equation [3.3.2] above, again forms the foundation of the analysis, with $v_w \delta u/\delta y$ a dominant term.

The continuity equation is $\frac{\delta u}{\delta x} + \frac{\delta v}{\delta y} = 0$ ..... [3.3.6]

and the shear is $\tau/\rho = \nu\frac{\delta u}{\delta y} - \overline{u'v'}$ .... [3.3.7]

with boundary conditions $u = 0$, $v = v_w$ at $y = 0$ [3.3.8]

Close to the wall, with $dp/dx \to 0$, equation [3.3.2] reduces to

$$v_w \frac{\delta u}{\delta y} = \frac{1}{\rho}\frac{\delta \tau}{\delta y} \qquad \text{....... [3.3.9]}$$

[3.3.9] was integrated, to yield :

$$v_w u = \frac{\tau - \tau_w}{\rho} \qquad \text{....... [3.3.10]}$$

and using the definition $\frac{\tau_w}{\rho} = u_\tau^{\,2}$ .... [3.3.11]

[3.3.12] was obtained :-

$$u_\tau^{\,2} + v_w u = \tau/\rho \qquad \text{....... [3.3.12]}$$

The momentum integral equation for the transpired boundary layer is thus :

$$\frac{d}{dx}(U_\infty^{\,2}\theta) + \frac{dU_\infty}{dx}U_\infty\delta^* = \frac{\tau_w}{\rho} + v_w U_\infty \qquad \text{....... [3.3.13]}$$

Using the vorticity transfer theory of G.I. Taylor with $l = \kappa y$ resulted in an expression which, for $v_w = 0$, did not reduce to the generally accepted law for flat plate flow. Prandtl's momentum transfer theory in conjuntion with a linear mixing length yielded what Black and Sarnecki (1958) called the bilogarithmic law. This referred to the squared logarithmic term in their expression, derived as follows :

Substitute the momentum transfer formulation,

$$\frac{\tau}{\rho} = \kappa^2 y^2 \left(\frac{\delta u}{\delta y}\right)^2 \qquad \ldots\ldots\ [3.3.14]$$

into [3.3.12] :

$$u_\tau^{\ 2} + v_w u = \kappa^2 y^2 \left(\frac{\delta u}{\delta y}\right)^2 \qquad \ldots\ldots\ [3.3.15]$$

From [3.3.9],

$$\frac{\delta u}{\delta y} = \frac{1}{\rho v_w} \frac{\delta \tau}{\delta y} = \frac{1}{v_w} \frac{\delta(\tau/\rho)}{\delta y}$$

$$u_\tau^{\ 2} + v_w u = \kappa^2 \left[\frac{y}{v_w} \cdot \frac{\delta(u_\tau^{\ 2} + v_w u)}{\delta y}\right]^2 \qquad \ldots\ldots\ [3.3.16]$$

$$(u_\tau^{\ 2} + v_w u) = \left(\frac{\kappa}{v_w}\right)^2 \left[\frac{\delta(u_\tau^{\ 2} + v_w u)}{\delta(\ln y)}\right] \qquad \ldots\ldots\ [3.3.17]$$

This integrates to :

$$u_\tau^{\ 2} + v_w u = \left(\frac{v_w}{2\kappa} \ln y/d\right)^2 \qquad \ldots\ldots\ [3.3.18]$$

where d is a constant of integration.

Equation [3.3.18] is expected to hold for 2-D incompressible flow, with $\delta p/\delta y$ negligible (Prandtl's assumption for [3.3.2], and a thin laminar sublayer.

[3.3.18] was expressed in a manner which allows both u_τ and d to be determined from the slope and the intercept on the ordinate of a straight line drawn through the experimental points in the bilog region. κ was treated as a univer-al constant.

Thus

$$\frac{u}{U_\infty} - \frac{1}{4\kappa^2}\frac{v_w}{U_\infty}\left(\ln\frac{U_\infty y}{\nu}\right)^2 = \left[\frac{1}{4\kappa^2}\frac{v_w}{U_\infty}\left(\ln\frac{U_\infty d}{\nu}\right)^2 - \frac{u_\tau^2}{v_w U_\infty}\right]$$

$$- \left(\frac{1}{2\kappa^2}\frac{v_w}{U_\infty}\ln\frac{U_\infty d}{\nu}\right)\ln\frac{U_\infty y}{\nu} \qquad \text{..... [3.3.19]}$$

Let $\frac{1}{2\kappa}\sqrt{\frac{v_w}{U_\infty}}\ln\frac{U_\infty y}{\nu} = Y_i$ .... [3.3.20]

$$n_i = -\frac{1}{2\kappa}\sqrt{\frac{v_w}{U_\infty}}\ln\frac{U_\infty d}{\nu} \qquad \text{....... [3.3.21]}$$

$$p_i^2 = \frac{u_\tau^2}{v_w U_\infty} \qquad \text{....... [3.3.22]}$$

then $\frac{u}{U_\infty} - Y_i^2 = (n_i^2 - p_i^2) + 2n_i Y_i$ ..... [3.3.23]

Clearly, if $\frac{u}{U_\infty} - Y_i^2$ is plotted against Y_i, and a straight line is fitted through the experimental points, the slope would be $2n_i$, and the ordinate intercept $n_i^2 - p_i^2$. This technique has numerous advantages over that of Mickley and Davis because the velocit, scale is now the known, measured valued of U_∞, rather than u_τ, obtained from the momentum integral equation. $d\theta/dx$ could be calculated from :

$$U_\infty^2\frac{d\theta}{dx} = u_\tau^2 + v_w U_\infty \qquad \text{....... [3.3.24]}$$

(3.3.13 for $dU_\infty/dx = 0$)

$$\frac{d\theta}{dx} = \frac{v_w}{U_\infty}(p_i^2 + 1) \qquad \text{....... [3.3.25]}$$

For values of F>0,005, it was found that the wall shear velocity became imaginary, ie. $p_i^2<0$. This gave $c_f<0$, which was what Mickley and Davis (1956) found, but ascribed to experimental error. It is very important to note that in the above technique, negative c_f does not imply reversed flow, as was found in un-injected flows with adverse pressure gradient.

This lengthy discussion has been given because the bilog technique is used for comparing the present results with those of Mickley and Davis (1956). Values of u_τ were not reported, as they were imaginary, and were only needed for the graphical presentation. Surface roughness was mentioned in the paper, but did not feature in the analysis.

McQuaid (1967) introduced intemittency into his formulation. A two parameter family of curves was mentioned, but not given in this paper. The velocity profiles generated from the family were compared with some experimental data. Results were good, also when fitted to the Mickley and Davis results.

The law of the wall for $v_w = 0$ is

$$\frac{u}{u_\tau} = f\left(\frac{u_\tau y}{\nu}\right) \qquad \text{..... [3.3.26]}$$

This could be extended for injected flows by adding v_w, e.g.

$$\left.\begin{aligned} \frac{u}{u_\tau} &= f\left(\frac{u_\tau y}{\nu}, \frac{v_w}{u_\tau}\right) \\ \text{or} \quad \frac{u}{v_w} &= f_2\left(\frac{u_\tau y}{\nu}, \frac{v_w}{u_\tau}\right) \end{aligned}\right\} \qquad \text{..... [3.3.27]}$$

and to include surface roughness

$$\left.\begin{aligned} \frac{u}{u_\tau} &= f\left(\frac{u_\tau y}{\nu}, \frac{v_w}{u_\tau}, \frac{u_\tau k}{\nu}\right) \\ \text{ie.} \quad u^+ &= f(y^+, v_w^+, k^+) \end{aligned}\right\} \qquad \text{..... [3.3.28]}$$

McQuaid, however, suggested a function using U_∞ as a velocity scale, and retained wall shear in the term c_f, thus :

$$\frac{u}{U_\infty} = g(y/\theta,\ H,\ Re_\theta,\ \frac{v_w}{U_\infty}) \qquad \text{.......} [3.3.29]$$

and

$$\left.\begin{aligned} c_f &= c_f(H,\ Re_\theta,\ \frac{v_w}{U_\infty}) \\ Re_{\delta_B} &= Re_{\delta_B}(H,\ Re_\theta,\ \frac{v_w}{U_\infty}) \end{aligned}\right\} \qquad \text{.......} [3.3.30]$$

(δ_B was defined as "twice the distance from the wall to the position where γ = 0,5").

McQuaid assumed the law presented by Black and Sarnecki for the sublayer [3.3.3], and modified Stevenson's 'law of the wall' for the turbulent region with suction or injection :

$$2\frac{u_\tau}{v_w}[(1 + \frac{v_w}{U_\infty}\cdot\frac{U_\infty^2}{u_\tau^2})^{\frac{1}{2}} - 1] = A \log \frac{u_\tau \delta_B}{\nu} + B \qquad \text{...} [3.3.31]$$

A pressure gradient term was also derived, and was shown to be analogous to the pressure gradient term for unblown flows. This was given as :

$$\Delta_i = \frac{\nu}{(u_\tau^2 + v_w u)^{3/2}}\cdot\frac{1}{\rho}\cdot\frac{dp}{dx} \qquad \text{.......} [3.3.32]$$

It was found that the model gave good agreement provided $-0{,}004<\Delta_i<0{,}006$. Furthermore, and this is of importance to the present work, the "fully developed state was not attained even at 33 boundary layer lengths downstream after a sudden change in injection rate".

Although this paper clearly indicates the importance of θ in transpired boundary layers, the objections raised previously to τ_w being calculated from the velocity profile, and not direct measurement, again apply.

Pletcher (1969) analysed an axisymmetric configuration, and developed a mixing length based on the Van Driest damping factor (Van Driest, 1956). An explicit finite difference technique is explained in the paper, and purports to give good results for flat plate, uninjected flows. The injected velocity profile shown agrees well with data from one of the Mickley and Davis tests. It was pointed out that the explicit method is more direct, and simpler to programme than an implicit method. Furthermore, it was not necessary to linearize the boundary layer equation before solving it, thus eliminating the need for an iterative process. However, it is well known that explicit methods are prone to instability, especially if the step length becomes too small.

Cebeci and Smith (1970a) also solved the Prandtl boundary layer equation for axisymmetric, compressible flow. This paper was preceded by numerous others that were very similar. This particular version showed the equations, boundary conditions, the finite difference grid and transformations in some detail. An implicit finite difference technique was employed to solve the linearized momentum equation with boundary conditions. A mixing length formulation based on Van Driest (1956) was used for the sublayer and the blending region, and a formulation using intermittency for the fully turbulent region. The energy equation was solved simultaneously, as this was a compressible flow situation. Grid spacing and CPU time required for solution were discussed.

Cebeci (1970b) showed how the Van Driest damping factor could be modified for pressure gradient and injection. Comparison with experimental results appeared excellent. The Van Driest velocity gradient relationship was extended to flows with injection :-

$$\frac{du^+}{dy^+} = \frac{2(v_w^+u^+ + 1)}{1 + \{1 + 4(v_w^+u^+ + 1)\kappa^2(y^+)^2[1 - \exp(-y^+/A^+)]^2\}^{\frac{1}{2}}} \quad \text{..... [3.3.33]}$$

where A^+ is the modified Van Driest damping constant.

Equation [3.3.33] suggests an iterative solution for u^+.

This work by Cebeci will be discussed in greater detail in Chapter 4.

Cebeci and Smith (1974) and Cebeci and Bradshaw (1977) continued the above work, but suggest changes to the Reynolds stress formulation, and a very much more sophisticated finite difference technique, known as Keller's box method. The Falkner-Skan equation requires additional transformation before computer solution is possible. The second book is of more general interest showing how Runge-Kutta can be used, and gives examples of computer programmes.

Bale (1975) concentrated on axial flow through a tube with mass extraction at the walls. A potential flow solution was obtained, which gave a good representation of the flow field inside the porous pipe, but gave no information with respect to shear stress at the wall.

Schetz and Nerney (1977), as mentioned above, concentrated on experimental work, and the direct measurement of skin friction. It was shown that an extension to the Van Driest mixing length could not account for surface roughness, but the Reichardt model could. The momentum equation could thus be written :

$$\frac{du^+}{dy^+} = \frac{1 + v_w^+u^+}{1 + \kappa[1 + v_w^+u^+)(y^+ - y_a^+ \tanh (y^+/y_a^+)]} \quad [3.3.34]$$

(cf. equation 3.3.33)

y_a^+ is a length scale, and is of the order of the laminar sublayer thickness. It was expected that y_a^+ would decrease with roughness, and $y_a^+ = y_a^+(k^+)$ was determined. The relationship $y_a^+ = y_a^+(k^+, v_w^+)$ still needs to be found experimentally for various values of k, v_w and types of roughness. For the unblown case, the Clauser shift for roughness was confirmed :

$$\frac{u}{u_\tau} = A \log \frac{y u_\tau}{\nu} + B - \Delta(u/u_\tau) \qquad \text{....... [3.3.35]}$$

ie. roughness did not change the slope of the fully turbulent region, only the intercept on the ordinate.

Presented above are a few papers written on the subject of the transpired boundary layer. There are innumerable papers on this topic : studying each one would result in a great deal of repetition, and possibly be of little use until the skin friction for shear flows with transpiration has been truly established. From this section, it should be clear that the present situation bears close resemblance to the confusion which existed in the 1940's as regards the fully turbulent region of the solid-wall turbulent boundary layer. With the introduction of reliable skin friction transducers, that position was clarified.

CHAPTER 4

A THEORETICAL APPROACH TO THE TURBULENT BOUNDARY LAYER WITH TRANSPIRATION

4.1 Introduction

The analysis follows the classical treatment by Prandtl for the boundary layer on a flat plate. For the turbulent shear layer, the Prandtl momentum transfer theory is considered and is modified by introducing the Van Driest damping factor. This technique is used to extend the analysis to include transpiration and pressure gradient. For the fully turbulent region, intermittency is introduced into the transport equation.

It was felt that more information regarding the boundary layer could be obtained following this type of analysis than using a potential flow solution. Knowledge with respect to skin friction, boundary layer growth and intermittency became available, and the analysis could be extended to include heat transfer and compressible flows.

4.1.1 Definition of parameters featured in turbulent flow analysis

One of the most important quantities in any analysis of this type is τ_w, the shear stress at the wall. In non-dimensional form, τ_w appears in the local skin friction coefficient, c_f

$$c_f = \frac{\tau_w}{\rho u_s^2} \qquad \text{....... [4.1.1]}$$

When analysing the turbulent shear layer, the wall shear velocity is invariably the velocity scale. By definition,

$$u_\tau{}^2 = \frac{\tau_w}{\rho} \qquad \text{....... [4.1.2]}$$

$$u_\tau = u_e\sqrt{\frac{c_f}{2}} \qquad \text{....... [4.1.3]}$$

The thickness of the boundary layer is denoted by δ. $y \to \delta$ as $\partial u/dy \to 0$. A more practical definition is

$$y = \delta \quad \text{when } u = 0{,}99U_\infty \qquad \text{..... [4.1.4]}$$

$$\text{Thus} \quad u_e = 0{,}99U_\infty \qquad \text{....... [4.1.5]}$$

The displacement thickness, δ^*, is the mass flow deficit which occurs in the boundary layer owing to the reduced velocity near the surface :

$$\left.\begin{aligned} \rho u_e \delta^* &= \int_0^\delta \rho(u_e - u)du \\ \frac{\delta^*}{\delta} &= \int_0^1 \left(1 - \frac{u}{u_e}\right) d\left(\frac{y}{\delta}\right) \end{aligned}\right\} \qquad \text{....... [4.1.6]}$$

A deficiency in momentum in the boundary layer may be expressed as a momentum thickness, θ:

$$\left.\begin{aligned} \rho u_e{}^2\theta &= \int_0^\delta \rho u(u_e - u)dy \\ \frac{\theta}{\delta} &= \int_0^1 \frac{u}{u_e}\left(1 - \frac{u}{u_e}\right) d\left(\frac{y}{\delta}\right) \end{aligned}\right\} \qquad \text{....... [4.1.7]}$$

Note that the upper integrated limit is given here as δ, but is more correctly ∞.

The ratio of displacement to momentum thickness, H, is a very useful shape factor,*

$$H = \delta^*/\theta \qquad \text{....... [4.1.8]}$$

* see Addendum for further explanation.

4.2 The Continuity and Momentum Equations

The derivation of the Prandtl boundary layer equations for an incompressible, newtonian fluid is well known (see Schlichting, 1968).

Continuity : $\frac{\delta \bar{u}}{\delta x} + \frac{\delta \bar{v}}{\delta y} = 0$ ..... [4.2.1]

Momentum : $\bar{u}\frac{\delta \bar{u}}{\delta x} + \bar{v}\frac{\delta \bar{u}}{\delta y} = u_e\frac{du_e}{dx} + \frac{1}{\rho}\frac{\delta}{\delta y}(\mu\frac{\delta \bar{u}}{\delta y} - \rho\overline{u'v'})$ [4.2.2]

The bar denotes a time based average quantity, and is assumed in the following equations.

At the edge of the boundary layer :

$u_e\frac{du_e}{dx} = -\frac{1}{\rho}\frac{dp}{dx}$ .... [4.2.3]

4.3 Formulation for the Reynolds Stress

To solve equation [4.2.2], it is necessary to relate the Reynolds stress, $\rho\overline{u'v'}$ to the mean velocity. Following Schlichting (1968), a formulation analogous to the laminar shear stress is assumed :

$\tau_t = \rho\varepsilon\frac{\delta \bar{u}}{\delta y}$ .... [4.3.1]

and then substitute Prandtl's momentum transfer theory for the eddy kinematic viscosity :

$\varepsilon = l^2(\frac{\delta \bar{u}}{\delta y})$ .... [4.3.2]

where $l = \kappa y$ .... [4.3.3]

This approach leads to a useful velocity distribution for the fully turbulent region. Near the wall the profile is linear. See Grimson (1971) for the derivation of [4.3.4] and [4.3.5].

Laminar sublayer : $u^+ = y^+$ .... [4.3.4]

Fully turbulent region : $u^+ = \frac{1}{\kappa} \ln y^+ + B$ ..... [4.3.5]

The Buffer or Blending region is not predicted.

Van Driest (1956) derived a continuous velocity and shear distribution by modifying the mixing length. By considering Stokes flow (ie. an infinite plate oscillating sinusoidally parallel to itself).

The modified mixing length became :-

$$l = \kappa y[1 - \exp(-y/A)]$$ .... [4.3.6]

Clearly, as y increases, the exponential term decreases, and $l \to \kappa y$, as before, for the fully turbulent region.

Using [4.3.6], [4.3.2] and [4.3.1],

$$\tau_t = -\rho\overline{u'v'} = \rho\kappa^2 y^2[1 - \exp(-y/A)]^2 \left|\frac{\delta u}{\delta y}\right|\frac{\delta u}{\delta y}$$ ..... [4.3.7]

A is the Van Driest damping length, dependent on the turbulence intensity and kinematic viscosity of the flow. It was determined experimentally, and in non-dimensional form, $A^+ = 26$ for $\kappa = 0,4$.

$$\tau = \tau_l + \tau_t$$ .... [4.3.8]

$$\tau = \mu\frac{\delta u}{\delta y} + \rho\kappa^2 y^2[1 - \exp(-y/A)]^2 \left|\frac{\delta u}{\delta y}\right|\frac{\delta u}{\delta y}$$ ..... [4.3.9]

Cebeci (1970b) modified A to include injection and pressure gradient :

$$A^+ = \frac{A u_\tau^*}{\nu}$$ .... [4.3.10]

$$\text{Modified, } A^{+} = 26\left\{-\frac{p^{+}}{v_w^{+}}\left[\exp(11{,}8 v_w^{+}) - 1\right] + \exp(11{,}8 v_w)\right\}^{-\frac{1}{2}} \quad \text{..... [4.3.11]}$$

$$\text{where } p^{+} = -\frac{dp}{dx}\,\frac{\nu}{\rho(u_w^{*})^{3}}; \quad v_w^{+} = \frac{v_w}{u_w^{*}} \quad \text{....... [4.3.12]}$$

4.4 Eddy Viscosity Formulation for the Fully Turbulent Region

In turbulent boundary layers, the potential core often extends well into the boundary layer. A pictorial representation of the instantaneous layer is depicted below :-

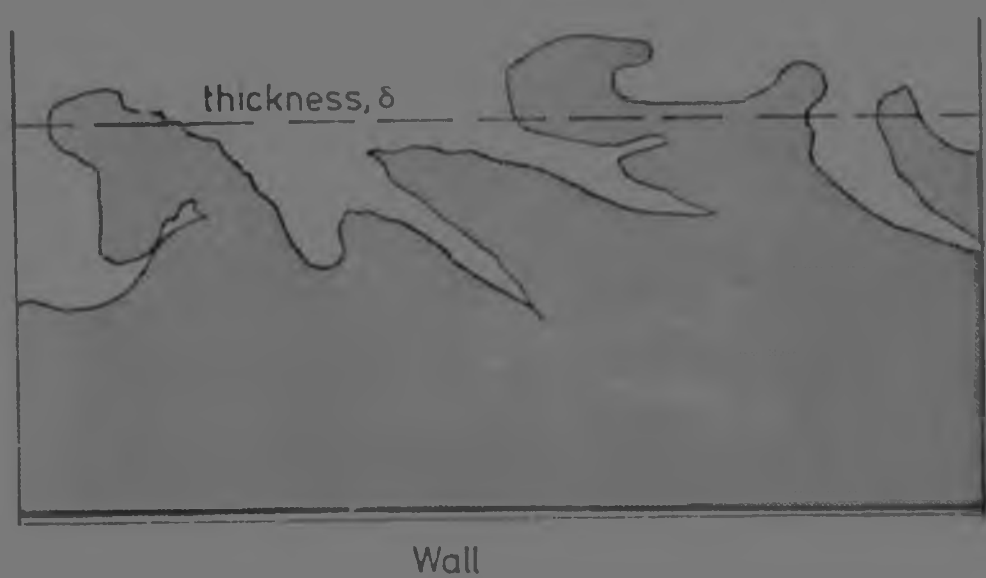

FIG 4.1 : SKETCH OF THE INSTANTANEOUS TURBULENT BOUNDARY LAYER, SHOWING THE EXTENSION OF THE POTENTIAL CORE BELOW THE AVERAGE THICKNESS

If the Reynolds stress in the potential core is zero, then the intermittent extension of this 'clean' flow into the boundary layer must influence the shear distribution across the outer turbulent region. Sarnecki postulated that γ, the intermittency, was the fraction of total time for which the flow was turbulent at a fixed distance from the plate. γ ranges from 0 to 1, where γ = 1 inside the continuously turbulent boundary layer, and γ→0 at the edge of the layer.

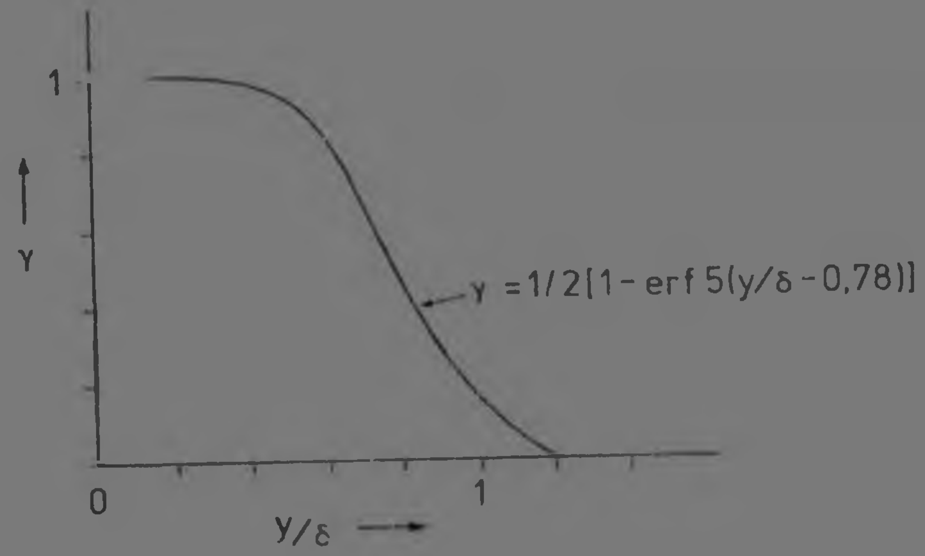

FIG 4.2 : INTERMITTENCY DISTRIBUTION ACROSS A TURBULENT BOUNDARY LAYER (CEBECI, 1974)

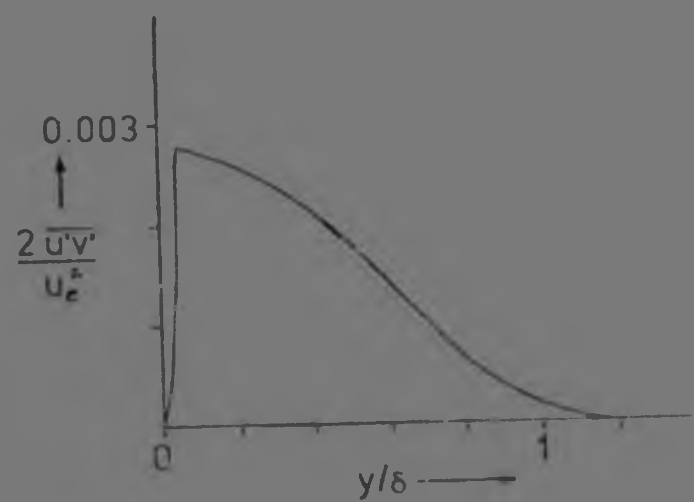

FIG 4.3 : REYNOLDS STRESS ACROSS THE BOUNDARY LAYER FOR A SMOOTH FLAT PLATE, ZERO PRESSURE GRADIENT

Intermittency and Reynolds stress were determined experimentally with hot wire anemo etry by Klebanoff (Cebeci 1974, Schlichting 1968).

Clearly, even the modified mixing length theory cannot predict ε across the entire boundary layer. For in the outer region, ε must decrease, and experiments have shown that the decrease follows the intermittency curve, as could be expected. The eddy viscosity in the outer region was given as :

$$\varepsilon_0 = 2[\int_0^\infty (u_e - u)dy] \times \tfrac{1}{2}[1 - \mathrm{erf}\, 5(y/\delta - 0{,}78)] \qquad [4.4.1]$$

The intermittency curve may be approximated (Cebeci 1974) by :

$$\gamma \quad \frac{1}{[1 + 5{,}5(y/\delta)^6]} \qquad \ldots\ldots\ [4.4.2]$$

γ is a constant, with a value between 0,016 and 0,02. In the present work, γ = 0,0168 is used. In the programme, the turbulent transport eddy viscosity was used until it was equal to the outer eddy viscosity. From this point outwards, ε_0 was used.

[4.4.1] may be writte :-

$$\varepsilon_0 = \alpha u_e \delta^* \gamma \qquad \ldots\ldots\ [4.4.3]$$

4.5 Boundary Conditions

The boundary conditions for the turbulent shear layer are :-

$$u(x,0) = 0 \qquad \ldots\ldots\ [4.5.1]$$

$$v(x,0) = 0 \text{ or } v_w \text{ with mass transfer} \qquad \ldots\ [4.5.2]$$

$$\lim_{y \to \infty} u(x,y) = u_e(x) \qquad \ldots\ldots\ [4.5.3]$$

4.6 The Transformed Momentum and Related Equations : A Summary

Only the transformed equations are given here. Details of the transformation appear in Appendix A1. ϕ is a transformed, non-dimensionalized stream function.

Momentum :

$$[(1 + \varepsilon^{+})\phi'']' + (\phi + \eta)\phi'' - \beta(\phi' + 2)\phi' = 2\xi[(\phi' + 1)\frac{\delta\phi'}{\delta\xi} - \phi''\frac{\delta\phi}{\delta\xi}] \qquad \text{..... [4.6.1]}$$

Boundary conditions :

$$\phi(\xi,0) = 0 \quad \text{for no transpiration} \qquad \text{..... [4.6.2a]}$$

$$\phi(\xi,0) = -\frac{1}{(2\xi)^{\frac{1}{2}}}\int_0^{\xi}\frac{\rho v_w}{\mu u_e}d\xi \quad \text{with } v_w \neq 0 \qquad \text{..... [4.6.2b]}$$

$$\phi'(\xi,0) = -1 \qquad \text{..... [4.6.3]}$$

$$\lim_{\eta\to\eta_\infty} \phi'(\xi,\eta) = 0 \qquad \text{..... [4.6.4]}$$

Eddy viscosity equations :

$$\varepsilon_i = \kappa^2(2\xi)^{\frac{1}{2}}\eta^2\frac{\phi''}{\rho}[1 - \exp\{-\eta(\frac{(2\xi)^{\frac{1}{2}}}{\mu}\cdot\phi_w'')^{\frac{1}{2}}/A^{+}\}]^2 \qquad \text{... [4.6.5]}$$

$$\varepsilon_o = \alpha.[-\frac{(2\xi)^{\frac{1}{2}}}{\rho}\int_0^{\eta_\infty}\phi' d\eta] \times [1 + 5{,}5(\frac{\eta}{\eta_\infty})^6]^{-1} \qquad \text{..... [4.6.6]}$$

Boundary layer parameters :

$$c_f = \mu(\frac{2}{\xi})^{\frac{1}{2}}\phi''(\xi,0) \qquad \text{....... [4.6.7]}$$

$$\delta^* = -\frac{(2\xi)^{\frac{1}{2}}}{\rho u_e}\int_0^{\eta_\infty}\phi'(\xi,\eta)d\eta \qquad \text{....... [4.6.8]}$$

$$\theta = -\frac{(2\xi)^{\frac{1}{2}}}{\rho u_e}\int_0^{\eta_\infty}\phi'(\xi,\eta)[1 + \phi'(\xi,\eta)]d\eta \qquad \text{....... [4.6.9]}$$

CHAPTER 5

COMPUTER SOLUTION OF THE MOMENTUM EQUATION

5.1 Introduction

If a generalised computer programme is developed and proved with respect to reliable experimental results, it becomes possible to calculate such parameters as boundary layer thickness, skin friction and heat transfer. Such a programme could be simple, e.g. for the case of a flat plate, and may be made more versatile to include transition, pressure gradient, roughness, transpiration, heat transfer, compressible flow, axisymmetric flow and three dimensional flow.

A finite difference technique, rather than a finite element method, is used in this dissertation to solve equation [4.6.1]. Because of the well known stability problems experienced with explicit methods, an implicit scheme was selected, with its attendant requirement to linearise the equation. In this chapter the linearisation and matrix solution are discussed.

5.2 Linearisation of the Momentum Equation

Linearisation is achieved by allowing those terms which make the equation non-linear to be set to values known from a previous station or interation. Clearly an iterative process is necessary, in which the latest value approaches that of the previous iteration. When linearising, care must be taken to retain at least one term of each derivative. The subscript o here denotes a previously known quantity :-

$$[(1 + \epsilon^+)_o \phi'']' + (\phi_o + \eta)\phi'' - \phi' B(\phi_o' + 2) =$$
$$2\xi[(\phi_o' + 1)\frac{\delta\phi'}{\delta\xi} - \phi_o''\frac{\delta\phi}{\delta\xi}] \qquad \text{.......} \; [5.2.1]$$

5.3 The Finite Difference Grid

Cebeci (1974) suggested a grid in which the step lengths normal to the wall were very small, near the wall, ie. in the region of rapid change in velocity, and increasing in size towards the edge. He proposed a grid of the form :-

$$\Delta\eta_i = K.\Delta\eta_{i-1} \qquad \text{.......} \; [5.3.1]$$

$\Delta\eta_i$ is the general step length, and for $K>1$, this step length is larger than the previous step. If the first step length is h, the distance to the i^{th} grid point is :-

$$\eta_i = h\frac{K^{i-1} - 1}{K - 1} \qquad \text{.......} \; [5.3.2]$$

The exponential growth in grid spacing ties up with the turbulent velocity profile.

An alternate expression for the i^{th} grid spacing is :-

$$\Delta\eta_i = K^{i-2}.h \qquad \text{.......} \; [5.3.3]$$

The programme was written in a manner to allow variable step length in the streamwise direction. This may be a completely random step length. Because the programme "marches" in the x-direction when solving, the grid points in this direction were called stations, and are denoted by, e.g. the n^{th} station.

The ordinate was divided into points or steps, denoted by i. Note that the first η value, ie. at the wall, is point $i = 1$, therefore $\eta_1 = 0$.

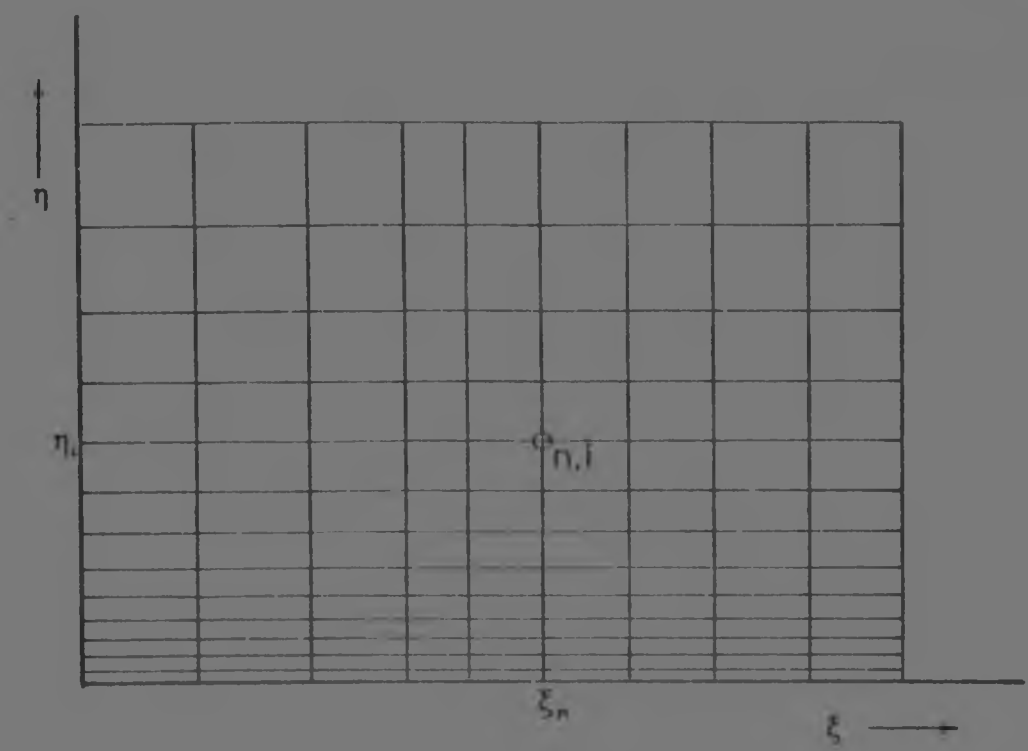

FIG 5.1 : THE FINITE DIFFERENCE GRID FOR k = 1,2 AND h = 1,5

5.4 The Momentum Equation in Finite Difference Form

Equation [5.2.1] is given with the subscripts as used in the programme :-

$$[(1 + \varepsilon^+_{n,i_0})\phi''_{n,i}]' + (\phi_{n,i_0} + \eta_i)\phi''_{n,i} - \phi'_{n,i}\cdot\beta_n(\phi'_{n,i_0} + 2)$$
$$= 2\xi_n[(\phi'_{n,i_0} + 1)\frac{\delta\phi'}{\delta\xi}\Big|_{n,i} - \phi''_{n,i_0}\frac{\delta\phi}{\delta\xi}\Big|_{n,i}] \quad \ldots [5.4.1]$$

By taking the derivative of the first term at this stage $d\varepsilon^+/dy$ would be introduced, which may be determined numerically, but with the attendant error inherent in any such calculation, with the added difficulty that ε was not a continuous function. $\phi'''_{n,i}$ would also appear. The derivative was solved implicitly in the final equation by treating the term as a separate function, say g. This is why the term $(1 + \varepsilon^+)_{n,i-1_0}$ and at $(n,i + 1)$ feature in the following equation. Values of ϕ are known at n-1, n-2 and o. All these terms were kept on the right hand side, while those in n,i were retained on the left hand side. The capital letters denote constants based on step size, and are defined in Appendix A2.

$$\phi_{n,i-2}\{A.X1.(1+\varepsilon_0^+)_{n,i-1}\}$$

$$+\ \phi_{n,i-1}\{A.X2.(1+\varepsilon_0^+)_{n,i-1} + B.D.(1+\varepsilon_0^+)_{n,i} + (\phi_{0_{n,i}} + \eta_i)D$$
$$-\ \beta.A.(\phi'_{0_{n,i}} + 2) - 2\xi_n(\phi'_{0_{n,i}} + 1).A.N\}$$

$$+\ \phi_i\{A.X3.(1+\varepsilon_0^+)_{n,i-1} + B.E.(1+\varepsilon_0^+)_{n,i} + C.X4.(1+\varepsilon_0^+)_{n,i+1}$$
$$+\ E.(\phi_{0_{n,i}} + \eta_i) - \beta.B.(\phi'_{0_{n,i}} + 2) - 2\xi_n(\phi'_{0_{n,i}} + 1)N.B$$
$$+\ 2\xi_n\phi''_{0_{n,i}}.N\}$$

$$+\ \phi_{i+1}\{B.F.(1+\varepsilon^+)_{n,i} + C.X5.(1+\varepsilon_0^+)_{n,i+1} + F.(\phi_{0_{n,i}} + \eta_i)$$
$$-\ \beta.C.(\phi'_{0_{n,i}} + 2) - 2\xi_n(\phi'_{0_{n,i}} + 1).N.C\}$$

$$+\ \phi_{i+2}\{C.X6.(1+\varepsilon_0^+)_{n,i+1}\}$$

$$= 2\xi_n\{(\phi'_{0_{n,i}} + 1)[L.\phi'_{n-2,i} + M\phi'_{n-1,i}] - \phi''_{0_{n,i}}[L.\phi_{n-2,i} + M\phi_{n-1,i}]\}$$

.... [5.4.2]

Lumping the coefficients into single constants reduces [5.4.2] to :-

$$\phi_{n,i-2}.A_i + \phi_{n,i-1}.B_i + \phi_{n,i}.C_i + \phi_{n,i+1}.D_i + \phi_{n,i+2}.E_i = F_i$$

.... [5.4.3]

Remembering that $i = 1$ denoted $\eta = 0$, a system of linear simultaneous equations could be written starting with $i = 3$. If N is the number of η steps, a total of N-4 equations can be set up (because [5.4.3] must end with N-2). There are thus N unknowns and N-4 equations. Using boundary conditions, ϕ_1, ϕ_2, ϕ_{N-1} and ϕ_N were determined.

$$\phi_{n,1}A_3 + \phi_{n,2}B_3 + \phi_{n,3}C_3 + \phi_{n,4}D_3 + \phi_{n,5}E_3 = F_3$$

$$0 \quad \phi_{n,2}A_4 + \phi_{n,3}B_4 + \phi_{n,4}C_4 + \phi_{n,5}D_4 + \phi_{n,6}E_4 = F_4$$

$$0 \quad 0 \quad \phi_{n,3}A_5 + \phi_{n,4}B_5 + \phi_{n,5}C_5 + \phi_{n,6}D_5 + \phi_{n,7}E_5 = F_5$$

$$\vdots \qquad \qquad \vdots$$

$$\phi_{n,N-4}A_{N-2} + \phi_{n,N-3}B_{N-2} + \phi_{n,N-2}C_{N-2} + \phi_{n,N-1}D_{N-2} + \phi_{n,N}E_{N-2}$$

$$= F_{N-2} \qquad \ldots\ldots [5.4.4]$$

Because $\phi_{n,1}$ and $\phi_{n,2}$ are known from boundary conditions, they are taken to the right hand side :-

$$\left.\begin{aligned} \phi_{n,3}C_3 + \phi_{n,4}D_3 + \phi_{n,5}E_3 &= F_3 - \phi_{n,1}A_3 - \phi_{n,2}B_3 \\ \phi_{n,3}B_4 + \phi_{n,4}C_4 + \phi_{n,5}D_4 + \phi_{n,6}E_4 &= F_4 - \phi_{n,2}A_4 \end{aligned}\right\} \quad [5.4.5]$$

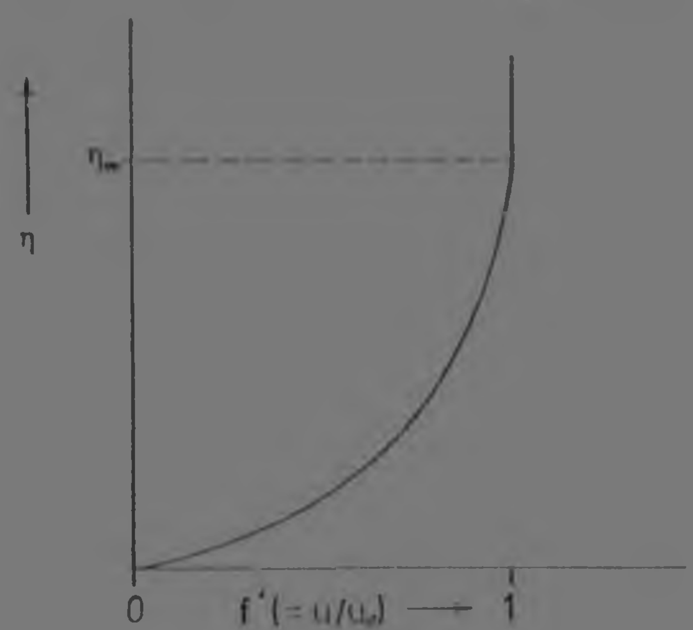

FIG 5.2 : SKETCH OF VELOCITY PROFILE IN TRANSFORMED CO-ORDINATES

From Fig 5.2 it is seen that as $\eta \to \eta_\infty$, $f'(\xi,\eta) \to 1$ and therefore $\phi'(\xi,\eta) \to 0$.

Equation [4.6.4] states that

$$\lim_{\eta \to \eta_\infty} \phi'(\xi,\eta) = 0 \qquad \text{....... [5.4.6]}$$

If $N-2$, $N-1$ and N are in this region, then using a simple finite difference approximation :-

$$\phi'_{N-1} = \frac{\phi_N - \phi_{N-1}}{\eta_N - \eta_{N-1}} = 0 \qquad \text{....... [5.4.7]}$$

$$\therefore \phi_N = \phi_{N-1} \qquad \text{....... [5.4.8]}$$

Similarly :-

$$\phi'_{N-1} = \frac{\phi_N - \phi_{N-2}}{\eta_N - \eta_{N-2}} = 0 \qquad \text{....... [5.4.9]}$$

$$\therefore \phi_N = \phi_{N-1} = \phi_{N-2} \qquad \text{....... [5.4.10]}$$

The $N-3$ equation is :-

$$A_{N-3}\phi_{n,N-5} + B_{N-3}\phi_{n,N-4} + C_{N-3}\phi_{n,N-3} + \phi_{n,N-2}(D_{N-3} + E_{N-3}) = F_{N-3} \qquad \text{....... [5.4.11]}$$

and the $N-2$ equation (last) is :-

$$A_{N-2}\phi_{n,N-4} + B_{N-3}\phi_{n,N-3} + \phi_{n,N-2}(C_{N-2} + D_{N-2} + E_{N-2}) = F_{N-2} \qquad \text{....... [5.4.12]}$$

The general equation may be stated :-

$$[A]\{\phi\} = \{B\} \quad i=3 \text{ to } i=N-2 \qquad \text{....... [5.4.13]}$$

5.5 The Finite Difference Molecule

The general finite difference molecule is shown in Fig 5.3

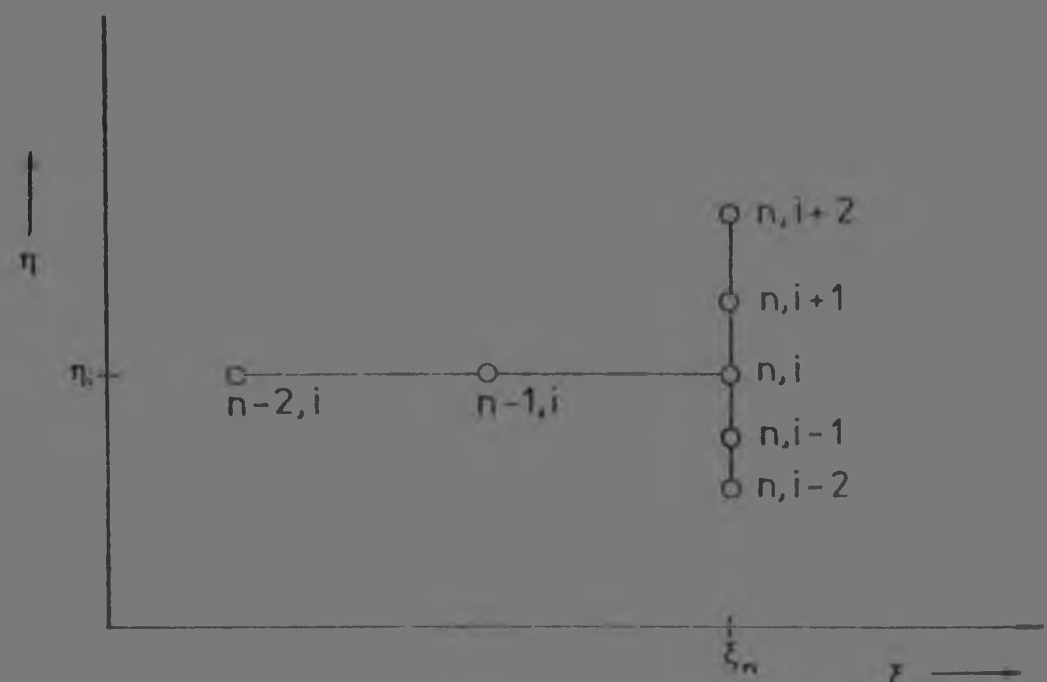

FIG 5.3 : THE FINITE DIFFERENCE MOLECULE

To solve for ϕ at station n, it is necessary to know the values of ϕ, ϕ' and ϕ'' at stations $n-2$ and $n-1$. Two profiles were therefore required to start the solution at the third station. The programme then marched to $n+1$ and used $n-1$ and n to solve for ϕ at $n+1$, and so on. For the first solution at say n, the values on the right hand side, denoted by o, were substituted by the values at $n-1$. Similarly in generating ε. The iterative process was based on the convergence of $\phi''_{n,1}$ and $\phi''_{o\,n,1}$ and $\delta_n{}^*$ and $\delta_o{}^*$.

To economise on core storage on the computer, only four vectors for ϕ, ϕ', ϕ'' and ε^+ were used. Solutions at $n-2$, $n-1$ and n were stored in the first three vectors; the present iteration, o, in the fourth. The first three rotated cyclicly. If the vectors are denoted by V_1, V_2 and V_3, the solutions were stored :-

$n=1$, V_1

$n=2$, V_2

o, V_4

Once convergence was achieved, $V_4 \rightarrow V_3$ and print/plot. V_1 could be overwritten and the solution march to $n=4$

$n=2$, V_2

$n=3$, V_3

o V_4

After convergence, $V_4 \rightarrow V_1$, print/plot, and delete V_2

$n=3$, V_3

$n=4$ V_1

o V_4

After convergence, $V_4 \rightarrow V_1$, print/plot, etc.

A tremendous saving was possible when storing matrix $[A]$ because it was banded. It had two upper and two lower co-diagonals. Typically, the banded matrix required 500 storage locations, compared with 10 000 for full square matrix storage. In double precision, this is equivalent to 80 k bytes.

$n=1$, V_1

$n=2$, V_2

o, V_4

Once convergence was achieved, $V_4 \rightarrow V_3$ and print/plot V_1 could be overwritten and the solution march to $n=4$

$n=2$, V_2

$n=3$, V_3

o V_4

After convergence, $V_4 \rightarrow V_1$, print/plot, and delete V_5

$n=3$, V_3

$n=4$ V_1

o V_4

After convergence, $V_4 \rightarrow V_2$, print/plot, etc.

A tremendous saving was possible when storing matrix [A] because it was banded. It had two upper and two lower co-diagonals. Typically, the banded matrix required 500 storage locations, compared with 10 000 for full square matrix storage. In double precision, this is equivalent to 80 k bytes.

FIG 5.4

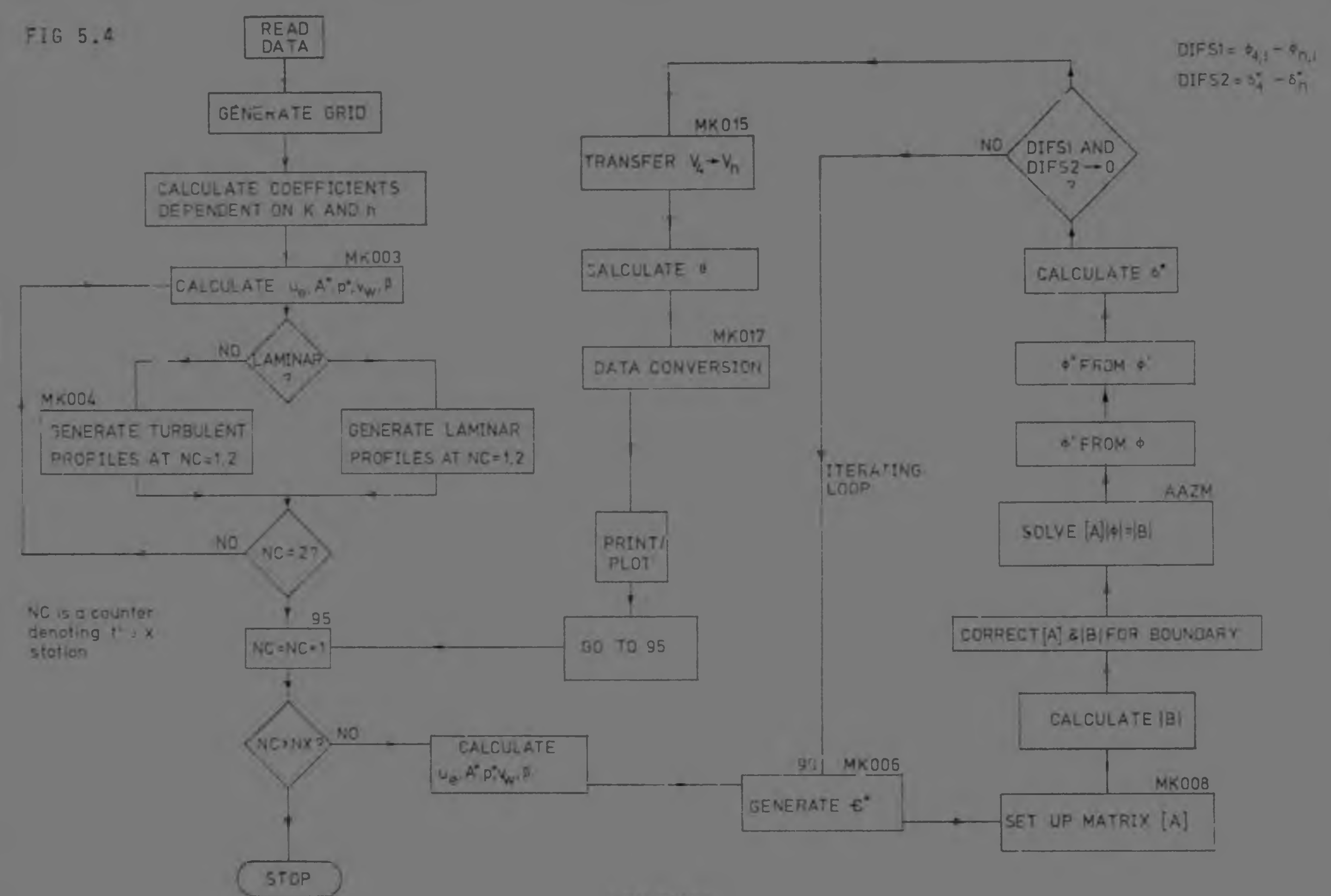

5.6 FLOW CHART

5.7 Discussion of Various Features of the Programme

5.7.1 Initial profiles

As stated above, profiles at $n=1$ and $n=2$ were required to start the solution. These were generated in MK001L (laminar) or MK004 (turbulent) - see Fig 5.5. Distance along the abcissa was used as a criterion for laminar or turbulent flow. Various stability techniques, critical Reynolds numbers and shape factors have been suggested (Cebeci 1974). However, these are often limited, and not sufficiently accurate, e.g. critical Reynolds number is for flat plate flow with zero pressure gradient, and spans a large range ($3{,}5 \times 10^5$ to 10^6).

If $\varepsilon=0$, the solution is laminar, and from a given ξ station, $\varepsilon>0$ and the programme entered the transition and hence turbulent solutions.

The laminar profile was generated from an equation given by Grimson (1971) :-

$$\frac{u}{U_\infty} = f(y/\delta) = f(\bar{y}) \qquad \text{.......} \; [5.7.1]$$

If a fourth order polynomial is used, a pressure gradient may be included :-

$$\frac{u}{U_\infty} = A_0 + A_1\bar{y} + A_2\bar{y}^2 + A_3\bar{y}^3 + A_4\bar{y}^4 \qquad \text{.......} \; [5.7.2]$$

A pressure gradient related shape factor was introduced :-

$$\Lambda = \frac{\delta^2}{\nu}\cdot\frac{du}{dx} \qquad \text{.......} \; [5.7.3]$$

$$\frac{u}{U_\infty} = \bar{y}(2 - 2\bar{y}^2 + \bar{y}^3) + \frac{\Lambda}{6}\,\bar{y}(1 - 3\bar{y} + 3\bar{y}^2 - \bar{y}^3) \qquad \text{...} \; [5.7.4]$$

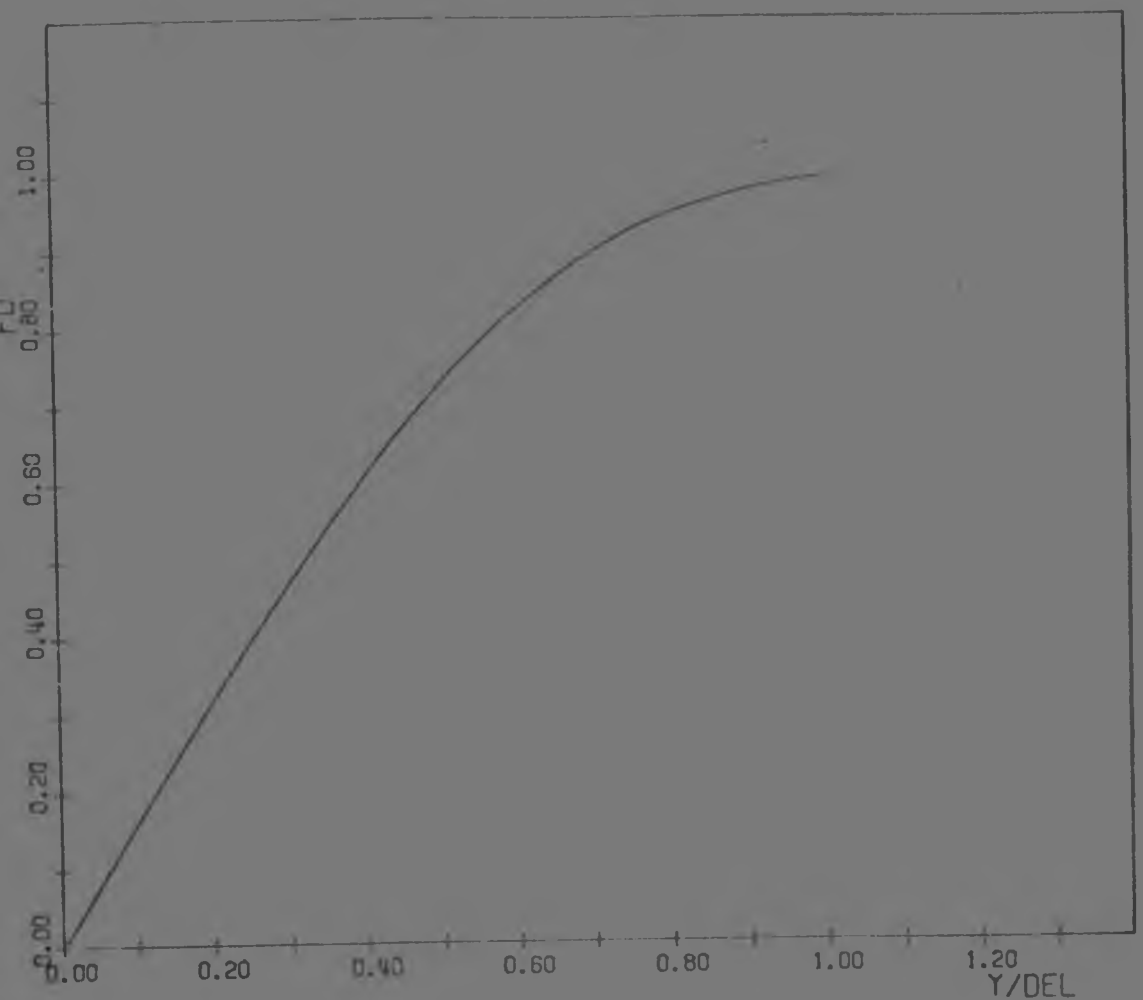

FIG 5.5 LAMINAR INPUT PROFILE

The turbulent profile was generated using Van Driest's mixing length theory. One difficulty here was that the edge of the boundary layer was over-estimated, and pressure gradient was not included. However, the programme would obtain the correct profile at $n=6$ after some iteration. In developing this subroutine, it was found that the results were significantly improved if the unequal, exponential type η grid was used. See Fig 5.6 for equal step length, and Fig 5.7 for exponential grid, using the well known semi-log plot. Fig 5.7 is reproduced on simple non-dimensionalised axes in Fig 5.8. The dashed lines on Fig 5.7 are for :-

$$u^+ = y^+ \quad \text{....... [5.7.5]}$$

and $u^+ = 5{,}757 \log y^+ + 5{,}24$ .... [5.7.6]

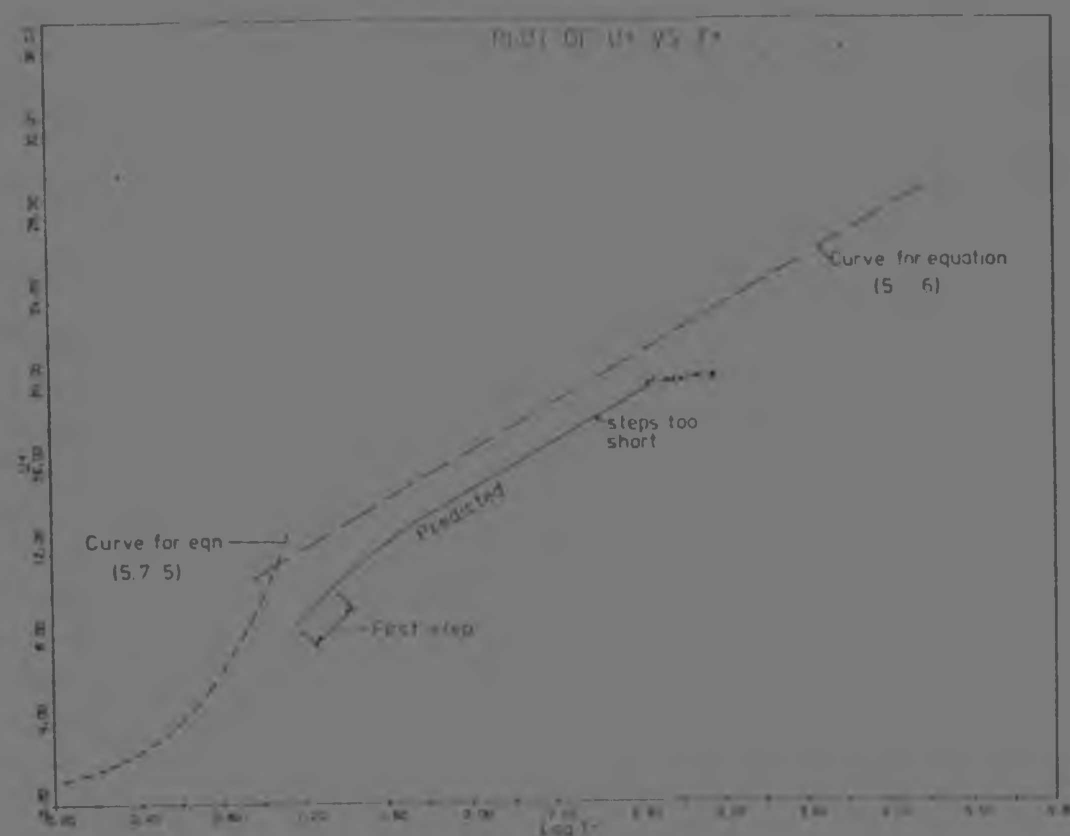

FIG 5.6 : TURBULENT PROFILE GENERATED WITH EQUAL STEP LENGTH

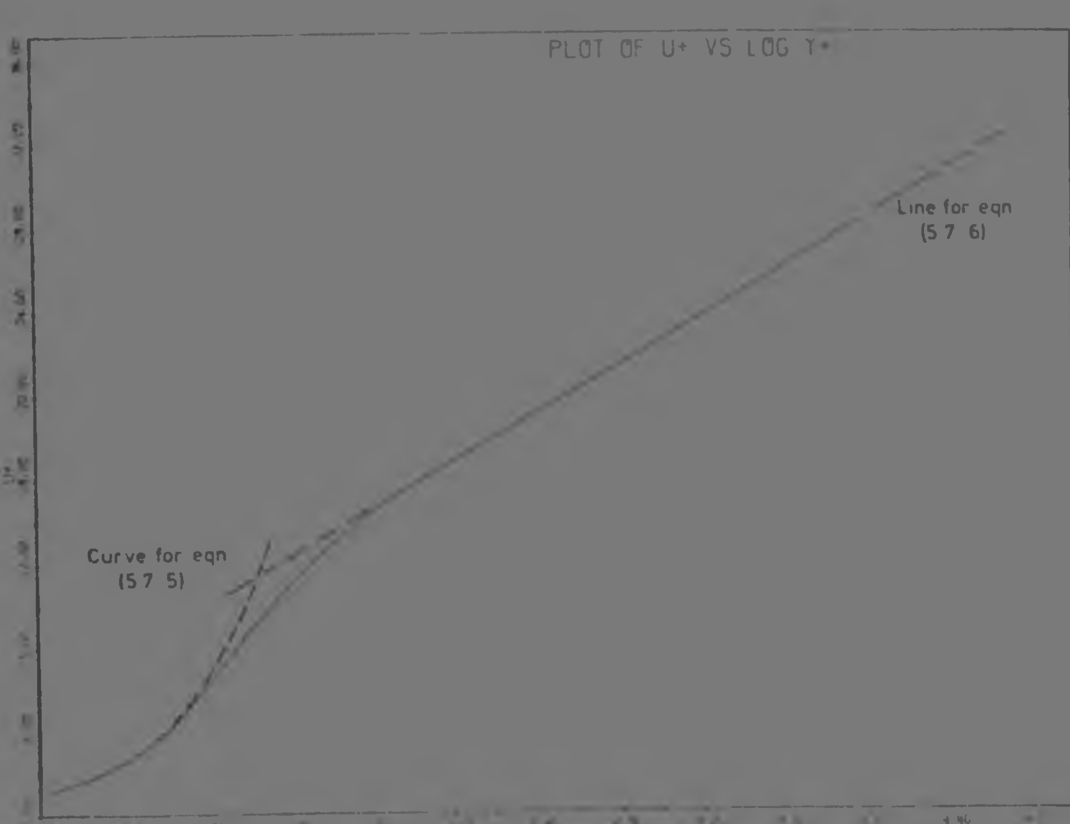

FIG 5.7 : TURBULENT PROFILE GENERATED WITH UNEQUAL STEP LENGTH

FIG 5.8 : TURBULENT PROFILE GENERATED WITH UNEQUAL STEP LENGTH

Equation [3.3.33], with $v_w^+ = 0$, simplified to that derived by Van Driest (1956) :-

$$\frac{du^+}{dy^+} = \frac{2dy^+}{1 + \sqrt{1 + 4\kappa^2 y^{+2}[1 - \exp(-y^+/A^+)]^2}} \qquad \text{..... [5.7.7]}$$

by integrating this expression, $u_i^+ = \int_0^{y_i^+} f(y^+)$. This was performed numerically in subroutine MK004. u_i^+ had to be converted to u/u_e, ie. u_w^+ was required. c_f was estimated in subroutine TAUF from the simplified equation

$$c_f = \frac{0{,}0595}{Re_x^{1/5}} \qquad \text{....... [5.7.8]}$$

In both laminar and turbulent profile generators, it was necessary to convert $u/u_e(=f')$ to ϕ', and to calculate ϕ and ϕ''. The edge of the boundary layer was taken to be where $\phi' < 0{,}0001$.

To obtain δ^* and θ, the profile had to be integrated. This was done by using the trapezoidal rule, which was considered sufficiently accurate because the step length was so small. Note that the experimental profiles were integrated in a similar manner, and for a very coarse grid (20 points compared with 100 for the computer programme) the difference in θ when using Simpson's rule was 1%. A typical equation appears in Appendix F1.

As the injection increased, the shear stress at the wall tends to zero, or even a negative value. However, reverse flow is not thought to occur. The programme was not designed to handle these possibilities. If ϕ'' was obtained from ϕ using Newtons Divided Difference technique at the wall, negative shear was indicated at values of $F \geq 0{,}005$. This is in accordance with experiment, but resulted in difficulties when calculating u_w^*, and hence also v_w^+ and p^+. The programme was written for a continuous velocity profile and the condition of no-slip at the wall. Note too that the derivation of A^{+} was for very small injection rates, and $y_{B}{}^{+} = 11,8$ was the value for unblown flat plate flow.

By using a reasonably large initial η step (0,06 compared with values as low as 0,001 suggested by Cebeci (1970a), and calculating ϕ'' from ϕ', the programme remained stable up to values of $F = 0,017$.

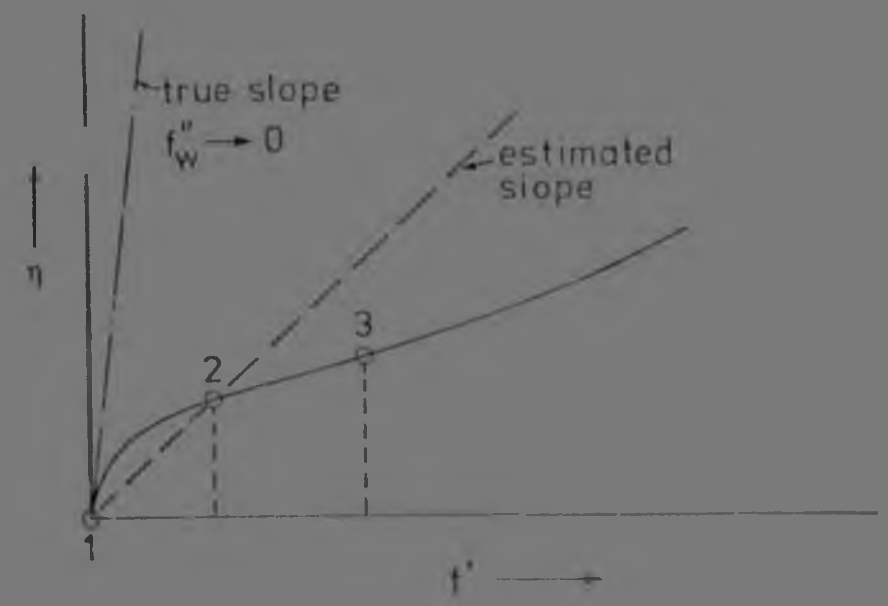

FIG 5.9 : u-VELOCITY PROFILE NEAR THE WALL

The numbers shown in Fig 5.9 denote η grid points. If 2 is outside the point of inflexion, the programme would effectively be unaware of this behaviour. ϕ'' would be predicted to be the dashed line (depending on the finite difference equation). This value is incorrect, but allows real values of $u_{\omega}{}^{*}$, $v_{\omega}{}^{+}$, p^{+} etc. to be calculated. Although these errors are large, the effect of this on the complete solution of [5.4.13] appeared to be very small.

Because this technique produced results which appeared very promising, the loss of accuracy in $u_w{}^*$, and hence meaningless c_f for injected flows, was considered unimportant in the present phase of research. As will be pointed out later in Chapter 7, $u_w{}^*$ as characteristic velocity for injected boundary layers may well require reconsideration.

For zero pressure gradient flat plate flow, c_f predicted by the programme was very close to that experimentally measured and fitted by [5.7.8].

CHAPTER 6

EXPERIMENTAL APPARATUS AND PROCEDURE

6.1 Introduction

The object of the experiments was to obtain a number of mean velocity profiles on a porous plate preceded by a solid plate, ie. to subject a fully developed turbulent profile to injection. The next step was to constrict the lower porous surface, to ascertain whether this made a measurable difference to the profiles. To this end an open circuit wind tunnel with rectangular working section was designed. Three different grades of porous plate were tested.

6.2 The Wind Tunnel

6.2.1 General

The open circuit wind tunnel consisted of a Sirrocco centrifugal fan (see Appendix B1 for the performance curve). Drive was provided by a Siemens A.C. induction motor rated at 22 kW, through three Fenner β type belts. By changing pulleys, the rotational speed of the fan could be varied, resulting in different flow rates and pressures. A flow damper at the fan inlet could be used to vary the flow rate, as could a by-pass at the beginning of the tunnel. This by-pass was only used at start-up (minimize starting load), because a power spectrum measured in the working section produced two additional spikes when the trap door was not fully closed (see 6.4).

The ducts leading to the Working Section were made up of a diffuser, settling chamber and contraction. Screens and honeycomb straightened the flow and decreased the turbulence intensity.

FIG 6.1 : GENERAL VIEW OF WIND TUNNEL SHOWING (1) THE SETTLING CHAMBER, (2) CONTRACTION, (3) ENTRY TO WORKING SECTION, (4) REAR OF INSTRUMENT PANEL (5) BETZ MANOMETER

6 2.2 The working section

A rectangular working section 209 x 496 mm was built. The side walls were made of perspex, the roof and solid floor sections of aluminium. A boundary layer bleed was installed in the floor in the entry section. The plate preceding the porous section was 800 mm long, the leading edge milled to 45°. This configuration could be altered such that the initial solid plate was 150 mm long. Theoretically a laminar boundary layer would reach the porous plate, but tests were not done with the short plate installed.

A traversing rig (Disa type 55H01) was mounted on slides. The probe could be lowered through a slit in the roof of the working section. The distance of the probe from the wall was measured with a Mitutoyo Dial Gauge. This entire rig was mounted on a separate frame which was isolated from the tunnel to prevent vibration being transmitted to the probe. The traversing rig allowed 4 degrees of freedom.

Fig 6.2 shows the working section and the traversing rig. In the next photograph, Fig 6.3, a close-up of the working section interior is given. In this figure the hot wire probe can be seen mounted above the porous plate. Note that the short plate configuration is depicted.

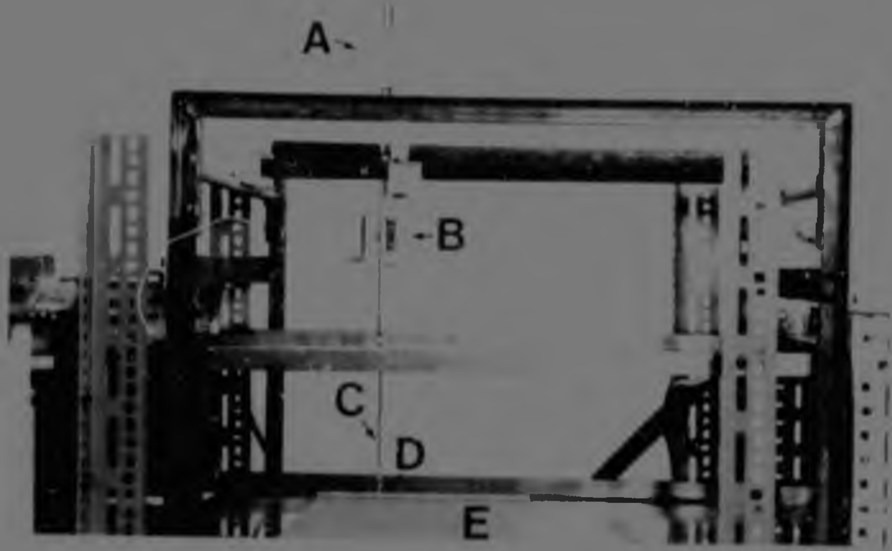

FIG 6.2 : THE WORKING SECTION AND THE TRAVERSING RIG : (A) DIAL GAUGE, (B) DISA TRAVERSING MECHANISM, (C) PROBE HOLDER, (D) HOT WIRE PROBE, (E) POROUS PLATE

FIG 6.3 : INSIDE OF THE WORKING SECTION : (A) ENTRY TO WORKING SECTION, (B) PROBE HOLDER, (C) HOT WIRE PROBE, (D) SHORT LEADING PLATE, (E) POROUS PLATE

6.2.3 Transpiration flow supply

The transpiration or secondary flow was drawn from the laboratory compressed air supply. An Ingersoll-Rand compressor fed two receivers, from which a 50 mm i.d. pipe ducted the air to a pressure regulator (Norgren type AG20). The flow rate was measured with an orifice plate, preceded by an entry length of 30 diameters. The orifice plate was calibrated according to British Standards 1042. A fibre-type filter, supplied by Vokes, was placed in the plenum chamber below the porous plate. The filter removed particles down to 5 microns, as well as grease. The front cover of the plenum chamber had to be removed when changing porous plates. The height of the porous plate was adjusted with screws inside the chamber. The plates were made of sintered bronze by Sintered Products Ltd. of Nottingham, England. Each plate was 6,35 mm thick. The front and rear edges were milled to 45°. Grades E (highly porous) C and A were tested.

FIG 6.4 :
THE WORKING SECTION AND THE PLENUM CHAMBER SHOWN WITH ITS FRONT COVER IN PLACE

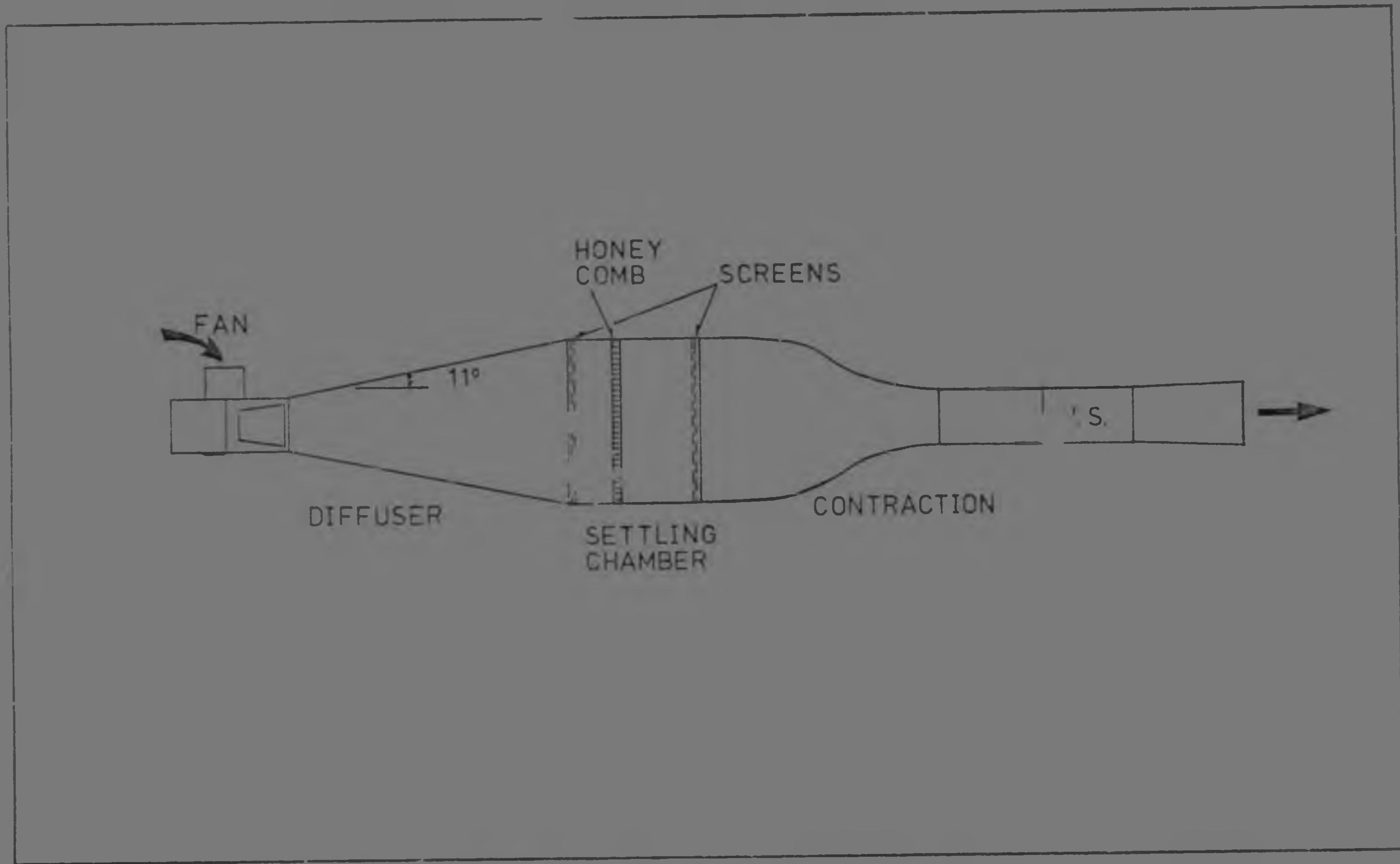

FIG 6.5 : PLAN VIEW OF THE WIND TUNNEL

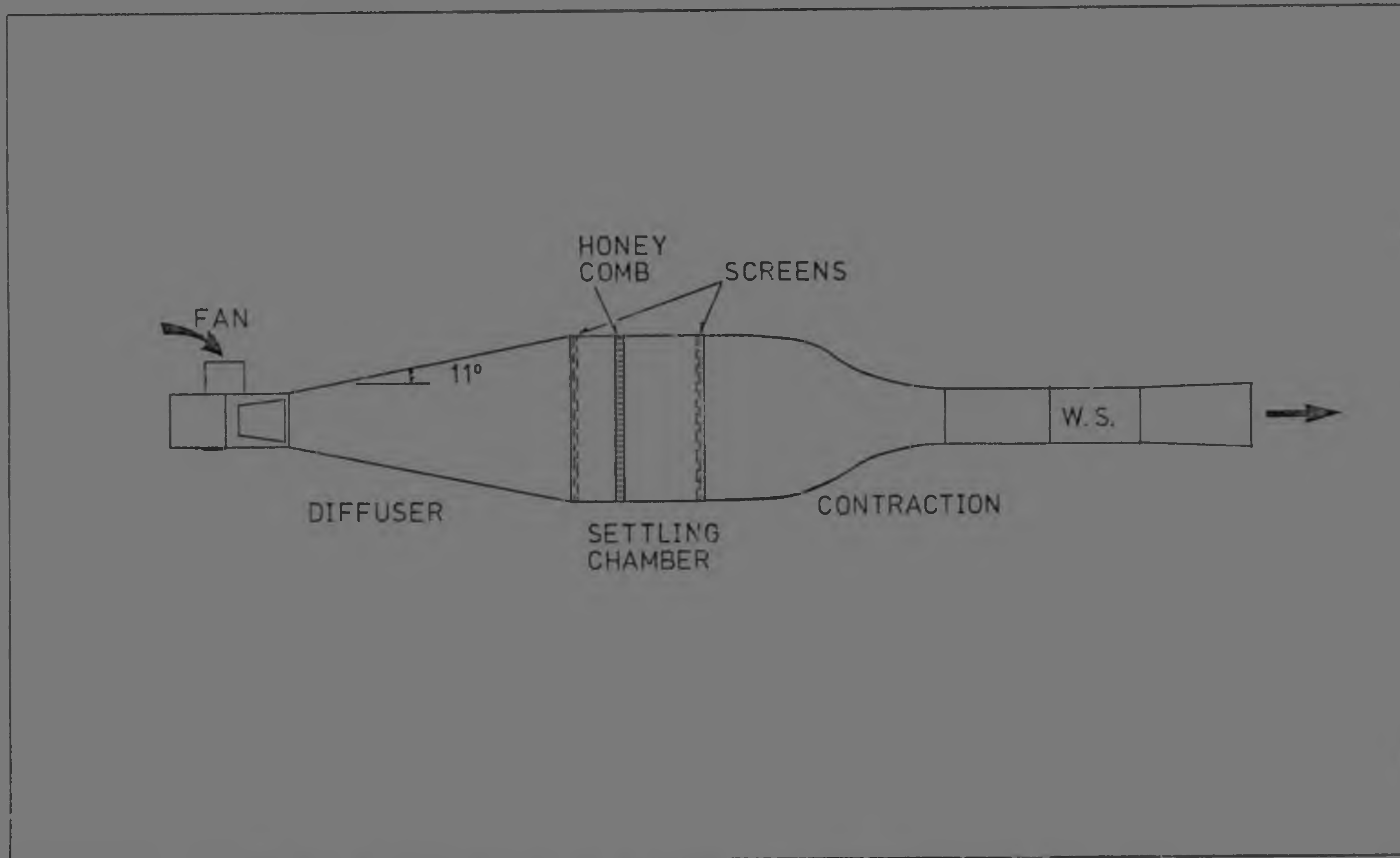

FIG 6.5 : PLAN VIEW OF THE WIND TUNNEL

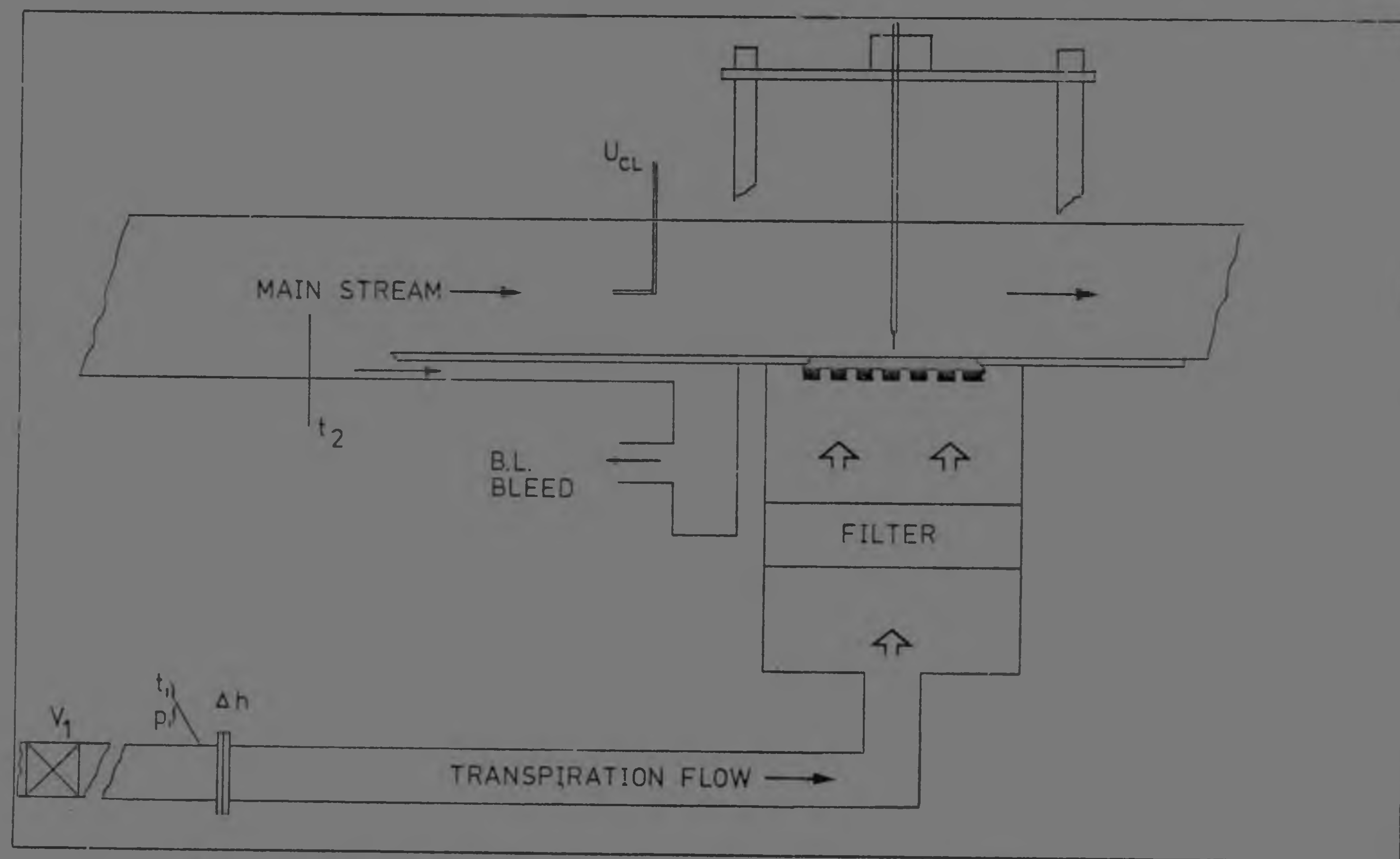

FIG 6.6 : SIDE VIEW OF THE WORKING SECTION SHOWING THE TRANSDUCERS

6.3 Hot-wire Anemometry

Velocity traverses were obtained using a Disa type 55D01 constant temperature anemometer. A single sensor, gold-plated wire probe (Disa type 55F01) was inserted in a probe holder with a protection pin attached. By adjusting this pin, it was possible to touch the pin on the working section floor, and treat that as the first point of traverse. By reading the dial gauge at that point, the height above the plate was determined, and subsequent increases in distance from the floor known to 0,01 mm.

The probe holder was held by the Disa traversing mechanism. This rig had a range of 100 mm, and was operated manually through a pinion drive, for slipless traversing. For increased accuracy, the dial gauge was mounted above the rig.

Apart from mean velocity, the turbulence intensity and power spectrum of the Working Section mainstream was measured. For this, the probe was mounted at a x-station, in the centre of the Working Section. Because the anemometer output is non-linear, it required processing. This was done with a Type 55D10 Lineariser. The linearised turbulent signal was integrated on a Type 55D35 R.M.S. Voltmeter, which gave $\sqrt{\overline{u'^2}}$. This unit, also made by Disa, had a voltage range of 0 - 300V. The integrator time constant could be set to 0,3, 1, 3, 10 and 30 seconds.

The calibration of the probes is discussed in Appendix C3.

To obtain the mean velocity in the boundary layer, a simple R.C. circuit was included in the circuit.

A Doric type DS100 digital voltmeter was used to measure the output from the anemometer.

6.4 The Energy Spectrum

Turbulent flow is so irregular that early investigators gave up hope of capturing the flow in universal expressions. In its very randomness lies the opportunity of using statistical methods to characterise the motion. Thus the time based mean velocity and thickness could be defined. The hot wire anemometer with its high frequency response, and oscilloscopes to record the output, made more sophisticated investigations possible. Thus the correlation function and energy spectrum are suitable means of presenting data.

$E_1(n)$ is defined such that $E_1(n)dn$ is the contribution to $\overline{u'^2}$ of the frequencies in the band n to $n + dn$.

$$\overline{u'^2} = \int_0^\infty E_1(n)dn \qquad \text{....... [6.4.1]}$$

As the frequency increases, $E_1(n)$ decreases rapidly because of the energy dissipation by viscous action.

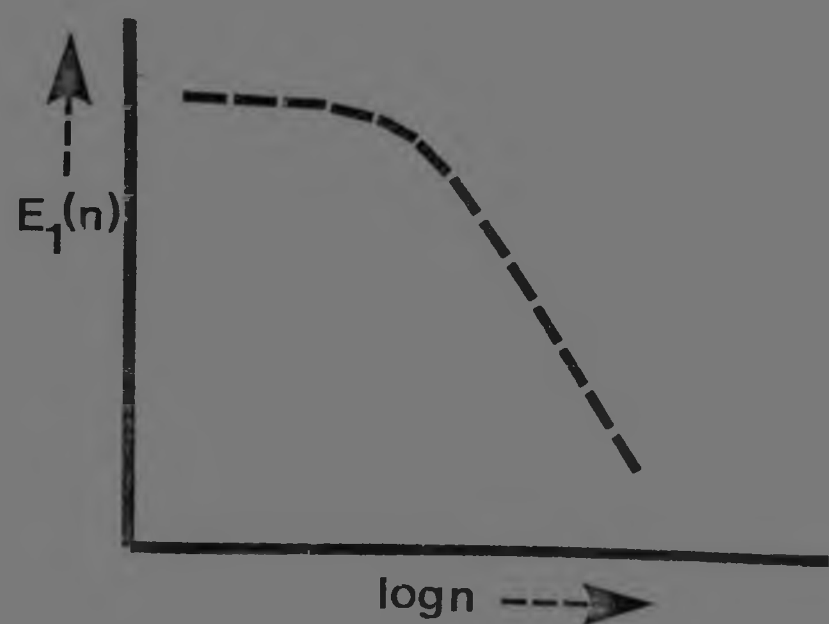

FIG 6.7 : SKETCH OF AN ENERGY SPECTRUM FOR TURBULENT FLOW

From Fig 6.7, $E_1(n)$ is c' ·ly greatest at low frequencies. The energy creating the rtices is drawn from the main-stream, and eventually ssipated through the action of viscosity.

Obtaining a plot of $E_1(n)$ vs n required the turbulent oscillations to be represented by a Fourier series, e.g.

$$f(n) = A_0 + A_1\cos\frac{\pi n}{L} + A_3\cos\frac{2\pi n}{L} + \ldots\ldots$$

and then plotting A_i vs n. Equipment employing a band pass filter could be used to generate the spectrum. For this work, a Hewlett-Packard Spectrum Analyser, model 3580A, was used in conjunction with the linearised output from the single sensor probe.

This unit produced a display on a screen, but a graphical output was obtained as well. The x-co-ordinate signal (frequency) was converted by a Hewlett-Packard Log Voltmeter/Converter, type 7562. Thus a log-log plot was produced directly on a Riken Denshi X-Y Recorder.

6.5 Experimental Procedure

It was found that the anemometer (in particular, the lineariser) was prone to drift with temperature. Before an experiment could be started, the lineariser was allowed a warm-up period of two hours (suggested by manufacturer). A linearised calibration curve was obtained, and the hot wire transducer transferred to the working section. It was essential that the anemometer was not switched off between calibration and test.

At the start of a test, valve V1 (see Fig 6.6) was opened, and the desired transpiration flow set.

After opening the by-pass, the fan was started. Once running, the trap door was closed, and the baffle at the fan inlet set for the required air velocity in the working section. This was checked with a pitot tube in the entry length. The free stream temperature was monitored, and once steady it was assumed that the wind tunnel had reached operating conditions. Ten to fifteen minutes was usually required for steady state to be attained.

The hot wire transducer was then positioned at X1, y=1, and the anemometer switched on. The anemometer output required about two minutes to settle, during which time the parameters required for measuring the secondary flow rate were noted. These were : pressure drop across the orifice plate, and the upstream static pressure and temperature, Δh, p_1 and t_1 respectively.

V_{LIN} was read on the DVM, and y on the dial gauge, and then the hot wire was moved to the next y point. This was continued to the end of the velocity traverse. Finally the centre line velocity was measured, which was assumed to be the local U_∞, and the free stream temperature, t_2.

The traversing rig was shifted to X2, and the transducer was traversed to y=1. The entire operation was repeated. Velocity profiles were measured at X1, X2, X3 and X4.

Special care was taken to seal the plenum chamber. Prestik was used at the porous plate edges, to ensure that the secondary flow did pass through the porous plate, and not form jets at the edges. This was more important when testing the A grade plate, which had very low porosity.

TABLE 6.1 : x-co-ordinate positions

Position denoted by :-	Distance from leading edge (mm)
X1	780
X2	856
X3	945
X4	1045

CHAPTER 7

PRESENTATION AND DISCUSSION OF RESULTS

7.1 Introduction

This chapter is divided into three main sections : the proving of the tunnel, the experimental results and the computer runs.

A spanwise velocity traverse is presented, and some difficulties with regard to the tunnel are discussed. In the first part, turbulence intensity and the spectrum analysis are given.

Secondly, the velocity traverses are shown in the popular non-dimensional form, u/u_e vs y/θ. Graphs containing information more compactly are given to illustrate trends when the lower porous surface was partially blocked. The bilog plotting technique of Black and Sarnecki (1959) is used to show the development of the profile with injection ratio, and also to compare the present results with those of Mickley and Davis (1956). The possibility of a new two-parameter family of curves is discussed, which appear to be independent of $u_w{}^*$ and F.

Plots obtained from the computer runs are included in the third section. Comparing these results with experimental work proved more problematic than was expected. For low injection ratio, it was possible to compare one of the profiles with that of Mickley and Davis (1959).

7.2 Initial Tests

7.2.1 Transverse velocity profile

The transverse velocity profile was measured to ensure that two dimensional flow was approximated at the centre line. The transducer was fixed at a particular value of y and x. The traversing rig was moved across the tunnel, taking readings at various intervals. One of these profiles is reproduced in Fig 7.2.

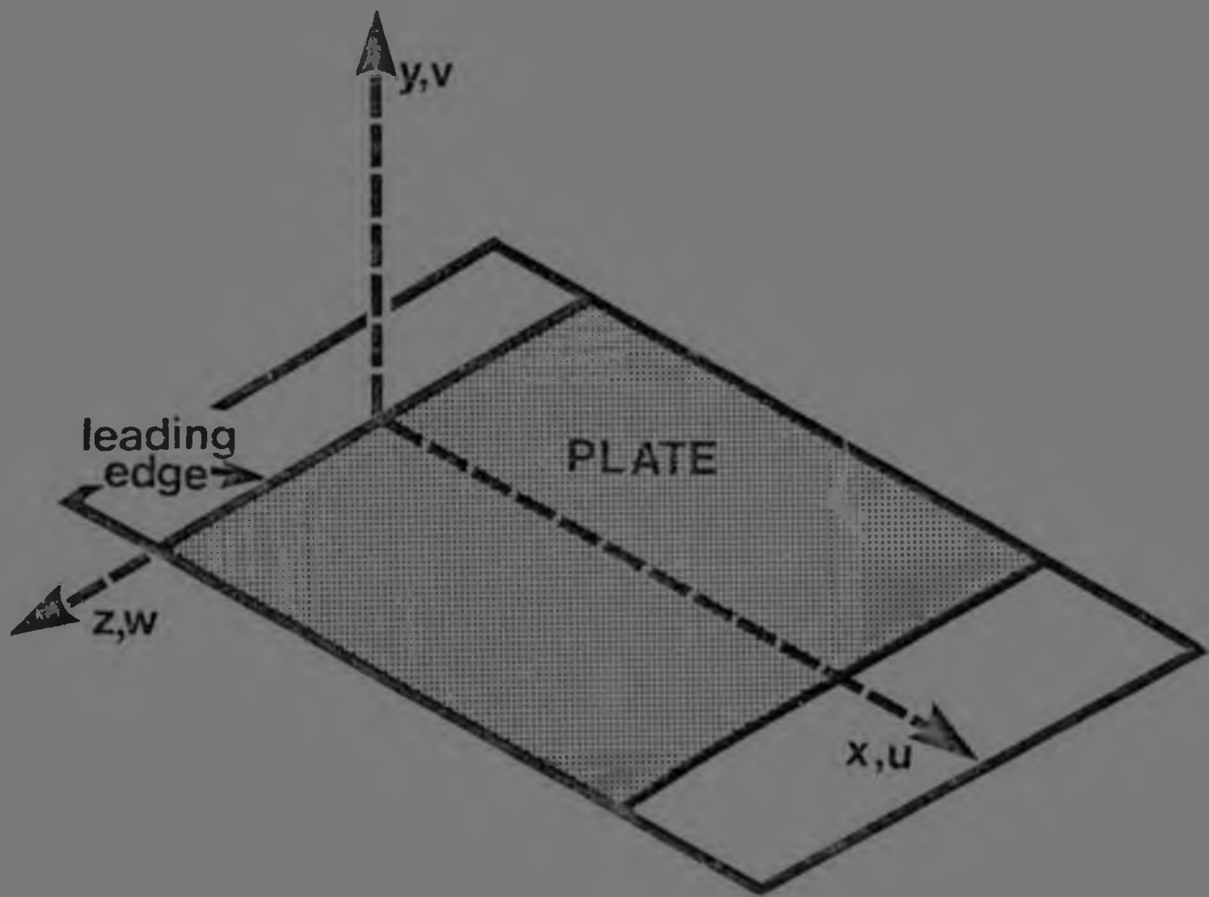

FIG 7.1 : DEFINITION OF AXES : THE X-AXIS LIES ON THE CENTRE-LINE OF THE WORKING SECTION, COINCIDING WITH THE FLOOR. Y WAS NORMAL TO THE FLOOR, AND Z TRANVERSELY COINCIDENT WITH THE FLOOR. THE VELOCITY COMPONENTS ARE INDICATED BY u, v AND w RESPECTIVELY

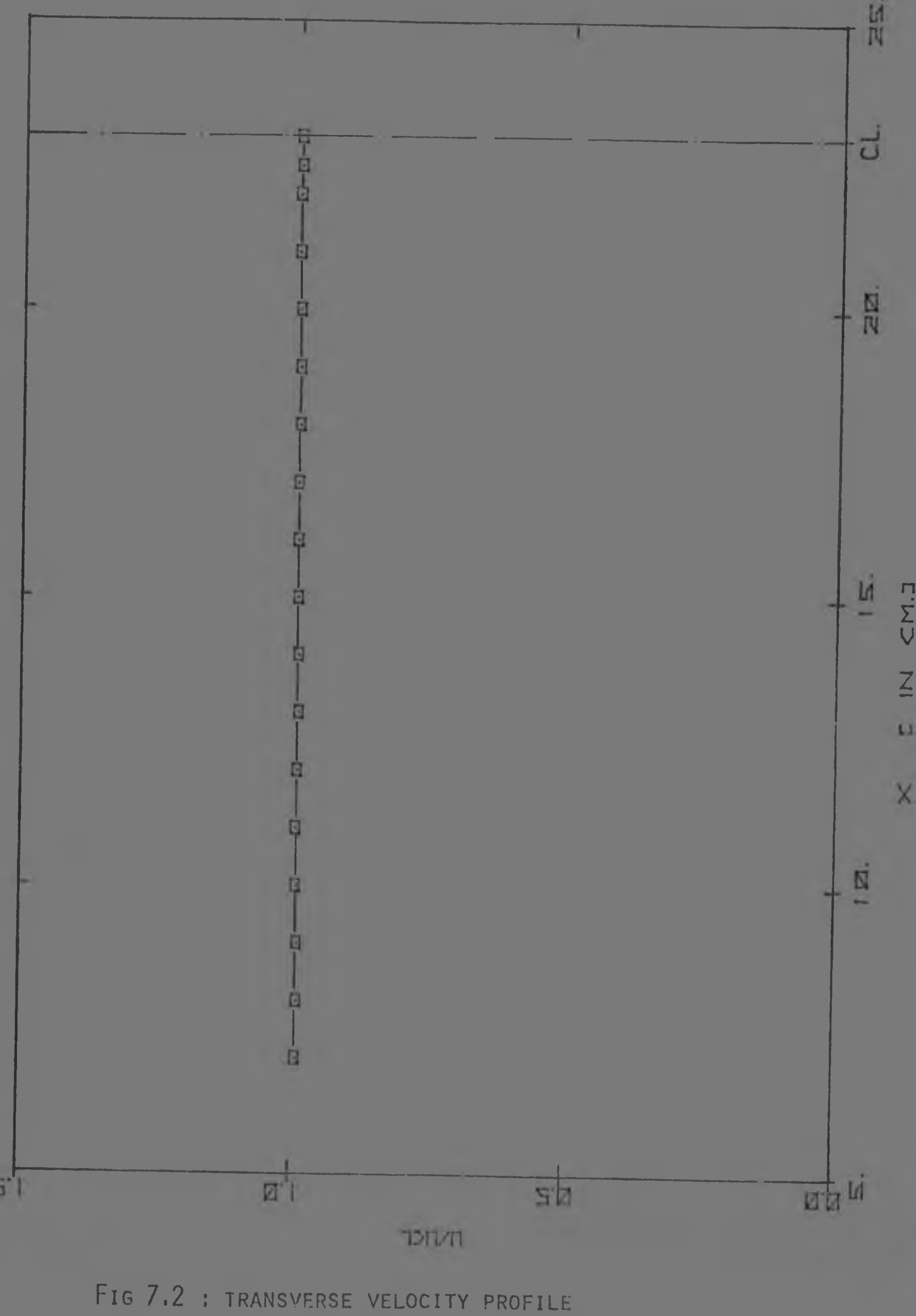

FIG 7.2 : TRANSVERSE VELOCITY PROFILE

The standard deviation of the transverse profile is s = 0,048 m/s, which is within the expected accuracy of the anemometer. The wind tunnel thus produced essentially two dimensional flow in the Working Section. All profiles were measured on the centre line, ie. at z = 0.

7.2.2 Turbulence and turbulence intensity

The turbulent fluctuations were observed by connecting the output of the lineariser to a Tektronix oscilloscope. This output was recorded and is presented in Figs 7.3 to 7.5. The first two traces show that the fluctuations were low in the main-stream. The trace depicted in Fig 7.5 was obtained by placing the probe 1 mm from the working section floor. It should be noted that the single wire sensor necessarily registered u', v' and a small percentage of w'. The probe was placed normal to the flow for all tests. Consideration of the results of Klebanoff, reproduced in Schlichting (1968), showed u', v' and w' all increased near the wall.

Figs 7.3 and 7.4 gave an indication of the autocorrelation, because the two superimposed traces were taken at time t and $t + \tau$. This was not quantified.

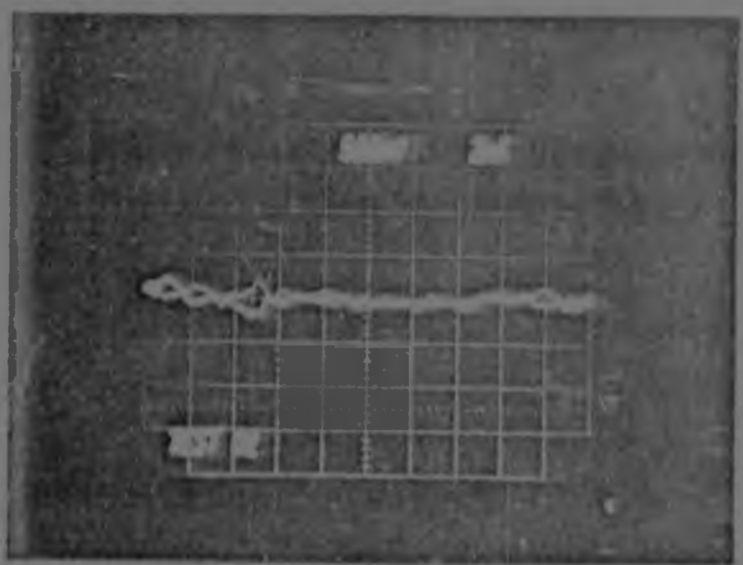

FIG 7.3 :
TWO TRACES FOR U_∞=16 m/s, PROBE AT CENTRE LINE

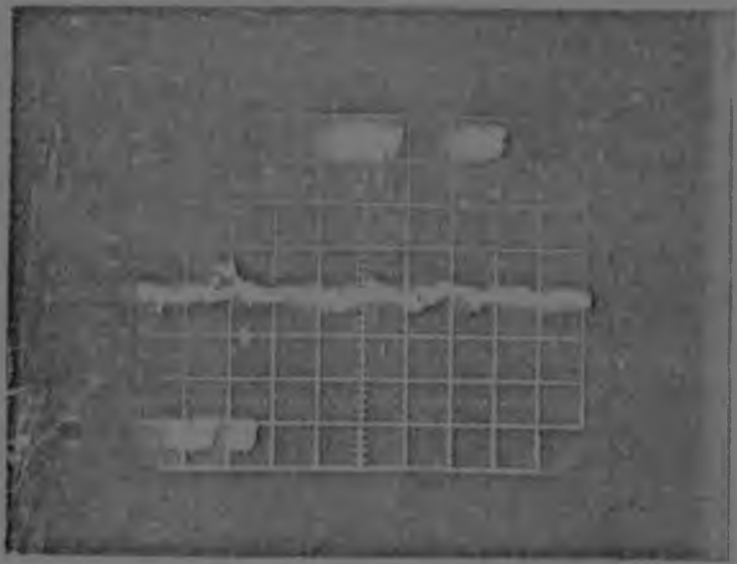

Fig 7.4 :
TWO TRACES FOR U_∞=12m/s, PROBE AT CENTRE LINE

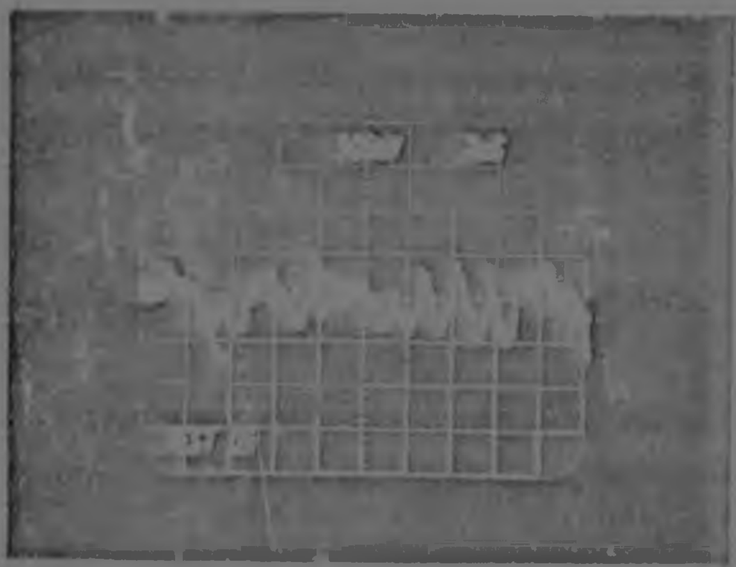

Fig 7.5 :
SINGLE TRACE FOR U_∞=16 m/s, PROBE 1 mm ABOVE SOLID WALL

A series of tests were performed to ascertain the turbulence intensity of the wind tunnel. By definition,

$$T = \sqrt{1/3(\overline{u'^2} + \overline{v'^2} + \overline{w'^2})}/U_\infty \qquad \text{.......} [7.2.1]$$

For isotropic flow (produced in wind tunnels behind a grid or screen) $\overline{u'^2} = \overline{v'^2} = \overline{w'^2}$, so for wind tunnels this equation becomes (Schlichting 1968)

$$T = \sqrt{\overline{u'^2}}/U_\infty \qquad \text{.......} [7.2.2]$$

The transducer was subject to u' and v'. Because w' was parallel to the sensor wire, this contribution should have been small. If $\overline{r'^2} = \overline{u'^2} + \overline{v'^2}$, then define a wind tunnel turbulence intensity

$$T = \sqrt{\tfrac{1}{2}\overline{r'^2}}/U_\infty \qquad \text{....... [7.2.3]}$$

The results of a number of runs at different velocities are given in Table 7.1. The integrator time constant was 10 sec. The probe was positioned at x = 800 mm, y = 112,5 mm, z = 0.

TABLE 7.1

Test	V_∞(volts)	U_∞(m/s)	$\sqrt{\overline{r'^2}}$(volts)	T%
A	3,190	15,359	0,891	0,59
B	2,558	12,335	0,640	0,53
C	2,191	10,579	0,504	0,49
D	1,835	8,876	0,457	0,53
E	1,392	6,756	0,368	0,56

U_∞ was varied by opening the by-pass. Considering Fig 7.6, it would be expected that T would have been lower had a more sophisticated method for decreasing U_∞ been employed. In the main test, this was done by closing the fan intake with a baffle plate. The increased angle of the trap door may explain why T dropped initially, but then increased in the last two tests.

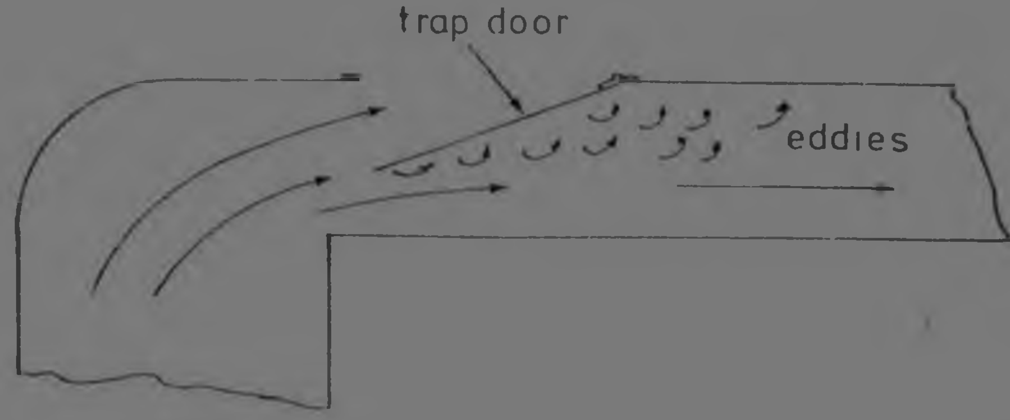

FIG 7.6 : DETAIL OF BY-PASS, SHOWING POSSIBLE EFFECTS OF OPENING THE TRAP DOOR

7.2.3 The energy spectrum

The energy spectrum was measured in tests A through E. The results are reproduced in Figs 7.7a to 7.7e. These are plots of log $E_1(n)$ vs log n. The inertial subrange was established ie. the portion of the curve which is fitted by the -5/3 law. This is a range in which vortices were neither generated or dissipated. It has been proposed that the large, low frequency eddies are formed by drawing energy from the main stream, creating the turbulent stresses. Because of the instability of the flow, smaller and smaller eddies appear until they are dissipated as heat (see Schlichting, 1968).

These plots show that a full spectral distribution of the energy of fluctuation was present in the tunnel, throughout the range of free stream velocities of interest.

In each spectrum the initial, eddy generating region can be seen. Furthermore, the function $E_1(n) \propto n^{-5/3}$ fitted the data in the inertial subrange. Noise from the anemometer and analyser disguised the high frequency range.

Fig 7.7b to Fig 7.7e show an energy bulge at high frequency. This occurred at approximately 6 and 10 Hz and is thought to have been caused by vortex shedding behind the trap door. This was discussed in section 7.2.2 in relation to Fig 7.6, and resulted in the discontinued use of the by-pass as a method of flow control.

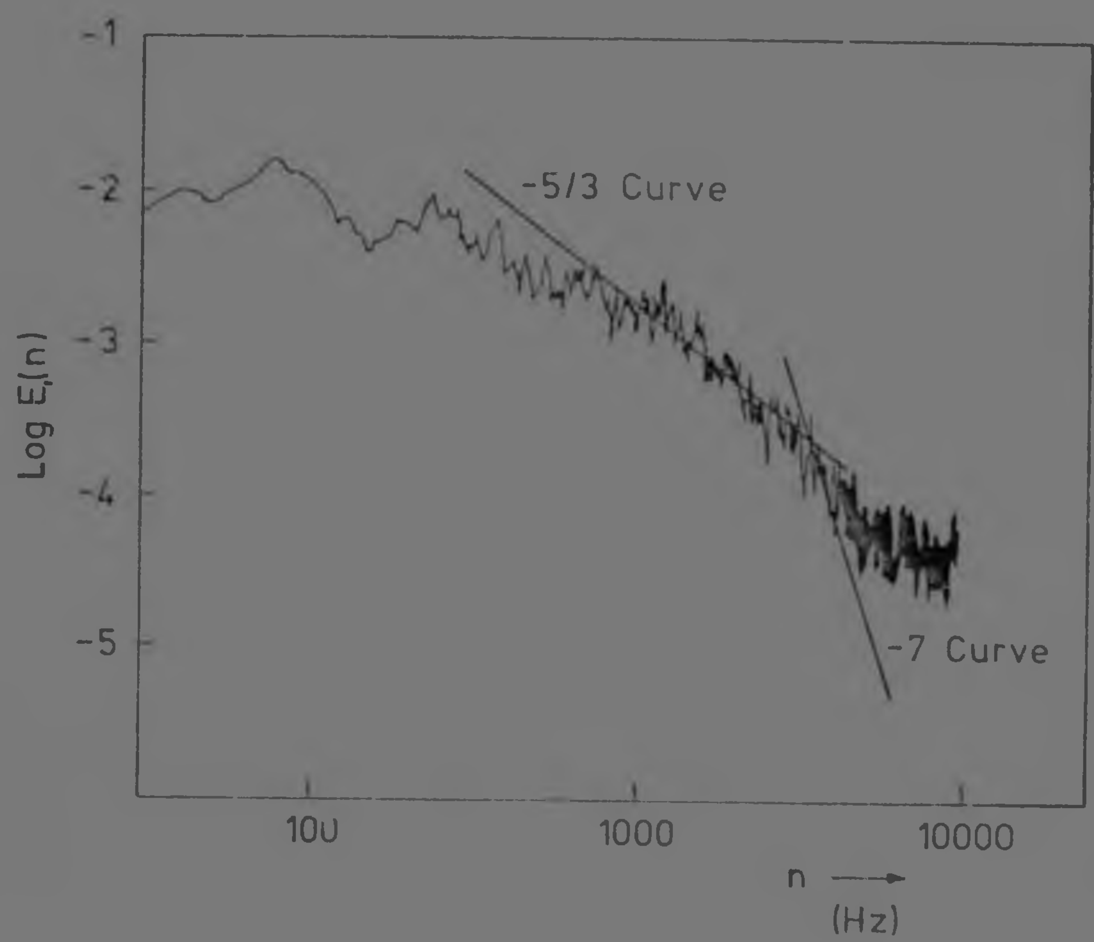

FIG 7.7a : TEST A

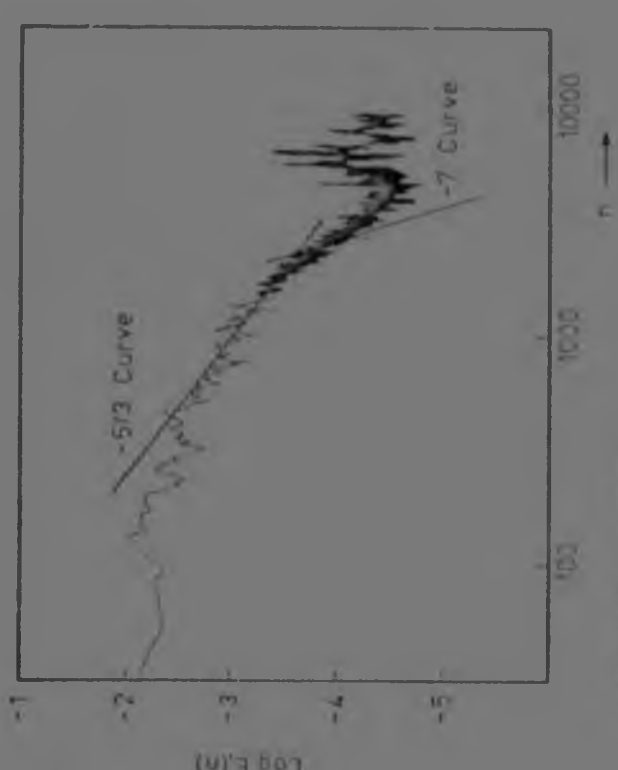

Fig 7.7b : TEST B

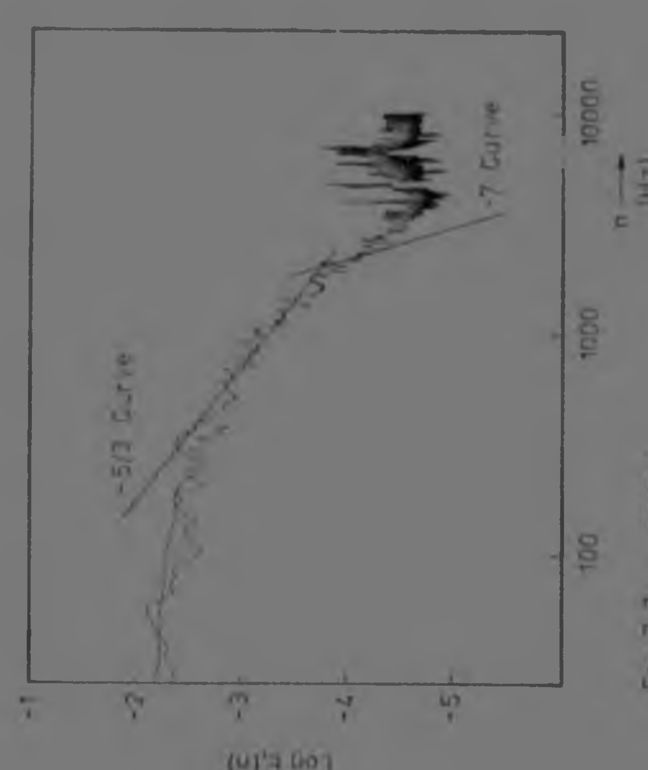

Fig 7.7c : TEST C

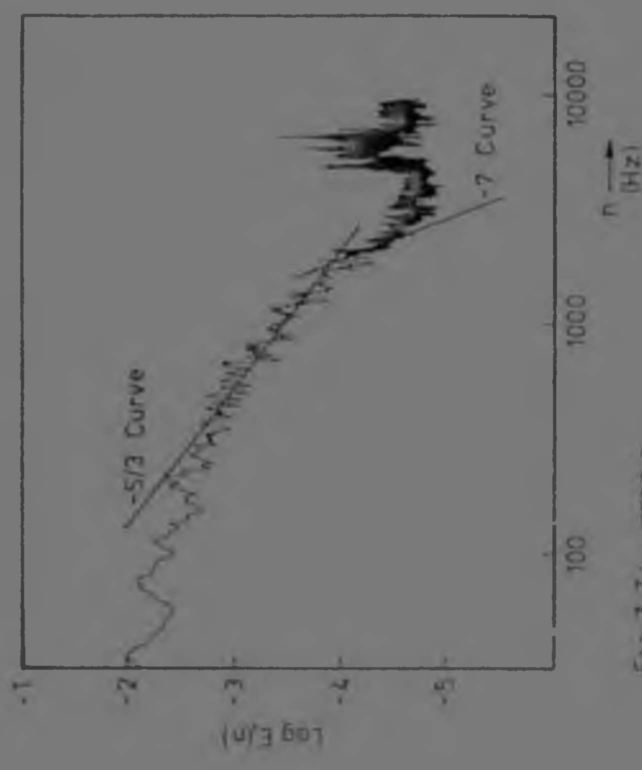

Fig 7.7d : TEST D

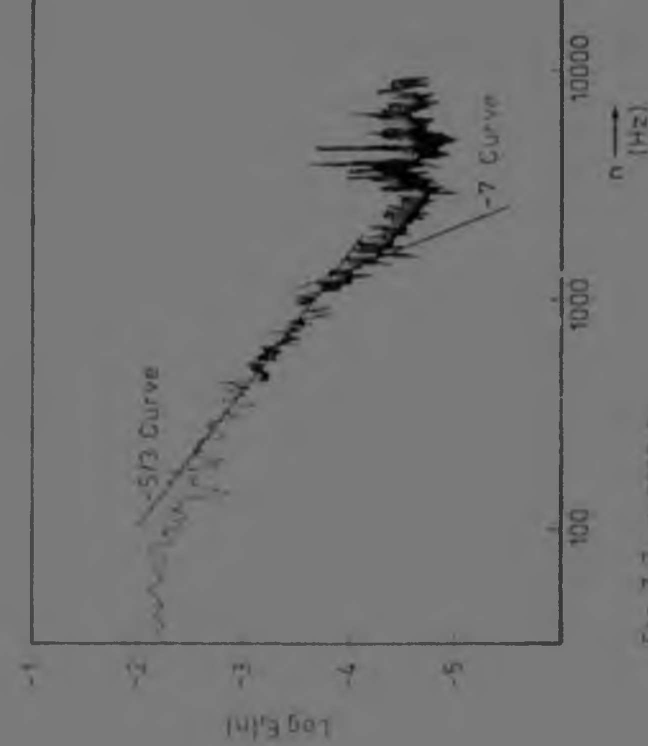

Fig 7.7e : TEST E

7.3 Experimental Work

In each test, the profile at a station just prior to the start of the porous section was measured. This station was denoted X1. The shape factor for these profiles ranged between 1,27 and 1,30, which is the correct value of H for the unblown, zero pressure gradient turbulent boundary layer. The simple Blasius profile was found not to fit the experimental data. Theoretical curves were constructed from Thompson's two parameter family (Thompson, 1965). Near the wall agreement was not as good, but it should be borne in mind that the given families had to be interpolated to obtain the approximate value of y/θ. Two of these profiles are given in Figs 7.8 and 7.9.

The reason for this result is thought to be as follows. The contraction was in the XZ-plane, and thus the transverse profile was exceptionally flat. In the YZ-plane, the tunnel height remained constant from the start of the diffuser. This resulted in a very thick boundary layer arriving in the entry section. It was therefore not possible to draw the entire boundary layer off through the boundary layer bleed. Almost duct flow resulted, rather than the ideal "flat plate in a free stream". Large δ did have the advantage that the y measurement was less critical, and the rate of change of u with y was much smaller. The disturbance of a transducer in the shear layer was thus decreased.

It must be pointed out that numerous investigators used a pitot tube for measuring the velocity. Because this device is larger than the miniature hot wire transducer used in the present work, the disturbance to the flow in the region of measurement was necessarily greater. In addition, it was found to be essential that the pitot tube was exposed to the correct static pressure. When a pitot tube was used in the tunnel running at a pressure slightly higher than atmospheric, incorrect readings were obtained. The same comments would apply to a pitot rake.

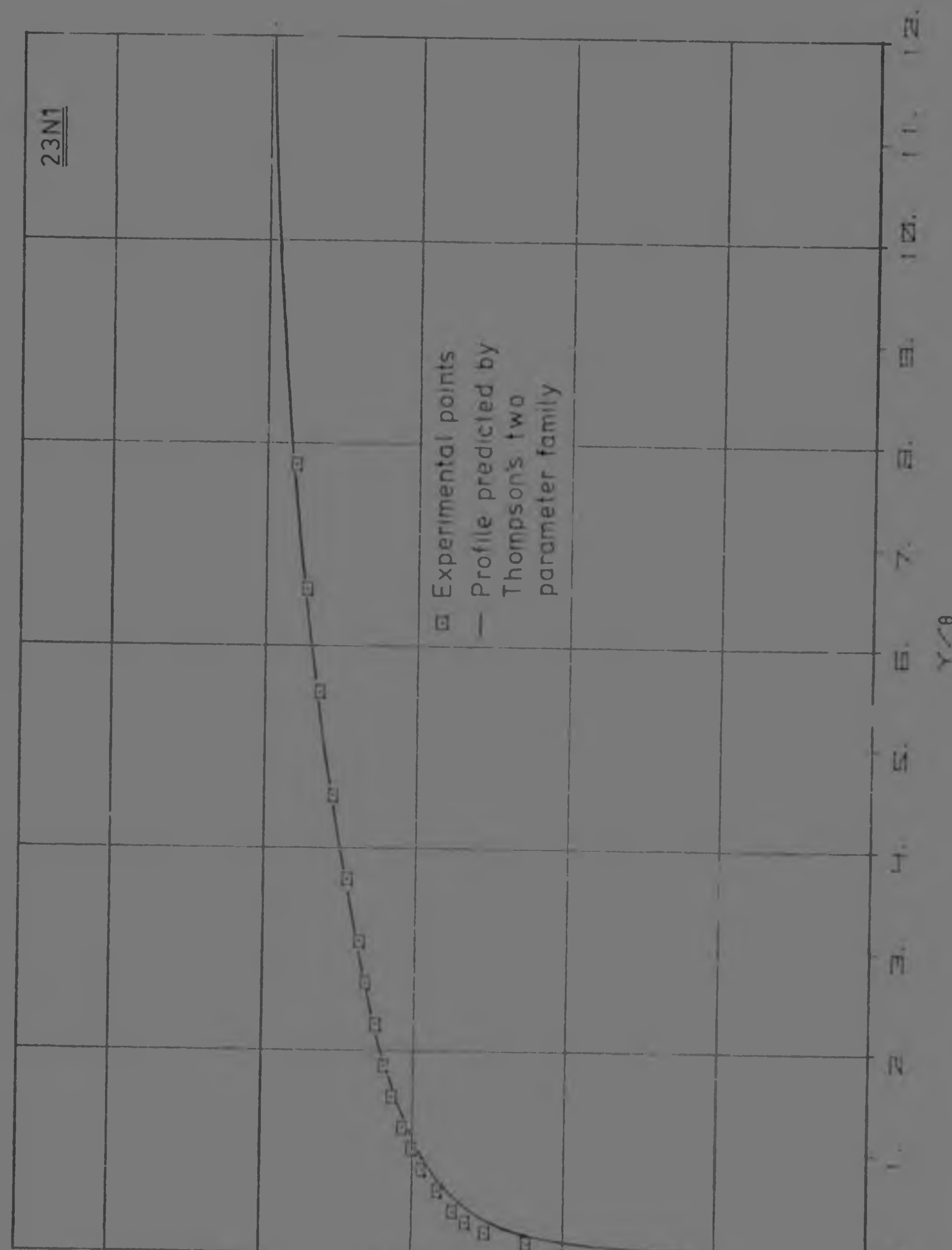

FIG 7.8 : EXPERIMENTAL PROFILE MEASURED ON THE SOLID PLATE FOR TEST 23N1

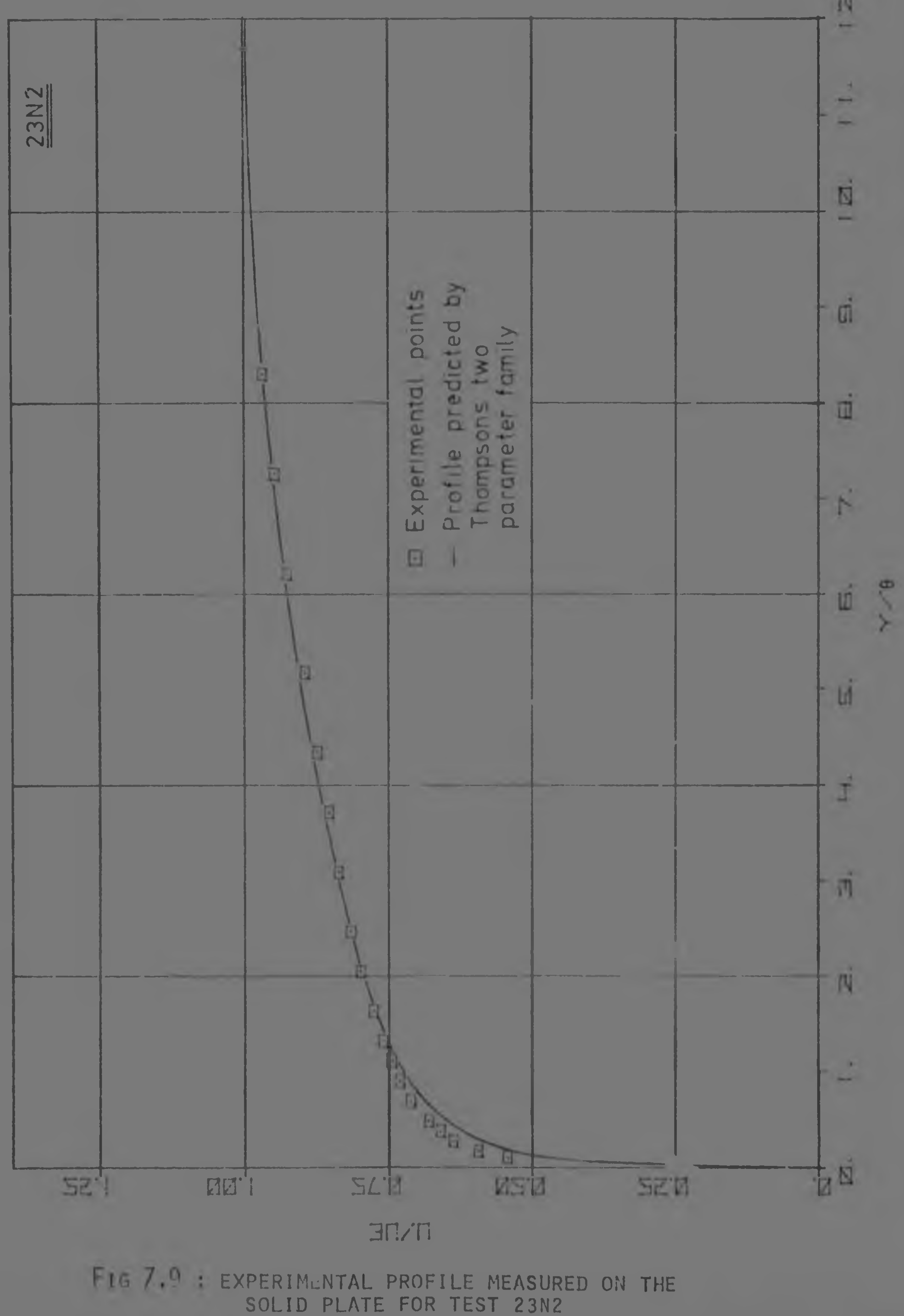

FIG 7.9 : EXPERIMENTAL PROFILE MEASURED ON THE SOLID PLATE FOR TEST 23N2

Great care was taken in measuring the profiles for the present work. The hot wire was re-calibrated for each run. A difficulty always present when using hot wires is that the transducer is not to be traversed to $y = 0$ to determine that point. A shield was attached to the probe holder with a broken probe. This probe was traversed down until it just touched the floor, and the dial gauge reading noted. The calibrated transducer was then placed in the holder. Since the two transducers were of equal length, y was calculated.

The results were processed on an IBM 370 computer, which printed and plotted the data.

7.3.1 The experimental results

The basic data is given in Appendix E1. The non-dimensionalized plots for all the tests, and baseline data for each test are given in Fig 7.10. The velocity profiles are followed by graphs of shape factor, H vs physical x for the maximum main stream velocity tests, and the tests with blockage. In these graphs the change in profile caused by blockage is indicated.

In the tables of Fig 7.10 the heading includes the date, e.g. test 28S1 was run on the 28th September, the 1 stands for the number of the test. The second part indicates the grade of porous plate, then F_{av} x 10^{-3} and finally the main stream velocity, U_{CL}, in m/s. Re_x was based on the distance measured from the leading edge. These were X1 = 0,7805 m, X2 = 0,8565, X3 = 0,9455, X4 = 1,0455. X1 was on the solid plate, X2 = 18,66%, X3 = 49,13% and X4 = 83,36% along the porous plate. F_{av} was based on the inlet velocity.

In Fig 7.10, the symbols used for plotting are :- A for X1, + for X2, X for X3 and ⊙ for X4. The co-ordinates used are u/u_e vs y/θ. This is preferred to y/δ, because δ is less easy to determine.

The first five tests were run at maximum free stream velocity, with an E grade plate installed. Results are shown in Fig 7.10a to e. In all tests, the increasing 'laminarisation' with x is evident, the curves coinciding at approximately y/θ = 3,5→5, this value increasing with F. For high F, the profiles at X3 and X4 tended to be very similar (see Fig 7.10e).

In test 28S3, the profile at X3 showed a strange step. This profile was obtained with probe No.4, which appeared to be faulty, and was not used again. Although not broken, the calibration curve for this probe changed during a test. Possibly a particle in the stream collided with the transducer.

Five tests, very similar to the above, were performed on the E grade plate, but at the reduced free stream velocity; U_∞ = 13 m/s at the Working Section inlet. Very similar results to the first set were obtained, but results were not identical. This indicates that the profile was not only dependent on F. Clearly Re_x was different, but probably also the effective roughness, k^+. These tests are shown in Fig 7.10f to j.

Tests 07O1 and 06O1 were also run over the unblocked E grade plate, but at U_{CL} = 9 m/s, and therefore at much lower Re_x.

The next set of tests, 09N1 to 11N2, shown in Fig 7.10m to q, were a repeat of the first 12 runs, but on the C grade, unblocked plate. The results were very similar, but showed a shift which was thought to have resulted from the change in roughness, k^+.

Finally, a sample test was performed, using the A grade plate. Because of the low porosity, and the resultant high pressure drop, great care was taken when sealing the plenum chamber. Powder metallurgy was used to make this plate, whereas the

PLOT OF U/UE VS Y/TTA

RUN 28-9 1,4-7,3-17

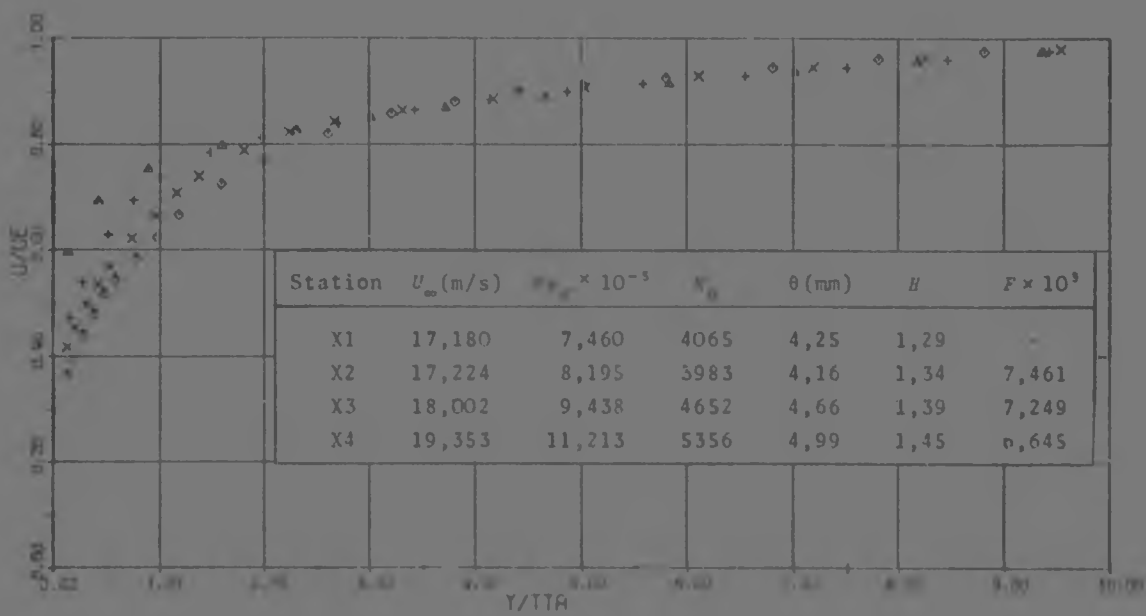

Station	U_∞ (m/s)	$Re_x \times 10^{-5}$	R_θ	θ (mm)	H	$F \times 10^3$
X1	17,180	7,460	4065	4,25	1,29	–
X2	17,224	8,195	3983	4,16	1,34	7,461
X3	18,002	9,438	4652	4,66	1,39	7,249
X4	19,353	11,213	5356	4,99	1,45	6,645

FIG 7.10a : TEST 28S1 E-7,58-17

PLOT OF U/UE VS Y/TTA

RUN 30-8/1,4-10,1-18

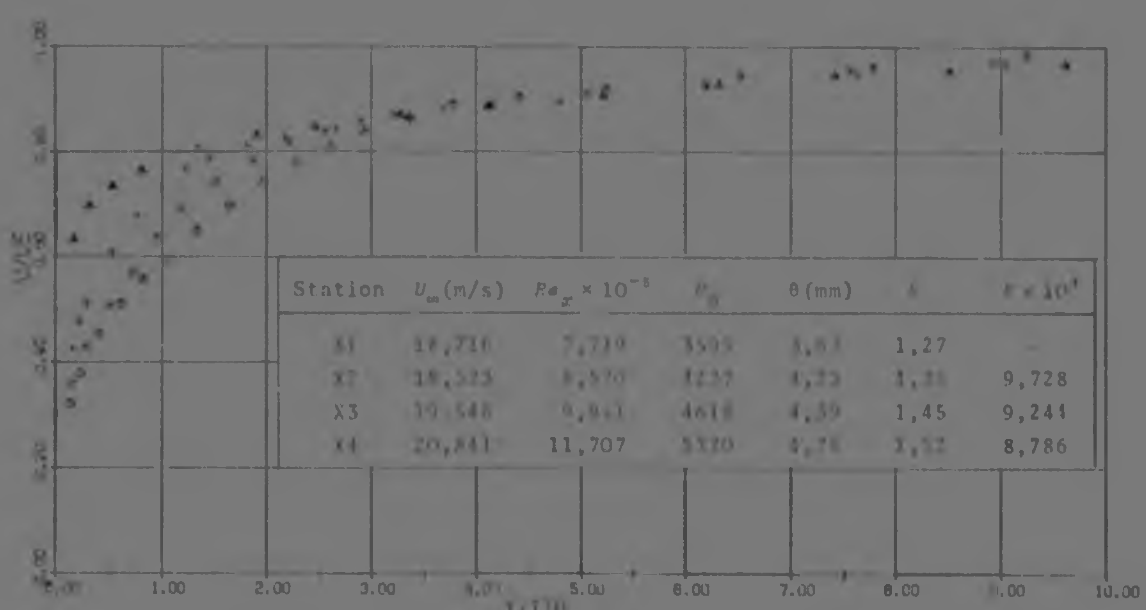

Station	U_∞ (m/s)	$Re_x \times 10^{-5}$	R_θ	θ (mm)	H	$F \times 10^3$
X1	[illegible]	[illegible]	[illegible]	[illegible]	1,27	–
X2	[illegible]	[illegible]	[illegible]	[illegible]	[illegible]	9,728
X3	[illegible]	[illegible]	4618	4,39	1,45	9,241
X4	20,841	11,707	[illegible]	[illegible]	[illegible]	8,786

FIG 7.10b : TEST 28S1 E-7,58-17

PLOT OF U/UE VS Y/TTA

RUN 28-8/5.8-12.0-17

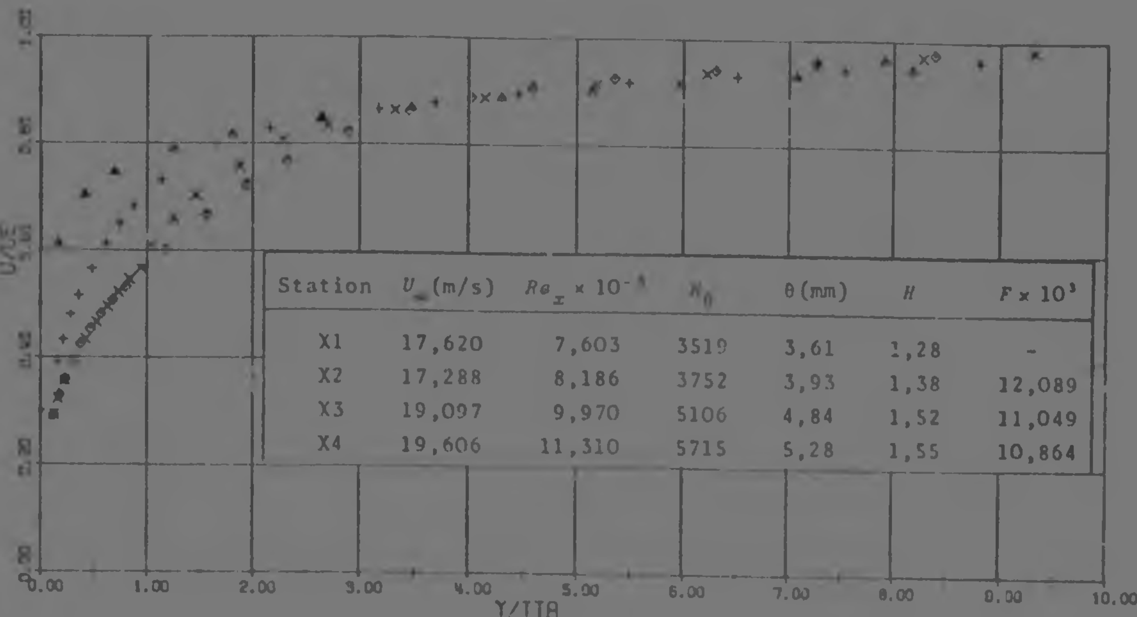

Station	U_∞ (m/s)	$Re_x \times 10^{-5}$	R_θ	θ (mm)	H	$F \times 10^3$
X1	17,620	7,603	3519	3,61	1,28	-
X2	17,288	8,186	3752	3,93	1,38	12,089
X3	19,097	9,970	5106	4,84	1,52	11,049
X4	19,606	11,310	5715	5,28	1,55	10,864

FIG 7.10c : TEST 28S2 E-12,41-17

PLOT OF U/UE VS Y/TTA

RUN 30-8/5.8-12.1-17

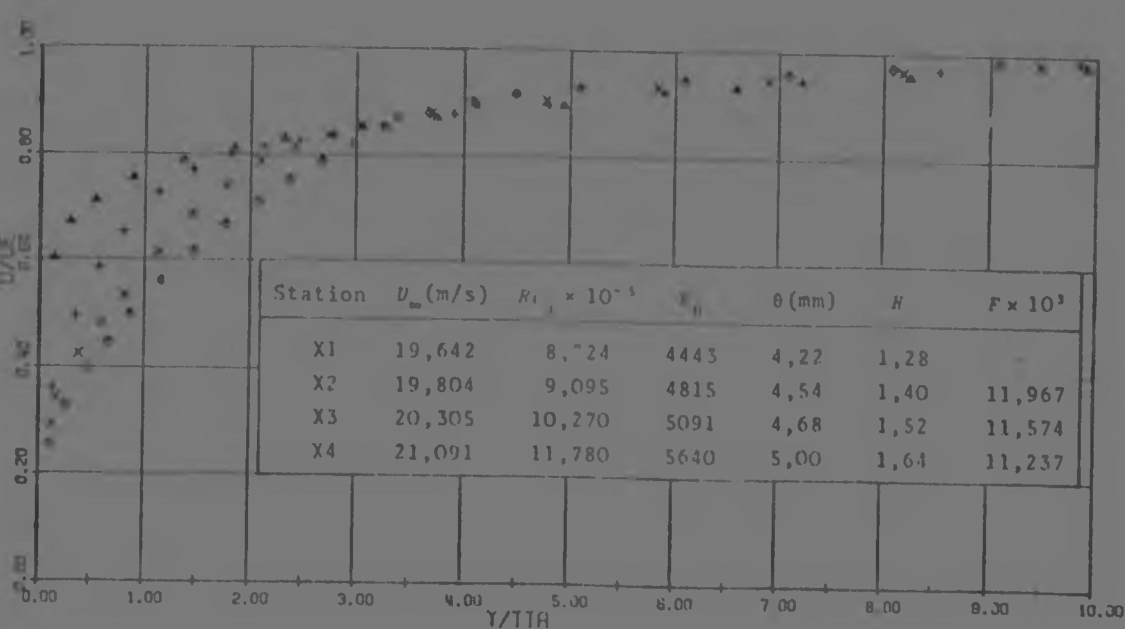

Station	U_∞ (m/s)	$Re_x \times 10^{-5}$	R_θ	θ (mm)	H	$F \times 10^3$
X1	19,642	8,724	4443	4,22	1,28	-
X2	19,804	9,095	4815	4,54	1,40	11,967
X3	20,305	10,270	5091	4,68	1,52	11,574
X4	21,091	11,780	5640	5,00	1,64	11,237

FIG 7.10d : TEST 30S2 E-13,79-17

PLOT OF U/UE VS Y/TTA

RUN 28-9/9,12-15,5-17

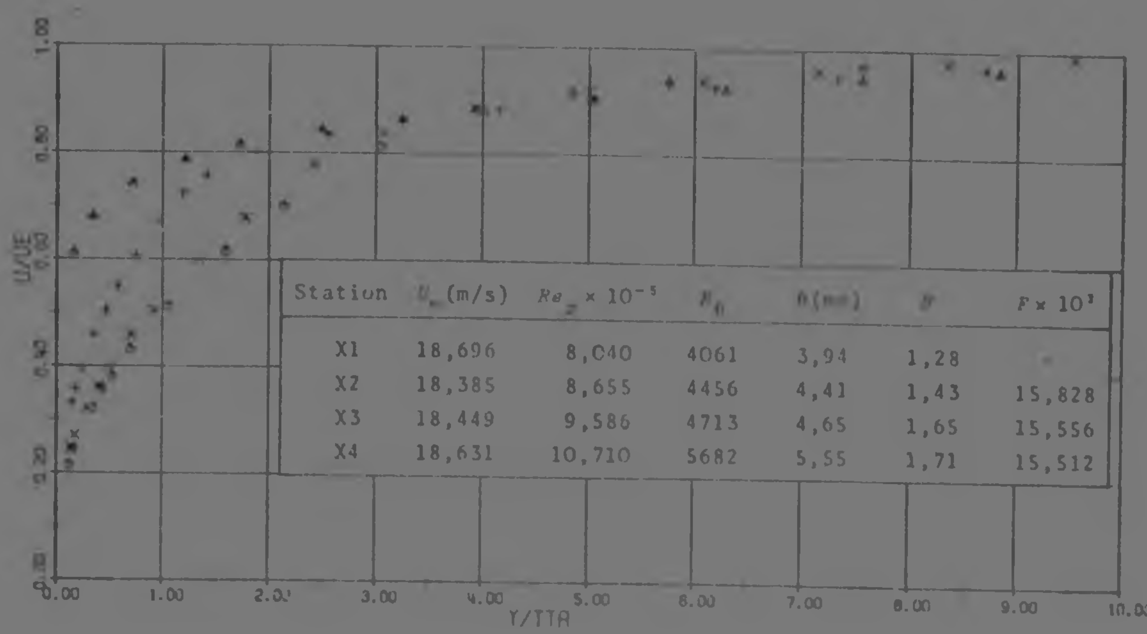

Station	U_∞ (m/s)	$Re_x \times 10^{-5}$	R_θ	θ (mm)	H	$F \times 10^3$
X1	18,696	8,040	4061	3,94	1,28	-
X2	18,385	8,655	4456	4,41	1,43	15,828
X3	18,449	9,586	4713	4,65	1,65	15,556
X4	18,631	10,710	5682	5,55	1,71	15,512

FIG 7.10e : TEST 2853 E-17,0-17

PLOT OF U/UE VS Y/TTA

RUN 03-10/5,8-5,3-13

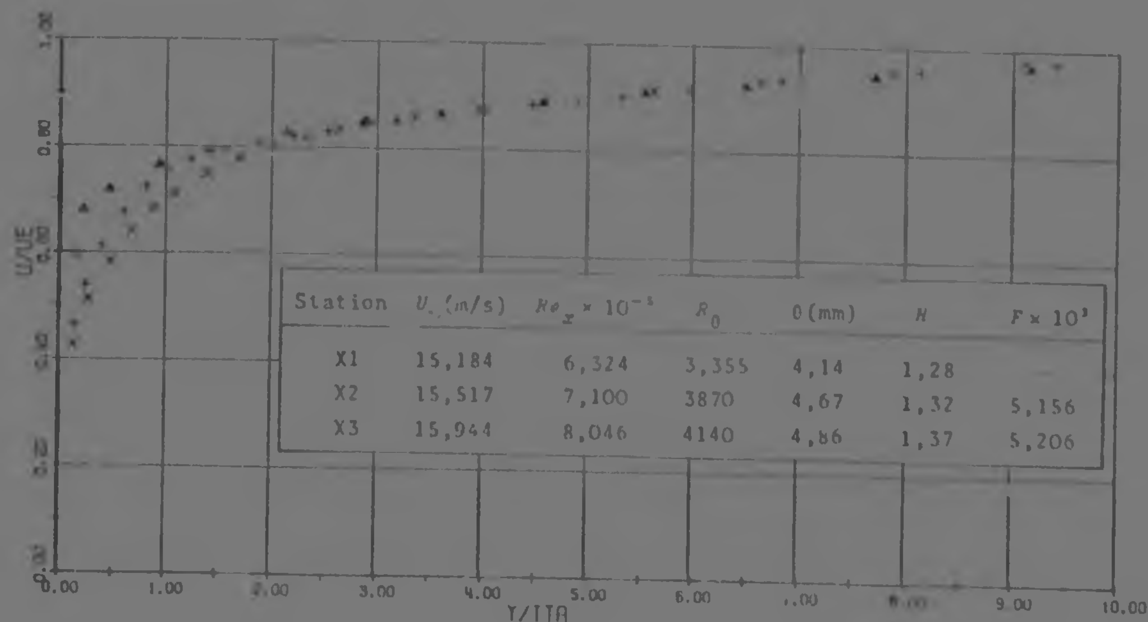

Station	U_∞ (m/s)	$Re_x \times 10^{-5}$	R_θ	θ (mm)	H	$F \times 10^3$
X1	15,184	6,324	3,355	4,14	1,28	
X2	15,517	7,100	3870	4,67	1,32	5,156
X3	15,944	8,046	4140	4,86	1,37	5,206

FIG 7.10f : TEST 0302 E-6,43-13

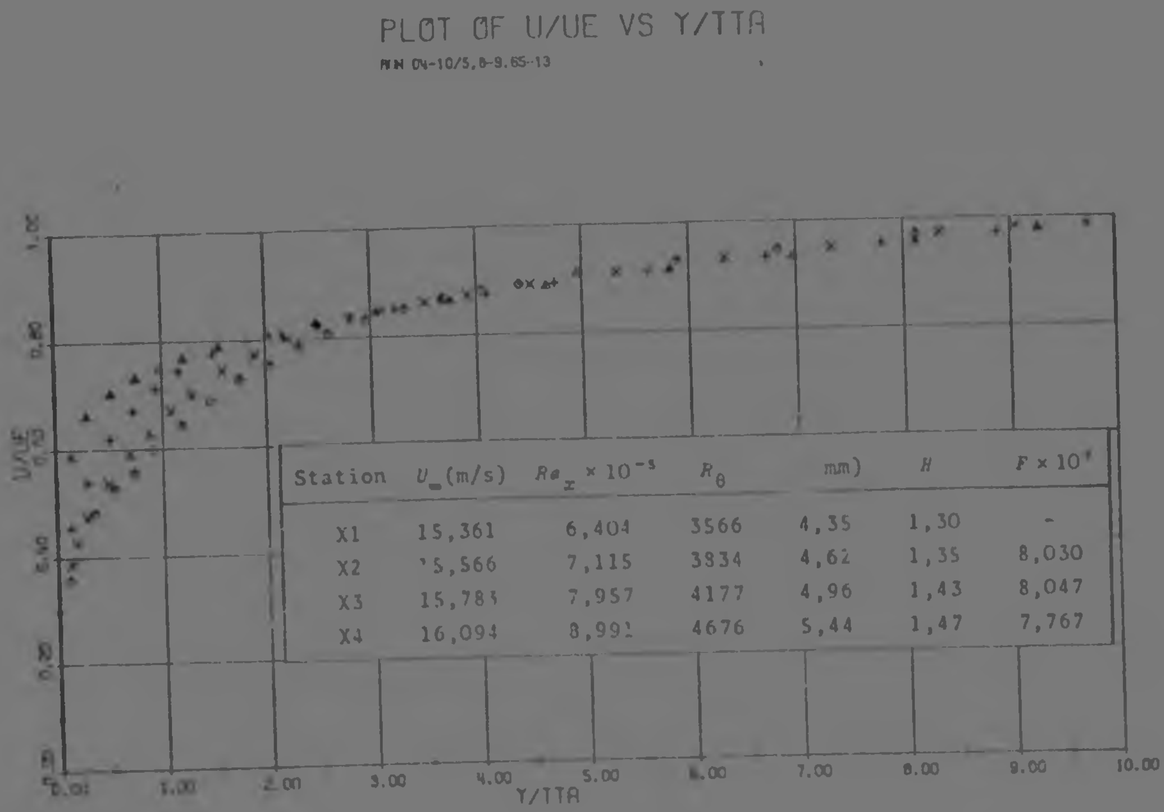

Station	U_∞ (m/s)	$Re_x \times 10^{-5}$	R_θ	θ(mm)	H	$F \times 10$
X1	15,361	6,404	3566	4,35	1,30	-
X2	?5,566	7,115	3834	4,62	1,35	8,030
X3	15,783	7,957	4177	4,96	1,43	8,047
X4	16,094	8,991	4676	5,44	1,47	7,767

FIG 7.10g : TEST 0402 E-9,69-13

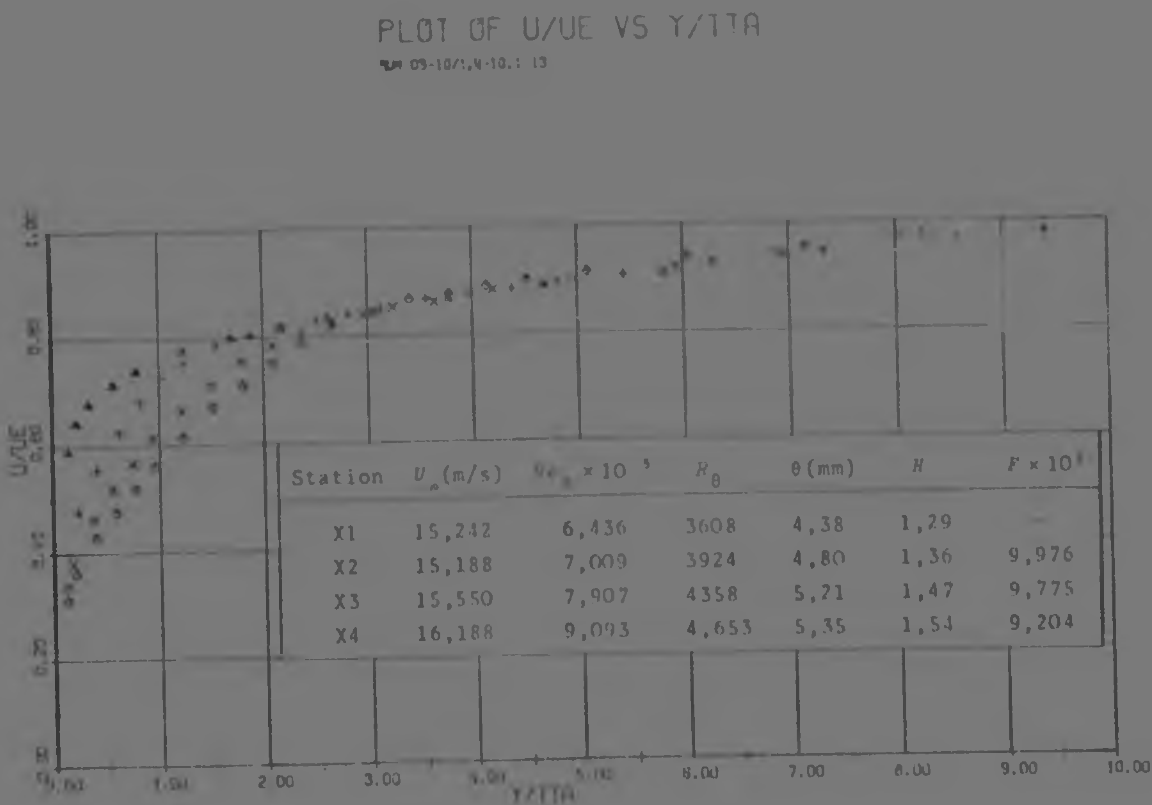

Station	U_∞ (m/s)	$Re_x \times 10^{-5}$	R_θ	θ(mm)	H	$F \times 10$
X1	15,242	6,436	3608	4,38	1,29	-
X2	15,188	7,009	3924	4,80	1,36	9,976
X3	15,550	7,907	4358	5,21	1,47	9,775
X4	16,188	9,093	4,653	5,35	1,54	9,204

FIG 7.10h : TEST 0301 E-11,59-13

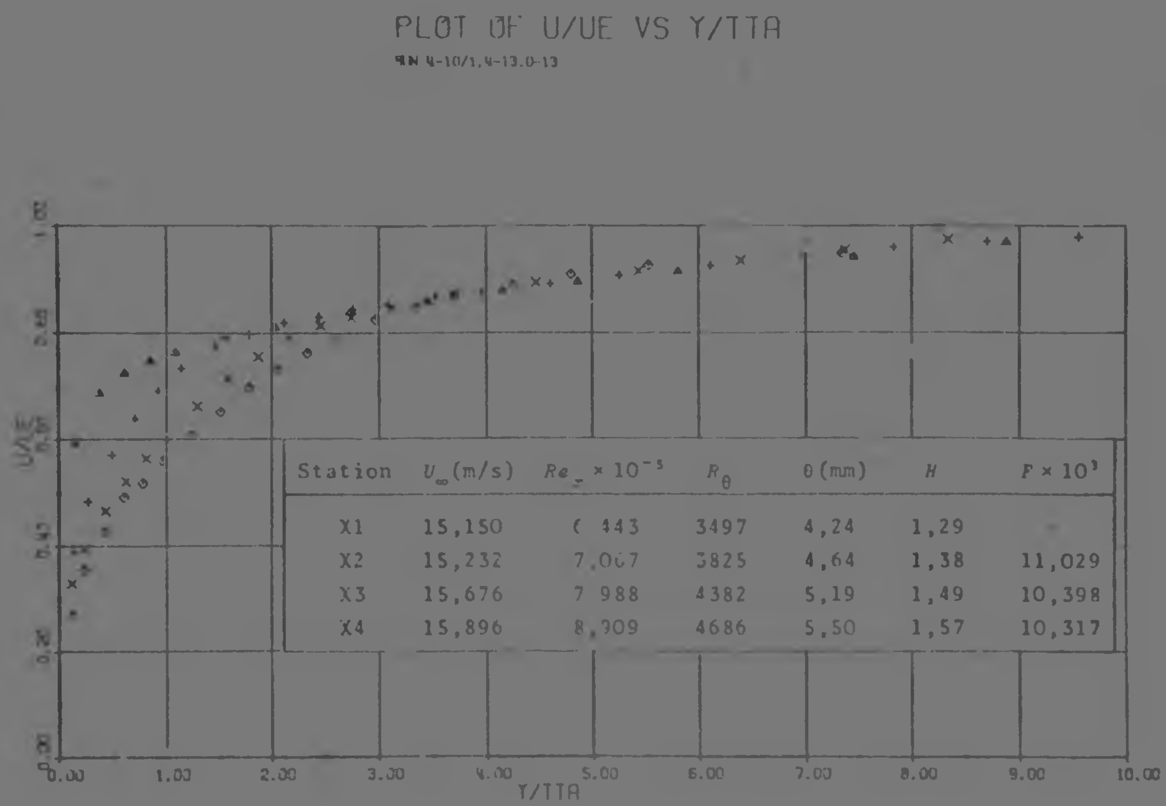

Station	U_∞(m/s)	$Re_x \times 10^{-5}$	R_θ	θ(mm)	H	$F \times 10^3$
X1	15,150	(443	3497	4,24	1,29	
X2	15,232	7,067	3825	4,64	1,38	11,029
X3	15,676	7 988	4382	5,19	1,49	10,398
X4	15,896	8,309	4686	5,50	1,57	10,317

FIG 7.10i : 0401 E-12,79-13

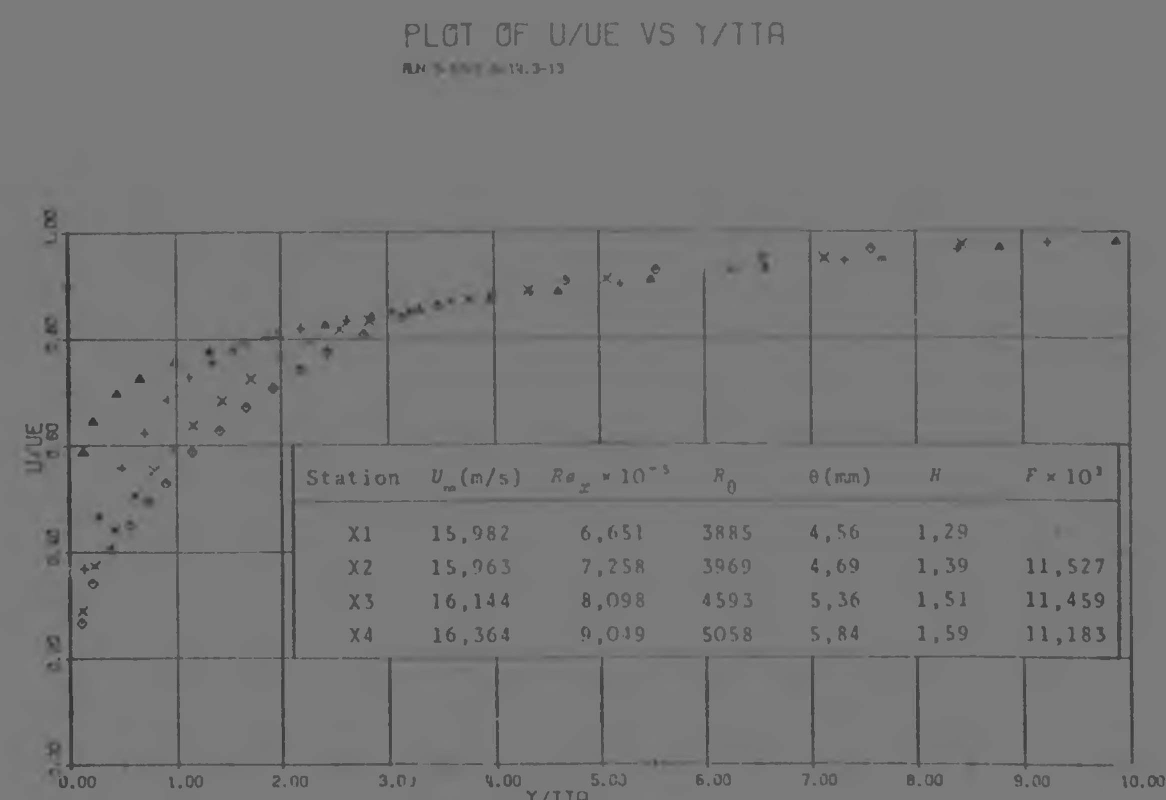

Station	U_∞(m/s)	$Re_x \times 10^{-5}$	R_θ	θ(mm)	H	$F \times 10^3$
X1	15,982	6,651	3885	4,56	1,29	
X2	15,963	7,258	3969	4,69	1,39	11,527
X3	16,144	8,098	4593	5,36	1,51	11,459
X4	16,364	9,049	5058	5,84	1,59	11,183

FIG 7.10j : TEST 0501 E-14,13-13

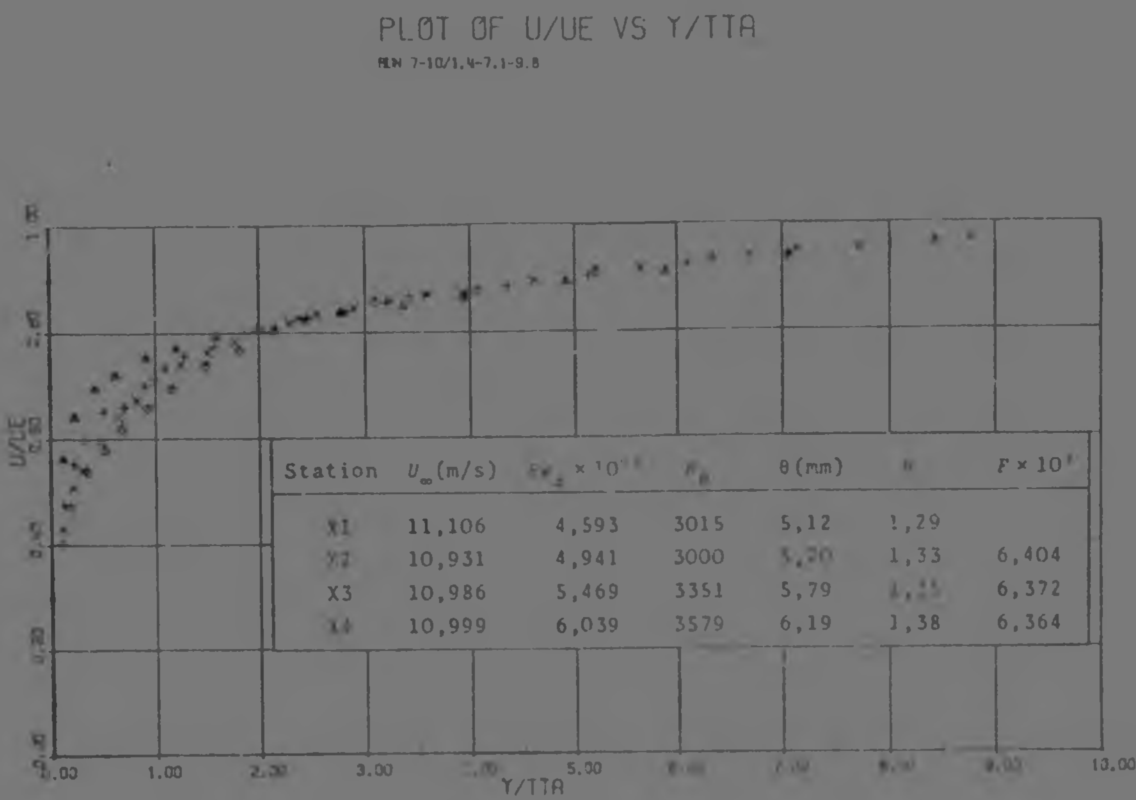

Station	U_∞(m/s)	$Re_x \times 10$[illegible]	R_θ	θ(mm)	[illegible]	$F \times 10$[illegible]
X1	11,106	4,593	3015	5,12	1,29	
X2	10,931	4,941	3000	[illegible]	1,33	6,404
X3	10,986	5,469	3351	5,79	[illegible]	6,372
X4	10,999	6,039	3579	6,19	1,38	6,364

FIG 7.10k : TEST 0701 E-7,74-9

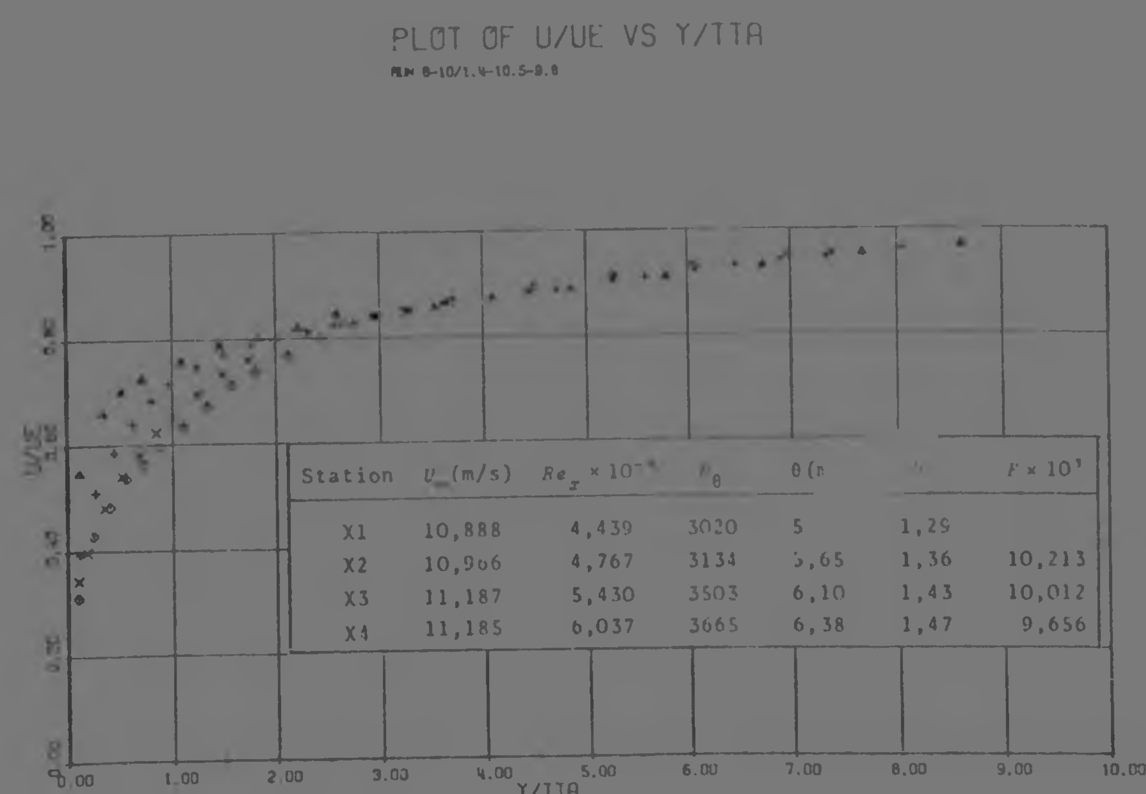

Station	U_∞(m/s)	$Re_x \times 10^{-6}$	R_θ	θ(r	[illegible]	$F \times 10$[illegible]
X1	10,888	4,439	3020	5	1,29	
X2	10,966	4,767	3134	5,65	1,36	10,213
X3	11,187	5,430	3503	6,10	1,43	10,012
X4	11,185	6,037	3665	6,38	1,47	9,656

FIG 7.101 : TEST 0601 E-12,03-9

PLOT OF U/UE VS Y/TTA

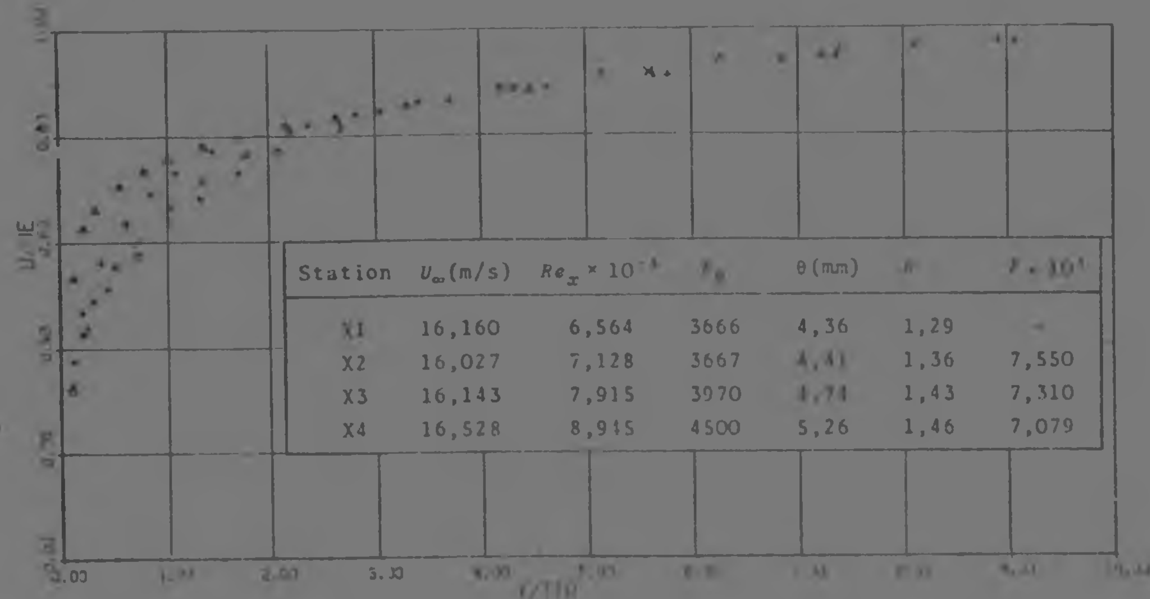

Station	U_∞(m/s)	$Re_x \times 10^{-5}$	R_θ	θ (mm)	H	F × 10^3
X1	16,160	6,564	3666	4,36	1,29	-
X2	16,027	7,128	3667	4,41	1,36	7,550
X3	16,143	7,915	3970	4,74	1,43	7,310
X4	16,528	8,945	4500	5,26	1,46	7,079

FIG 7.10m : TEST 09N1 C-7,07-17

PLOT OF U/UE VS Y/TTA

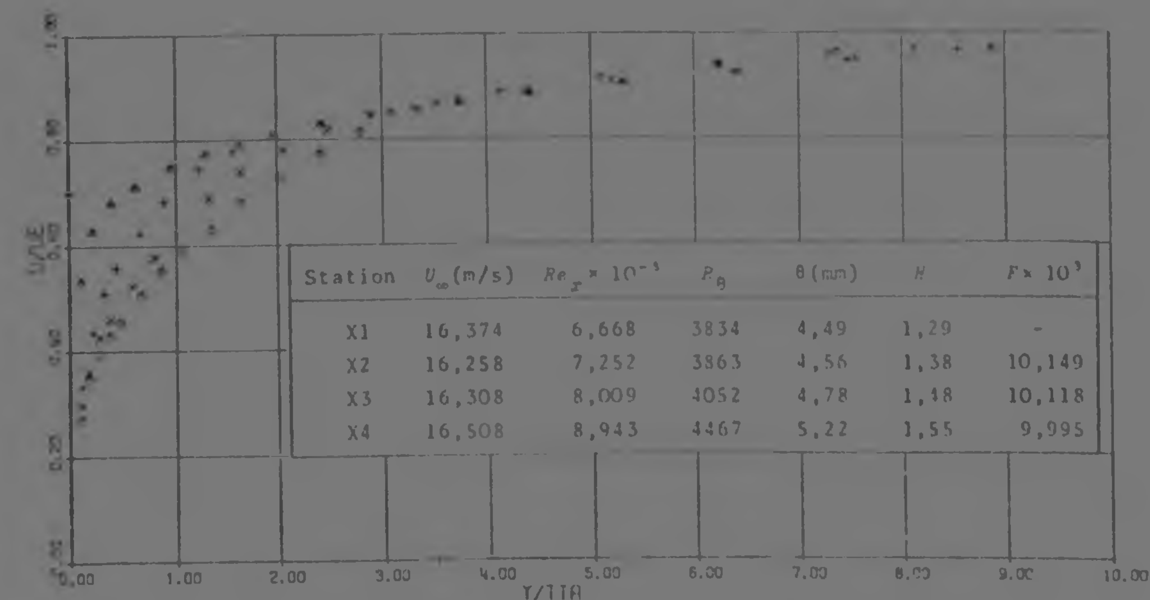

Station	U_∞(m/s)	$Re_x \times 10^{-5}$	R_θ	θ (mm)	H	F × 10^3
X1	16,374	6,668	3834	4,49	1,29	-
X2	16,258	7,252	3863	4,56	1,38	10,149
X3	16,308	8,009	4052	4,78	1,48	10,118
X4	16,508	8,943	4467	5,22	1,55	9,995

FIG 7 10n : TEST 10N1 C-9,82-17

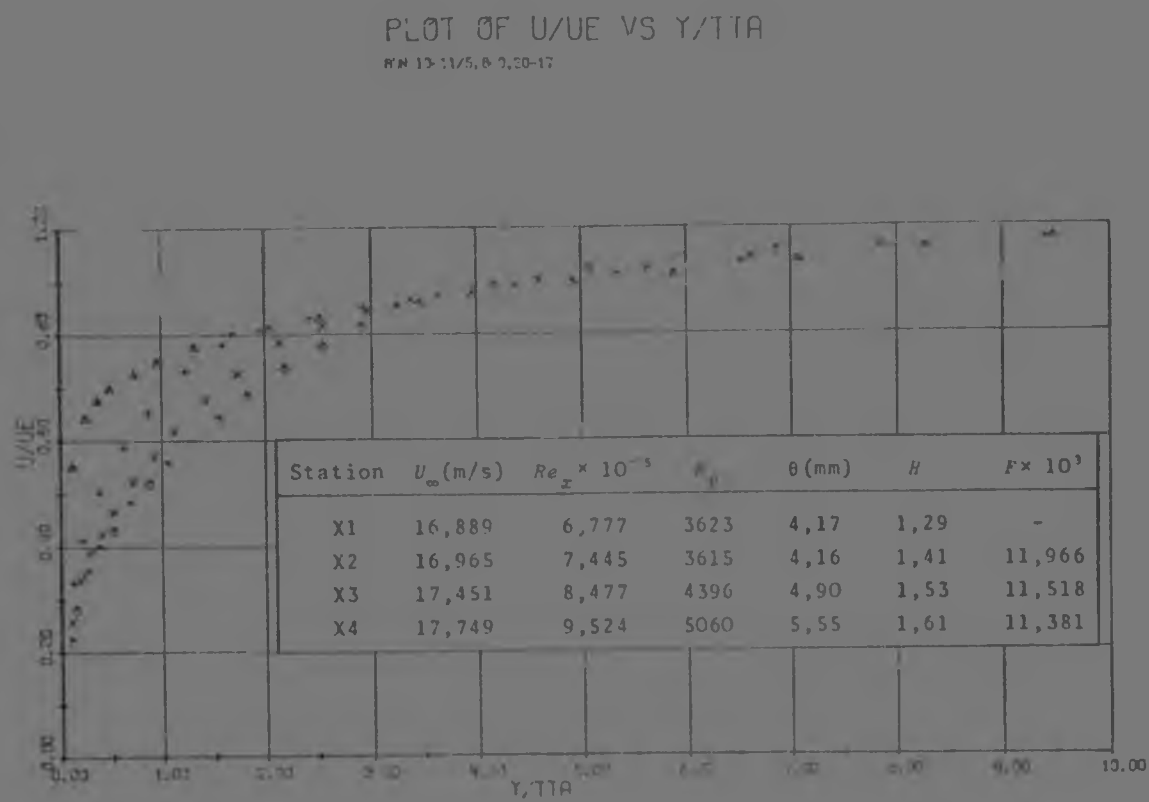

Station	U_∞(m/s)	$Re_x \times 10^{-5}$	R_θ	θ(mm)	H	$F \times 10^3$
X1	16,889	6,777	3623	4,17	1,29	-
X2	16,965	7,445	3615	4,16	1,41	11,966
X3	17,451	8,477	4396	4,90	1,53	11,518
X4	17,749	9,524	5060	5,55	1,61	11,381

FIG 7.10o : TEST 10N2 C-12,02-17

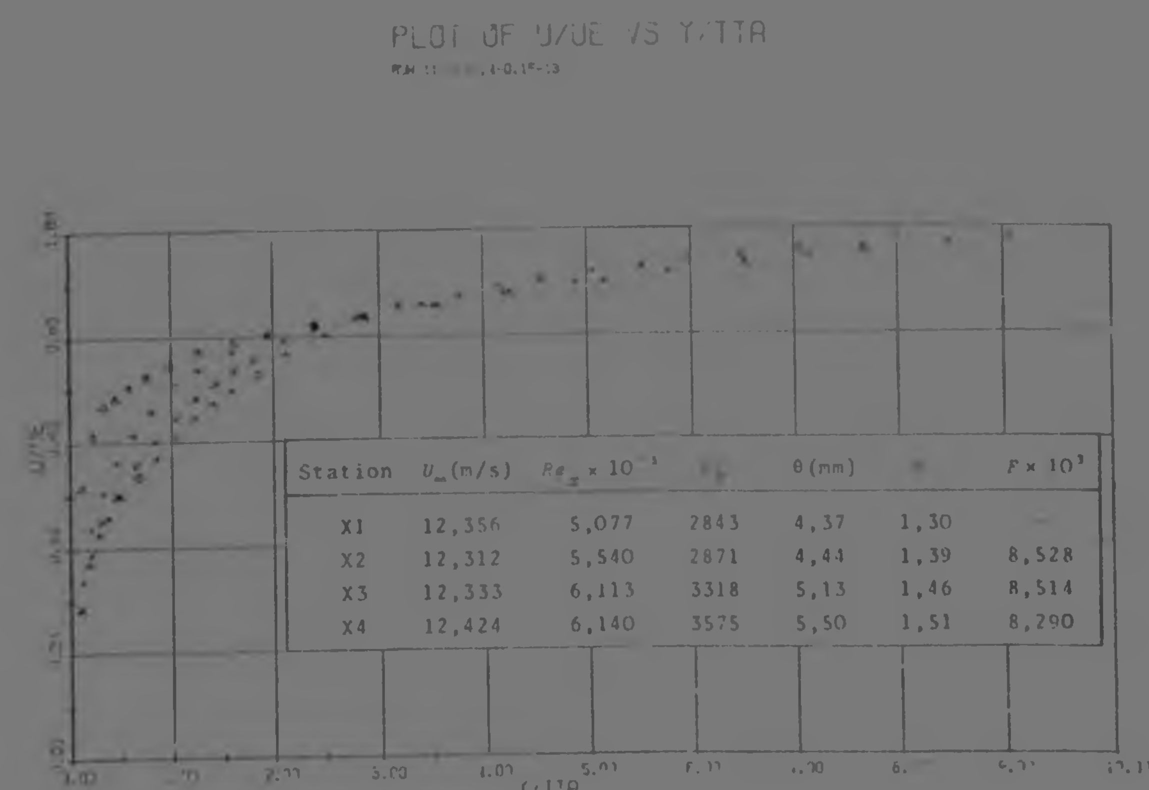

Station	U_∞(m/s)	$Re_x \times 10^{-5}$	R_θ	θ(mm)	H	$F \times 10^3$
X1	12,356	5,077	2843	4,37	1,30	-
X2	12,312	5,540	2871	4,44	1,39	8,528
X3	12,333	6,113	3318	5,13	1,46	8,514
X4	12,424	6,140	3575	5,50	1,51	8,290

FIG 7.10p : TEST 11N1 C-8,39-13

PLOT OF U/UE VS Y/TTA

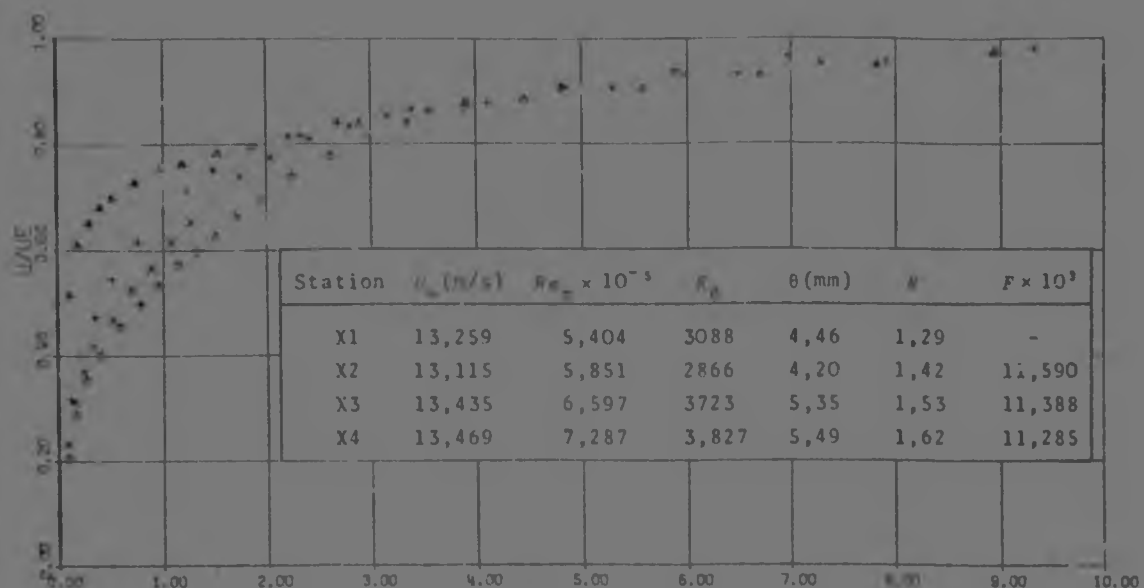

Station	U_∞ (m/s)	$Re_x \times 10^{-5}$	R_θ	θ (mm)	H	$F \times 10^3$
X1	13,259	5,404	3088	4,46	1,29	-
X2	13,115	5,851	2866	4,20	1,42	11,590
X3	13,435	6,597	3723	5,35	1,53	11,388
X4	13,469	7,287	3,827	5,49	1,62	11,285

FIG 7.10q : TEST 11N2 C-12,22-13

PLOT OF U/UE VS Y/TTA

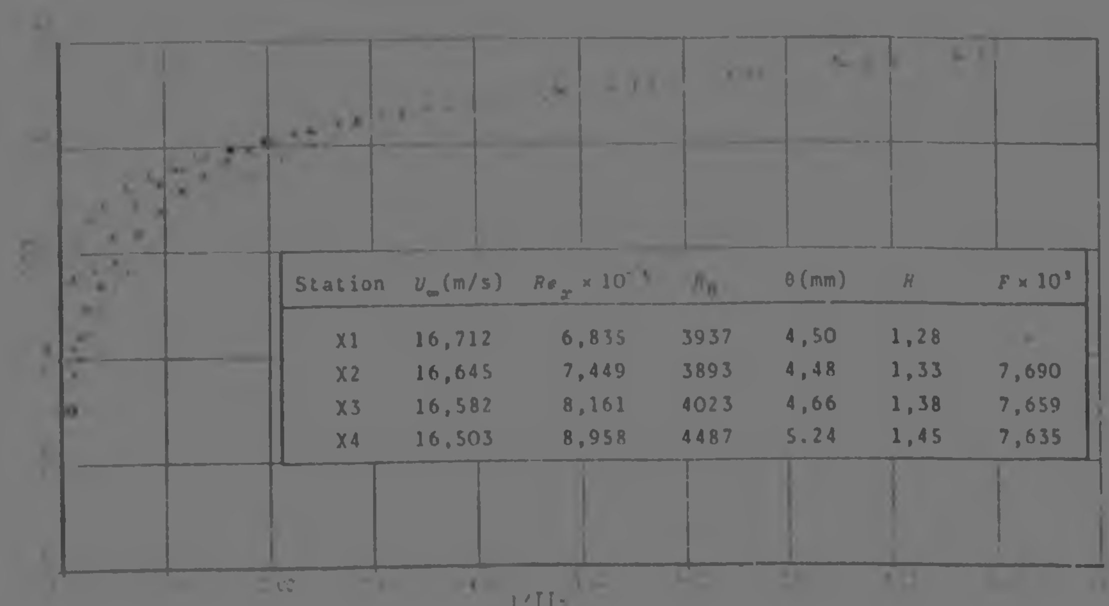

Station	U_∞ (m/s)	$Re_x \times 10^{-5}$	R_θ	θ (mm)	H	$F \times 10^3$
X1	16,712	6,835	3937	4,50	1,28	-
X2	16,645	7,449	3893	4,48	1,33	7,690
X3	16,582	8,161	4023	4,66	1,38	7,659
X4	16,503	8,958	4487	5.24	1,45	7,635

FIG 7.10r : TEST 16N1 A-7,55-17

PLOT OF U/UE VS Y/TTA

RUN 23 11/1,4-8-17E

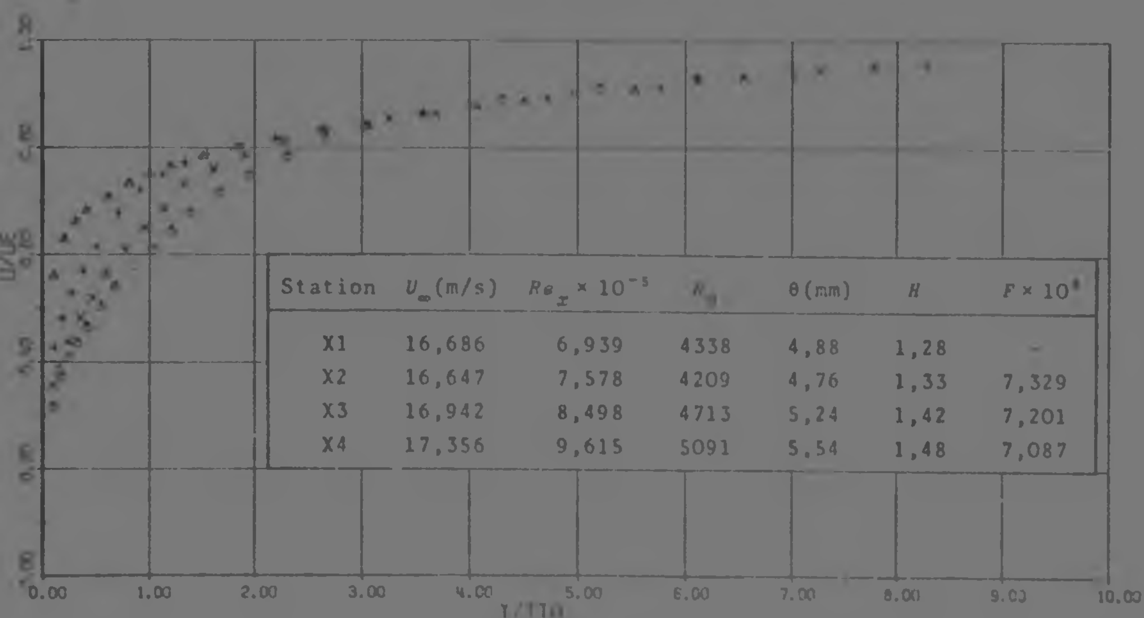

Station	U_∞(m/s)	$Re_x \times 10^{-5}$	[illegible]	θ(mm)	H	$F \times 10^3$
X1	16,686	6,939	4338	4,88	1,28	-
X2	16,647	7,578	4209	4,76	1,33	7,329
X3	16,942	8,498	4713	5,24	1,42	7,201
X4	17,356	9,615	5091	5,54	1,48	7,087

FIG 7.10s : TEST 23N1 E-7,27-17 50% BLOCKED

PLOT OF U/UE VS Y/TTA

RUN 23-11/5,8-8-17E

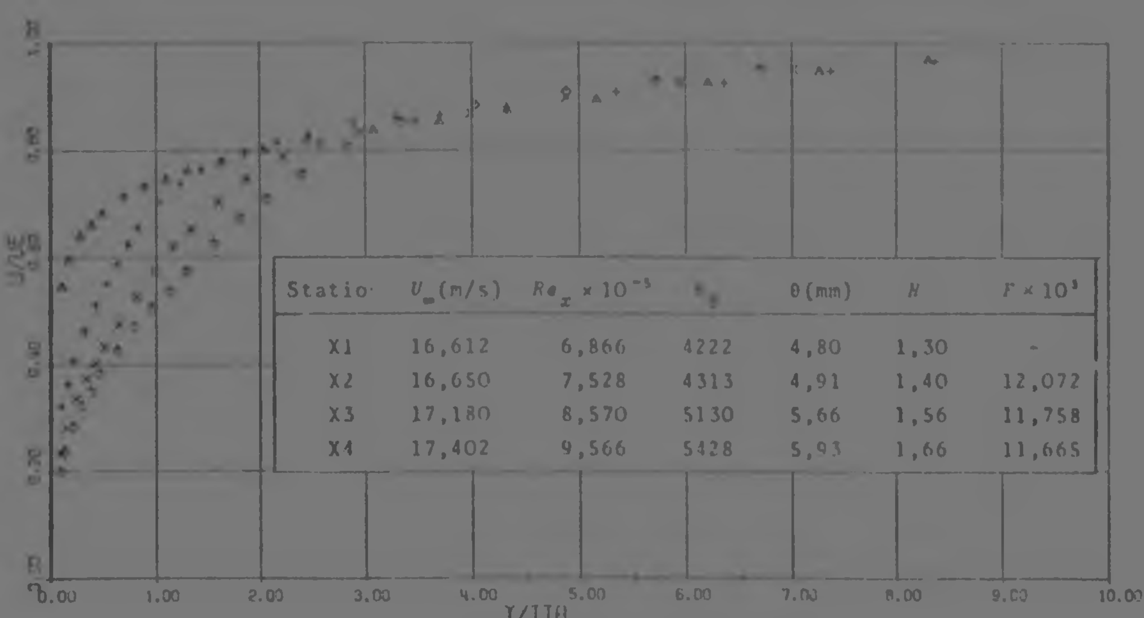

Statio	U_∞(m/s)	$Re_x \times 10^{-5}$	[illegible]	θ(mm)	H	$F \times 10^3$
X1	16,612	6,866	4222	4,80	1,30	-
X2	16,650	7,528	4313	4,91	1,40	12,072
X3	17,180	8,570	5130	5,66	1,56	11,758
X4	17,402	9,566	5428	5,93	1,66	11,665

FIG 7.10t : TEST 23N2 E-12,0-17 50% BLOCKED

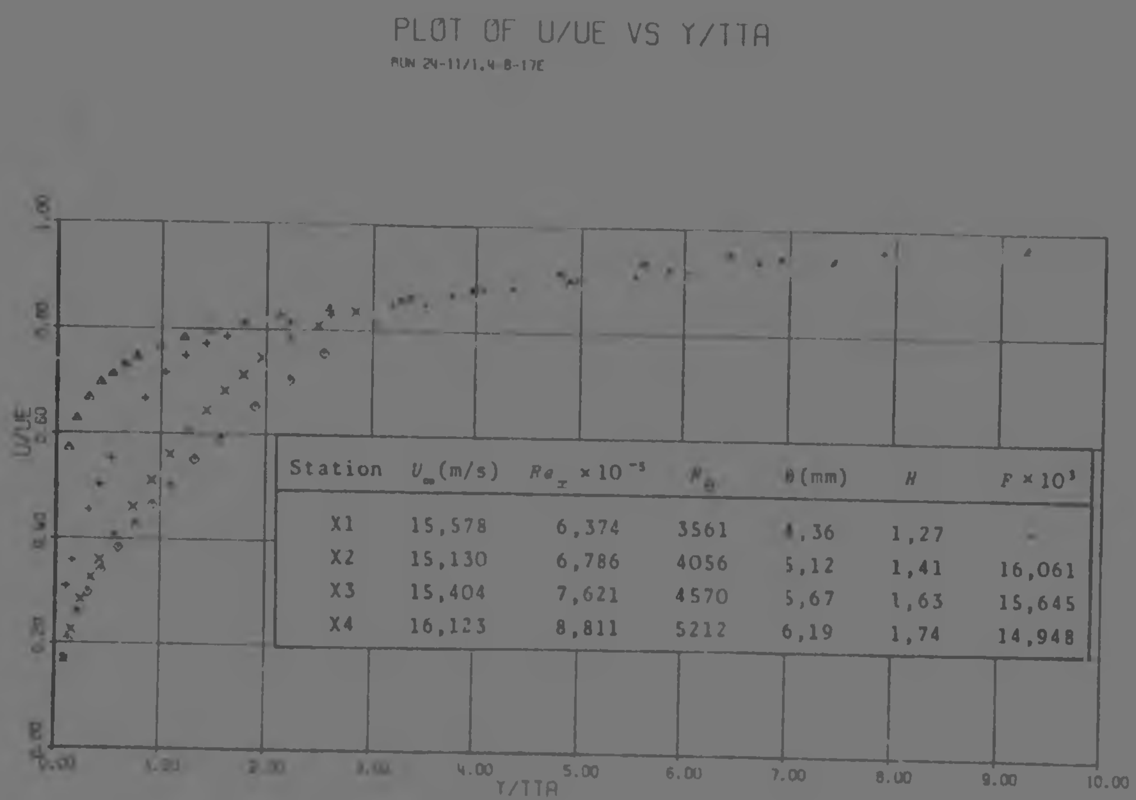

Station	U_∞(m/s)	$Re_x \times 10^{-5}$	R_θ	θ(mm)	H	$F \times 10^3$
X1	15,578	6,374	3561	4,36	1,27	–
X2	15,130	6,786	4056	5,12	1,41	16,061
X3	15,404	7,621	4570	5,67	1,63	15,645
X4	16,123	8,811	5212	6,19	1,74	14,948

FIG 7.10u : TEST 24N1 E-14,51-17 50% BLOCKED

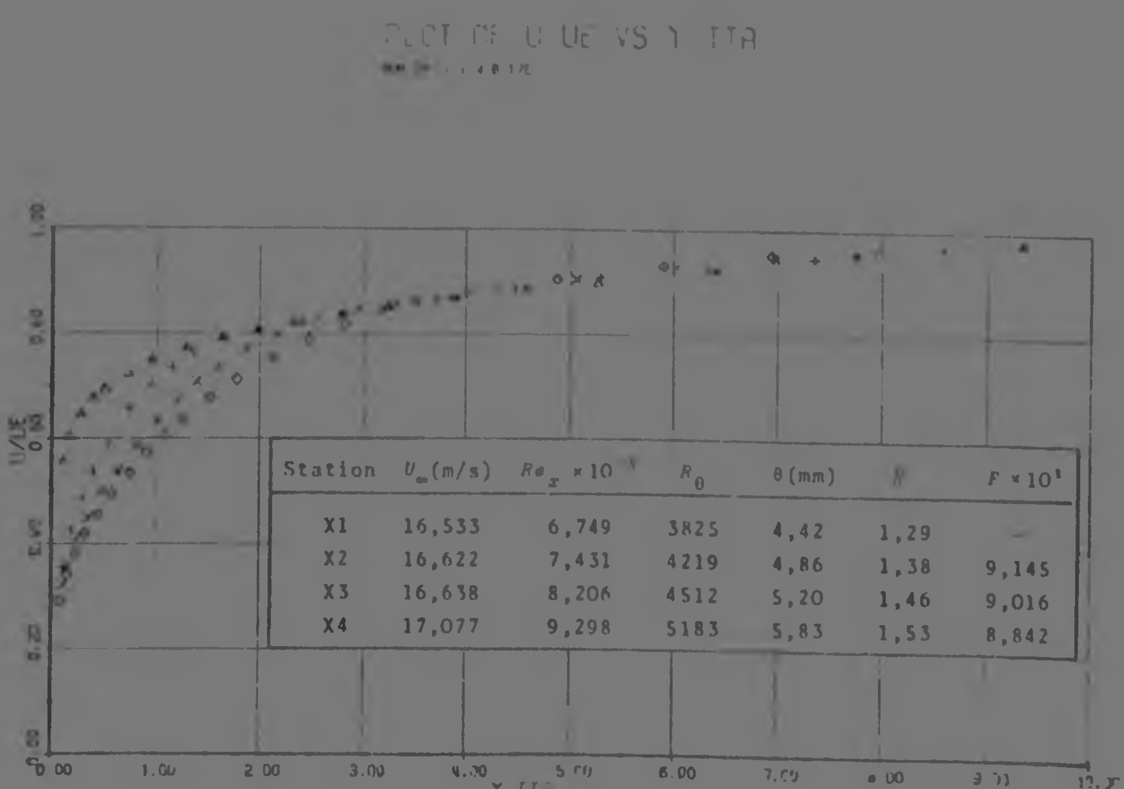

Station	U_∞(m/s)	$Re_x \times 10^{-5}$	R_θ	θ(mm)	H	$F \times 10^3$
X1	16,533	6,749	3825	4,42	1,29	–
X2	16,622	7,431	4219	4,86	1,38	9,145
X3	16,638	8,206	4512	5,20	1,46	9,016
X4	17,077	9,298	5183	5,83	1,53	8,842

FIG 7.10v : TEST 28N1 E-9,04-17 67% BLOCKED

PLOT OF U/UE VS Y/TTA

RUN 29 11/1.4 8 17E

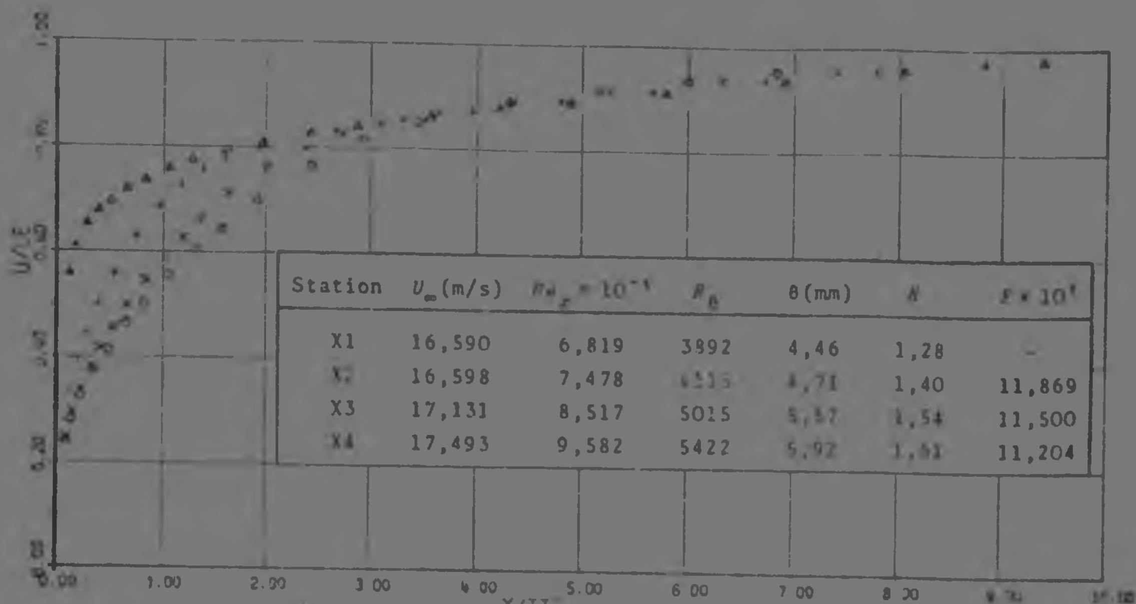

Station	U_∞(m/s)	$Re_x \times 10^{-5}$	R_θ	θ(mm)	H	$F \times 10^6$
X1	16,590	6,819	3892	4,46	1,28	-
X2	16,598	7,478	4515	4,71	1,40	11,869
X3	17,131	8,517	5015	5,57	1,54	11,500
X4	17,493	9,582	5422	5,92	1,61	11,204

FIG 7.10w : TEST 29N1 E-11,77-17 67% BLOCKED

PLOT OF U/UE VS Y/TTA

RUN 30 11/1 4 8 17E

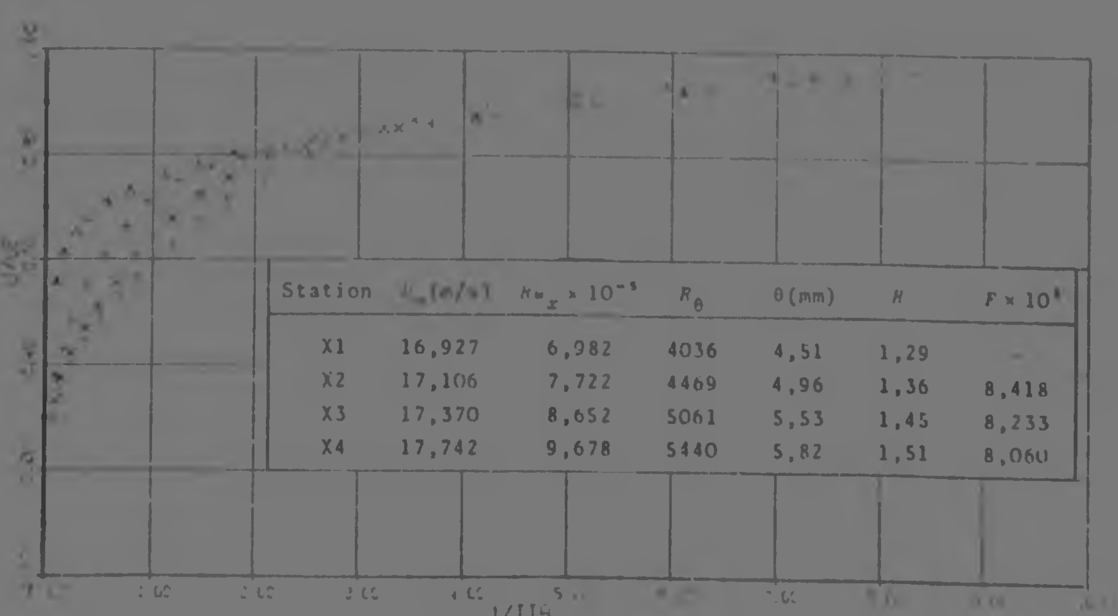

Station	U_∞(m/s)	$Re_x \times 10^{-5}$	R_θ	θ(mm)	H	$F \times 10^6$
X1	16,927	6,982	4036	4,51	1,29	-
X2	17,106	7,722	4469	4,96	1,36	8,418
X3	17,370	8,652	5061	5,53	1,45	8,233
X4	17,742	9,678	5440	5,82	1,51	8,060

FIG 7.10x : TEST 30N1 E-6,56-17 80% BLOCKED

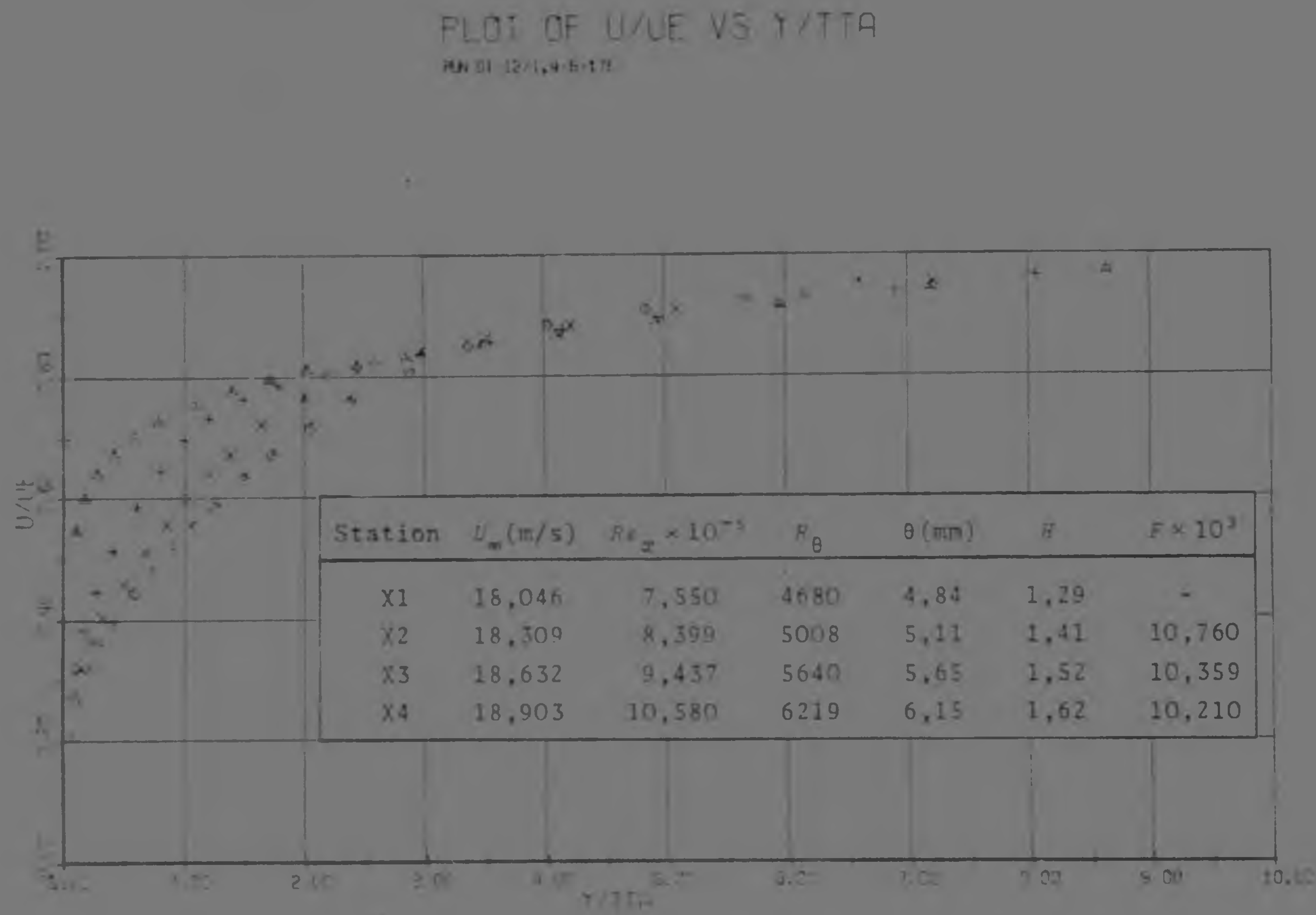

Station	U_∞ (m/s)	$Re_x \times 10^{-5}$	R_θ	θ (mm)	H	$F \times 10^3$
X1	18,046	7,550	4680	4,84	1,29	-
X2	18,309	8,399	5008	5,11	1,41	10,760
X3	18,632	9,437	5640	5,65	1,52	10,359
X4	18,903	10,580	6219	6,15	1,62	10,210

FIG 7.10y : TEST 01D1 E-11,66-17 80% BLOCKED

E and C grade plates were made by sintering spherical particles. The surface of the A grade plate was therefore much smoother, and the injection pattern was expected to be different from that experienced using grades E and C. (See Fig 7.11 and Appendix B).

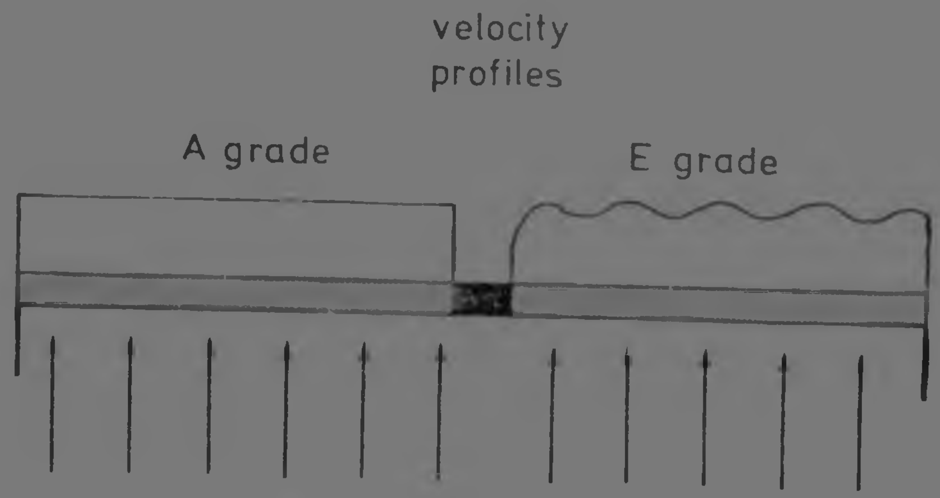

FIG 7.11 : v_w PROFILES EXPECTED FOR A AND E GRADE PLATES

Profiles obtained for the A grade plate and for test 28S1 were virtually identical. Note that for the former, F_{av} = 0,00755, for the latter F_{av} = 0,00758. The input profiles were the same as well. It was concluded that the velocity profile was mainly a function of injection ratio.

Having compiled a set of data for the unblocked porous plate, a few tests were done in which the lower porous surface was partially sealed with masking tape. The first tests were run with 50% blockage, as is shown in Fig 7.12.

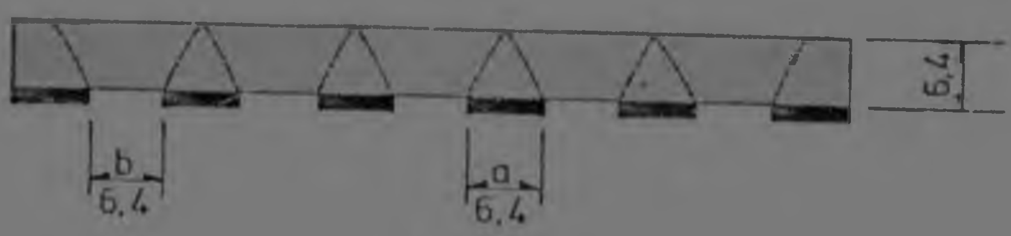

FIG 7.12 : SKETCH SHOWING THE PARTIALLY BLOCKED POROUS PLATE, 50% BLOCKED

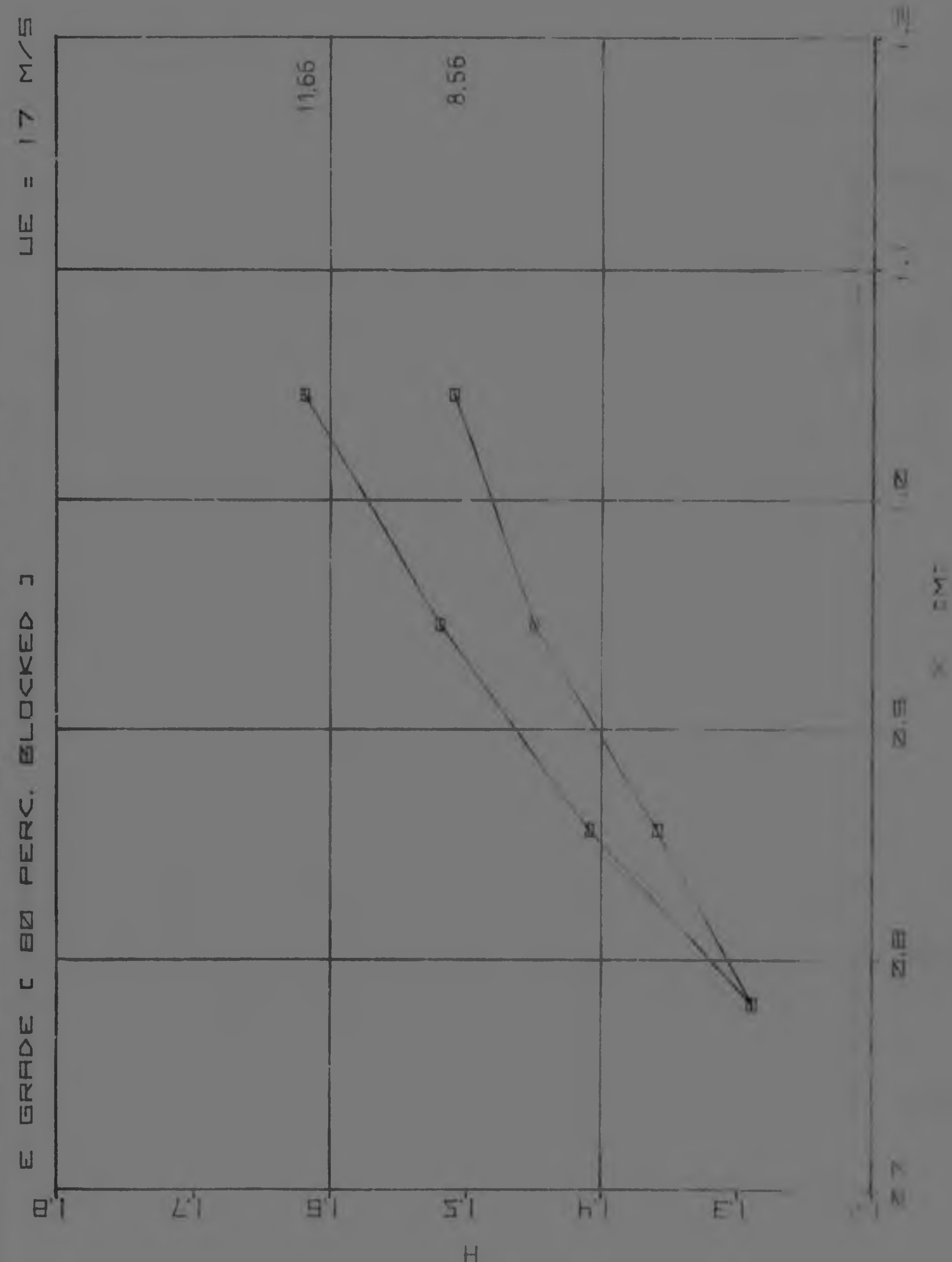

FIG 7.13d : PLOT OF VS x FOR u_e 17 m/s, 80% BLOCKED

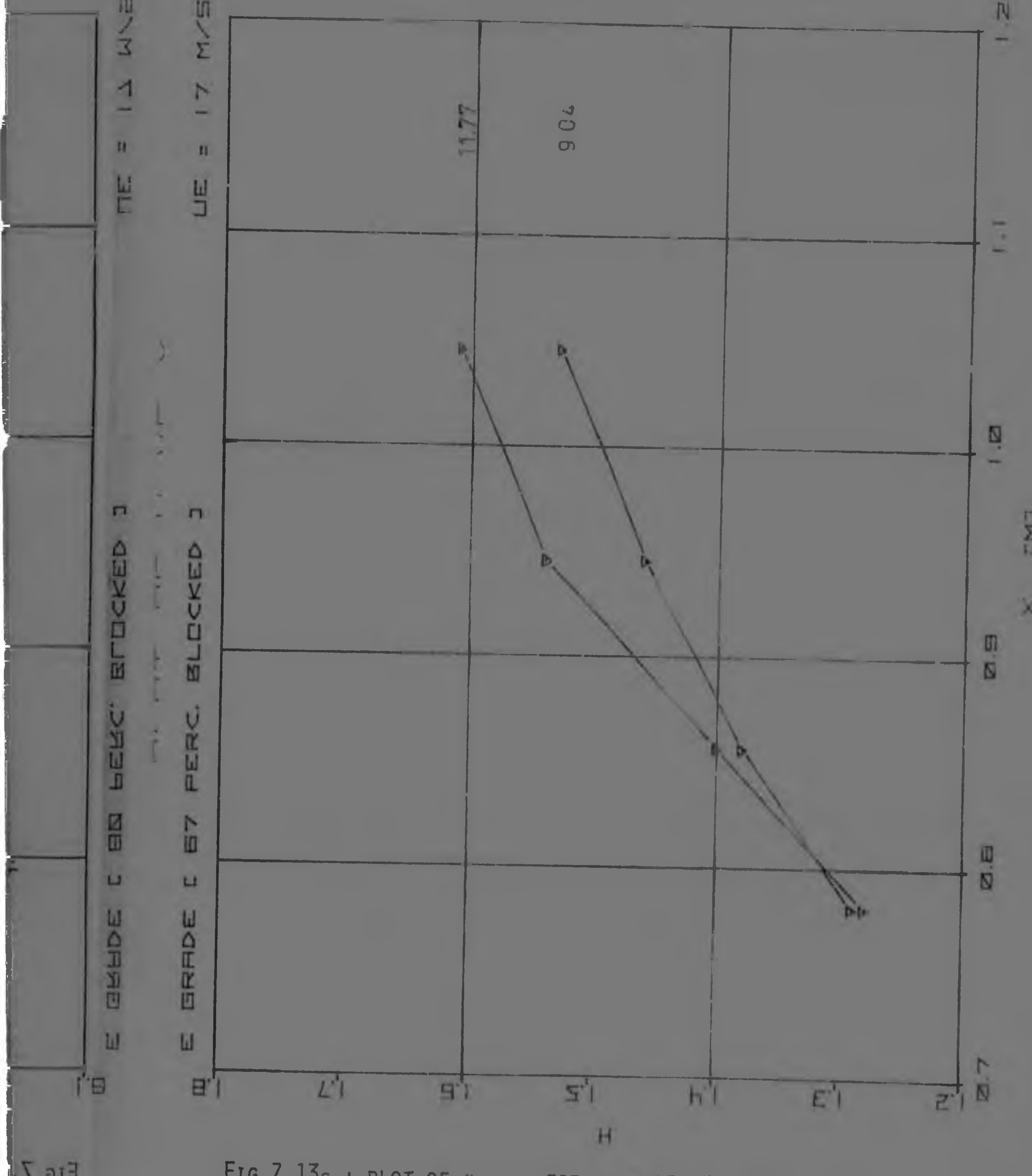

FIG 7.13c : PLOT OF H vs x FOR u_e = 17 m/s, 67% BLOCKED

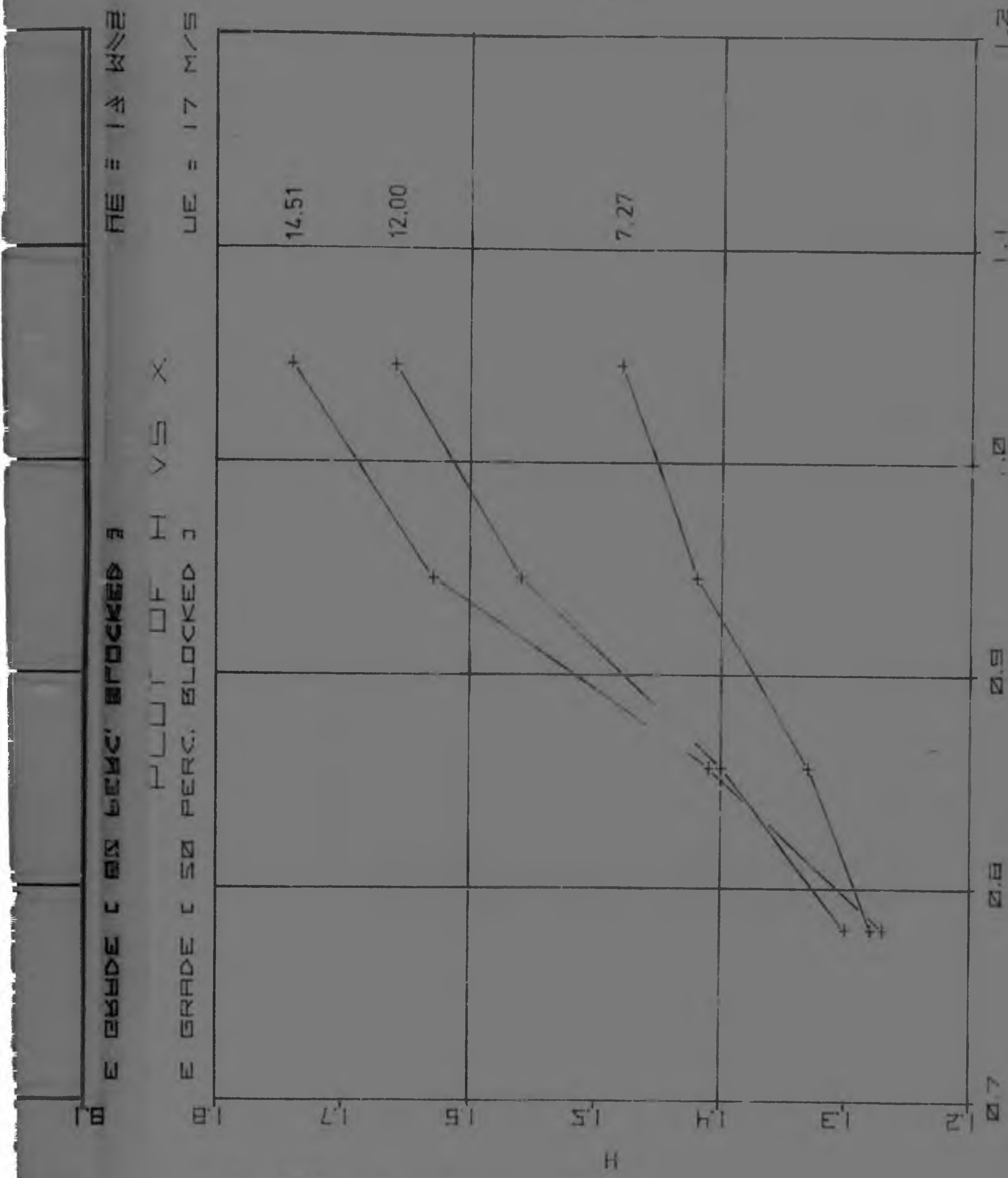

FIG 7.13b : PLOT OF H vs x FOR u_e = 17 m/s, 50% BLOCKED

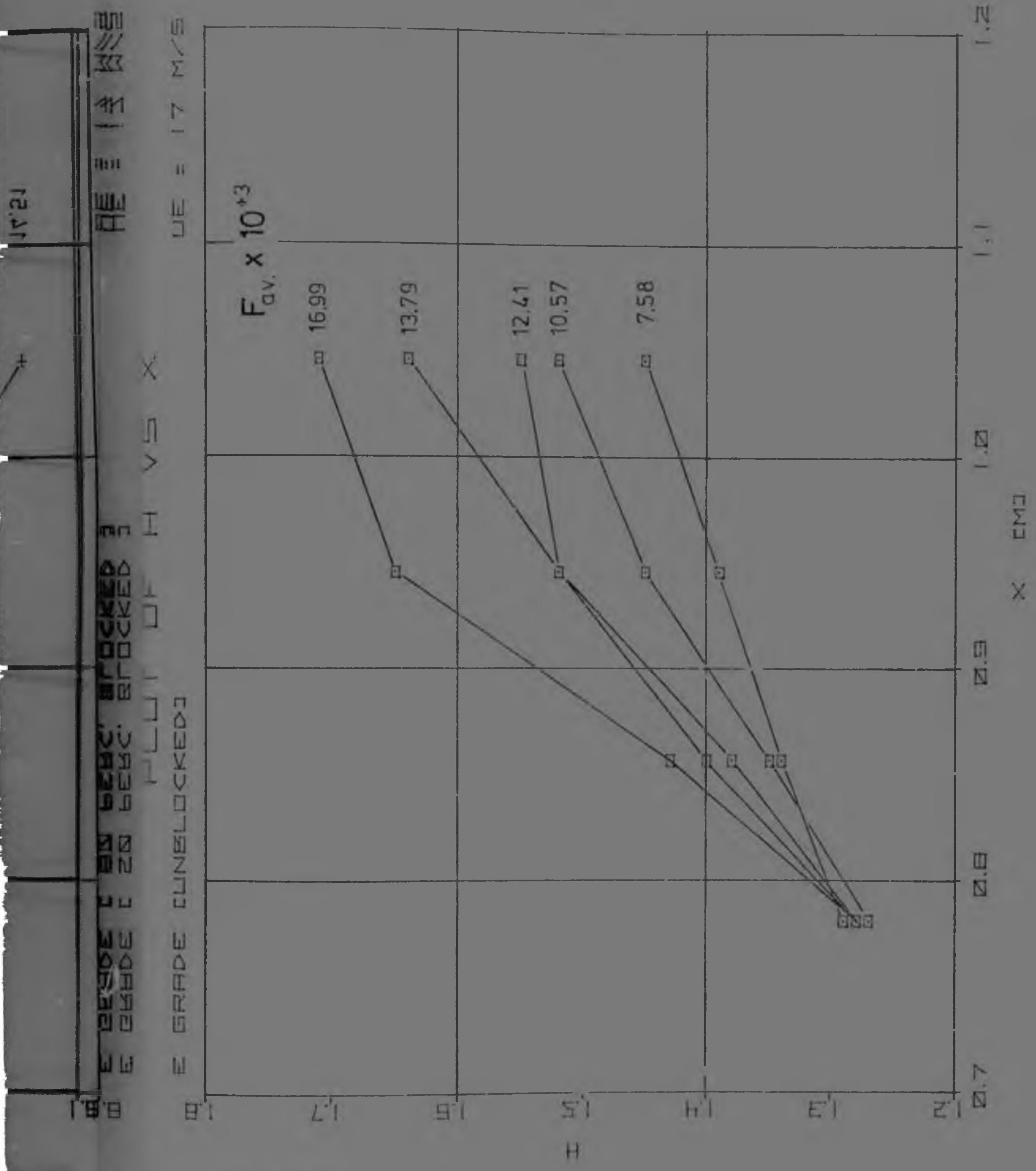

FIG 7.13a : PLOT OF H vs x FOR u_e = 17 m/s, UNBLOCKED

Tests 23N1 to 24N1 were run at U_∞ = 17 m/s, 50% blockage of the E grade plate. See Fig 7.10s to u.

With the tape covering 67% of the plate, a = 12,7 mm and b = 6,35 mm, tests 28N1 and 29N1 were performed. These profiles are presented in Fig 7.10v and w.

Two tests were run with a = 12,7 mm, b = 3,18 mm; this resulted in 80% blockage. Fig 7.10x and y are the profiles for these tests.

The effect of blockage is shown in Fig 7.13. This plot of shape factor, H vs x-station, was thought to present the change in a more succinct way than the usual velocity profile of Fig 7.10. The injection ratio, F, became a very average parameter. The definition of F now becomes :

$$F = \frac{Q_{trans}}{A_{upper} U_\infty} \quad \text{for } \rho \text{ constant} \qquad \ldots.. [7.3.1]$$

Where Q_{trans} was the transpiration flow rate and A_{upper} the area of porous plate exposed to the main stream.

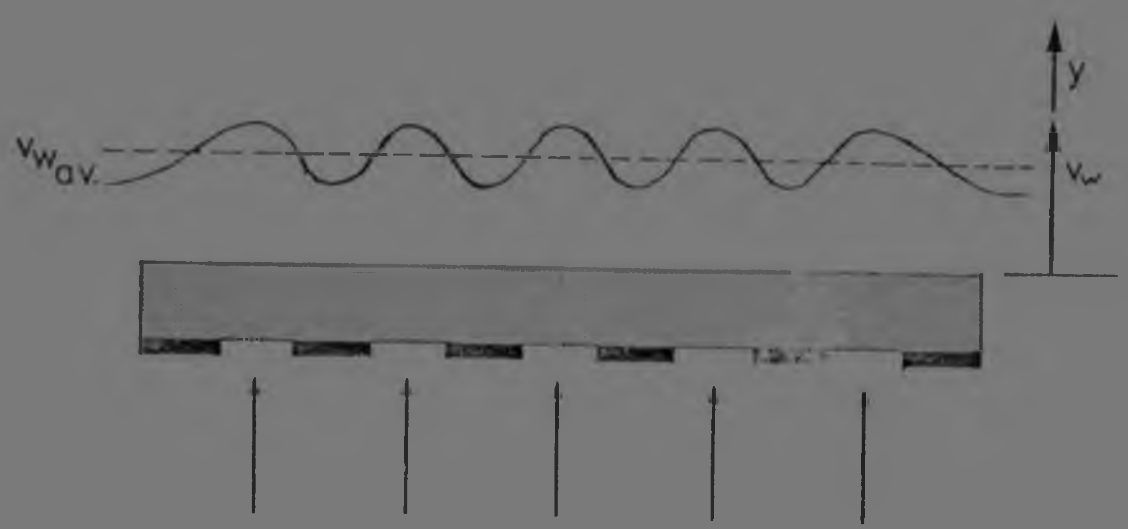

FIG 7.14 : DISTRIBUTION OF v_w WITH x FOR THE PARTIALLY BLOCKED POROUS PLATE, AND THE SPREAD OF THE FLOW IN THE POROUS MEDIUM WITH y

By considering Fig 7.13, it is seen that the curves do not increase with F as they do for the unblocked plate. The profile is developing for an apparently higher F. Clearly v_w was alternately above and below the average transpiration velocity. The average momentum in the y-direction must remain the same as for the unblocked porous plate, however, some of the injected flow penetrates deeper into the shear layer. Thus it is concluded that with the same transpiration flow rate, blockage results in an apparent increase in F and . If the Stanton number is expected to be a function of (see Moffat and Kays, 1968), a decreased heat transfer coeff. would become possible with blockage.* Intuitively, the opposite may be expected, however, only experiment is expected to resolve the matter.

It would therefore appear that the blockage caused by strengthening ribs below the porous surface, could result in improved performance.

7.3.2 The bilogular plotting technique

This method for determining from the velocity profile was discussed in Chapter , section 3, at some length. It was developed by Black and Sarnecki (1958), and yielded an effective imaginary shear velocity at the wall. This was merely a technique, and did not imply reverse flow, as may be encountered for flows in an adverse pressure gradient. The results are given in Fig 7.15a to c, Fig 7.16 and Fig 7.17. These graphs are presented because (i) Fig 7.15 showed the trend in the profiles for increasing F, and (ii) the graphs allowed an interesting comparison of the present results with those of Mickley and Davis (1956).

Fig 7.15a to c are graphs of $u/u_e - Y_*^2$ vs Y_* for the basic data of Mickley and Davis (1956), and the present work. Fig 7.15a is for U_∞ = 17 m/s, E grade. This graph also shows the limiting curves, ie. for $u/u_e = 0$ and $u/u_e = 1$, ie. the edge of the boundary layer. Plots shown in

* see Addendum for further explanation.

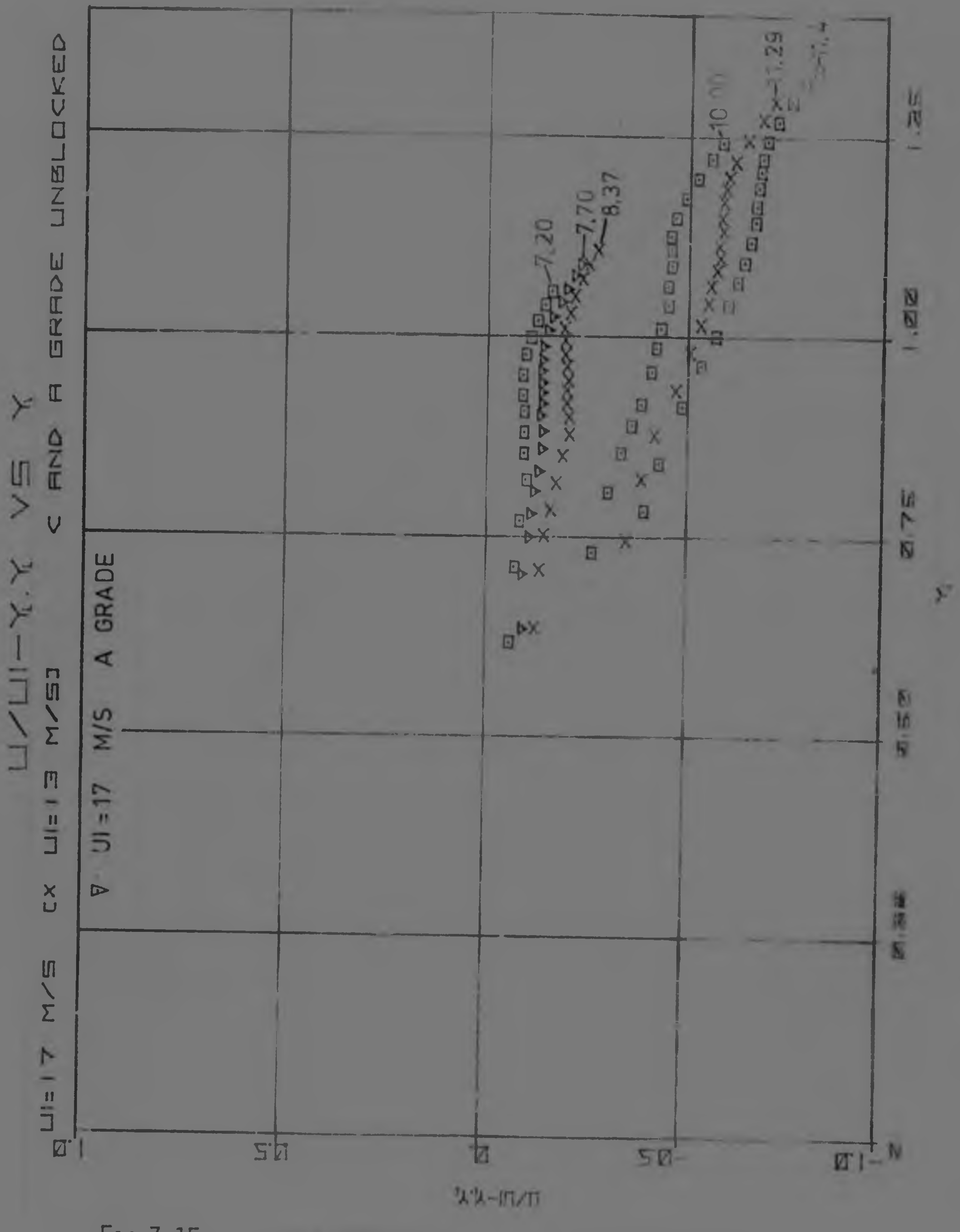

FIG 7.15c : SOME EXPERIMENTAL RESULTS PLOTTED ON THE BILOG CO-ORDINATES

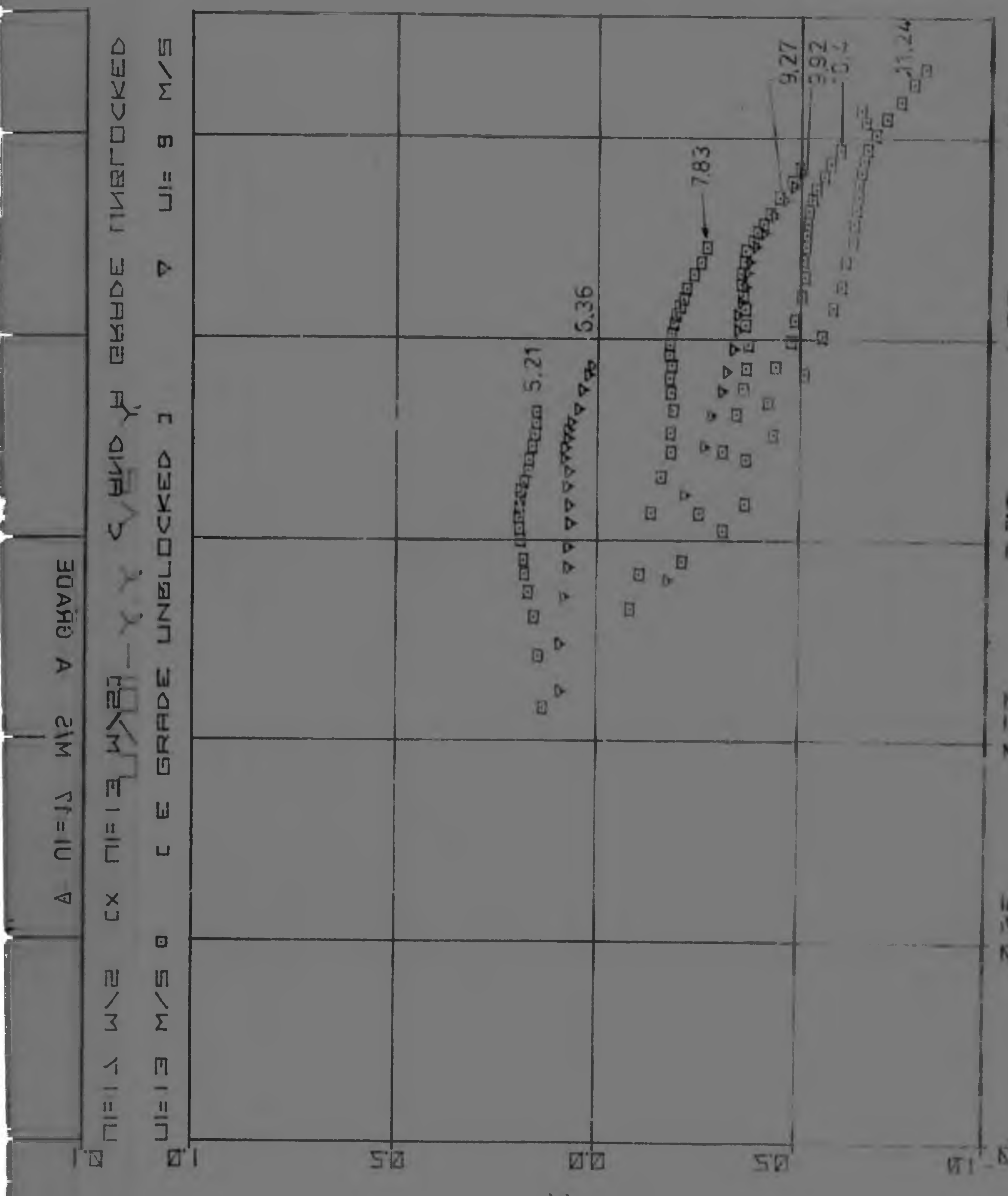

FIG 7.15B : SOME EXPERIMENTAL RESULTS PLOTTED ON THE BILOG CO-ORDINATES

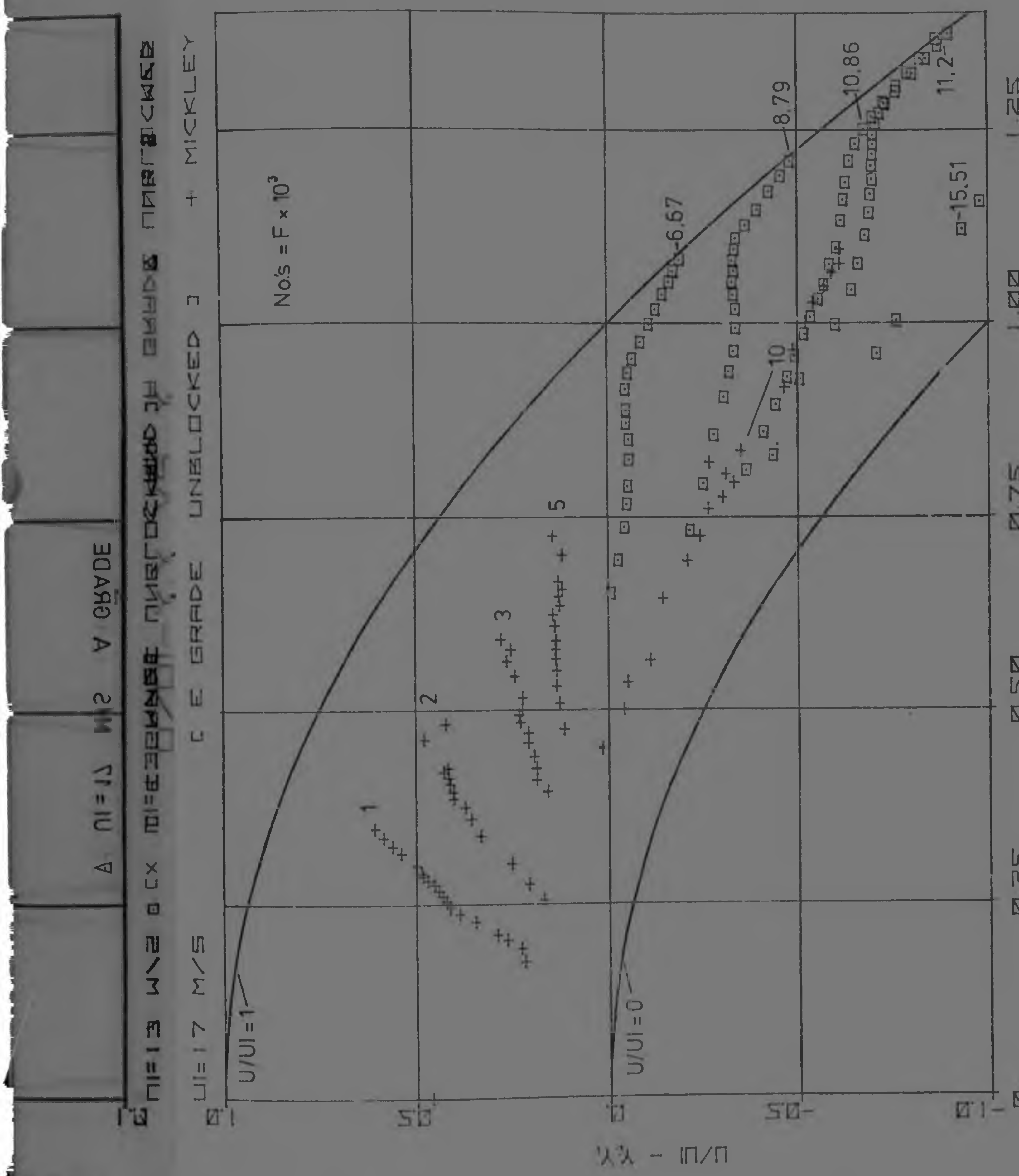

FIG 7.15A : PRESENT DATA AND THAT OF MICKLEY AND DAVIS (1956) PLOTTED ACCORDING TO THE BILOG LAW TECHNIQUE

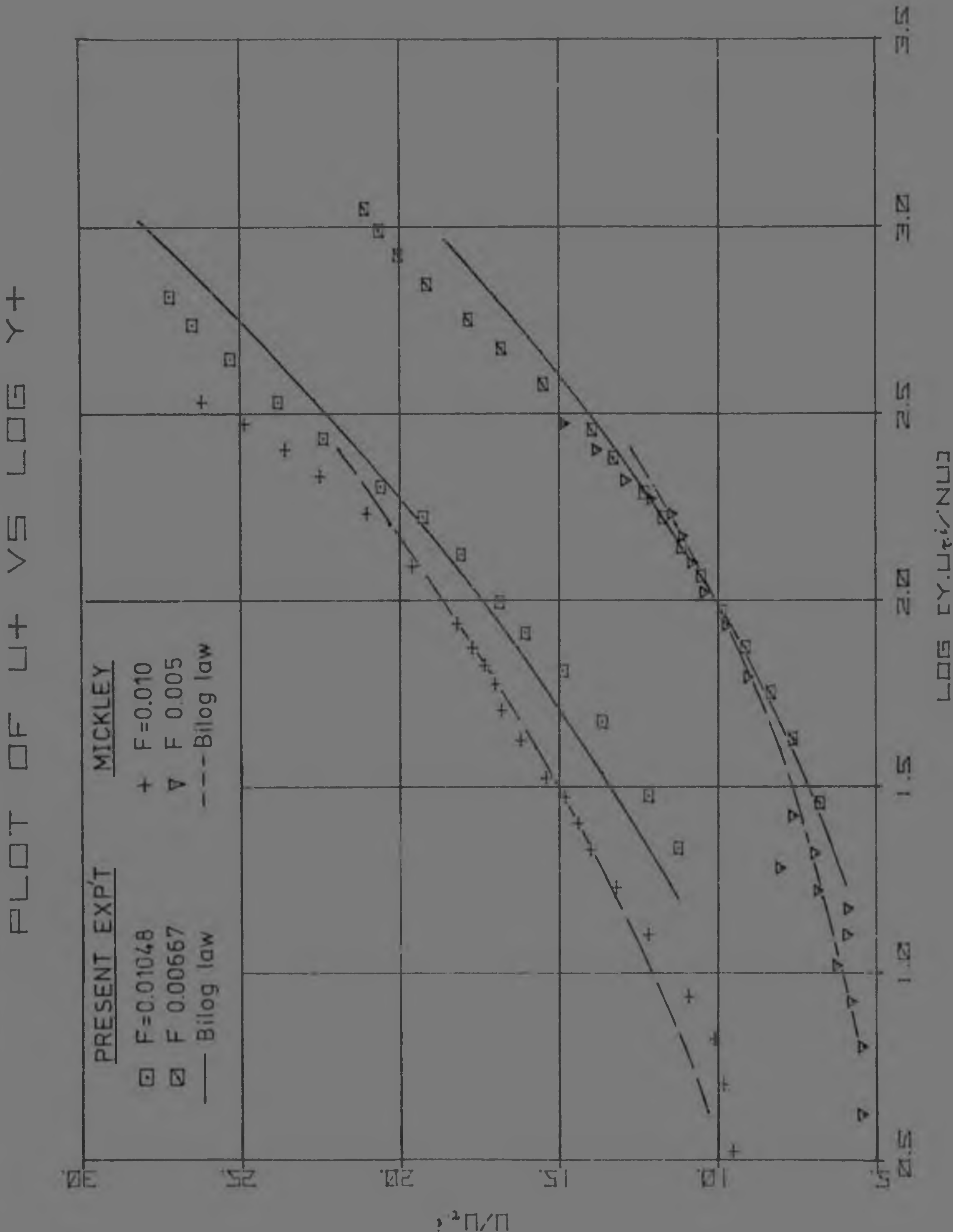

FIG 7.16 : EXPERIMENTAL DATA AND BILOG PREDICTED PROFILE

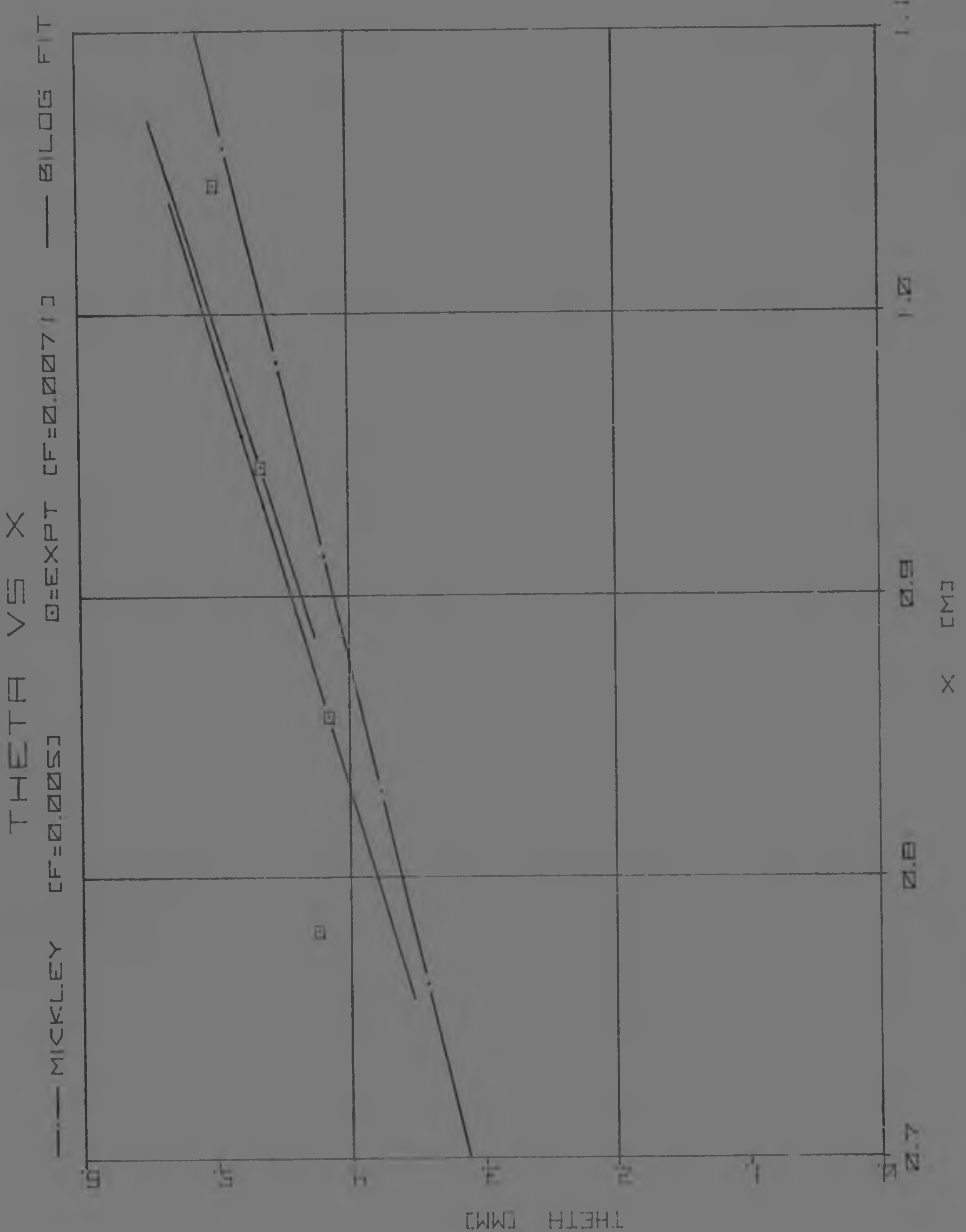

FIG 7.17 : GRAPH OF θ vs x - EXPERIMENTAL AND BILOG PREDICTED SLOPE

Fig 7.15b are for U_∞ = 13 m/s (⊡) and U_∞ = 9 m/s (∇), both sets on the E grade plate. Results obtained for U_∞ = 17 m/s (⊡), U_∞ = 13 m/s (×) on the C grade plate, and for the single run using the A grade plate (U_∞ = 17 m/s (∇)) are plotted on Fig 7.15c.

By fitting a straight line to the experimental points of a run (in the bilog region), u_τ could be calculated from the slope and ordinate intercept of that line (see equations 3.3.21 to 3.3.23). If this line did not pass through the limiting line of $u/u_\infty = 0$, u_τ would be imaginary. This was the case for all values of $F \geq 5$. The uncertainty in fitting the straight line can be seen from the scatter of the points. Two examples are shown in the non-dimensional plot of u/u_τ vs log $y.u_\tau/\nu$ in Fig 7.16. Again comparable results of Mickley and Davis (1956) are included. The lines represent the profiles predicted by the bilog law.

Because it was of importance to know $d\theta/dx$, it was thought useful to show that the bilog technique could predict this derivative, but gave no indication of the origin of the boundary layer. Fig 7.17 shows a typical example for F = 0,0071. The slope was calculated at a point, nd a straight line with that gradient drawn through the [illegible]. Good agreement was again obtained with the result [illegible]kley and Davis (1956).

It is felt that as this method yielded imaginary shear, it is only useful as a plotting technique, and is inadequate for estimating c_f. The graphs did allow comparison of the present work with that of other researchers.

7.3.3 A two-parameter family of curves

The two-parameter family of curves of Thompson (1965) was used to construct the mean velocity profile ahead of the porous wall. McQuaid (1967) suggested a family of curves for the transpired boundary layer. This set of curves predicted the velocity profile and the skin friction. Intermittency was included in the formulation (by the term δ_s, see eqn.[3.3.30]). This author showed that u/U_∞ was a function of y/δ_s, c_f, $R\delta_0$, v_w/U_∞, which was transformed to eqn.[3.3.29]. This was a function of y/θ, H, R_θ, v_w/U_∞.

A cross-plot of the present results was attempted, and is shown in Fig 7.18. These values were obtained from the velocity profiles (Fig 7.10) by keeping u/U_∞ constant, and reading y/θ for the various x stations (effectively Re_x, or Re_θ). It was thought that for constructing mean velocity profiles, it would be more useful to have u/u_e as one of the axes. Thus y/θ was kept constant, and the value of u/u_e read from Fig 7.10. These values were plotted, and a number of points from the experimental work of Mickley and Davis (1956) and McQuaid (1967) added. A series of curves were obtained, apparently independent of v_w/U_∞, and are presented as Fig 7.19 a to d.

This result may be stated :

$$H = H(R_\theta, v_w/U_\infty) \qquad \text{....... [7.3.2]}$$

$$u/U_\infty = f(y/\theta, H) \qquad \text{....... [7.3.3]}$$

A limitation of this family is that c_f is not accounted for. McQuaid (1967) presented a skin friction law, for v_w/U_∞ up to 0,010 :

$$c_f = c_f(H, R_\theta, v_w/U_\infty) \qquad \text{....... [7.3.4]}$$

These curves were assumed to hold for a porous wall, continuous from $x = 0$. It was thought that the values of c_f would be very different for discontinuous injection. However, it must again be emphasised that only direct measurement of τ_w would give reliable values of c_f. This would be necessary in each individual test, for its particular input profile, porous plate configuration, surface roughness, pressure gradient, etc.

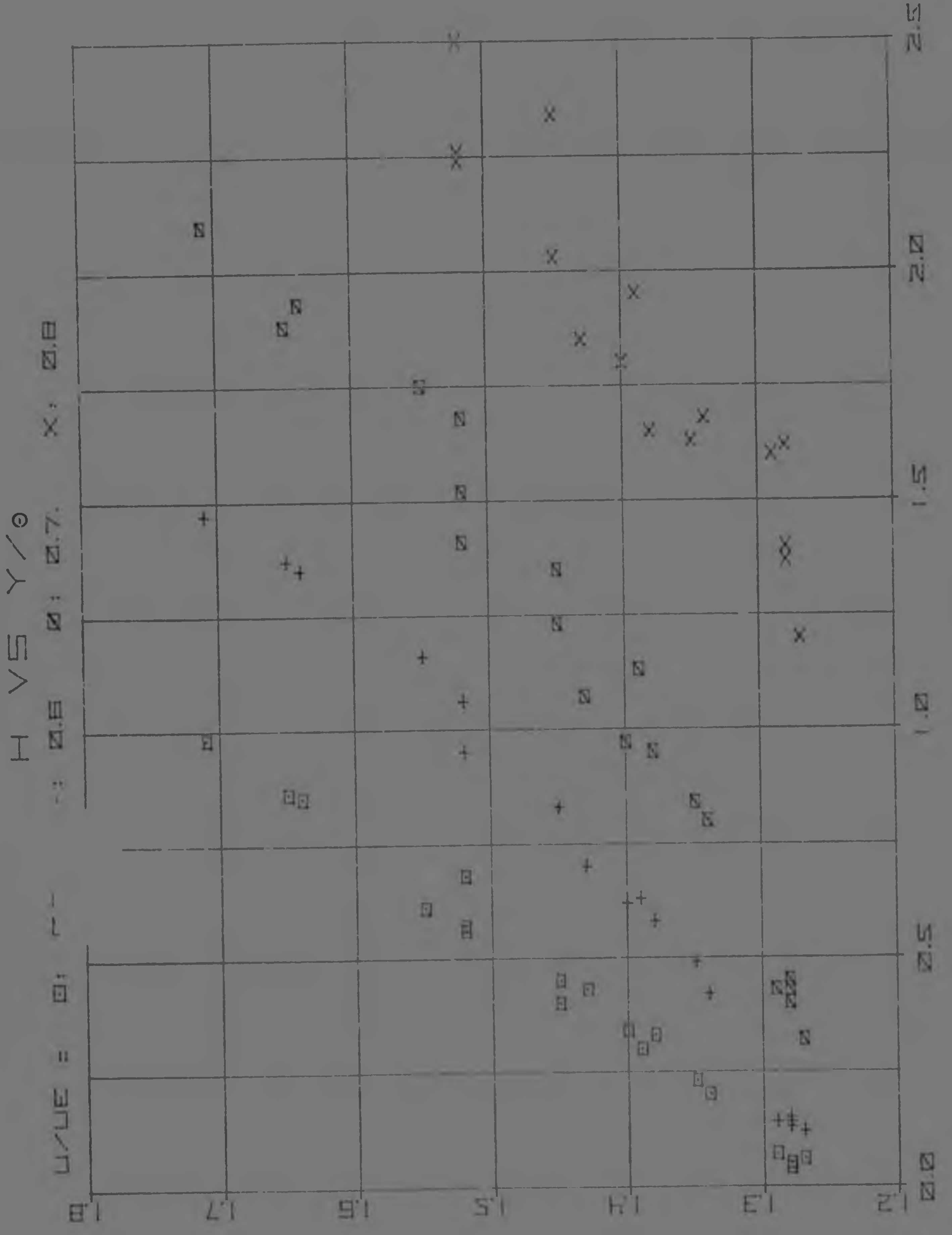

FIG 7.18 : CROSS PLOT OF PRESENT RESULTS, u/u_e CONSTANT

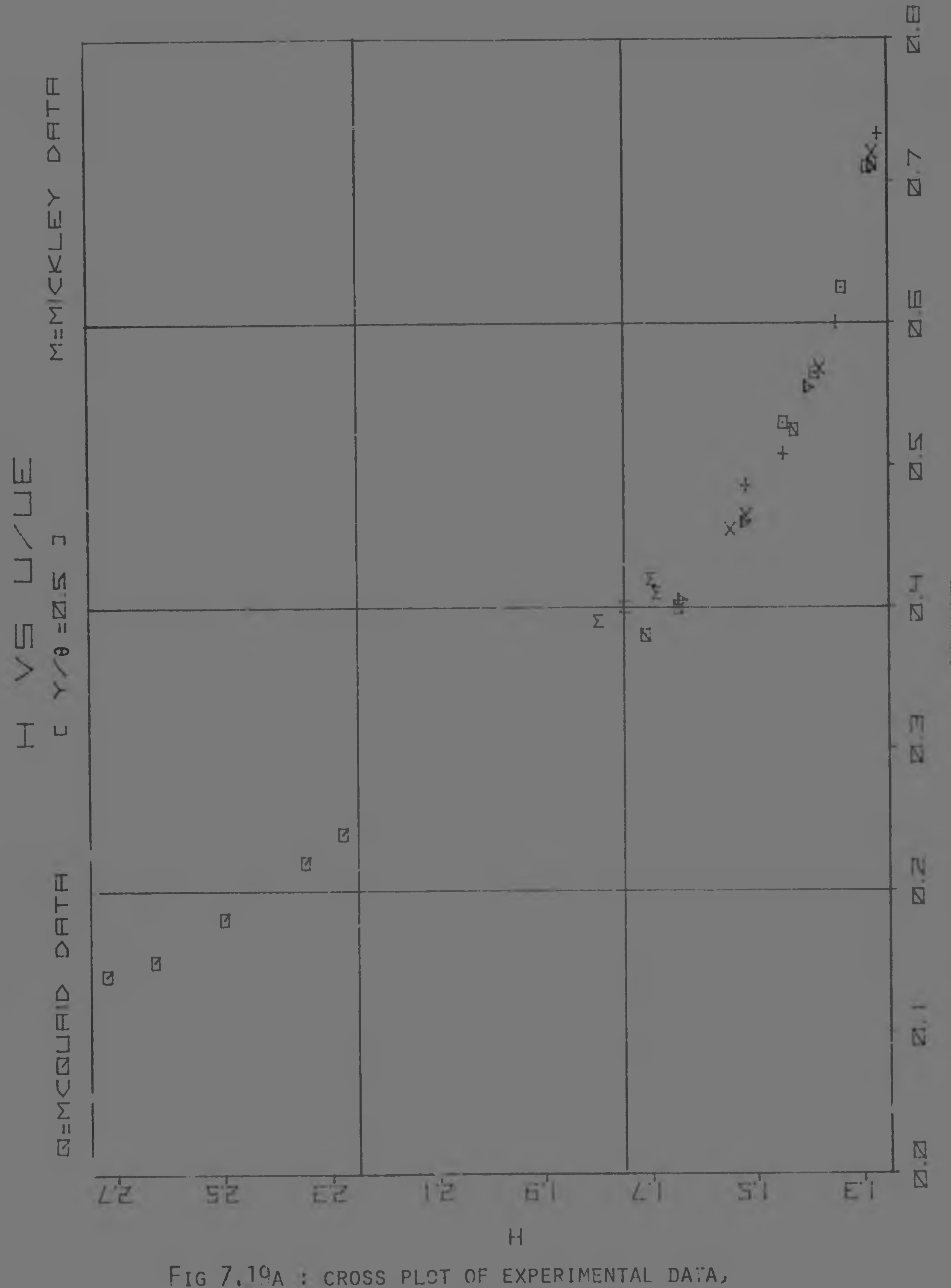

FIG 7.19A : CROSS PLOT OF EXPERIMENTAL DATA, FOR y/θ CONSTANT

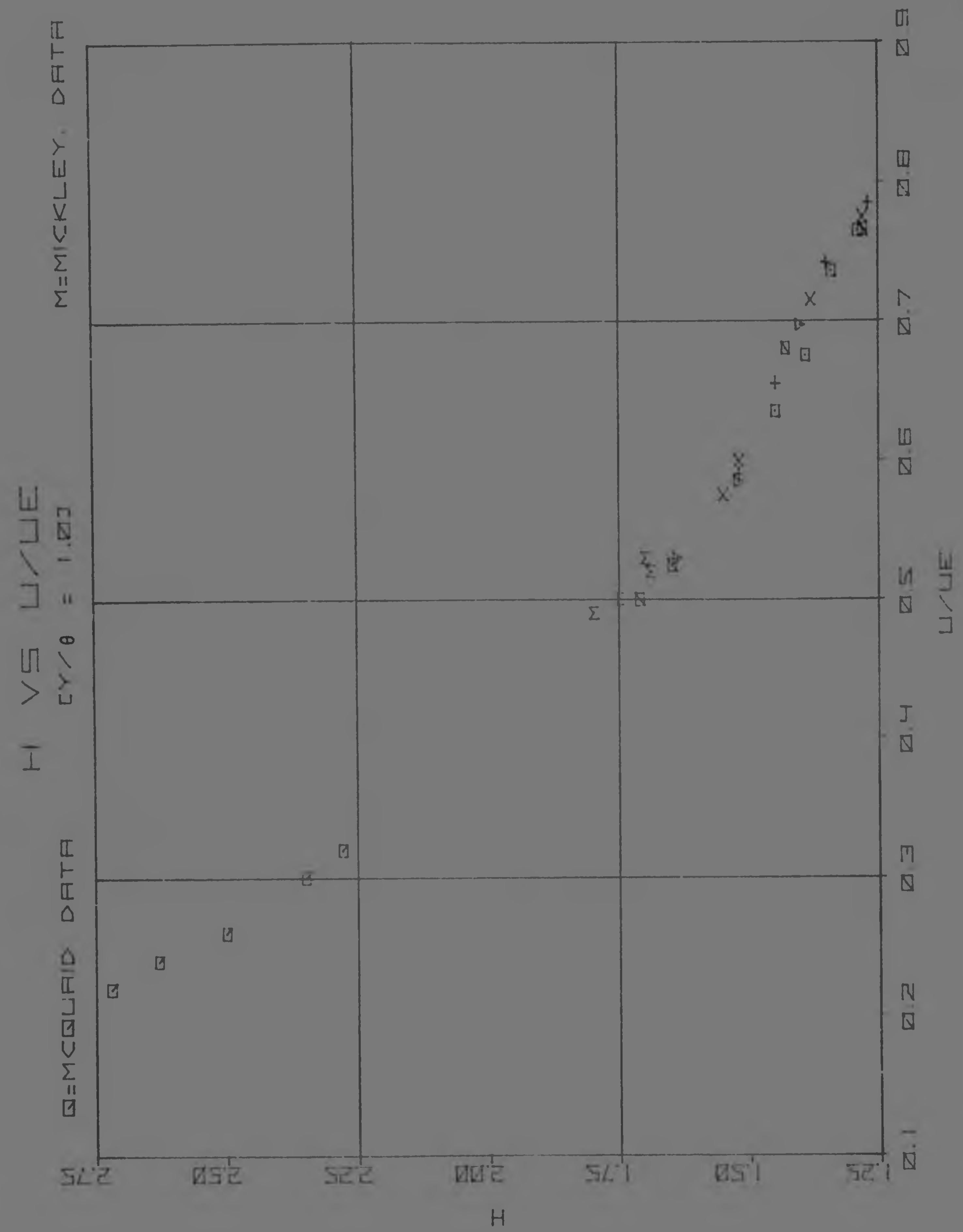

FIG 7.10B : CROSS PLOT OF EXPERIMENTAL DATA,
FOR y/θ CONSTANT

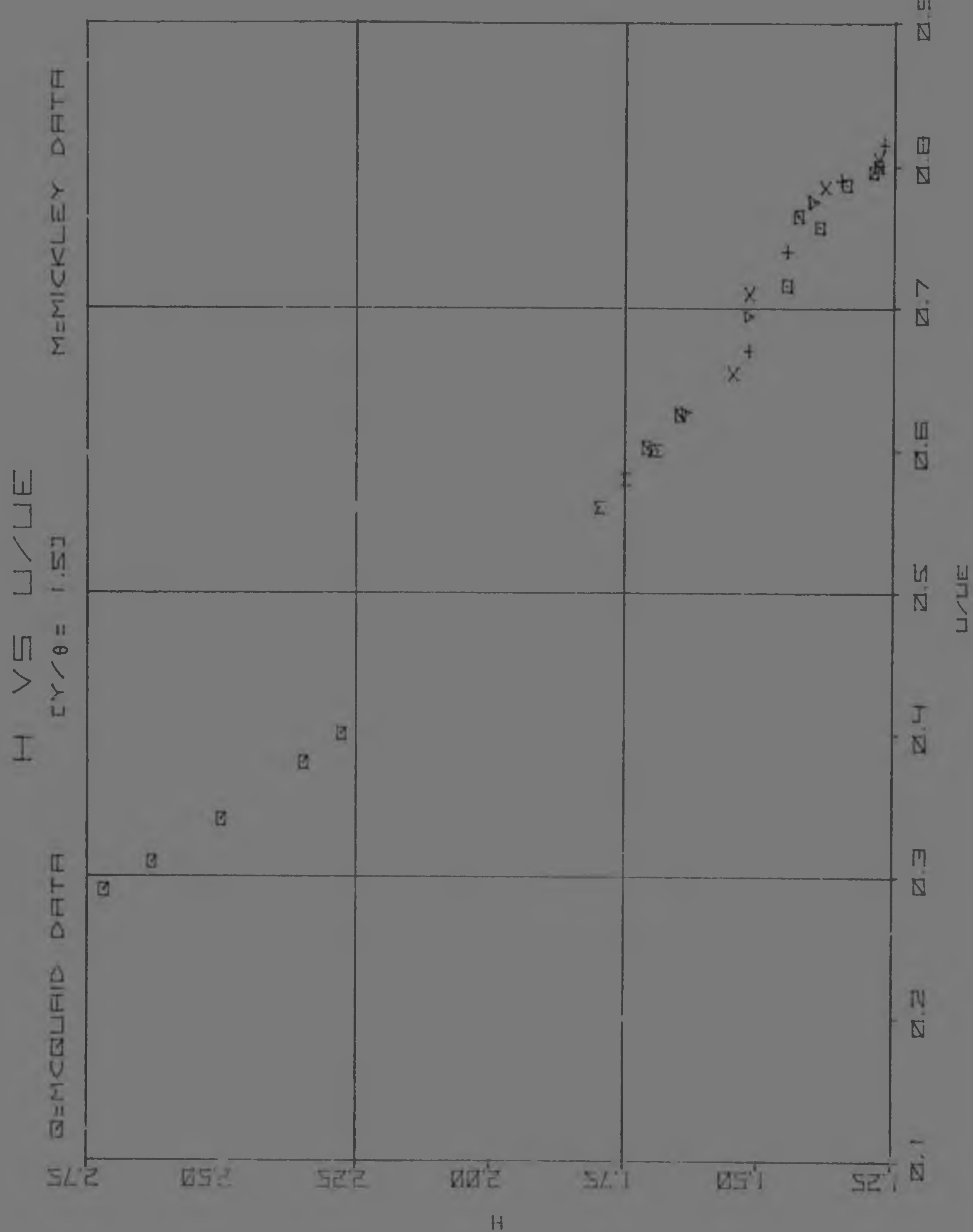

FIG 7.19C : CROSS PLOT OF EXPERIMENTAL DATA, FOR y/θ CONSTANT

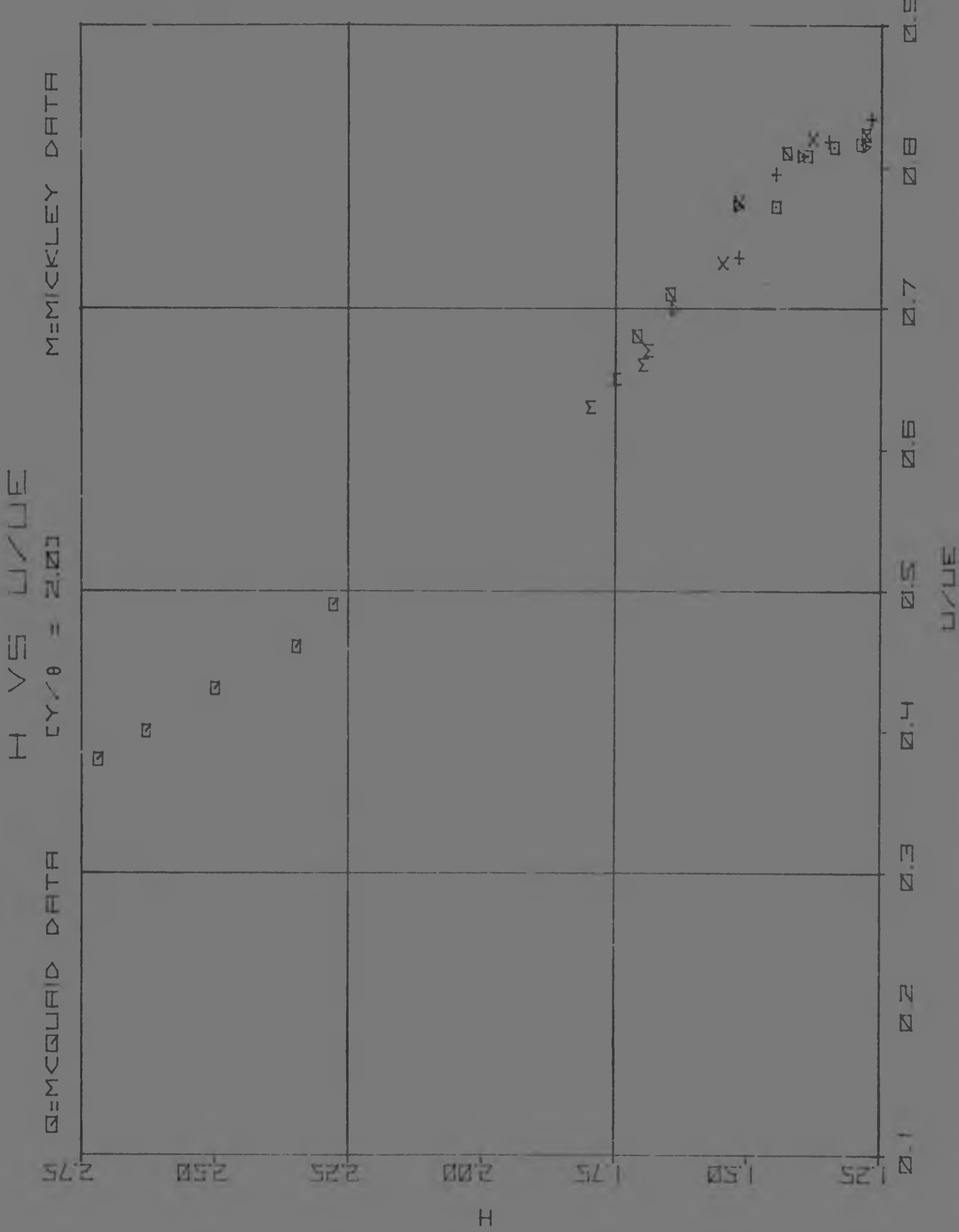

FIG 7.19D : CROSS PLOT OF EXPERIMENTAL DATA, FOR y/θ CONSTANT

7.4 Computer Programme Results

As discussed previously, the programme required two initial profiles to start the solution. These could be either laminar or turbulent, but with $v_w = 0$. Starting the solution with transpiration from the boundary layer origin was therefore not possible. By installing a trip wire, it is possible to obtain a turbulent profile for very low values of Re_x experimentally. However, the equation used to generate the turbulent profile was valid for $Re_x > 5\times10^4$. Thus it was not possible to simulate experimental conditions very effectively.

The boundary layer thickness was over-estimated because the equation used was valid only to $y^+ = 10^4$ (depending on Reynolds number). This is illustrated below in Fig 7.20.

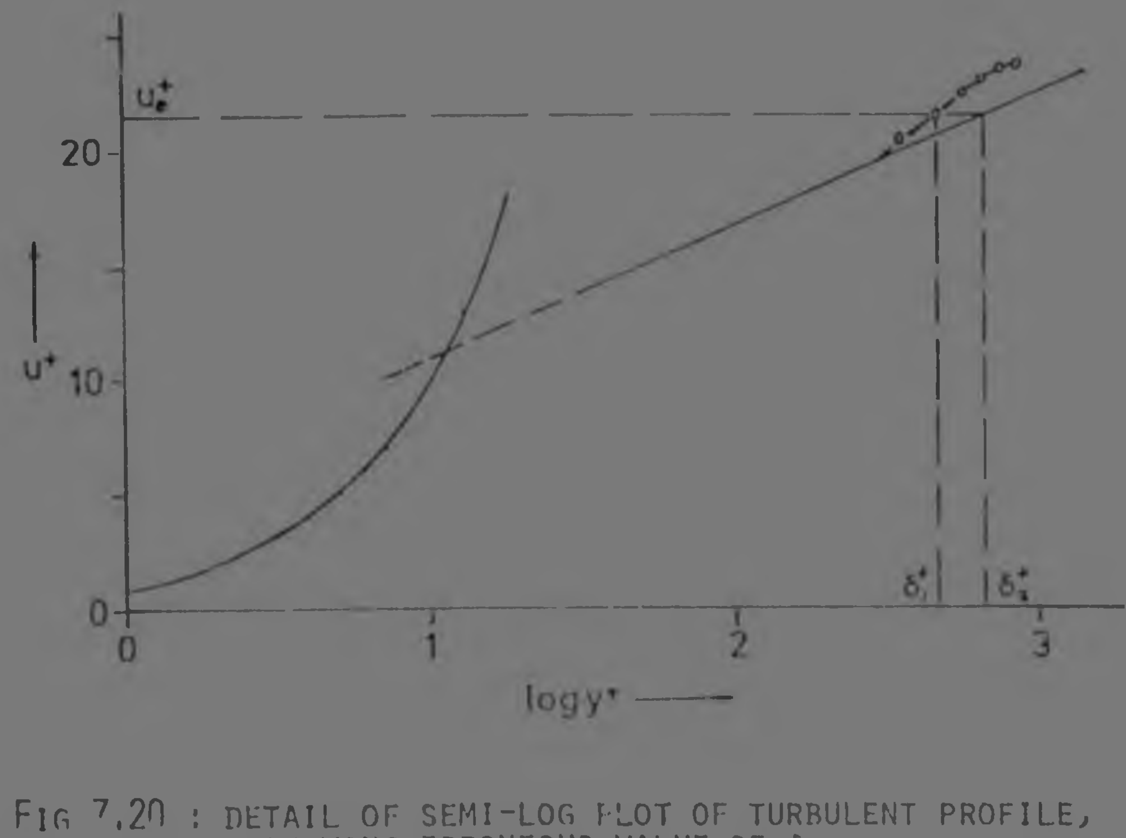

FIG 7.20 : DETAIL OF SEMI-LOG PLOT OF TURBULENT PROFILE, SHOWING ERRONEOUS VALUE OF δ

Clearly, if the straight line was used, $\delta^+ = \delta_2^+$, instead of δ_1^+, obtained from experimental points. If a wake law was not used in this region, a power law would probably be the easiest method of generating u^+ near the edge of the layer.

7.4.1 Main computer runs

The results of the main computer runs are shown graphically in Fig 7.21 a to j. See also Appendix F3 for tabulated values of Re_θ, H, etc.

By generating the input profiles on a flat plate, the programme was a close simulation of the experimental work. It was, however, not possible to obtain the identical input profile that was measured experimentally without extensive reprogramming - the Van Driest profile was used instead. Furthermore, the programme as written is for the 'flat plate in an infinite stream', whereas almost channel flow was obtained in the tunnel, ie. the boundary layer growth in the tunnel was limited to the centre line of the tunnel.

Examination of Fig 7.21 shows that the profiles generated are very similar to those depicted in Fig 7.10. The trends with x and F were identical, ie. increased 'laminarisation' with x and F.

The values of c_f appear to be highly erroneous. On the other hand, there is no experimental data for the step change in transpiration and surface roughness with which these values could be compared. If ϕ_ω'' is obtained from ϕ, negative c_f results, and hence imaginary u_τ^+, p^+ and v_ω^+. Although this is predicted by the bilog law, this is not of much use, as the programme cannot solve the equations for imaginary shear velocity. ϕ_ω'' was therefore obtained from ϕ', and it is expected that the error in ϕ_ω'' does not affect the solution significantly (Note:- ϕ_ω'' affects the inner eddy-viscosity equation). Clearly the finite difference equation which yields satisfactory values of c_f for the unblown layer was inadequate for the blown boundary layer. By decreasing the step size more accurate results would be obtained, but this would increase the cost of running the programme significantly. In this work, H=0,065 was common, whereas other investigators have reported H=0,001, with 300 steps.

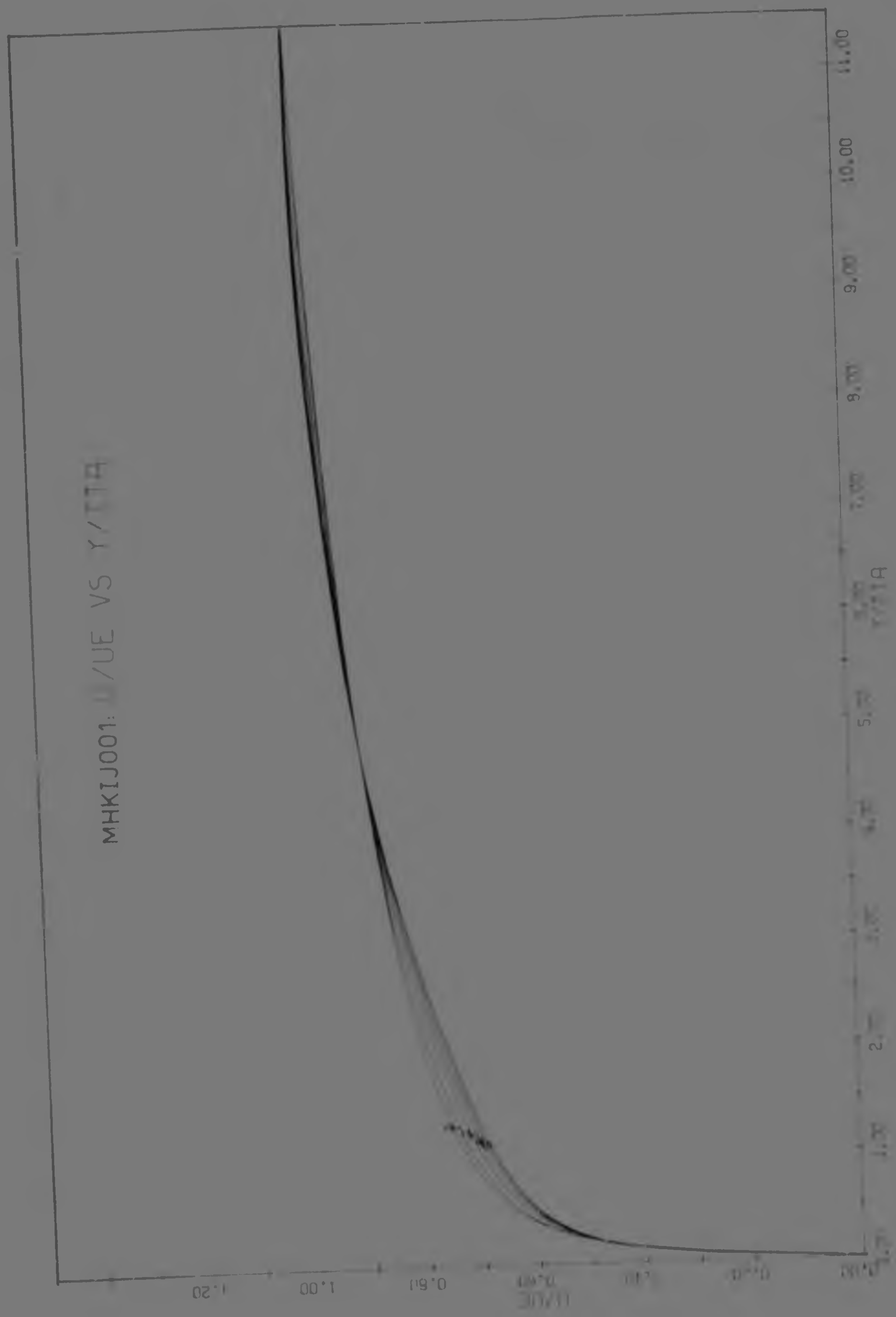

FIG 7.21A : TURBULENT PROFILES WITH INCREASING INJECTION, U_∞ = 17 m/s, F = 0,001

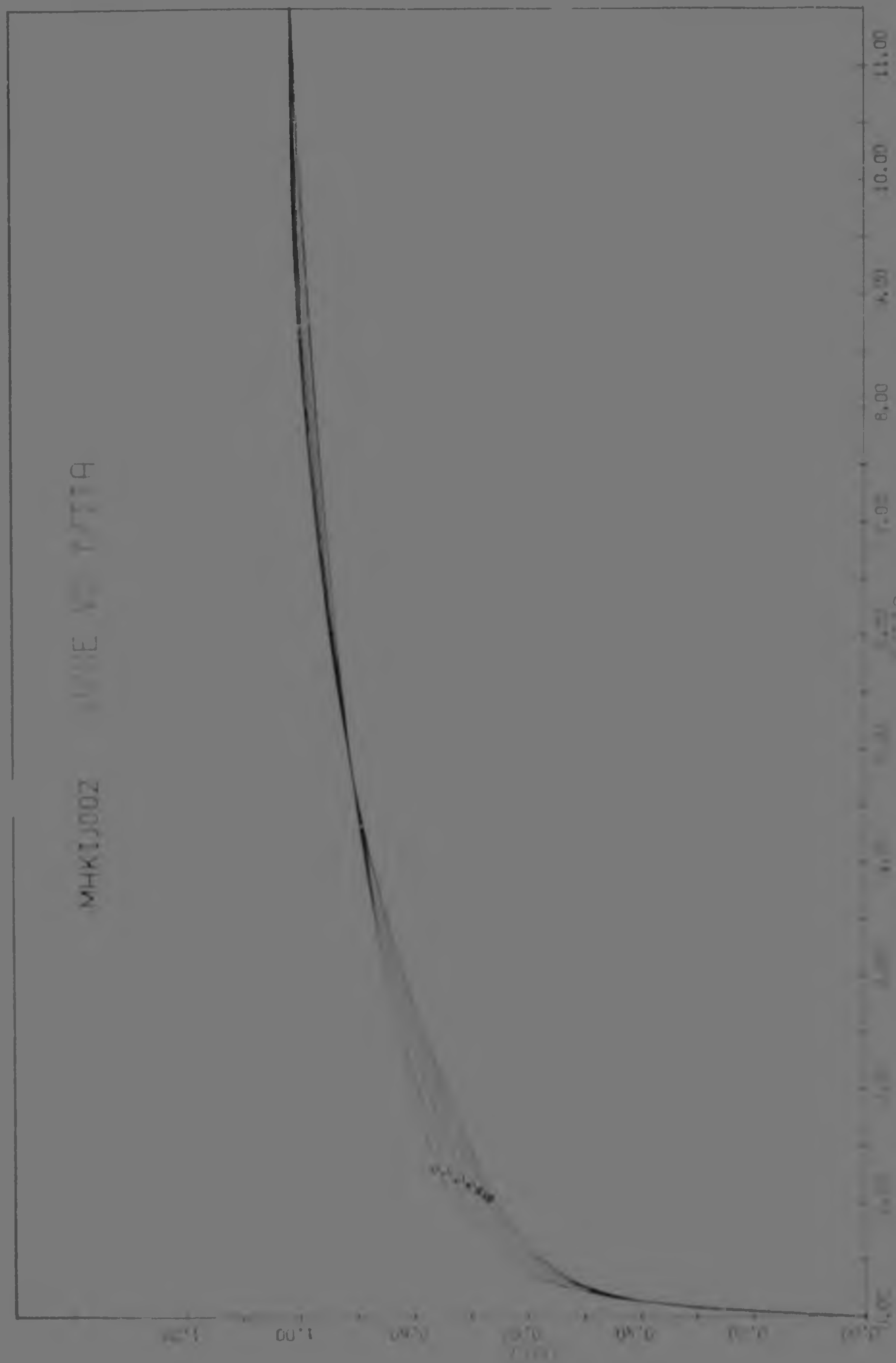

FIG 7.21B : INJECTED TURBULENT PROFILES FOR
U_∞ = 17 m/s, F = 0,002

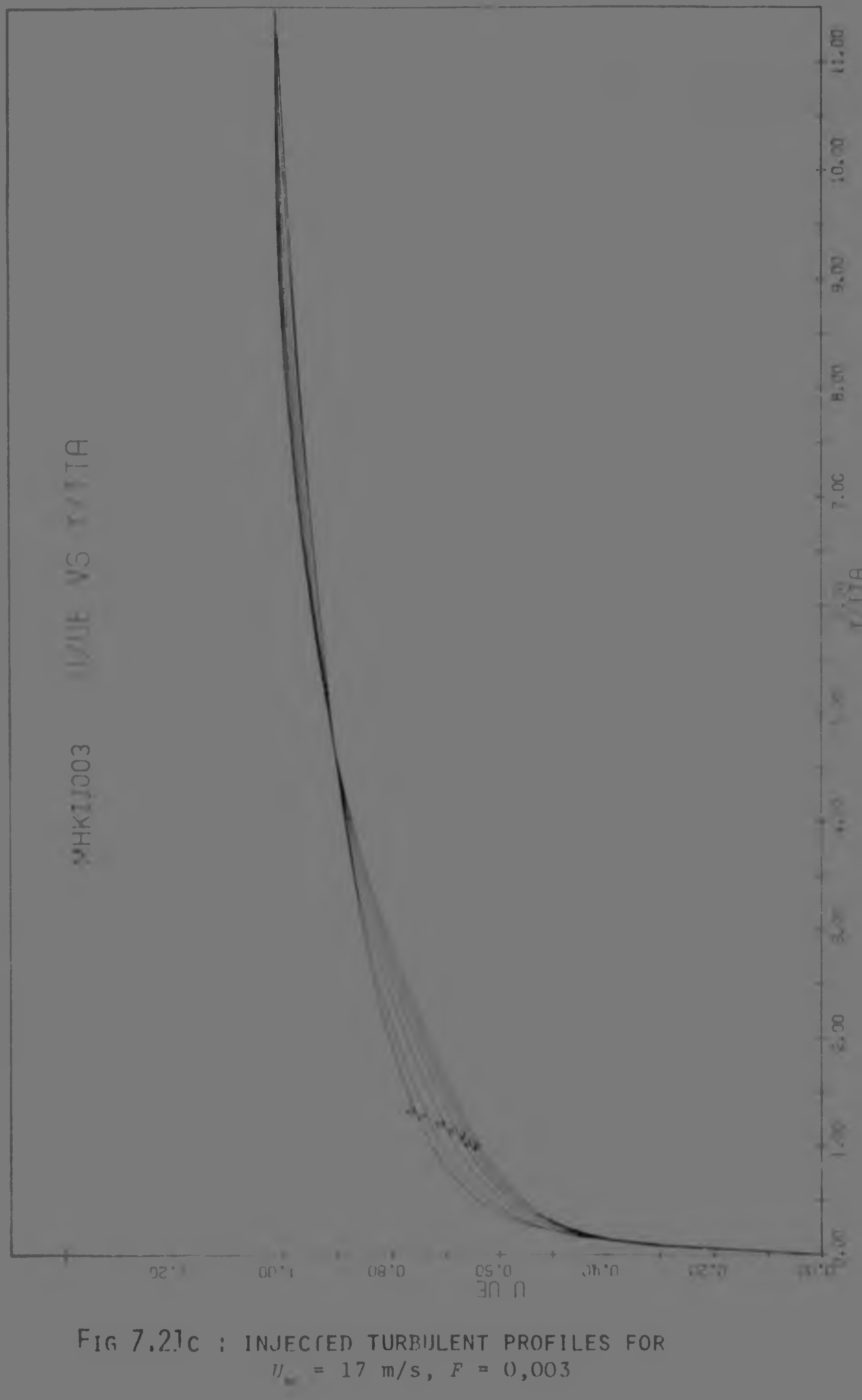

FIG 7.21c : INJECTED TURBULENT PROFILES FOR
U_{∞} = 17 m/s, F = 0,003

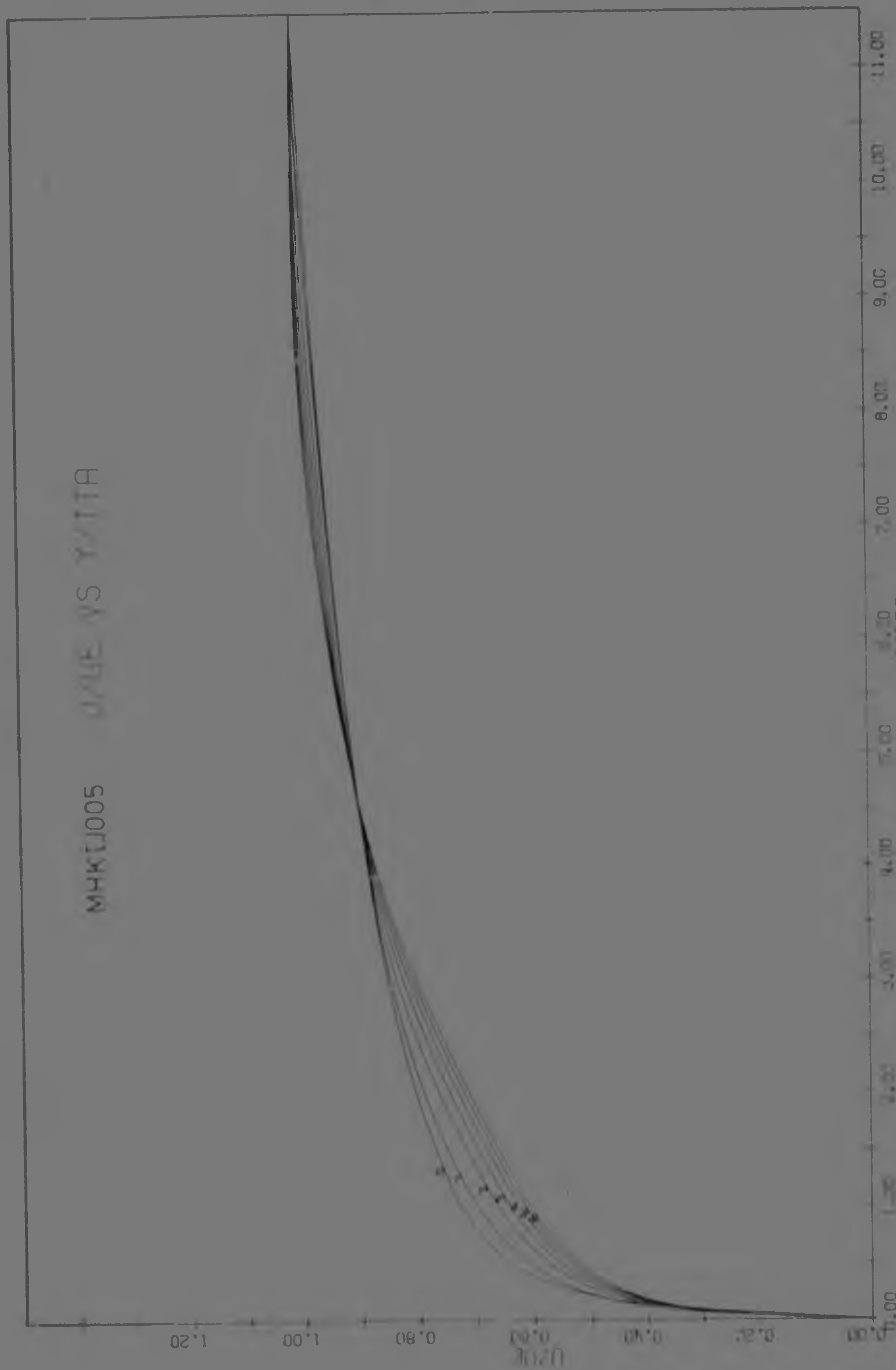

FIG 7.21D : INJECTED TURBULENT PROFILES FOR $U_\infty = 17$ m/s, $F = 0{,}005$

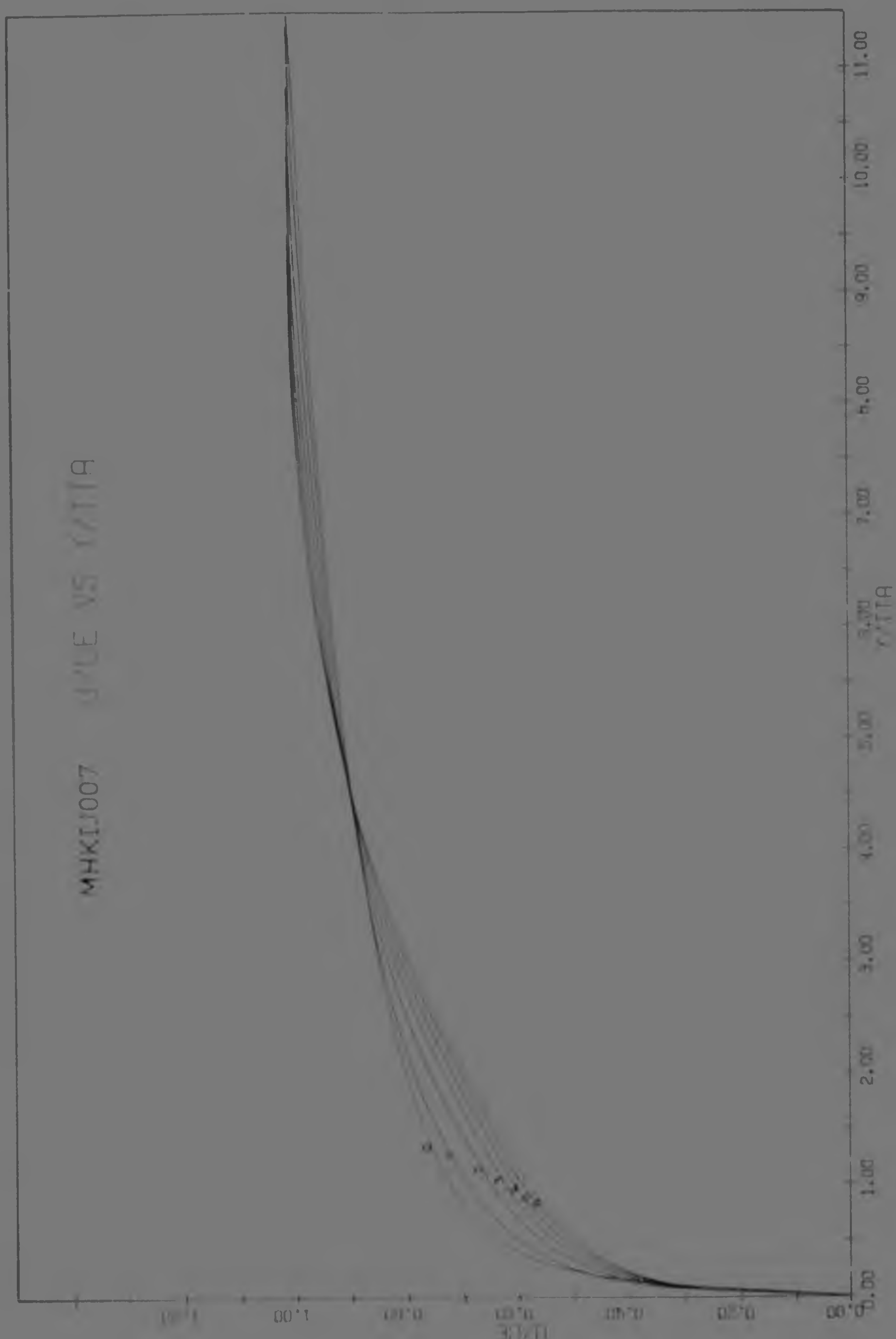

FIG 7.21E : INJECTED TURBULENT PROFILES FOR U_{∞} = 17 m/s, F = 0,007

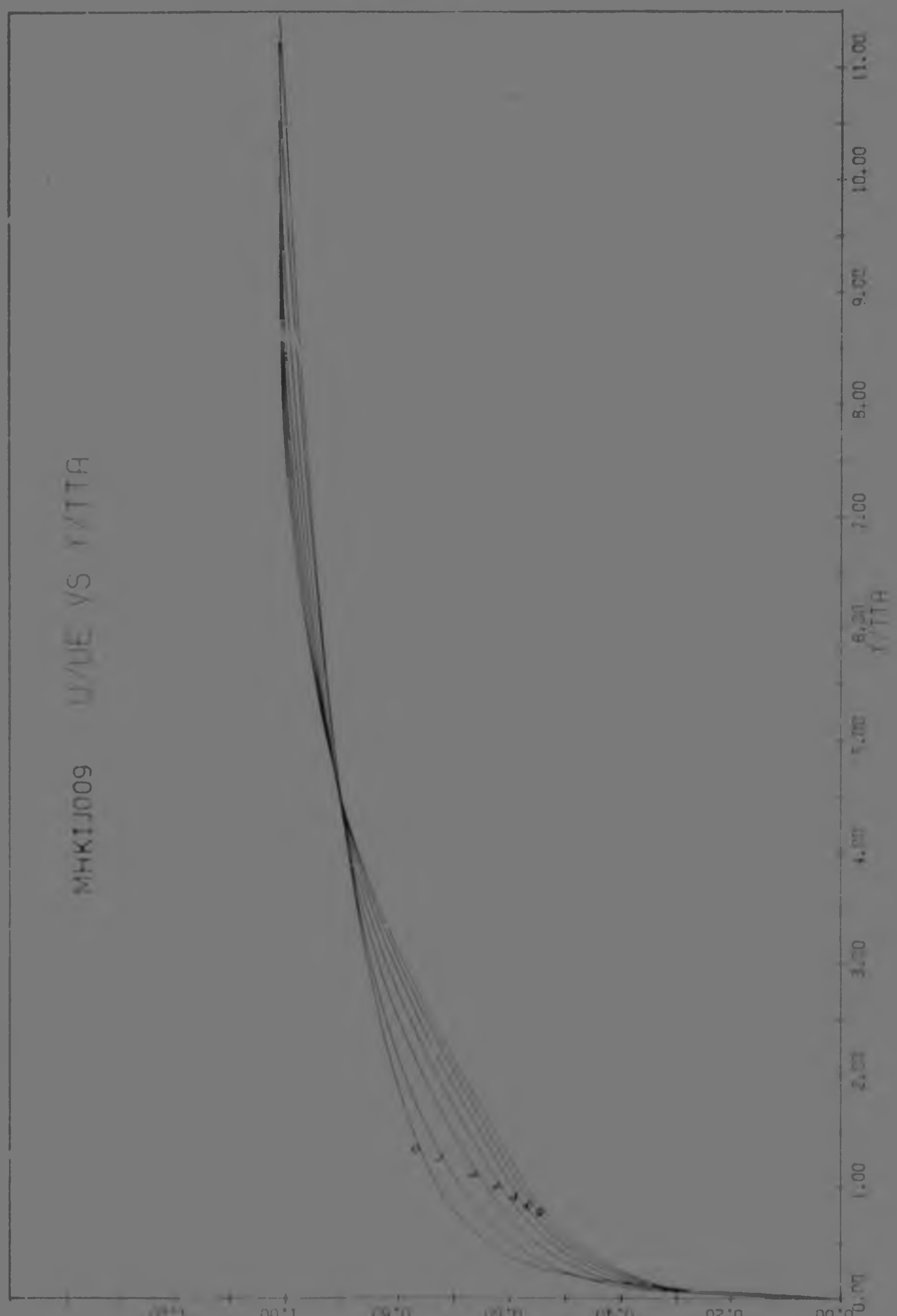

FIG 7.21F : INJECTED TURBULENT PROFILES FOR
$U_\infty = 17$ m/s, $F = 0{,}009$

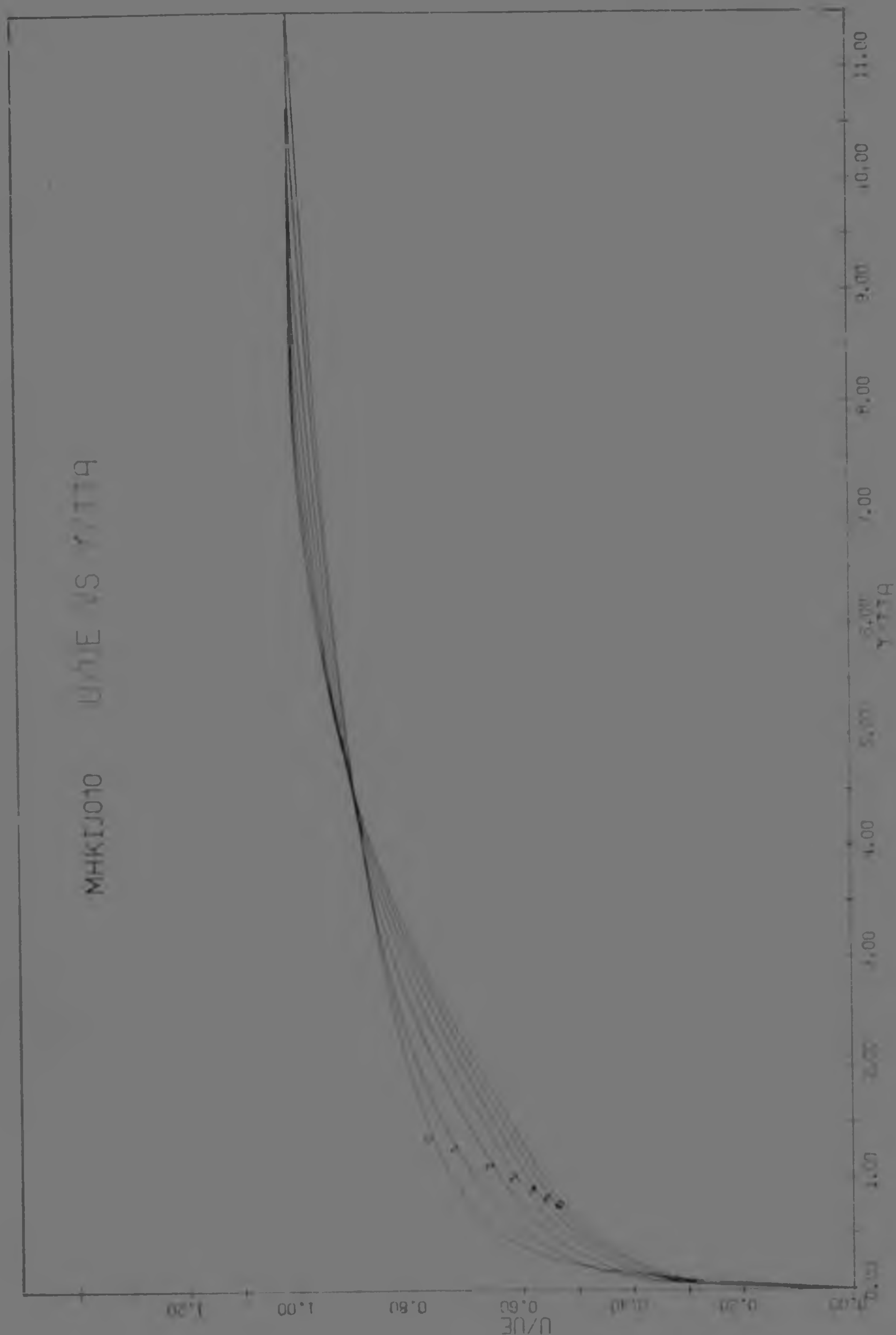

FIG 7.21G : INJECTED TURBULENT PROFILES FOR U_∞ = 17 m/s, F = 0,010

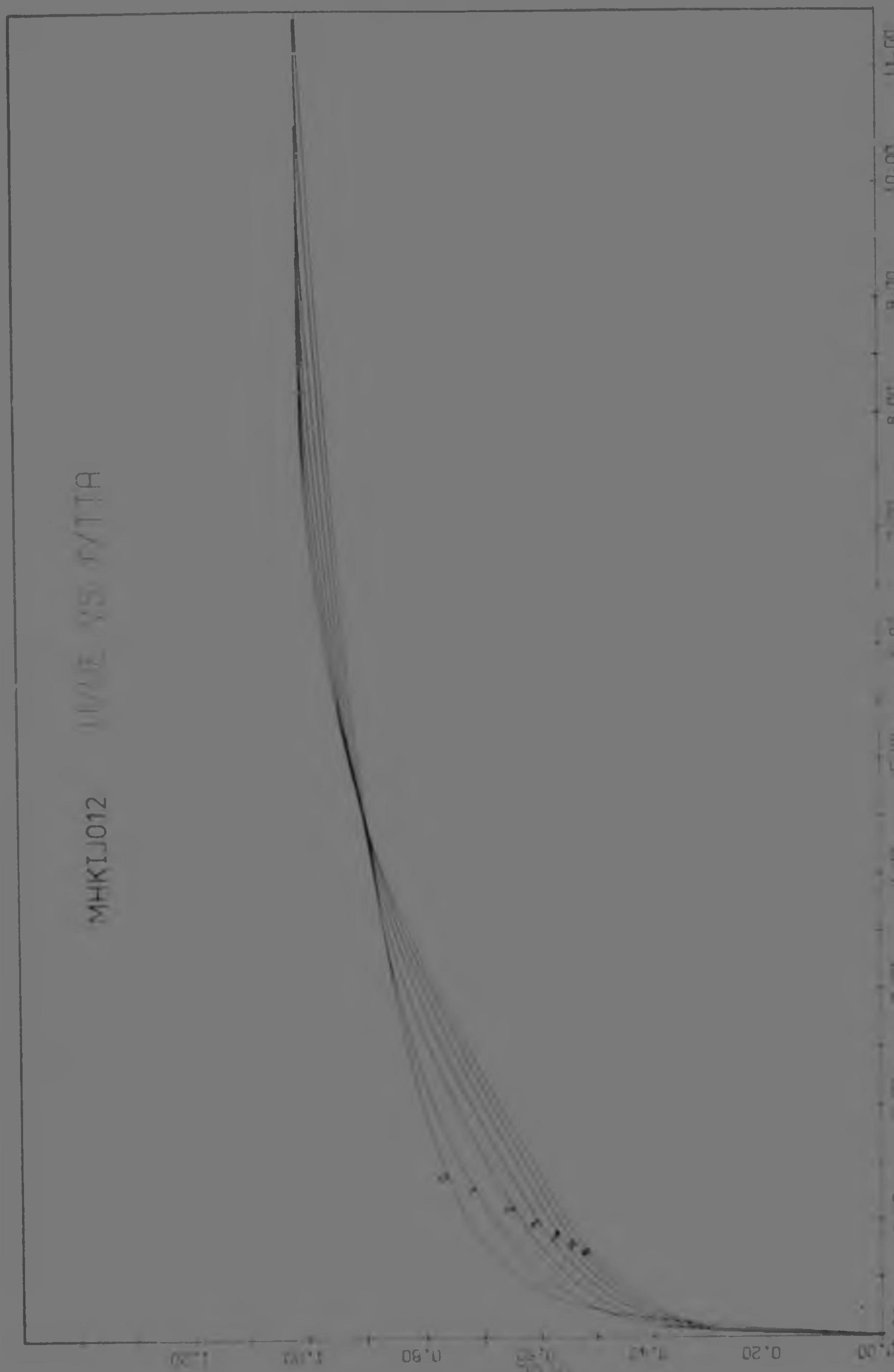

FIG 7.21H : INJECTED TURBULENT PROFILES FOR
U_{∞} = 17 m/s, λ = 0,012

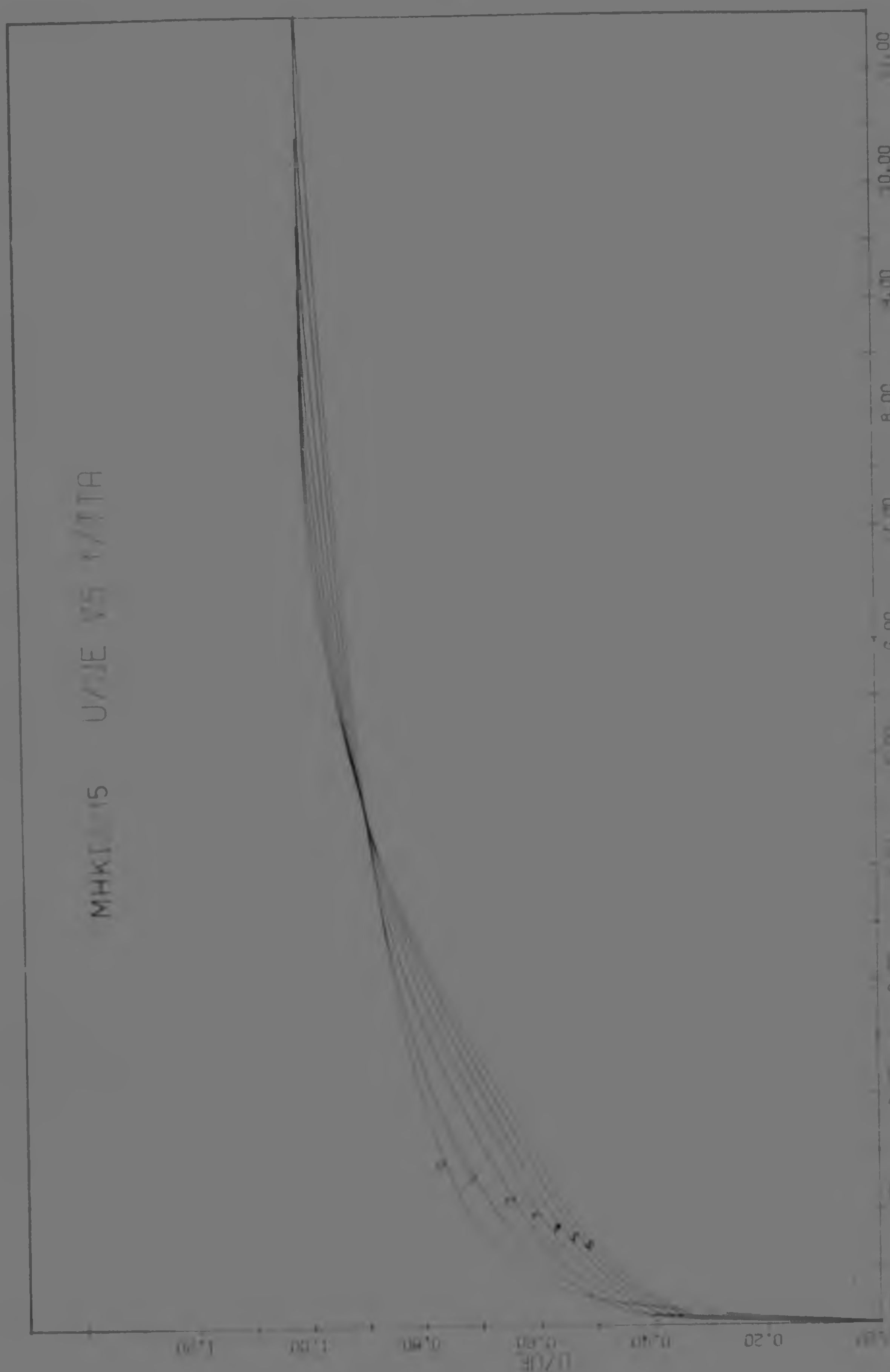

FIG 7.2J1 : INJECTED TURBULENT PROFILES FOR
U_∞ = 17 m/s, F = 0,015

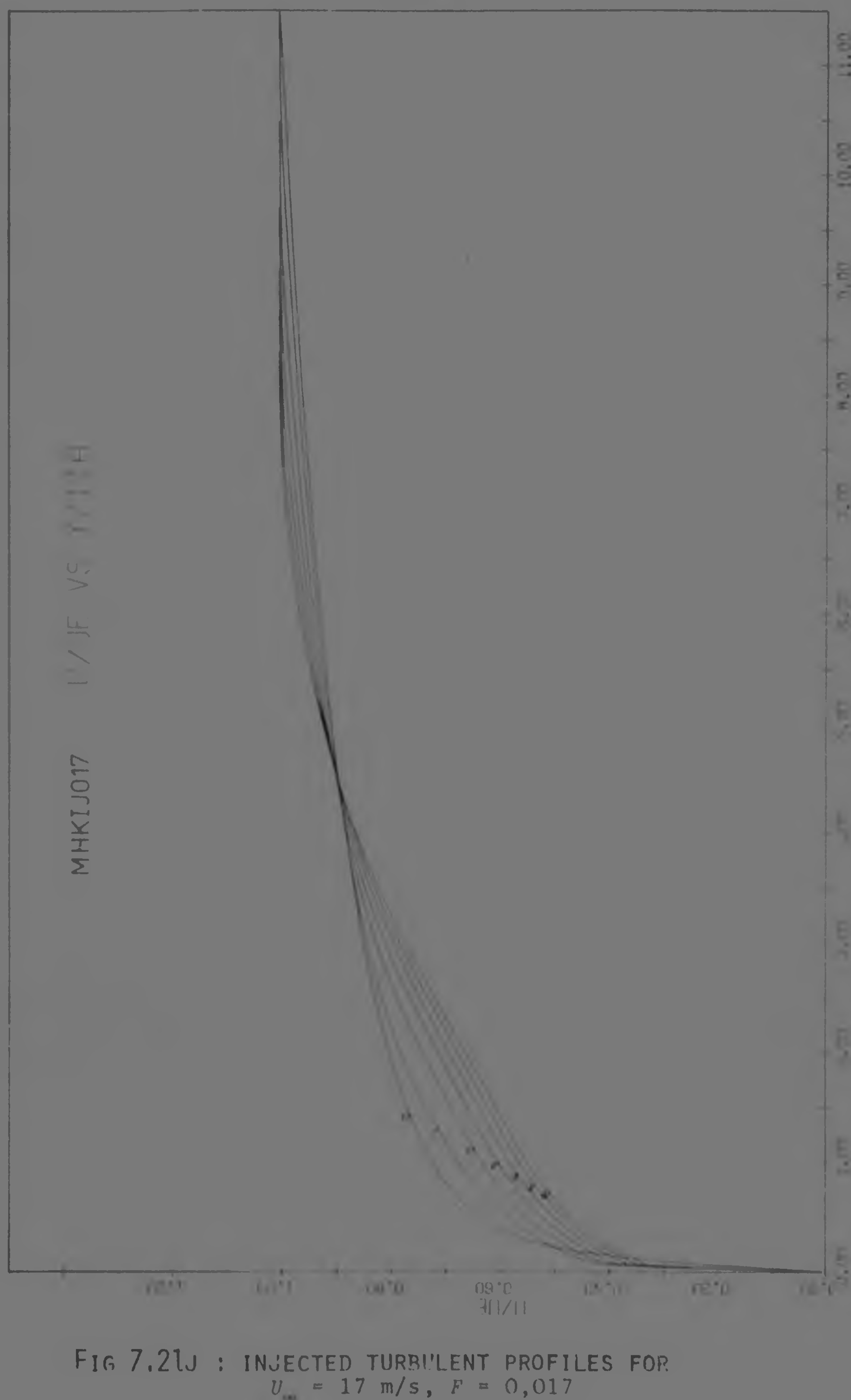

FIG 7.21J : INJECTED TURBULENT PROFILES FOR
U_{∞} = 17 m/s, F = 0,017

By using the approximat[illegible] ϕ'' as described, the programme was remarkedly s[illegible], solving for injection ratios up to F = 0,017. These high injection ratios have not been reported in the literature, and are approaching, if not exceeding, the limit of the boundary layer analysis.

The configuration and condition of the fluid for the main computer runs are reported in Table 7.2. Fig 7.22 shows the eddy viscosity distribution across the boundary layer.

TABLE 7.2 : Key to x-Stations used in Main Runs

Station	x(m)	$\xi \times 10^4$	$Re_x \times 10^5$	Plot symbol
3	0,790	2,416	7,274	0
10	0,825	2,523	7,596	1
20	0,875	2,676	8,056	2
30	0,925	2,829	8,516	3
40	0,975	2,982	8,977	4
50	1,025	3,135	9,437	5
60	1,075	3,288	9,898	6

U = 17 m/s
du/dx = 0 $^1/s$
ρ = 0,9971 kg/m^3
μ = 1,823 kg/ms
XTR = 0,8 m
IY = 100
K = 1,025
H = 0,065
DX = 0,005

7.4.2 Some additional runs

A run with injection and pressure gradient was performed - the results presented in Fig 7.23. MHKIJ003 was the comparable run with du_e/dx = 0 $^1/s$, and considering the shape factors at the same x stations show the difference very clearly, e.g. Station 60 : H_o = 1,45, $H_{du/dx=10}$ = 1,36. δ grew at a much slower rate (32,4 mm and 25,2 mm respectively), which is as expected.

MHKLONG3 and MHKLONG5 were runs in which an uninterrupted porous plate was simulated. The porous plate started at x = 0,312 m. This was improved in MHKTEST3, which is compared with the Mickley and Davis results for their run C-3-50. See Fig 7.26.

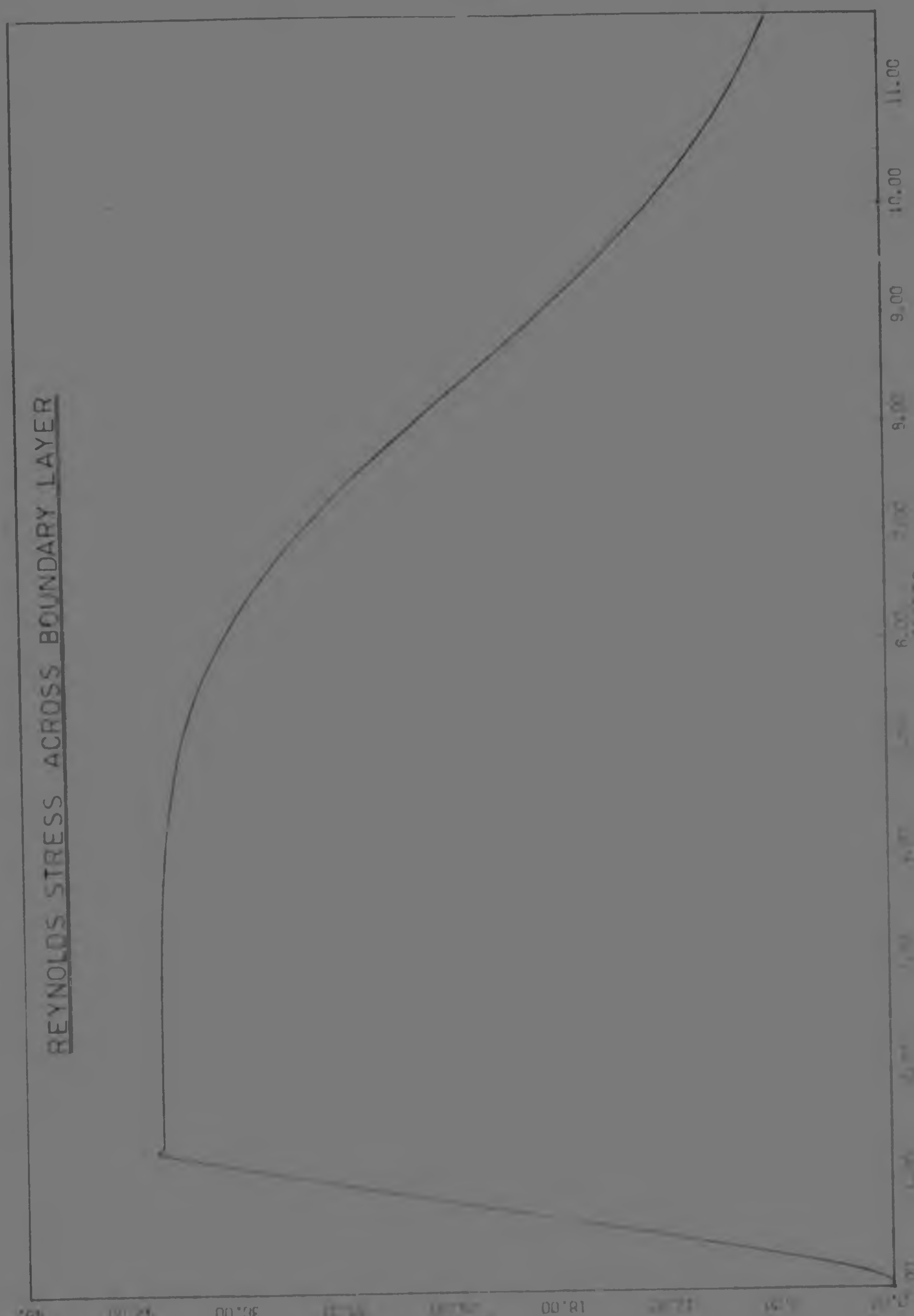

FIG 7.22 : EDDY-VISCOSITY ACROSS THE BOUNDARY LAYER
AT x = 0,790 m, U_∞ = 17 m/s

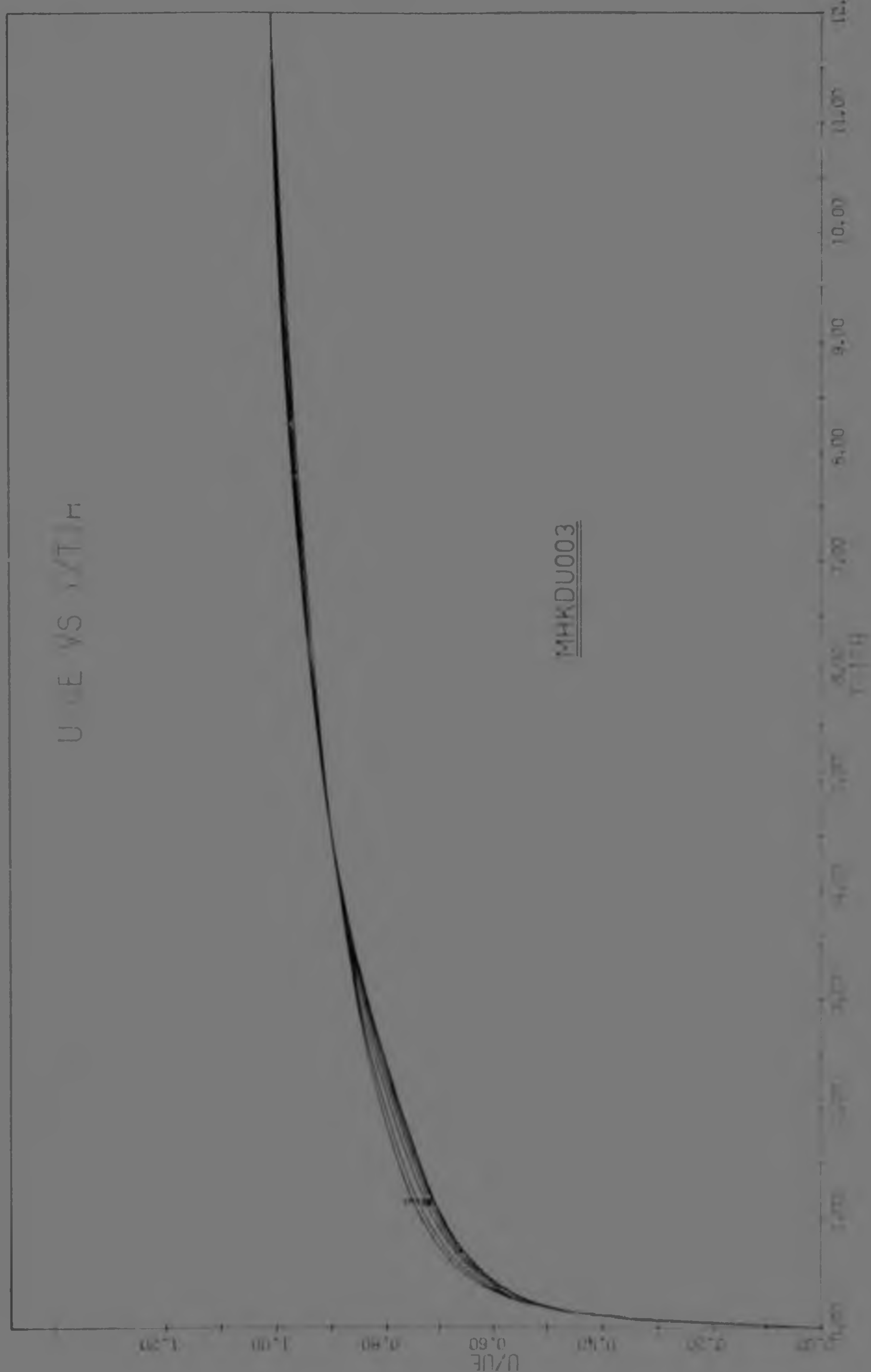

FIG 7.23 : VELOCITY PROFILE WITH INJECTION AND PRESSURE GRADIENT

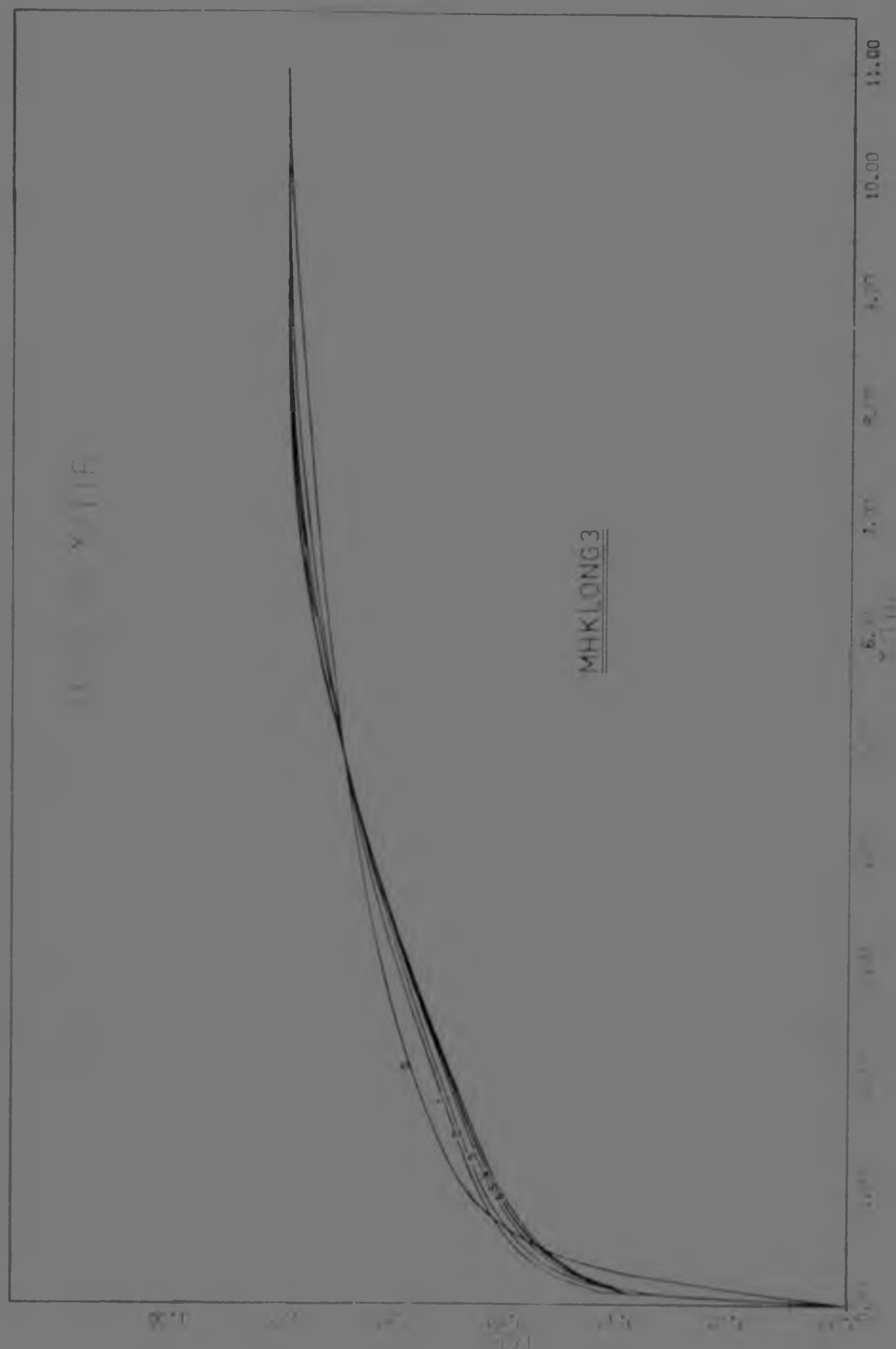

FIG 7.24 : VELOCITY PROFILE WITH INJECTION
STARTING AT x = 0,312 m

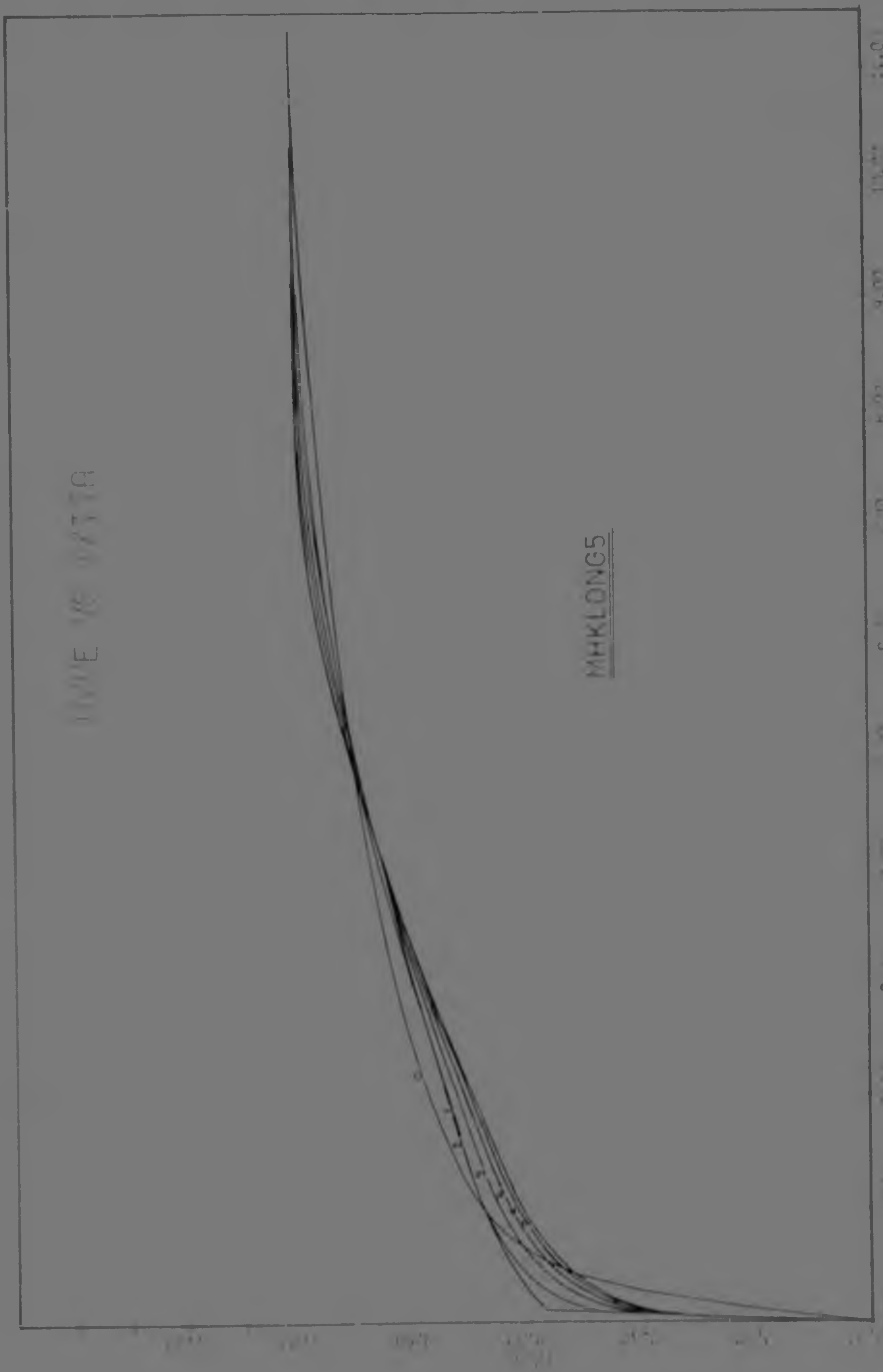

FIG 7.25 : VELOCITY PROFILE WITH INJECTION STARTING AT x = 0,312 m

TABLE 7.3 : Comparison Table

MHKTEST 3 STATION 60				MICKLEY AND DAVIS C-3-50 STATION H			
Re_θ	δ (mm)	θ (mm)	H	Re_θ	δ	θ (mm)	H
2687	25,87	2,94	1,50	2830	22,86	2,85	1,46

This is for the final station of run MHKTEST3, and Re_θ was still somewhat below that of the Mickley and Davis experiment. δ was again high, and hence also θ. The profiles compare well, and it is expected that if Re_θ were more accurately matched, the correspondence would be even better.

The programme was thus shown to produce results which compared well with experiment. Qualifying the programme more extensively would require many more runs, changing the free stream conditions and injection ratio, and finding similar experimental profiles. Note that the computer was using local (Johannesburg) density for air, which was why Re_θ was lower than that of Mickley and Davis given in Table 7.3, for similar values of θ and U_∞.

To allow smaller step lengths to be used, a thinner boundary layer was necessary. For this reason the main runs were performed from x=0,790 m, ie. fully turbulent flow, but δ≈23 mm, whereas the experiment produced δ~45mm. The latter would require a much coarser grid, and hence loss of accuracy. It was therefore not possible to compare the main runs with the experimental results. However, the trend of the 'transition' region from impermeable wall to injected flow obtained experimentally was clearly reflected by the computer results.

Skin friction results were thought to be in error by orders of magnitude. As presented, the programme calculated ϕ''_W from a second order fit, which was very satisfactory for the unblown profile. If Fig 5.9 is a correct representation of u, then a linear fit with very small step length at the wall would produce better results.

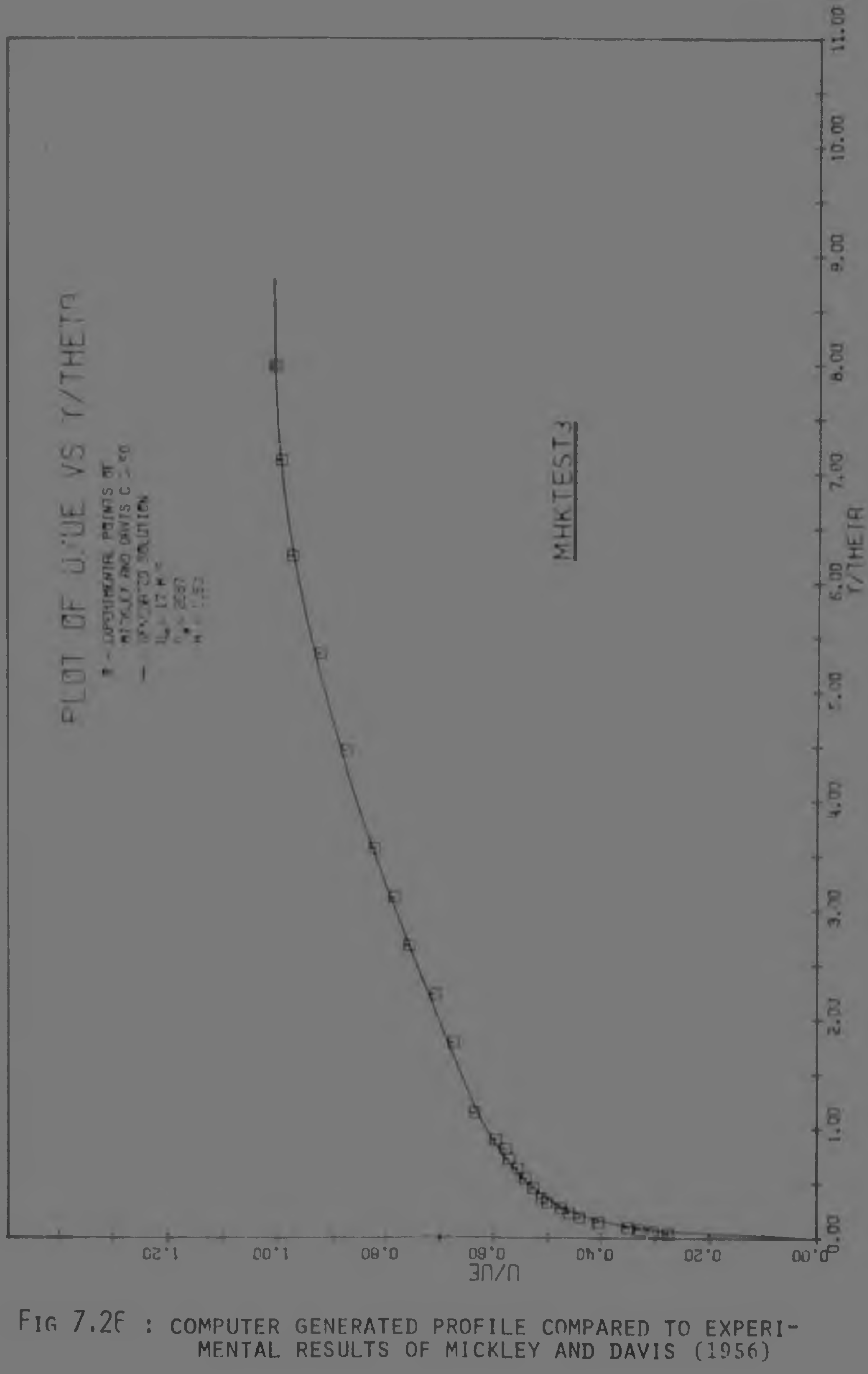

FIG 7.26 : COMPUTER GENERATED PROFILE COMPARED TO EXPERIMENTAL RESULTS OF MICKLEY AND DAVIS (1956)

CHAPTER 8

CONCLUSIONS

8.1 Experimental Features

A two dimensional, open circuit wind tunnel was designed, built and commissioned. A free stream velocity of 21 m/s could be obtained in the working section. To simulate the conditions described on page [illegible], a turbulent boundary layer was produced on a flat plate, which was interspersed with a porous plate. The boundary layer thus encountered injection, which was introduced through the porous plate.

Using the hot wire anemometer, a transverse velocity profile was obtained, and showed that the flow was two dimensional. The turbulence intensity was better than 0.[illegible], which is less than the expected level for this type of tunnel (ref. Schlichting, 1968). Measured energy spectra at a number of free stream velocities compared favourably with accepted theoretical predictions and experimental data.

Velocity profiles on the smooth flat plate were ascertained and shown to follow the profiles predicted by the Thompson two parameter family of cu[illegible].

To further qualify the performance of the tunnel, profiles with injection were plotted on the Bilog axes suggested by Black and Sarnecki, together with experimental data of Mickley and Davis (1956). This allowed direct comparison with other authors work, and also showed the development of the profile with increasing injection. Furthermore, the need for accurate skin friction information was highlighted.

8.2 Velocity Profiles and General Experimental Results

Velocity profiles were measured for a range of free stream velocities and injection ratios. By using different grades of porous plate, the roughness of the wall was also varied. A set of data for the turbulent boundary layer with uniform injection was established. By partially blocking the lower surface of the porous plate, velocity profiles with non-uniform injection were ascertained, and compared with the initial set of results.

The experimental results gathered in the region in which the flow encountered the abrupt change in injection and roughness showed that the average velocity in the shear layer decreased with increasing x. The shape parameter H can be used to quantify this change in momentum. Plotting H vs x showed that H increased rapidly with x, with a decrease in slope for larger x. It also showed that H increased with injection ratio. Consideration of the results of Mickley and Davis confirms this result, and indicates that H may asymptote to a constant value for a fixed injection ratio.

When the results for the partially blocked porous plate were compared with the initial set of data, it was found that H was higher for a particular x station at the same average injection ratio. As is explained in the Addendum this result could indicate a lower wall temperature in the case of a heated stream and cold air injection (assuming constant heat transfer). This would be a very desirable result for the applications discussed on page 1, however, this can only be confirmed with extensive additional experimentation.

To the author's knowledge, these tests constituted original work for the following reasons :-

i) The turbulent boundary layer encountered a step change in surface roughness and injection ratio, an intended feature of the test rig. Previous investigators had considered the fully developed turbulent boundary layer with uniform injection.

ii) Partial blockage of the porous plate, thus altering the injection profile, constituted a further controlled parameter. This feature simulated the attachment of the porous matrix to a rigid base, which would thus enable these materials to be used for effusion cooling in highly stressed materials.

A technique for predicting the turbulent boundary layer velocity profile with injection was developed. A two parameter family of curves was presented, which was independent of injection ratio. The results of Mickley and Davis as well as McQuaid were added to these plots, and indicate the existence of a correlation equation over a significant range of injection ratios. It was thought that more experimental data was required before a correlation equation could confidently be deduced.

The lowest point is $H = 1{,}3$, which is the value for the uninjected turbulent boundary layer. As the layer encountered injection, the value of the shape parameter increased, while u/u_{∞} decreased for a fixed value of y/θ. This trend continued until the value at X1 was reached which was very close to the results of Mickley and Davis, whose tests were done in the 'fully developed turbulent boundary layer'.

8.3 Features Pertinent to the Numerically Obtained Results

The momentum equations were solved numerically, and the velocity profiles thus generated were plotted, reflecting the trends determined experimentally, ie. the decrease of velocity in the shear layer with increased injection ratio and distance along the plate. To qualify the programme, various test runs were performed. Firstly, the laminar profile generated was compared with analytical results given in Schlichting. Then a turbulent profile was plotted on semi log axes and compared with established experimental and empirical data. Various test cases were investigated, in which Re_x was varied with and without pressure gradient, and also one in which the computer solution was allowed to march into the transition region.

Finally, runs with injection were performed. One of these was compared with the experimental results of Mickley and Davis. In all these comparisons, correlation was excellent, and the programme was considered to yield accurate velocity profiles.

The programme was run for a range of injection ratios of F = 0,017. This was the highest ratio investigated experimentally, and was thought to be at the limit of the assumption of the analysis. It should be noted that F = 0,017 is significantly higher than any injection ratio encountered in the literature survey, both in experimental or numerical work. The programme remained exceptionally stable, even at high values of F.

CHAPTER 9

SUGGESTIONS FOR FURTHER WORK

1. Modifications to the wind tunnel, which would result in a thin boundary layer arriving in the entry section, allowing greater control.

2. Measurement of the local skin friction by direct means, so that this matter may be cleared up satisfactorily. Initially, the effect of surface roughness with transpiration would have to be determined. If a floating element balance was used, the element must be made of porous material with the same roughness as the plate; and with injection at its surface.

3. To establish the heat transfer characteristics of step change, distributed injection, with and without blockage, tests must be done with a heated mainstream. This latter provision is intended to obviate the inverted temperature profile which results from heating the transpiration flow. The inverted temperature profile acts as a turbulence inhibiter, thus affecting the heat transfer mechanism.

4. The computer programme requires an improved finite difference technique for obtaining the second derivative, especially at the wall. From this, more realistic values of c_f may be expected. A more sophisticated turbulence transport equation will be necessary to account for surface roughness.

5. Alterations to the programme could be designed to allow for enclosed flow, and for more complicated pressure gradient situations.

6. By including the Energy Equation, the heat transfer to the plate could be calculated.

7. A deeper understanding of the flow in the porous matrix should be obtained, mainly from experiment. The spread of the jet, and the exit velocity of the air at the exposed surface should be studied.

8. Turbine blades in cascade with porous inserts should be manufactured and tests on heat transfer characteristics done. These could be compared with tests for blades with discrete hole injection.

APPENDIX A

A1 Transformation of the Momentum Equation

For convenience, the continuity and momentum equations of section 4.2 are restated here :-

Continuity : $\frac{\delta u}{\delta x} + \frac{\delta v}{\delta y} = 0$ .... [A1.1]

Momentum : $u\frac{\delta u}{\delta x} + v\frac{\delta u}{\delta y} = u_e\frac{\delta u_e}{\delta x} + \frac{\delta}{\delta y}(\nu\frac{\delta u}{\delta y} - \overline{u'v'})$ [A1.2]

Numerous transformations exist for equation A1.2. a popular one is the transformation to the Von Mises plane. The equation takes on the form of an unsteady heat-conduction equation. The disadvantage in solving an equation which is pseudo-elliptic (ie. the entire flow-field has to be solved simultaneously), is the excessive computer time used. A transformation similar to the Falkner-Skan solution could be used in a finite difference scheme that marches in the direction of predominant flow. In this way, conditions at each successive step could be set as required, e.g. surface roughness, injection (steady or varying with x), and also step length.

Following the treatment of Cebeci and Smith (1970a), the Levy-Lees transformation was used. This resulted in combining two independent variables, u and , shortened the abscissa and lengthened the ordinate.

The Levy-Lees transformation for flat-plate, incompressible flow is :-

$d\xi = \rho\mu u_e dx; \quad d\eta = \frac{\rho u_e}{(2\xi)^{\frac{1}{2}}} dy$ .... [A1.3]

Define a dimensionless stream function, f

$\psi(x,y) = (2\xi)^{\frac{1}{2}} f(\xi,\eta)$ .... [A1.4]

ψ is the stream function which satisfies the continuity equation :-

$$\frac{\delta\psi}{\delta y} = \rho u \ ; \quad \frac{\delta\psi}{\delta x} = -\rho v \qquad \ldots\ldots\ [A1.5]$$

Substituting A1.5 into A1.2, for μ and ρ constant :

$$\frac{1}{\rho^2}\frac{\delta\psi}{\delta y}\cdot\frac{\delta^2\psi}{\delta x\delta y} - \frac{1}{\rho^2}\frac{\delta\psi}{\delta x}\cdot\frac{\delta^2\psi}{\delta y^2} = u_e\frac{du_e}{dx} + \frac{\nu}{\rho}\cdot\frac{\delta}{\delta y}[(1 + \varepsilon^+)\frac{\delta^2\psi}{\delta y^2}] \quad [A1.6]$$

With $\varepsilon^+ = \varepsilon/\nu$

Hence :-

$$\frac{\delta\psi}{\delta y}\cdot\frac{\delta^2\psi}{\delta x\delta y} - \frac{\delta\psi}{\delta x}\cdot\frac{\delta^2\psi}{\delta y^2} = \rho^2 u_e\frac{du_e}{dx} + \nu\frac{\delta}{\delta y}[(1 + \varepsilon^+)\frac{\delta^2\psi}{\delta y^2}] \quad \ldots\ [A1.7]$$

From A1.5 (see Cebeci and Smith, 1970a) :-

$$\left.\begin{aligned} \frac{\delta}{\delta x} &= \rho\mu u_e\left(\frac{\delta}{\delta\xi} + \frac{\delta\eta}{\delta\xi}\cdot\frac{\delta}{\delta\eta}\right) \\ \frac{\delta}{\delta y} &= \frac{\rho u_e}{(2\xi)^{\frac{1}{2}}}\frac{\delta}{\delta\eta} \end{aligned}\right\} \qquad \ldots\ldots\ [A1.8]$$

From A1.4 :-

$$\left.\begin{aligned} \frac{\delta\psi}{\delta\xi} &= (2\xi)^{\frac{1}{2}}\left(\frac{f}{2\xi} + \frac{\delta f}{\delta\xi}\right) \\ \frac{\delta\psi}{\delta\eta} &= (2\xi)^{\frac{1}{2}}f' \end{aligned}\right\} \qquad \ldots\ldots\ [A1.9]$$

Using [A1.9] and $\beta=(2\xi).(du_e/d\xi)/u_e$, eqn.[A1.7] becomes :

$$[(1 + \varepsilon^+)f'']' + ff'' + \beta(1 - f'^2) = (2\xi)[f'\frac{\delta f'}{\delta\xi} - f''\frac{\delta f}{\delta\xi}] \qquad \ldots\ldots\ [A1.10]$$

where the prime denotes $\delta/\delta\eta$, and $f' = \delta f/\delta\eta = u/u_e$.

The left hand side of [A1.10] will be recognised as the solution obtained by Falkner and Skan (1931) for the laminar boundary layer with $u_e(x) \propto x^m$ (ie. the potential flow was proportional to a power of the length measured from the stagnation point).

Now introduce a translated stream function, ϕ. (This was done to improve the numerical computation.)

$$\left.\begin{aligned} f &= \phi + \eta \\ f' &= \phi' + 1 \\ f'' &= \phi'' \end{aligned}\right\} \qquad \text{.......} \; [A1.11]$$

Substitute [A1.11] into [A1.10]:-

$$[(1 + \varepsilon^{+})\phi'']' + (\phi + \eta)\phi - \beta.\phi'(\phi' + 2) = 2\xi[(\phi' + 1)\delta\phi'/\delta\xi - \phi''\delta\phi/d\xi] \qquad \text{.......} \; [A1.12]$$

This equation was also given as [4.6.1], and is an o.d.e. in η at $\xi = \xi_n$.

A2 The Finite Difference Approximations

Consider a function f at grid points i-2, i-1, i, ... etc., and let the distance between these points be h_1, h_2, h_3 and h_4 :-

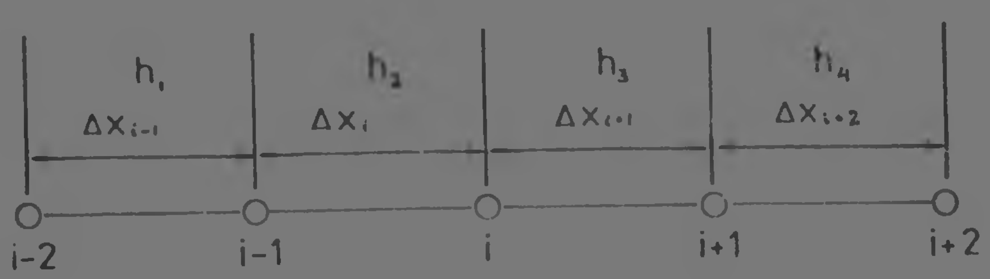

FIG A2.1 : SKETCH OF GRID POINTS, SHOWING NOMENCLATURE

Using Taylor's series to express :-

$$f(x_{i+1}) = f(x_i) + h_3 f'(x_i) + \frac{h_3{}^2 f''(x_i)}{2!} + O(h_3{}^3) \qquad [A2.1]$$

$$f(x_{i-1}) = f(x_i) - h_2 f'(x_i) + \frac{h_2^2}{2!} f''(x_i) + O(h_2^3) \text{...[A2.2]}$$

By doing the following manipulation : [A2.1] x h_2^2 - [A2.2] x h_3^2 obtain :

$$f'(x_i) = \frac{-h_3 f(x_{i-1})}{h_2(h_2 + h_3)} - \frac{(h_2 - h_3)}{h_2 h_3} f(x_i) + \frac{h_2 f(x_{i+1})}{h_3(h_2 + h_3)} + O(h^2)$$

.... [A.2.3]

This equation was written for $h_2 \neq h_3$, which creates some difficulty in expressing the order of error. In [A2.3] it is approximately $O(h_2 . h_3)$, and if $h_3 = h_2 = h$, $O(h^2)$.

Eliminating f' from [A2.1] and [A2.2] :

$$f''(x_i) = \frac{2f(x_{i-1})}{h_2(h_2+h_3)} - \frac{2f(x_i)}{h_2 h_3} + \frac{2f(x_{i+1})}{h_3(h_2+h_3)} \quad \text{..... [A2.4]}$$

This equation has an error $O(h_2)$ or $O(h_3)$, ie. much less accurate than [A2.3].

Equations derived in a similar manner are :-

$$f''(x_{i+1}) = \frac{2f(x_i)}{h_3(h_3+h_4)} - \frac{2f(x_{i+1})}{h_3 h_4} + \frac{2f(x_{i+2})}{h_4(h_3+h_4)} \quad \text{.... [A2.5]}$$

$$f''(x_{i-1}) = \frac{2f(x_{i-2})}{h_1(h_1+h_2)} - \frac{2f(x_{i-1})}{h_1 h_2} + \frac{2f(x_i)}{h_2(h_1+h_2)} \quad \text{.... [A2.6]}$$

Considering Fig A2.1 again, and using eqn.[5.3.3]

$$\left.\begin{aligned} h_1 &= \Delta x_{i-1} = h.K^{i-3} \\ h_2 &= \Delta x_i = h.K^{i-2} \\ h_3 &= \Delta x_{i+1} = h.K^{i-1} \\ h_4 &= \Delta x_{i+2} = h.K^{i} \end{aligned}\right\} \quad \text{...... [A2.7]}$$

Where h is the first step of the η grid.

Substituting [A2.7] into [A2.3] and [A2.4] :-

$$f'(x_i) = \frac{-f(x_{i-1})}{hK^{i-3}(1+K)} - \frac{(1-K)f(x_i)}{hK^{i-1}} + \frac{f(x_{i+1})}{hK^{i-1}(1+K)} \quad .... [A2.8]$$

$$f''(x_i) = \frac{2f(x_{i-1})}{h^2K^{2i-4}(1+K)} - \frac{2f(x_i)}{h^2K^{2i-3}} + \frac{2f(x_{i+1})}{h^2K^{2i-3}(1+K)} \quad [A2.9]$$

Each term in the last two equations could be divided into three parts, namely f_i, a constant in K and h, and a co efficient in i. This fact was used to simplify the equations. The first term of equation [A2.8] thus becomes :

$$\frac{-f(x_{i-1})}{hK^{i-3}(1+K)} = -f(x_{i-1}).A = -f(x_{i-1}).\frac{A1}{K^i} \quad ..... [A2.10]$$

So $A1 = -K^3/h(1+K)$, and all other coefficients dependent on h and K were calculated only once, ie. in subroutine MK002.

Because the x-stations were not restrained as the η points were, coefficients required for derivatives in the ξ-direction were calculated at each new station.

The coefficients that appeared in equation [5.4.2], are listed below :-

$$\left.\begin{aligned}
A &= \frac{-K^3}{h(1+K)}.\frac{1}{K^i} = \frac{A1}{K^i} \\
B &= \frac{-(1-K)K}{h}.\frac{1}{K^i} = \frac{B1}{K^i} \\
C &= \frac{K}{h(1+K)}.\frac{1}{K^i} = \frac{C1}{K^i} \\
D &= \frac{2K^4}{h^2(1+K)}.\frac{1}{K^{2i}} = \frac{D1}{K^{2i}} \\
E &= \frac{-2K^3}{h^2}.\frac{1}{K^{2i}} = \frac{E1}{K^{2i}} \\
F &= \frac{2K^3}{h^2(1+K)}.\frac{1}{K^{2i}} = \frac{F1}{K^{2i}}
\end{aligned}\right\} \quad .... [A2.11]$$

$$\left.\begin{aligned}
X1 &= \frac{2K^6}{h^2(1+K)} \cdot \frac{1}{K^2 i} \\
X2 &= \frac{-2K^5}{h^2} \cdot \frac{1}{K^2 i} \\
X3 &= \frac{2K^5}{h^2(1+K)} \cdot \frac{1}{K^2 i} \\
X4 &= \frac{2K^2}{h^2(1+K)} \cdot \frac{1}{K^2 i} \\
X5 &= \frac{-2K}{h^2} \cdot \frac{1}{K^2 i} \\
X6 &= \frac{2K}{h^2(1+K)} \cdot \frac{1}{K^2 i}
\end{aligned}\right\} \quad \ldots\ldots\ldots \text{[A2.11]}$$

Coefficients starting with X were not split up into two parts. This had been done initially, in a different form, and is the reason for real G1, H1, I1, J1, K1 being defined in subroutine MK002.

The streamwise derivatives were calculated as follows :-

$$\left.\frac{\delta\phi_i}{\delta\xi}\right|_n = L\phi_{n-2,i} + M\phi_{n-1,i} + N\phi_{n,i} \quad \ldots\ldots \text{[A2.12]}$$

$$\left.\frac{\delta\phi'_i}{\delta\xi}\right|_n = L\phi'_{n-2,i} + M\phi'_{n-1,i} + N\phi'_{n,i} \quad \ldots\ldots \text{[A2.13]}$$

These equations were obtained in a manner very similar to the derivation of [A2.3]. They were backward difference equations, and the step length remained variable.

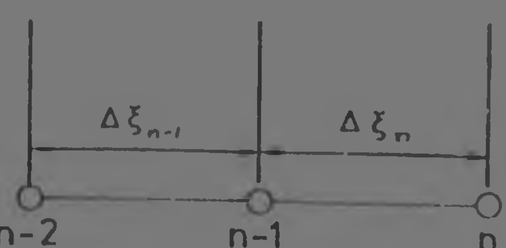

FIG A2.2 : SKETCH OF ξ GRID POINTS

$$\frac{\delta f(\xi_n)}{\delta \xi} = \frac{\Delta\xi_n f(\xi_{n-2})}{\Delta\xi_{n-1}(\Delta\xi_n + \Delta\xi_{n-1})} - \frac{(\Delta\xi_{n-1} + \Delta\xi_n) f(\xi_{n-1})}{\Delta\xi_{n-1}.\Delta\xi_n}$$

$$+ \frac{(\Delta\xi_{n-1} + 2\Delta\xi_n) f(\xi_n)}{\Delta\xi_n(\Delta\xi_{n-1} + \xi_n)} \qquad \text{....... [A2.14]}$$

Thus :-

$$L = \frac{\Delta\xi_n}{\Delta\xi_{n-1}(\Delta\xi_n + \Delta\xi_{n-1})}$$

$$M = \frac{-(\Delta\xi_{n-1} + \Delta\xi_n)}{\Delta\xi_{n-1}.\Delta\xi_n} \qquad \text{....... [A2.15]}$$

$$N = \frac{(\Delta\xi_{n-1} + 2\Delta\xi_n)}{\Delta\xi_n(\Delta\xi_{n-1} + \Delta\xi_n)}$$

To calculate ϕ_1'', Newton's Divided Difference method was used. The following equation was derived (see Milne-Thomson, 1933), from a second order fit :-

$$\phi_1'' = \frac{\phi_1'-\phi_2'}{\eta_1 - \eta_2} + (\eta_1 - \eta_2)\frac{\left\{\frac{\phi_1'-\phi_2'}{\eta_1 - \eta_2} - \frac{\phi_2'-\phi_3'}{\eta_2 - \eta_3}\right\}}{\eta_1 - \eta_3} \qquad \text{.... [A2.16]}$$

From Chapter 5, ϕ_1 and ϕ_2 were to be determined from boundary conditions. An equation was given for ϕ_1, but ϕ_2 still remained to be calculated. From eqn.[4.6.3], one of the boundary conditions is :-

$$\phi'(\xi,0) = \phi_1' = -1 \qquad \text{........ [A2.17]}$$

Using a very simple finite difference equation :-

$$\phi_1' = \frac{\phi_2 - \phi_1}{\eta_2 - \eta_1} = -1 \qquad \text{....... [A2.18]}$$

$$\therefore \phi_2 = \phi_1 - 1(\eta_2 - \eta_1)$$

[A2.18] did not give very satisfactory results, but by using the divided difference technique, the following relationship was derived :-

$$\phi_2 = \frac{\phi_1 \times K \times (K+2) + \phi_3 - K \times H \times (K+1)}{(K+1)^2} \qquad \text{.... [A2.19]}$$

The unblown profile was checked, and [A2.19] was found to agree to 6 figures. After the experience gained with calculating ϕ_1'' from a second order fit, it was felt that the plot of ϕ vs η should be reconsidered when injected, and a better fit developed for this curve. Although not tested, it was thought that a 4th order fit would be an improvement.

Except at the boundaries, central difference equations were used throughout. Note that these equations were derived to allow calculation of a function at i, and not mid-way between $i-1$ and $i+1$, which would have occurred had the function been calculated from a standard central difference equation for equal step length.

The equations derived were relatively simple, but produced a banded matrix with 5 columns. More complex equations, which become possible for equal step length, would have resulted in more columns in the banded matrix. This would require more core storage and more calculations, with related round-off errors, when solving $[A]\{\phi\} = \{B\}$. For generating the initial turbulent profile, it was found that the unequal step length improved the accuracy significantly. Because $\delta u/\delta y$ was much lower for laminar profiles, equal steps were more suitable for these calculations. This could be obtained by setting $K = 1$.

A3 Flow in Porous Media

One of the important aspects of using porous materials in transpiration cooling, is the need for strengthening the structure. As already suggested, this could be done by attaching the porous matrix to a rigid base with metering holes or slots.

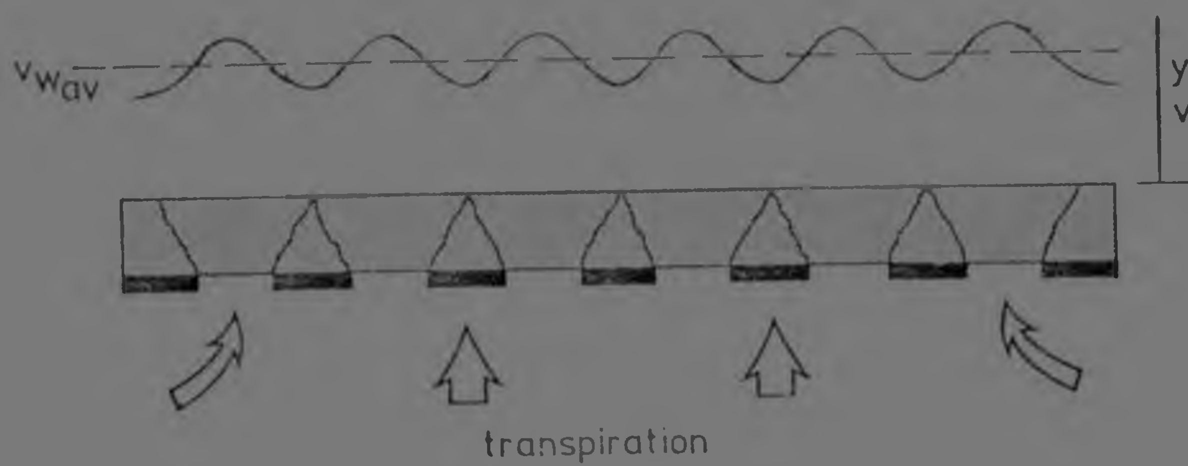

FIG A3.1 : THE POROUS MATRIX ( ) ATTACHED TO A RIGID BASE ( ) WITH METERING SLOTS

In the past, all results for pressure drop through the matrix have been obtained for the unrestricted case, ie, a one-dimensional flow situation. The average velocity at any y value in the porous material was constant. The pressure drop was found to be proportional to the superficial velocity, V_∞, for the so-called laminar region, and to V_∞^2 for the 'turbulent' region. This was found experimentally, and is useful if V_∞ is constant.

The configuration shown in Fig A3.1 was expected to behave very differently. Because the jet is spreading in the matrix, the velocity is changing, and hence also Δp. To design a porous cover for transpiration cooling, it is necessary to know : (i) the spread of the jet with y, and from that, the distance between metering slots or holes to ensure a suitable insulating layer of cool air on the upper surface of the porous material, and (ii) the pressure drop for the two-dimensional flow situation

Two approaches to the problem are possible. The microscopic, analytic approach, or the macroscopic approach, discussed in Appendix A4.

Because a porous matrix is made up of randomly sintered particles with sizes spanning a given tolerance, it is not meaningful to consider the flow at a point. Following

Slattery (1972) the momentum equation was volume averaged, in much the same way that turbulent flows were averaged on a time base.

Two theorems, developed by Slattery (1972), were used, as were the Reynolds rules of averages. The theorems were for the volume average of gradient, and of the divergence, of a second order tensor or a spatial vector field, called $\underline{B}$.

$$\overline{\nabla \underline{\underline{B}}} = \frac{1}{V} \int_{V_f} \nabla \underline{\underline{B}} dV = \nabla \overline{\underline{\underline{B}}} + \frac{1}{V} \int_{S_w} \underline{B}.\underline{n} dS \qquad \ldots\ldots\ [A3.1]$$

$$\overline{\text{div}B} = \frac{1}{V} \int_{V_f} \text{div}\underline{B} d = \text{div}\overline{\underline{B}} + \frac{1}{V} \int_{S_w} \underline{B}.\underline{n} dS \qquad \ldots\ldots\ [A3.2]$$

where V_f is the volume, S_w the surface area.

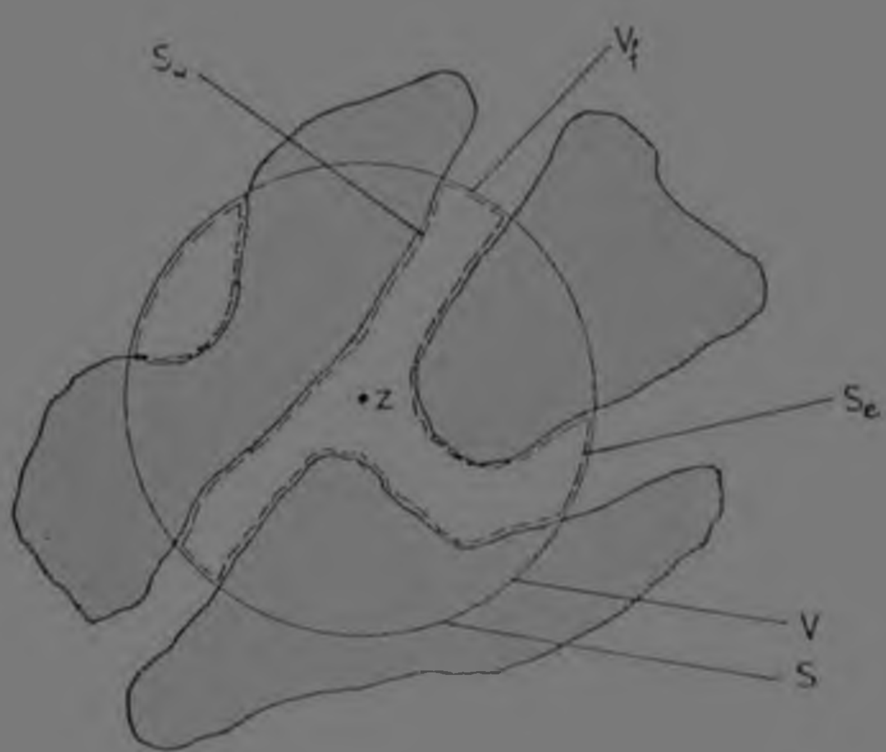

FIG A3.2 : THE POROUS MEDIUM, SHOWING VOLUME V_f, AND THE ENCLOSING SURFACE S. NOTE THAT S MUST ENCLOSE SOLID AND FLUID. S_w COINCIDES WITH THE PORE WALLS. $\underline{n}$ IS THE NORMAL VECTOR.

The Navier-Stokes equation for the steady flow of an incompressible newtonian fluid may be derived from Cauchy's first law of motion (assume no external forces were present) :

$$\rho \mathrm{div}(\underline{v}\,\underline{v})^{1} = -\nabla p + \mu \mathrm{div}(\nabla \underline{v}) \qquad \ldots\ldots\ [A3.3]$$

Taking the local volume average of eqn.[A3.3] :-

$$\frac{1}{V}\int_{V_f} \rho \mathrm{div}(\underline{v}\,\underline{v})\,dV = -\frac{1}{V}\int_{V_f} \nabla p\,dV + \frac{1}{V}\int_{V_f} \mu \mathrm{div}(\nabla \underline{v})\,dV \quad \ldots\ [A3.4]$$

Noting that $(\underline{v}\,\underline{v}.\underline{n}) = 0$ on the wall, S_w, and introducing a quantity v', representing the deviation of the local point velocity from the local volume average velocity :-

$$\underline{v} = \overline{\underline{v}} + \underline{v}' \qquad \ldots\ldots\ [A3.5]$$

Note $\overline{\overline{\underline{v}}} = \overline{\underline{v}}$ ∴ $\overline{\underline{v}'} = 0$

Equation [A3.3] becomes :-

$$\rho \mathrm{div}(\underline{v}\,\underline{v}) = -\nabla \overline{p} + \mu(\overline{\nabla^2 \underline{v}}) - \rho \mathrm{div}(\overline{\underline{v}'\underline{v}'}) + \frac{1}{V}\int_{S_w} p\underline{n}\,dS \qquad [A3.6]$$

The interesting feature of [A3.6] was the additional term, $-\rho \mathrm{div}(\overline{\underline{v}'\underline{v}'})$ which is very similar to the Reynolds stress term produced in the time based averaging process used for turbulent flows.

Various techniques have been suggested to simplify [A3.6], and for one dimensional creep flow (ie. delete inertial terms) the Darcy law can be derived. Another simplification for two dimensional, inertial flow, suggested by Whitaker (1969), introduced a total resistance tensor $\underline{R}$. The nine terms in this tensor would have to be evaluated experimentally, and were expected to be proportional to μ, some length scale and the permeability of the porous medium.

---

1 $\underline{v}\,\underline{v}$ is known as the dyadic product, and was treated as a second order tensor.

At the present stage it was felt that the above line of thought was not worth pursuing further : techniques for determining R were not known to the author.

A4 Tests on the Porous Matrix

At the pres· t state of the art, it was felt that a macroscopic approach could be expected to yield results more quickly. A preliminary investigation was done, starting with a dimensional analysis.

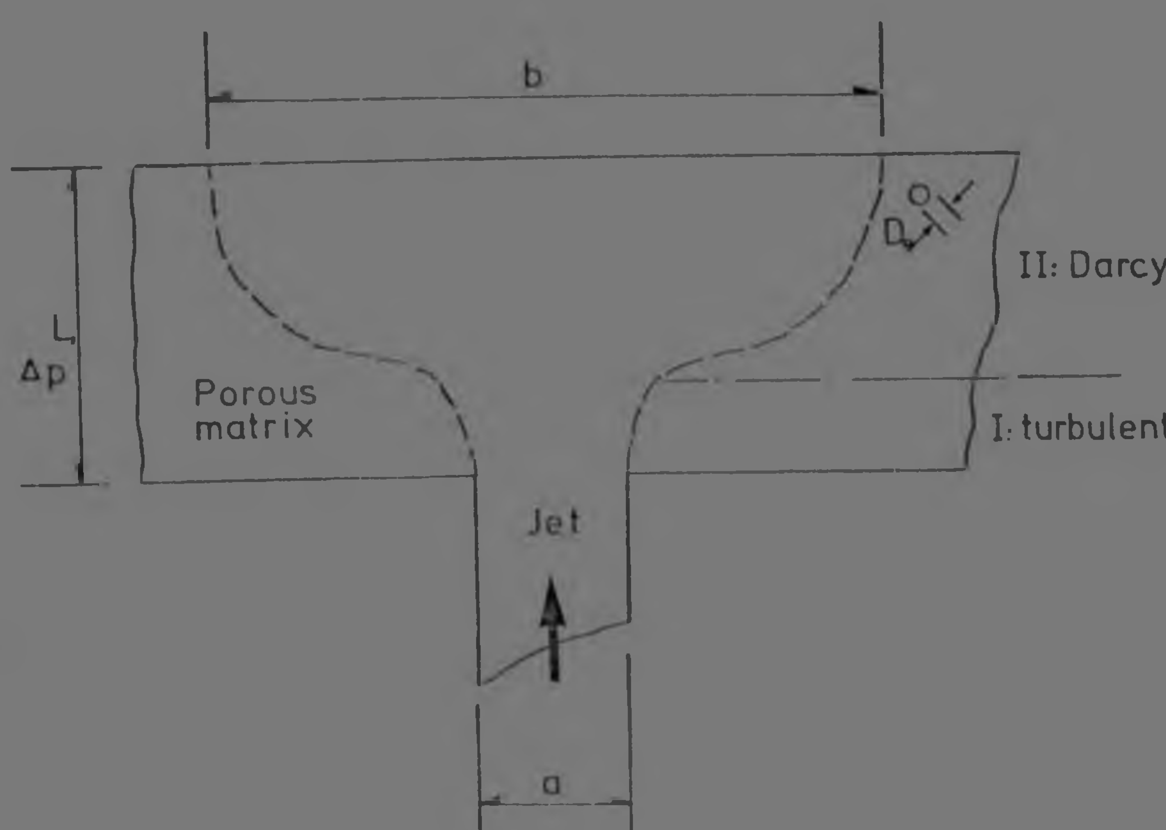

FIG A4.1 : SKETCH OF POROUS MATRIX WITH JET AT LOWER SURFACE

Because designers of transpiration cooled turbine nozzle guide vanes have a very limited pressure differential to work with, Δp was considered the most important quantity.

The variation of b with a, L and V is required if a uniform cold layer is to be present on the outer surface.

$$\Delta p = f(L, a, D, b, V, \mu, \rho) \qquad \text{....... [A4.1]}$$

Typically, the following relationship was produced :-

$$\frac{\Delta p}{\mu^2/\rho D^2} = (Re_D)^u (\tfrac{a}{D})^v (\tfrac{b}{D})^w (\tfrac{L}{D})^x$$

Because 3 length scales were present, these could be interchanged at will. The first dimensionless group was particularly interesting :-

$$\frac{\Delta p}{\mu^2/\rho D^2} = \frac{\Delta p}{\rho V^2}.Re_D^{\,2} \qquad \text{....... [A4.2]}$$

$\Delta p/\rho V^2$ is the well known pressure drop coefficient C_p.

Define

$$C_{p_D}{}' = C_p.Re_D^{\,2} \qquad \text{....... [A4.3]}$$

Some tests were performed on a matrix made of plastic spheres, D_o = 37,2 mm above an axisymmetric jet from a 80 mm pipe. The flow rate was measured with an orifice plate, and V was the average velocity in the pipe. A static pressure tapping was placed at the jet outlet.

A steam generator was placed upstream in the pipe, and the air passed over dry ice, thus producing a visible flow at the porous matrix surface. (See Fig A4.2). It was not possible to measure b with any reliability.

FIG A4.2 : LOW VELOCITY JET, V = 2,72 m/s, EMERGING FROM MATRIX

It was observed that at high velocity, the smoke formed a jet above the matrix, whereas at low velocity, the smoke filtered slowly through the matrix, and had spread much more. The conclusion reached was that for large L, an initial 'turbulent' region existed, causing a high pressure drop. This caused the jet to spread, hence slowing down to the laminar Reynolds number range. Creep flow resulted in this region - the loss of inertia being clearly visible when the smoke merely filtered through the last row of spheres. The 3 short lines on Fig A4.5 diverged from the solid line for increasing Re_L. This was thought to have been caused by the small additional pressure drop through the 'Darcy' region. Fig A4.3 shows turbulent flow emerging from the porous matrix.

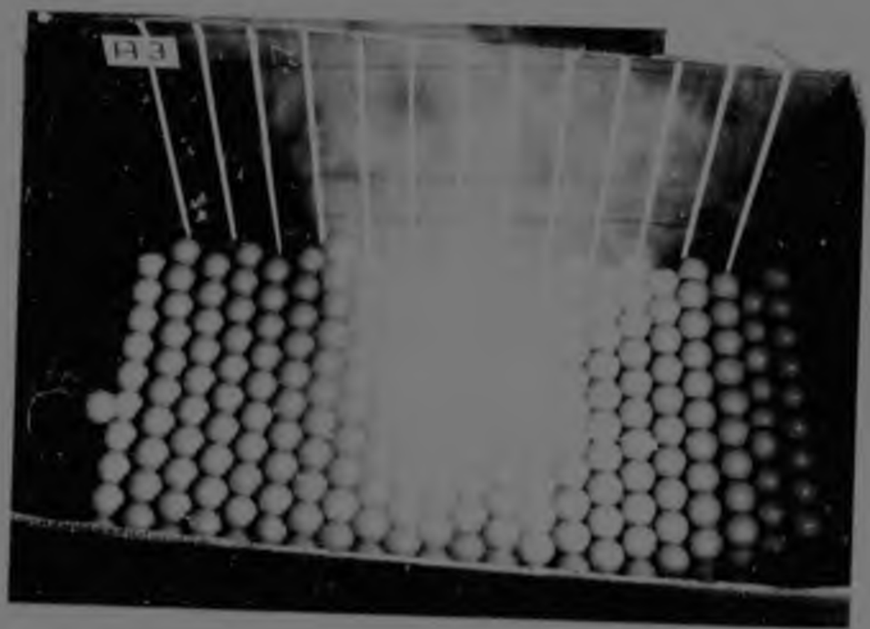

FIG A4.3 : TURBULENT JET : V = 6,5 m/s, EMERGING FROM MATRIX

The full results were not reported, but two of the graphs plotted are presented in Figs A4.4 and A4.5.

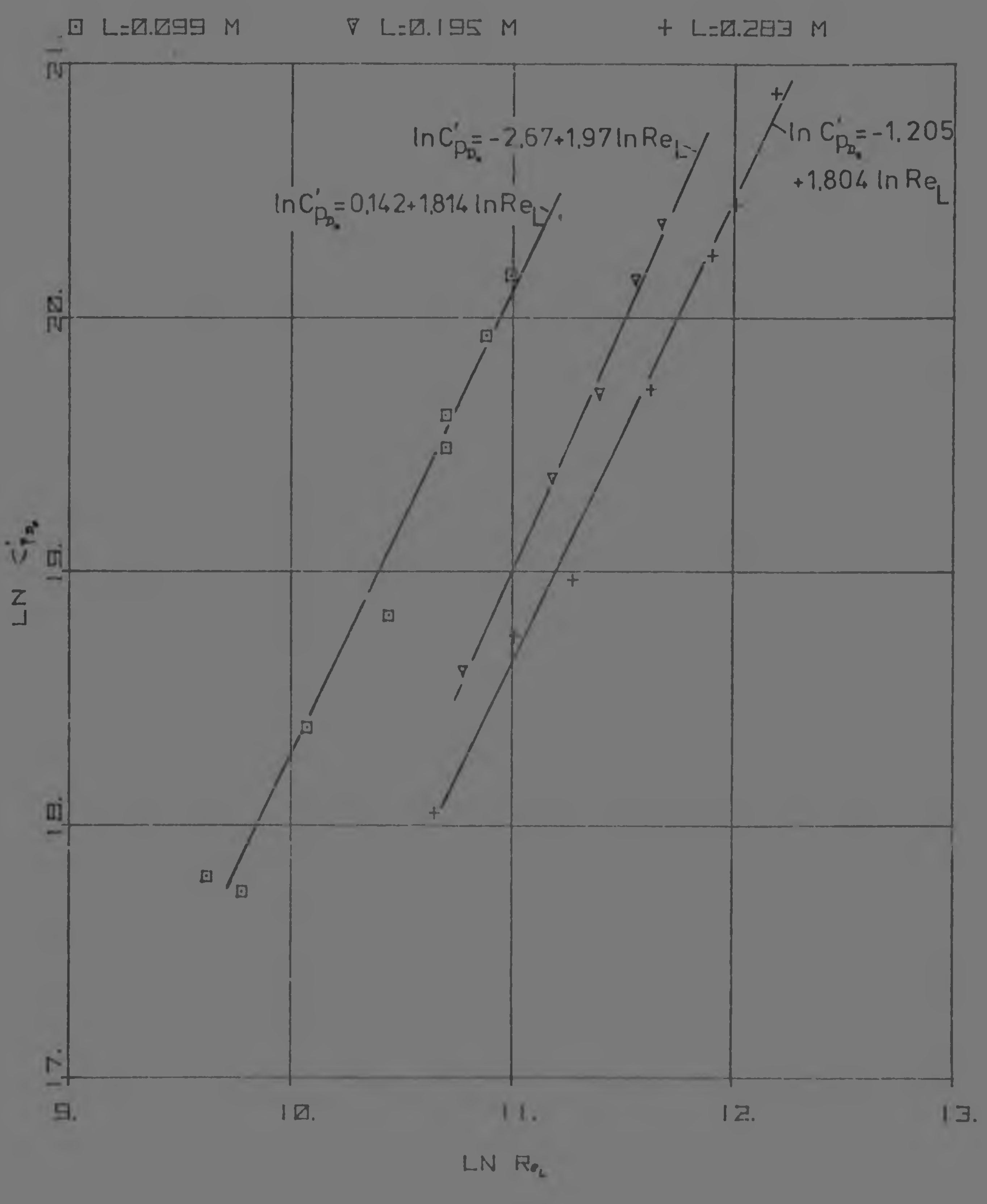

FIG A4.4 : PLOT OF C'_{pD_o} VS Re_L

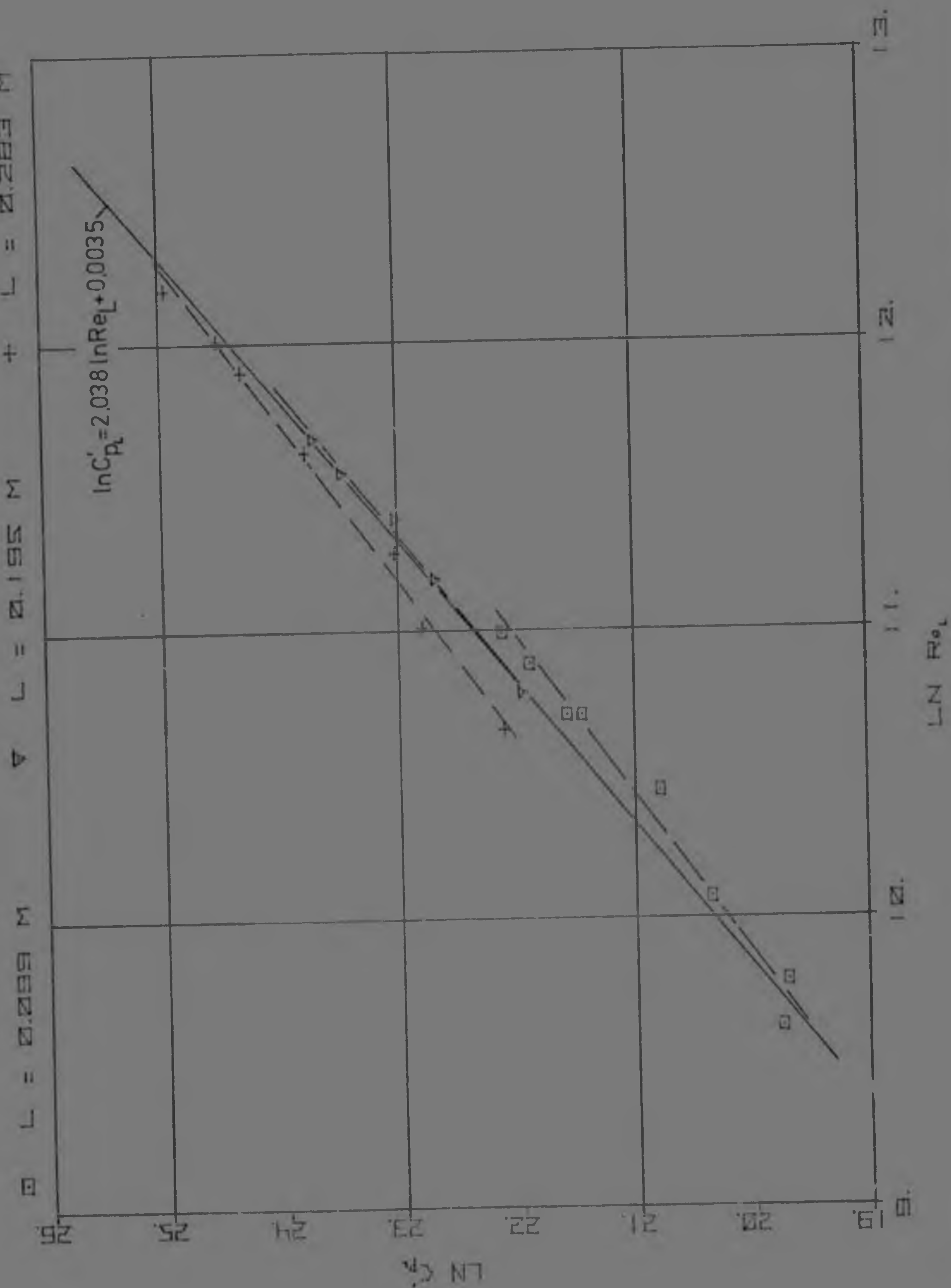

FIG A4.5 : PLOT OF C'_{pL} VS Re_L

APPENDIX B

B1 Design of the Wind Tunnel, Fan and Contraction

Subsonic wind tunnel design has become a well documented exercise. Basic decisions such as whether the tunnel should be open or closed circuit, and type of fan are very much cost dependent.

The tunnel built for this project was to form part of an existing unit. After certain sections had been constructed, it was found to be preferable to be independent of other research programmes, and a tunnel was designed around the parts already built. This was unfortunate, because the tunnel could have been better designed.

The open circuit tunnel consisted of a centrifugal fan, diffuser, settling chamber, contraction, entry section, working section and an exit diffuser.

Materials used were wood strips (100 mm wide), banded to 3 mm thick masonite, the smooth side of which formed the inside walls of the tunnel. The edges were supported with slotted angle iron. An outside company made the settling chamber and contraction of mild steel sheet. Details of the working section appear in Appendix B2. The entire tunnel is supported at shoulder height on wooden legs.

A centrifugal fan, somewhat overpowered by a 22 kW squirrel cage induction motor, was made available for the project. This unit was used to blow air down the tunnel, rather than sucking the air through the tunnel. If the ducting was attached to the fan inlet, it was expected that swirl due to the rotation of the fan would be transmitted back to the Working Section. The removal of such a vortex may have required straightener vanes, a complication which was to be avoided. The profile at the fan outlet was highly non-uniform, but this was to be controlled with screens. In the event, this proved more difficult than was expected. The profile in the entry section was much improved by the addition of honeycomb in the settling chamber. Aluminium honeycomb, 50 mm thick with a cell size of 6 mm, was used.

The contraction had an area ratio of 3:1. Theoretically this should have reduced the velocity fluctuations by a ninth. A potential flow analysis (see Cheers, 1945) was used to design the contraction. The equations were handled on a Hewlett-Packard 9810 calculator. The streamline denoted as contraction wall was plotted by the calculator (Fig B1.2).

FIG B1.1A : PLAN VIEW OF THE WIND TUNNEL, SHOWING (A) THE SETTLING CHAMBER, (B) THE CONTRACTION, (C) THE ENTRY SECTION, (D) THE WORKING SECTION uniform, but this was to be controlled with screens. In the event, this proved more difficult than was expected. The profile in the entry section was much improved by the addition of honeycomb in the settling chamber. Aluminium honeycomb, 50 mm thick with a cell size of 6 mm, was used.

The contraction had an area ratio of 3:1. Theoretically this should have reduced the velocity fluctuations by a ninth. A potential flow analysis (see Cheers, 1945) was used to design the contraction. The equations were handled on a Hewlett-Packard 9810 calculator. The streamline denoted as contraction wall was plotted by the calculator (Fig B1.2).

FIG B1.1A : PLAN VIEW OF THE WIND TUNNEL, SHOWING (A) THE SETTLING CHAMBER, (B) THE CONTRACTION, (C) THE ENTRY SECTION, (D) THE WORKING SECTION

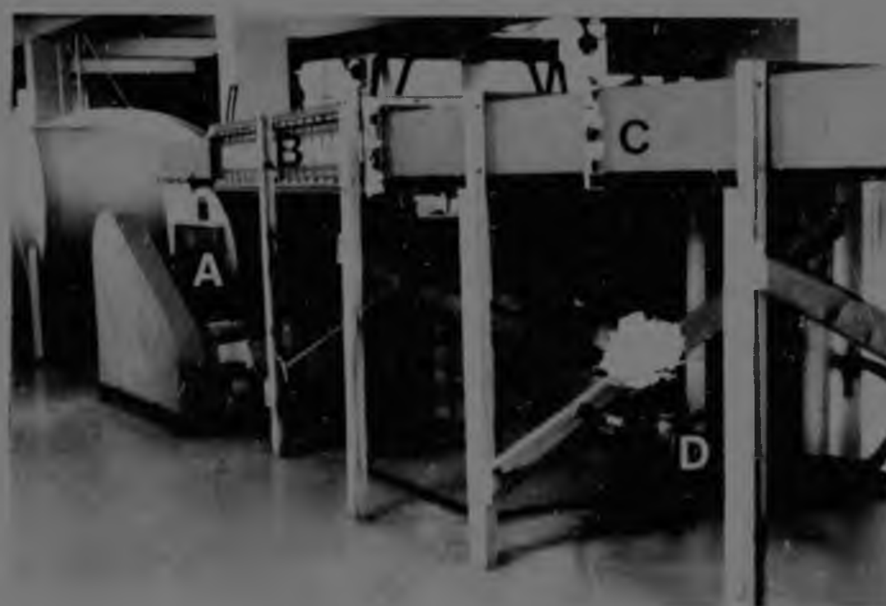

FIG B1.1B : SIDE VIEW OF THE TUNNEL WITH (A) THE FAN UNIT, (B) THE DIFFUSER, (C) SETTLING CHAMBER AND CONTRACTION, AND (D) THE COMPRESSED AIR SUPPLY

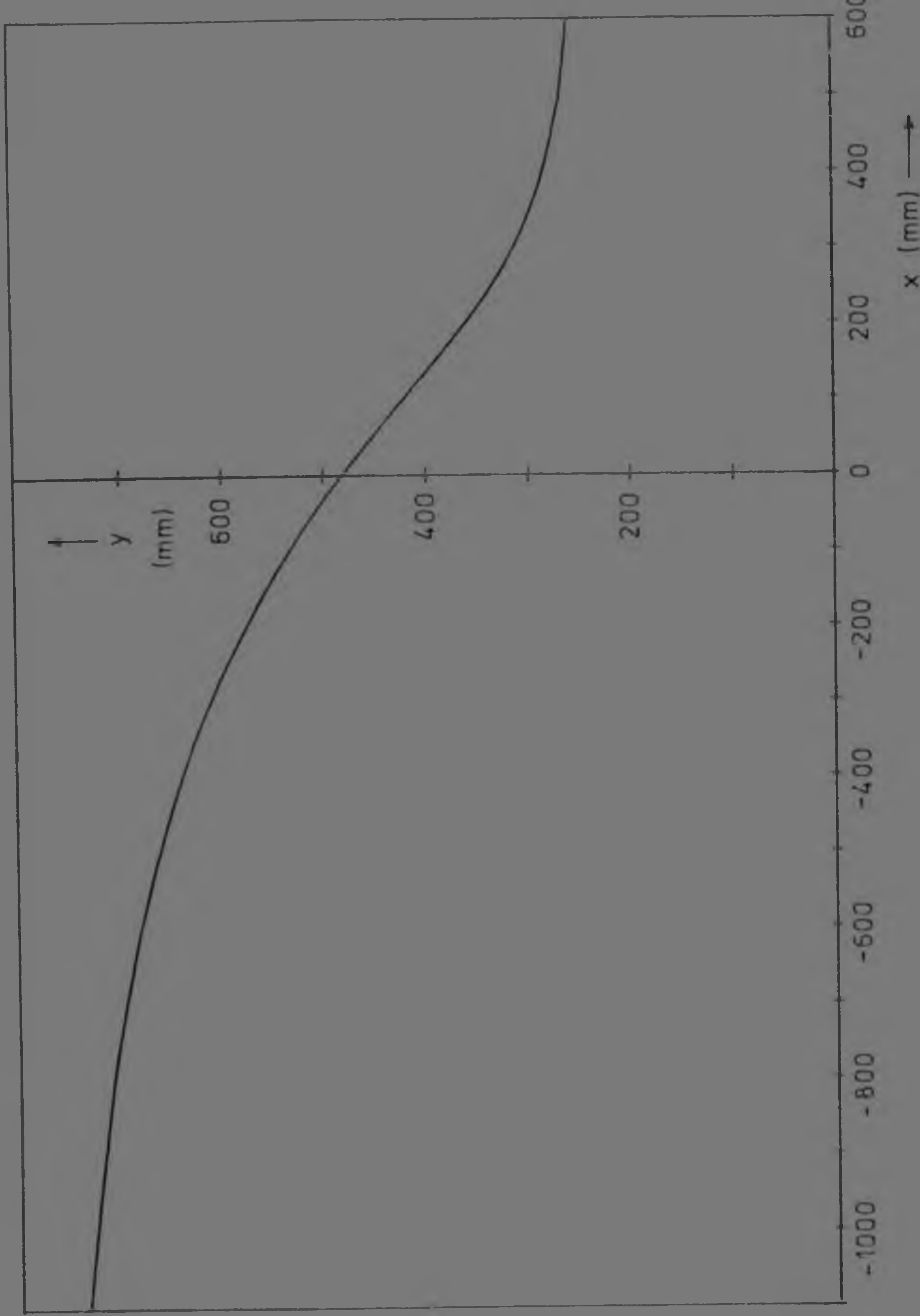

FIG B1.2 : CONTOUR OF WIND TUNNEL CONTRACTION

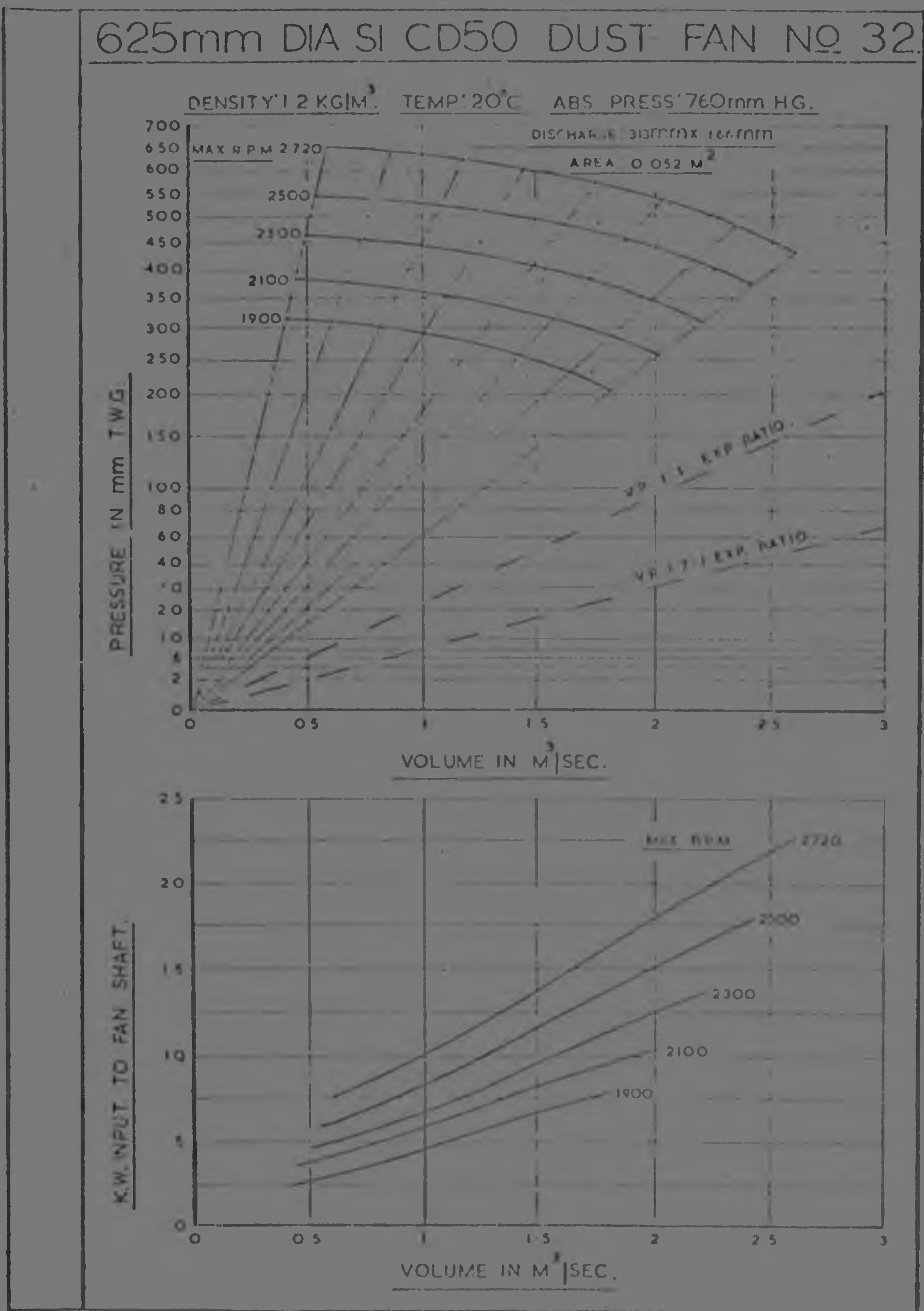

FIG B1.3 : FAN PERFORMANCE CURVE

B2 The Working Section

A working section producing two dimensional flow with $Re_L = 1{,}2 \times 10^6$ was required. The plate was to be solid, interspersed with a porous section through which a secondary flow could be introduced.

The working section was made rectangular, with dimensions 0,496 x 0,209 m. At a flowrate of 1,5 m^3/s, a velocity of 17 m/s was expected in the jet. With the 1 m long, parallel duct ahead of the working section, various plates could be attached to the leading plate, allowing variation of Re_L. With a leading plate 0,8 m long, as used in most of the tests, $Re_L = 1{,}2 \times 10^6$ was achieved at the end of the working section, which was 0,865 m long. A boundary layer bleed drew air off below the leading plate.

The plates and the roof of the working section were made of 3 mm aluminium sheet. Perspex (6,35 mm thick) was used for side walls. The porous plates had dimensions 500 x 244 x 6,35 mm. The porous plate leading and trailing edges were milled at 45°, and was pulled up to the aluminium plates with adjusting screws inside the plenum chamber. Filters were incorporated in the plenum chambers, to avoid the lower porous surface from becoming clogged with dirt or grease.

An exit diffuser was attached to the end of the working section. It was 1 m long, and prevented downstream conditions from affecting the flow in the jet. This section was on wheels, and could be removed to allow work inside the working section when setting up the hot wire transducer. The perspex sides were also removable.

B3 Engineering Drawing

Fig B3.1 is a reduction of the assembly drawing of the Working Section.

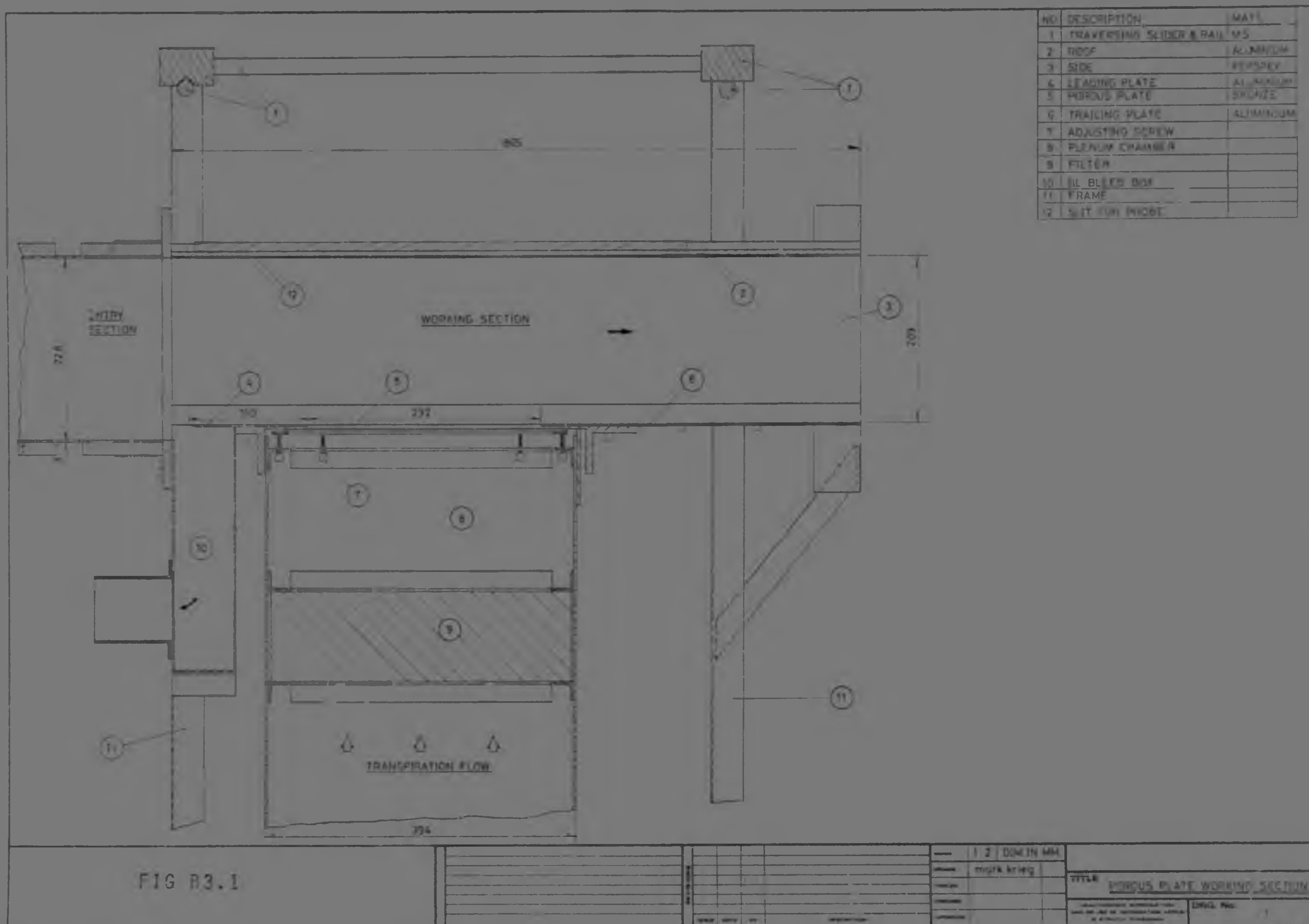
NO | DESCRIPTION | MAT'L
1 | TRAVERSING SLIDER & RAIL | M.S.
2 | ROOF | ALUMINIUM
3 | SIDE | PERSPEX
4 | LEADING PLATE | ALUMINIUM
5 | POROUS PLATE | BRONZE
6 | TRAILING PLATE | ALUMINIUM
7 | ADJUSTING SCREW
8 | PLENUM CHAMBER
9 | FILTER
10 | BL BLEED BOX
11 | FRAME
12 | SLIT FOR PROBE
ENTRY SECTION
WORKING SECTION
TRANSPIRATION FLOW
805
209
224
110
232
354
1:2 DIM IN MM
mark krieg
TITLE POROUS PLATE WORKING SECTION
DRG. No.

FIG B3.1

APPENDIX C

C1 Calibration of the Orifice Plate

The orifice plate was calibrated according to BS 1042.

C2 Calibration of Thermocouple

Copper-constanten thermocouples were used. The calibration curve is shown in Fig C2.1 below.

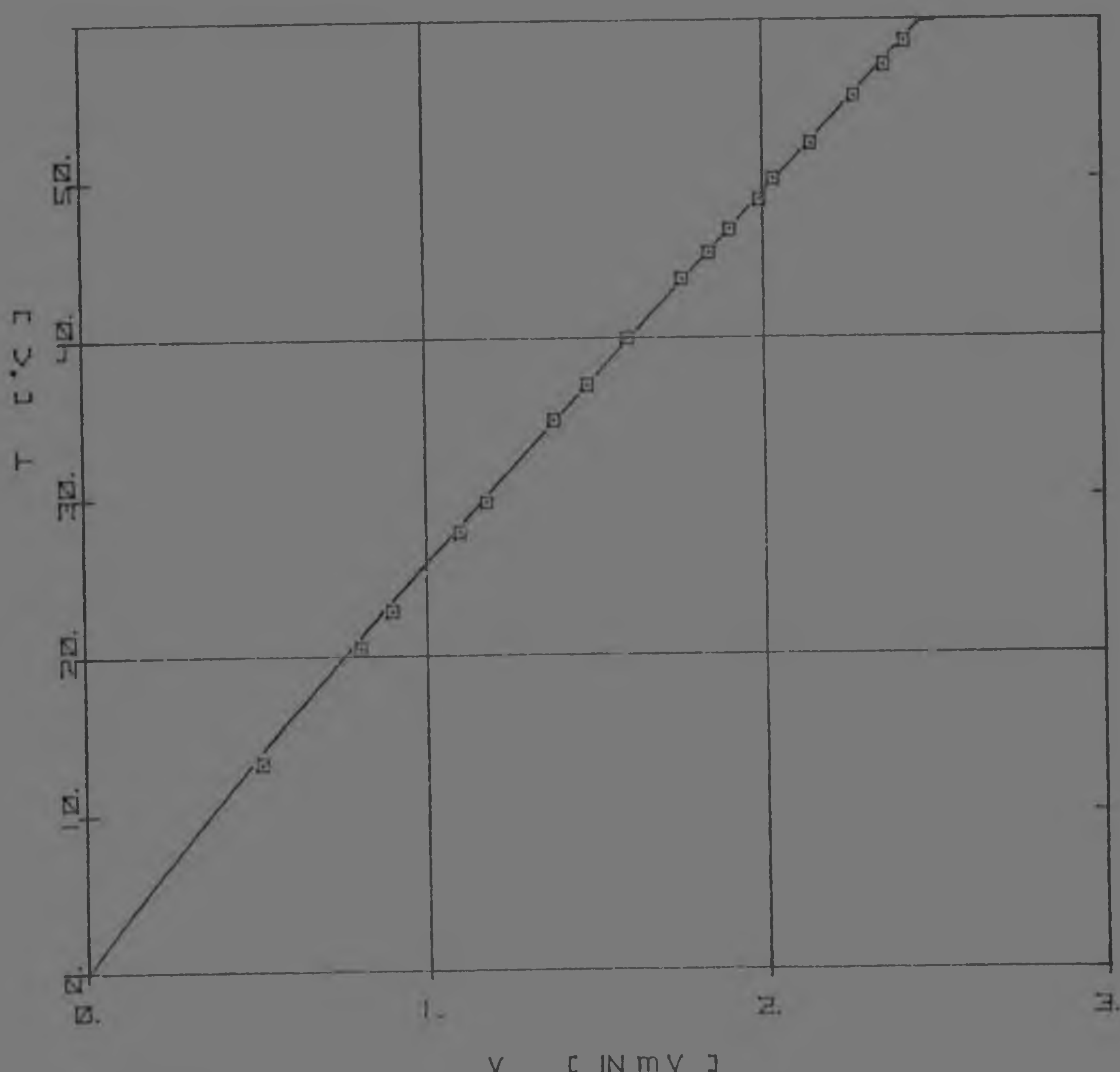

FIG C2.1

C3 The Calibration of the Hot Wires

The single sensor hot wires were calibrated using the Disa calibrating rig. This unit consisted of the Disa Pressure Control Unit, type 55 D 44, the Pressure Converter, type 55 D 46, and the nozzle unit, type 55 D 45. A Van Essen manometer model 6750 was used to measure the pressure drop across the nozzle.

The anemometer gain was adjusted using a square wave generator, and an oscilloscope to see when the amplifier became unstable. The zero flow voltage was determined, after amplification by the Auxilliary Unit, as was the hot wire resistance at the calibrating temperature.

Each hot wire (there were 4) was calibrated using the anemometer and the Auxilliary Unit.

King's Law was used to describe the calibration curves :-

$$V^2 = V_o^2 + BU^n \qquad \text{..... [C3.1]}$$

To obtain B and n, the data was plotted on log-log axes in the following form :-

$$\log\{(\frac{V}{V_o'})^2 - 1\} = n \log U$$

Clearly, if the lhs was plotted against log U, the slope was n. Note that $V_o' = cV_o$, where $c<1$. The value of c was varied to find the value which gave the best straight line through the points.

The lineariser used the function

$$V_{LIN} = K(V^2 - V_o^2)^{1/n} \qquad \text{....... [C3.2]}$$

$$\therefore V_{LIN} = K(V_o^2 - BU^n - V_o^2)^{1/n} \qquad \text{....... [C3.3]}$$

$$V_{LIN} = KBU = cU \qquad \text{....... [C3.4]}$$

to convert the non-linear anemometer output to a linear voltage. The exponent was set on the unit, and the hot wire was calibrated with the lineariser.

C4 Temperature Correction for the Anemometer Output

The heat loss from a hot-wire is influenced by the air velocity and by the air temperature. The anemometer output for a specific velocity must be corrected if the air temperature is different to the calibration temperature. This correction was performed from the following considerations :

The heat balance equation for a hot wire is :-

$$\frac{E^2}{R_w} = (T_w - T)h \qquad \text{....... [C4.1]}$$

E = voltage drop across the hot wire
R_w = working resistance of the hot wire
T_w = working temperature of the hot wire
T = fluid temperature
h = heat transfer coefficient.

For constant h, the expression for the correction of the anemometer output for a change in T :-

$$E_n{}^2 = E^2\frac{(T_w - T_n)}{(T_w - T)} \qquad \text{....... [C4.2]}$$

E_n = corrected voltage
T_n = calibration temperature

The resistance of the hot wire changes with temperature according to :

$$R = R_n\{1 + \alpha(T - T_n)\} \qquad \text{....... [C4.3]}$$

R is the resistance at temperature T, α is the thermal resistance coefficient :-

$\alpha = 0{,}0036\ 1/^{0}C$ .... [C4.4]

Equation C4.2 may be rewritten :-

$$E_n^{\ 2} = E^2 \frac{(R_w - R_n)}{(R_w - R)} \qquad \text{....... [C4.5]}$$

R was calculated from [C4.3], and the corrected anemometer reading from [C4.5].

C5 Correction for Proximity of the Wall

It was expected that the heat loss from the hot wire would increase very near a wall (y<2mm). Various attempts have been made to correct for this apparent increase in velocity, see Dryden (1936).

The change in voltage ΔV, can be calculated from

$$\Delta V = \sigma n \frac{(T_w - T)^2}{y^2}$$

which was given by Horsley (1975). The value of σ was estimated to be 2,53 x 10^{-6}, for y in mm. n was the exponent for the hot wire, discus[illegible]n C4.

APPENDIX D

D1 The Experimental Results

Presented here are the results of the velocity profiles measured in the boundary layer. The velocity measurements were corrected for temperature and the proximity of the wall.

Notes on experimental results

A pow r law was fitt to the input profile. It was given in the first lin of printout. FD was u/u_e. The coefficient of th first right hand term was the inverse of the power calculated.

A virtual origin for the first profile was calculated from

$$\delta = 0{,}383x/Re_x^{1/5} \qquad \text{....... [D1.1]}$$

Re_x was based on this virtual origin. The difference in x length between subsequent stations was added to the fir-- value.

The programme, DP2, performed the integrations for δ^* and θ, and plotted the results. The graphs are given in Fig 7.10.

CURVE 1 FIT: LOG(FD)= 0.1145E+00*LOG(Y/D)+-0.[illegible]E-02

E-758-17

2851

UINF= 17.[illegible] M/S
REX= 0.1037E+07 X= 2.079
T= 16.90 DEG.C RHO= 1.0002 KG/CU.M
MU= 0.179[illegible]E-04 KG/MS NU= 0.1788E-04 M*M/S

Y(MM)	U (M/S)	Y/TTA	U/UE	Y/DEL
0.61	10.134	0.143	0.5887	0.0124
1.81	11.788	0.426	0.6831	0.0368
3.81	12.400	0.890	0.7526	0.0774
5.81	[illegible]	1.361	0.7871	0.1383
8.81	14.[illegible]44	2.706	0.8257	0.1982
12.81	14.[illegible]49	3.012	[illegible]	0.2601
15.81	14.784	3.717	[illegible]	0.2711
19.81	15.[illegible]	4.6[illegible]	[illegible]	0.4023
24.81	15.[illegible]8	5.833	[illegible]	0.5038
29.81	15.[illegible]	7.028	0.9305	0.6354
34.81	16.277	8.184	0.9573	0.7069
39.81	16.[illegible]7	9.359	0.9741	0.8085
43.81	16.531	10.3[illegible]	0.9878	0.9100

DEL= 43.70 MM DSTR= 5.43 MM THETA= 4.25 MM
RDEL= 0.4[illegible]85E+05 RDSTR= 0.523[illegible]E+04 RTTA= 0.4065E+04
SHAPE FACTOR,H= 1.[illegible]

STATION 2

UINF= 17.22[illegible] M/S
REX= [illegible] X= 2.155
T= 17.15 DEG.C RHO= 0.99[illegible]3 KG/CU.M
MU= 0.179[illegible]E-04 KG/MS NU= 0.1800E-04 M*M/S

Y(MM)	U (M/S)	Y/TTA	U/UE	Y/DEL
0.63	[illegible]	0.1[illegible]1	0.4732	0.0136
1.13	[illegible]	0.271	[illegible]	0.0241
2.13	10.[illegible]	0.512	[illegible]	0.04[illegible]
3.13	11.[illegible]43	0.7[illegible]	[illegible]	0.0[illegible]
4.13	12.577	0.992	0.7276	0.0[illegible]
6.13	[illegible]	1.472	0.7040	0.1[illegible]
8.13	[illegible]	1.953	0.8113	0.1[illegible]
11.13	14.[illegible]92	2.673	0.8387	0.2[illegible]
14.13	[illegible]	3.3[illegible]	0.8645	0.3[illegible]
17.13	15.[illegible]79	4.114	0.8843	0.3[illegible]
20.13	15.[illegible]	4.815	[illegible]	0.4[illegible]
23.13	15.[illegible]81	5.556	0.9133	0.4[illegible]
27.13	15.[illegible]	6.510	0.9292	0.5[illegible]
31.13	1[illegible].[illegible]15	7.477	0.9[illegible]	0.6[illegible]
35.13	16.[illegible]68	8.439	0.9[illegible]	0.7[illegible]
39.13	16.[illegible]30	9.399	0.9756	0.8[illegible]
44.13	16.[illegible]	10.600	0.9914	0.9[illegible]

DEL= 46.65 MM DSTR= 5.58 MM THETA= 4.[illegible]6 MM
RDEL= 0.4484E+05 RDSTR= 0.534[illegible]E+04 RTTA= 0.3983E+04

STATION 3

UINF= 18.00[illegible] M/S
REX= 0.22[illegible]E+07 X= 2.245
T= 17.40 DEG.C RHO= 0.9985 KG/CU.M
MU= 0.180[illegible]E-04 KG/MS NU= 0.1803E-04 M*M/S

Y(MM)	U (M/S)	Y/TTA	U/UE	Y/DEL
0.62	7.[illegible]	0.133	0.4178	0.0119
0.95	[illegible]	0.204	0.4548	0.0183
1.45	[illegible]	0.311	0.4997	0.0279
1.95	[illegible]	0.419	0.5392	0.0375
2.45	10.[illegible]	0.526	0.5703	0.0471
3.45	11.[illegible]	0.740	0.6227	0.0663
4.45	11.[illegible]	0.955	0.6661	0.0855
5.45	12.[illegible]	1.170	0.7089	0.1048
6.45	13.[illegible]	1.384	0.7396	0.1240
8.45	14.[illegible]	1.814	0.7891	0.1624
10.45	14.[illegible]	2.243	0.8226	0.2009
12.45	15.[illegible]	2.672	0.8434	0.2393
14.45	15.[illegible]	3.316	0.8641	0.2777
19.45	15.[illegible]	4.174	0.8865	0.3739
24.45	16.[illegible]	5.[illegible]	0.9069	0.45[illegible]
29.45	16.[illegible]	6.106	0.9295	0.5[illegible]
34.45	16.[illegible]	7.170	0.9457	0.6[illegible]
39.45	17.192	8.2[illegible]	0.9647	0.77[illegible]
44.45	17.471	9.5[illegible]	0.9803	0.8544

DEL= 52.02 MM DSTR= 6.48 MM THETA= 4.65 MM
RDEL= 0.51[illegible]E+05 RDSTR= 0.6472E+04 RTTA= 0.4652E+04

STATION 4

UINF= 19.393 M/S
REX= 0.2[illegible]E+07 X= 2.344
T= 17.50 DEG.C RHO= 0.9980 KG/CU.M
MU= 0.180[illegible]E-04 KG/MS NU= 0.1804E-04 M*M/S

Y(MM)	U (M/S)	Y/TTA	U/UE	Y/DEL
0.63	6.[illegible]	0.134	0.3[illegible]	0.0121
0.87	7.[illegible]	0.174	0.3959	0.0167
1.37	8.[illegible]65	0.274	0.4415	0.0263
1.87	9.[illegible]20	0.374	0.4912	0.0359
2.37	9.[illegible]	0.475	0.5[illegible]	0.0455
2.87	10.[illegible]	0.575	0.5[illegible]	0.0551
3.87	11.[illegible]15	0.775	0.5853	0.0743
4.87	11.[illegible]	0.975	0.6242	0.0935
5.87	12.[illegible]73	1.176	0.6606	0.1127
7.87	13.[illegible]	1.576	0.7251	0.1511
9.87	14.[illegible]	1.977	0.7713	0.1895
12.87	15.[illegible]37	2.577	0.8100	0.2470
15.87	16.[illegible]22	3.178	0.8571	0.3046
18.87	16.[illegible]57	3.779	0.8797	0.3622
21.87	17.[illegible]	4.380	0.8994	0.4198
24.87	17.[illegible]	4.981	0.9111	0.4774
28.87	17.731	5.782	0.9259	0.5542
33.87	18.[illegible]01	6.783	0.9443	0.6501
38.87	18.[illegible]24	7.784	0.9616	0.7461
43.87	18.[illegible]02	8.786	0.9761	0.8421

DEL= 52.10 MM DSTR= 7.25 MM THETA= 4.00 MM
RDEL= 0.5587E+05 RDSTR= 0.7780E+04 RTTA= 0.5356E+04

CURVE FIT: LOG(F0)= 0.[illegible]E-01*LOG(Y/D)+ 0.10[illegible]E-02

E-10.57-17

3051

UINF= 18.216 M/S
REX= 0.170[illegible]E+07 H= 1.723
T= 2[illegible].91 DEG.C RHO= 0.9856 KG/CU.M
MU= 0.1817E-04 KG/MS NU= 0.1842E-04 M*M/S

Y(MM)	U (M/S)	Y/TTA	U/UE	Y/DEL
0.67	11.474	0.171	0.6335	0.0125
1.17	12.574	0.322	0.6672	0.0236
1.57	13.[illegible]	0.542	0.7341	0.0307
2.57	13.[illegible]	[illegible].817	0.7[illegible]	0.0528
[illegible]	14.[illegible]	1.367	[illegible]42	0.1031
[illegible].57	14.[illegible]	1.[illegible]	[illegible]	0.1[illegible]
[illegible].57	15.243	2.455	0.8451	0.1876
11.57	15.[illegible]54	3.[illegible]	0.8[illegible]81	0.2[illegible]0
[illegible].57	15.[illegible]	4.118	0.[illegible]947	0.[illegible]
1[illegible].57	1[illegible]	5.210	0.9075	0.3[illegible]0
[illegible].57	1[illegible].744	6.31[illegible]	[illegible].9285	0.4[illegible]
2[illegible].57	17.[illegible]	7.4[illegible]	[illegible]	0.5[illegible]
[illegible].57	17.[illegible]	8.[illegible]	[illegible]	0.[illegible]
[illegible].57	1[illegible]	9.621	[illegible]	0.7041
[illegible].57	[illegible]	1[illegible].[illegible]	0.[illegible]	0.7946
4[illegible].57	[illegible]	12.[illegible]72	[illegible].9[illegible]	0.9054

DEL= 37.47 MM DSTR= 4.6[illegible] MM THETA= 3.63 MM
RDEL= 0.3[illegible]01E+0[illegible] RDSTR= 0.4[illegible]E+04 RTTA= 0.359[illegible]E+04
SHAPE FACTOR,H= 1.27

STATION [illegible]

UINF= 1[illegible].[illegible] M/S
REX= [illegible]E+07 H= 1.799
T= 21.70 DEG.C RHO= 0.9[illegible] KG/CU.M
MU= 0.1[illegible]E-04 KG/MS NU= 0.1[illegible]51E-04 M*M/S

Y(MM)	U (M/S)	Y/TTA	[illegible]	Y/DEL
0.62	7.7[illegible]5	0.146	[illegible].4[illegible]8	0.0125
0.[illegible]	8.742	0.[illegible]17	0.476	0.[illegible]1
1.[illegible]	9.[illegible]	0.[illegible]93	0.5125	[illegible]
[illegible]	[illegible].15[illegible]	[illegible]	0.6[illegible]85	0.0443
[illegible]	12.[illegible]	0.[illegible]	0.6702	0.0644
4.[illegible]	13.3[illegible]	0.9[illegible]	[illegible]	0.0846
5.20	14.[illegible]	1.228	0.7[illegible]4	0.1047
6.2[illegible]	14.455	1.464	0.[illegible]	0.1249
7.7[illegible]	1[illegible]	1.8[illegible]	0.[illegible]117	0.1[illegible]
9.2[illegible]	15.17[illegible]	2.177	0.8277	0.1[illegible]53
11.[illegible]	15.4[illegible]	2.645	0.8432	0.225[illegible]
14.2[illegible]	15.8[illegible]7	3.[illegible]4	0.[illegible]29	0.28[illegible]
20.2[illegible]	16.47[illegible]	4.771	0.8963	0.4068
26.20	16.[illegible]	6.188	0.9250	0.5277
32.20	17.028	7.6[illegible]5	0.9[illegible]4	0.648[illegible]
38.20	17.8[illegible]	9.022	0.9708	0.7694
44.20	18.[illegible]	10.439	0.9861	0.8902

DEL= 4[illegible].65 MM DSTR= 5.74 MM THETA= 4.23 MM
RDEL= 0.4965E+0[illegible] RDSTR= [illegible].574[illegible]E+04 RTTA= 0.4237E+04

STATION 3

UINF= 1[illegible].[illegible] M/S
REX= 0.19[illegible]E+07 H= 1.[illegible]
T= [illegible].[illegible]5 DEG.C RHO= 0.9814 KG/CU.M
MU= 0.1825E-04 KG/MS NU= 0.1859E-04 M*M/S

Y(MM)	U (M/S)	Y/TTA	U/UE	Y/DEL
[illegible].[illegible]2	[illegible].9[illegible]	0.1[illegible]	0.3570	0.0[illegible]
1.[illegible]4	[illegible].314	0.2[illegible]	0.4296	0.[illegible]
2.[illegible]4	[illegible].[illegible]	0.[illegible]	0.50[illegible]	0.[illegible]
3.[illegible]4	11.[illegible]	[illegible]	0.5[illegible]	0.0[illegible]
[illegible].[illegible]4	12.[illegible]	0.[illegible]	0.6[illegible]	0.0[illegible]
[illegible].[illegible]4	1[illegible]	1.1[illegible]	0.[illegible]	0.1[illegible]
[illegible].[illegible]4	1[illegible]	1.[illegible]	0.7[illegible]	0.1[illegible]
[illegible]	1[illegible]	1.[illegible]	0.7[illegible]	[illegible]
[illegible]	1[illegible]	2.[illegible]	0.[illegible]	[illegible]
11.[illegible]4	1[illegible]	2.[illegible]	0.[illegible]	0.2[illegible]
1[illegible].[illegible]4	1[illegible]	2.[illegible]	0.[illegible]	0.2[illegible]
[illegible]	1[illegible]	3.24[illegible]	0.[illegible]605	0.2[illegible]
[illegible]	17.[illegible]	3.[illegible]	0.[illegible]	0.3[illegible]
[illegible]	1[illegible].24[illegible]	4.15[illegible]	0.[illegible]	0.3[illegible]
22.[illegible]	1[illegible].6[illegible]	[illegible]	0.9[illegible]95	0.4[illegible]
2[illegible].[illegible]4	1[illegible]	[illegible]	0.[illegible]315	0.[illegible]
[illegible]	1[illegible].4[illegible]1	7.[illegible]	0.9549	0.[illegible]
[illegible]	1[illegible].784	[illegible].9[illegible]5	0.9706	0.7[illegible]
4[illegible].[illegible]4	1[illegible].12[illegible]	1[illegible]	0.9891	0.9[illegible]

DEL= 49.3[illegible] MM DSTR= 6.[illegible] MM THETA= 4.3[illegible] MM
RDEL= 0.[illegible]E+05 RDSTR= 0.665[illegible]E+0[illegible] RTTA= 0.[illegible]E+04

STATION 4

UINF= [illegible] M/S
REX= 0.[illegible]E+07 H= 1.[illegible]
T= 22.60 DEG.C RHO= 0.9809 KG/CU.M
MU= 0.1825E-04 KG/MS NU= 0.1[illegible]61E-04 M*M/S

Y(MM)	U (M/S)	Y/TTA	U/UE	Y/DEL
[illegible]	6.[illegible]	0.1[illegible]1	0.[illegible]	0.0127
[illegible]	7.[illegible]24	0.223	0.[illegible]2	0.0217
1.[illegible]	[illegible]	0.[illegible]2	0.4[illegible]7	0.[illegible]
2.[illegible]	10.[illegible]	0.[illegible]2	0.511[illegible]	0.[illegible]
3.[illegible]	11.[illegible]	0.812	0.[illegible]	0.[illegible]
4.[illegible]	12.[illegible]	1.[illegible]3	0.[illegible]	0.[illegible]
[illegible]	13.[illegible]	1.[illegible]	0.[illegible]	0.[illegible]
7.[illegible]	14.[illegible]	1.[illegible]54	0.6973	0.1[illegible]
9.[illegible]	15.2[illegible]	1.[illegible]70	0.741[illegible]	[illegible]
1[illegible]	16.[illegible]1	2.2[illegible]	0.77[illegible]	0.22[illegible]
12.[illegible]	16.[illegible]	2.[illegible]	0.8005	0.2[illegible]1
1[illegible]	17.2[illegible]	2.[illegible]17	0.8[illegible]	0.2[illegible]
1[illegible].[illegible]	17.[illegible]44	3.[illegible]8	0.[illegible]	0.3[illegible]7
17.[illegible]	1[illegible]	3.750	0.[illegible]	0.365[illegible]
20.[illegible]	18.67[illegible]	4.391	0.[illegible]	0.4271
24.[illegible]	18.[illegible]	5.23[illegible]	0.[illegible]	0.5[illegible]
30.[illegible]	19.497	6.496	0.9450	0.6[illegible]
[illegible].[illegible]	19.[illegible]	7.[illegible]	0.9613	0.7547
4[illegible].[illegible]	20.3[illegible]	9.23[illegible]	0.9839	0.8981

DEL= 48.84 MM DSTR= 7.31 MM THETA= 4.75 MM
RDEL= 0.5469E+05 RDSTR= 0.8[illegible]72E+04 RTTA= 0.53[illegible]E+04

E-12.41-17

2852

CURVE 1 FIT: LOG(FO)= C.1068E+03*LOG(Y/D)+ C.1788E-02

UINF= 17.620 M/S
REX= C.1655E+07 X= 1.723
T= 17.92 DEG.C RHO= C.9968 KG/CU.M
MU= C.1808E-04 KG/MS NU= 0.1509E-04 M*M/S

Y(MM)	U (M/S)	Y/TTA	U/UE	Y/DEL
0.83	10.665	0.180	0.6116	0.0179
1.83	12.[illegible]	0.473	[illegible]	0.0378
2.55	12.[illegible]	0.736	0.7465	0.[illegible]3
4.55	13.746	1.255	0.7025	0.0[illegible]2
6.55	14.255	1.837	0.8172	0.1384
9.55	14.756	2.6[illegible]	0.8459	0.2019
12.55	15.136	3.494	0.8677	0.2403
15.55	15.497	4.[illegible]	0.8878	0.3287
18.55	15.734	5.1[illegible]	0.9029	0.3921
21.55	16.073	6.[illegible]	0.9160	0.4555
25.55	16.[illegible]	7.[illegible]	0.9327	0.5471
29.55	16.[illegible]	8.[illegible]	0.9473	0.6[illegible]
35.55	10.813	[illegible]	0.9638	0.7[illegible]5
40.55	17.[illegible]	10.[illegible]	0.9920	0.8[illegible]
44.55	17.[illegible]	12.233	0.9936	0.9417

DEL= 37.15 MM DSTR= 4.63 MM THETA= 3.61 MM
RDEL= [illegible] RDSTR= C.4915E+04 RTTA= 0.3510E+04
SHAPE FACTOR,H= [illegible]

STATION 2

UINF= 17.29[illegible] M/S
REX= [illegible]E+07 X= 1.784
T= 17.9[illegible] DEG.C RHO= C.9968 KG/CU.M
MU= [illegible]E-04 KG/MS NU= [illegible]E-04 M*M/S

Y(MM)	U (M/S)	Y/TTA	U/UE	Y/DEL
0.67	6.727	0.161	0.3938	0.0137
0.84	7.127	[illegible]	0.4177	0.0[illegible]
1.14	8.[illegible]	[illegible]	0.4[illegible]5	0.0[illegible]
1.44	8.[illegible]	[illegible]	0.5157	0.0[illegible]
1.94	9.[illegible]	[illegible]	0.5459	0.0[illegible]
2.44	10.[illegible]	[illegible]	0.6126	0.0[illegible]
2.94	11.1[illegible]	[illegible]	0.6512	0.0[illegible]
3.44	11.7[illegible]	[illegible]	0.6832	0.0[illegible]
4.44	12.[illegible]	1.171	0.7335	0.[illegible]
5.44	13.70[illegible]	1.641	0.7[illegible]	0.1267
6.44	14.195	2.155	0.8201	0.1609
10.44	14.574	2.6[illegible]	0.8402	0.2152
12.44	14.935	3.1[illegible]	0.8664	0.2[illegible]
14.44	15.[illegible]	3.670	0.8700	0.2[illegible]
17.44	15.3[illegible]	4.443	0.9075	0.3512
21.44	15.721	5.442	0.9196	0.4317
25.44	15.[illegible]	6.431	0.9325	0.5122
29.44	16.[illegible]	7.[illegible]	0.9[illegible]	0.5929
34.44	16.553	8.774	0.9[illegible]43	0.6935
39.44	16.772	10.049	0.9803	0.7941
44.44	16.925	11.322	0.9898	0.8949

DEL= 49.6[illegible] MM DSTR= [illegible] MM THETA= 3.9[illegible] MM
RDEL= 0.4747E+05 RDSTR= 0.5192E+04 RTTA= 0.3752E+04

STATION 3

UINF= 19.[illegible] M/S
REX= 0.197[illegible]E+07 X= 1.873
T= 18.12 DEG.C RHO= 0.9965 KG/CU.M
MU= C.1804E-04 KG/MS NU= 0.1811E-04 M*M/S

Y(MM)	U (M/S)	Y/TTA	U/UE	Y/DEL
0.62	5.[illegible]	0.130	0.2978	0.0119
[illegible]	6.[illegible]	0.165	0.3232	0.0153
1.10	6.[illegible]	[illegible]	0.3562	0.0211
[illegible]	7.[illegible]	[illegible]	0.3976	0.0306
[illegible]	[illegible]	[illegible]	0.4341	0.0[illegible]
[illegible]	[illegible]	[illegible]	0.4663	0.0409
3.10	[illegible]	[illegible]	0.4937	0.0503
[illegible]	[illegible]	[illegible]	0.5275	0.0[illegible]
4.10	1[illegible]	[illegible]	0.5461	0.0785
[illegible]	10.[illegible]	[illegible]	0.5671	0.0891
[illegible]	11.[illegible]	[illegible]	0.6101	0.0976
[illegible]	12.[illegible]	[illegible]	0.6504	0.1149
7.10	13.[illegible]	[illegible]	0.7033	0.1352
[illegible]	14.[illegible]	[illegible]	0.7590	0.1742
11.10	15.[illegible]	[illegible]	0.8066	0.2125
13.10	15.[illegible]	[illegible]	0.8363	0.2[illegible]
16.10	16.[illegible]	[illegible]	0.8637	0.3[illegible]
20.10	16.[illegible]	4.[illegible]	0.8882	0.3[illegible]
[illegible]	17.[illegible]	5.[illegible]	0.9146	0.4[illegible]
[illegible]	17.[illegible]	6.216	0.9373	0.5762
[illegible]	18.[illegible]	7.[illegible]	0.9542	0.6712
[illegible]	18.[illegible]	8.[illegible]	0.9690	0.7676
45.10	18.[illegible]	9.[illegible]	0.9823	0.8633

DEL= 52.24 MM DSTR= 7.35 MM THETA= [illegible] MM
RDEL= [illegible] RDSTR= C.7765E+04 RTTA= 0.5106E+04

STATION 4

UINF= 19.60[illegible] M/S
REX= 0.213[illegible]E+07 X= 1.973
T= 18.20 DEG.C RHO= 0.9955 KG/CU.M
MU= C.1804E-04 KG/MS NU= 0.1813E-04 M*M/S

Y(MM)	U (M/S)	Y/TTA	U/UE	Y/DEL
0.62	5.[illegible]	0.117	0.2923	0.0115
0.[illegible]	6.[illegible]	0.174	0.3201	0.0171
1.22	6.[illegible]	0.231	0.3592	0.0[illegible]
1.72	7.[illegible]	0.327	0.3041	0.0[illegible]
2.[illegible]	8.[illegible]	0.39[illegible]	0.4[illegible]	0.0378
2.[illegible]	8.412	0.477	0.4542	0.0[illegible]
3.02	9.[illegible]	0.572	0.4820	0.0[illegible]
3.62	9.[illegible]	0.685	0.5[illegible]	0.0[illegible]
4.22	10.[illegible]	0.700	0.5326	0.0782
[illegible]	11.121	0.[illegible]	0.5729	0.0[illegible]
[illegible]	11.[illegible]	1.177	0.6027	0.115[illegible]
8.22	12.072	1.556	0.6[illegible]	0.1[illegible]
10.21	14.[illegible]	1.932	0.7247	0.1[illegible]
12.22	14.93[illegible]	2.31[illegible]	0.7[illegible]	0.2[illegible]
15.22	16.01[illegible]	2.881	0.8253	0.2[illegible]
18.22	16.7[illegible]	3.448	0.8[illegible]	0.3[illegible]
21.22	17.26[illegible]	4.[illegible]	0.8[illegible]	0.3[illegible]
24.22	17.637	4.5[illegible]	0.9[illegible]	0.4[illegible]
28.22	17.[illegible]	5.341	0.9271	0.5231
33.22	18.31[illegible]	6.297	0.9437	0.6159
38.22	18.647	7.234	0.9607	0.7085
44.22	18.93[illegible]	8.269	0.9757	0.9198

DEL= 53.04 MM DSTR= 9.21 MM THETA= 5.20 MM
RDEL= 0.5823E+05 RDSTR= 0.8872E+04 RTTA= 0.5715E+04

E-13,79-17

3052

CURVE 1 FIT: LOG(FD)= 0.1103E+00*LOG(Y/D)+-0.2175E-04

UINF= 19.442 M/S
REX= 0.[illegible]E+07 X= 2.107
T= 22.[illegible] DEG.C RHO= 0.9800 KG/CU.M
MU= 0.1827E-04 KG/MS NU= 0.1864E-04 M*M/S

Y(MM)	U (M/S)	Y/TTA	U/UE	Y/DEL
0.[illegible]	[illegible].726	0.147	0.6033	0.0118
1.27	12.[illegible]	0.301	0.6711	0.0247
2.27	13.[illegible]6	0.533	0.7123	0.0474
3.77	14.[illegible]72	0.894	0.7543	0.0723
5.77	15.217	1.368	0.7877	0.1122
7.77	15.753	1.843	0.8101	0.1494
9.77	15.[illegible]25	2.317	0.8292	0.1866
12.77	16.[illegible]3	3.029	0.8513	0.2430
15.77	16.[illegible]31	3.740	0.[illegible]707	0.3012
20.77	17.[illegible]31	4.[illegible]	0.896[illegible]	0.3967
27.77	18.[illegible]5	6.585	0.9315	0.[illegible]54
34.77	18.[illegible]8	8.245	0.9569	0.6648
41.77	1[illegible].[illegible]27	9.905	0.[illegible]765	0.7977
46.77	[illegible]	10.617	0.9846	0.8[illegible]

DEL= 43.42 MM DSTR= 5.41 MM THETA= 4.22 MM
RDEL= 0.457[illegible]E+05 RDSTR= 0.5597E+04 RTTA= 0.[illegible]E+04
SHAPE FACTOR,H= 1.28

STATION 2

UINF= 19.804 M/S
REX= 0.2318E+07 X= 2.[illegible]
T= 23.02 DEG.C RHO= 0.9795 KG/CU.M
MU= 0.182[illegible]E-04 KG/MS NU= 0.186[illegible]E-04 M*M/S

Y(MM)	U (M/S)	Y/TTA	U/UE	Y/DEL
0.62	7.[illegible]3	0.[illegible]37	0.3601	0.0125
1.63	9.[illegible]	0.[illegible]	0.4[illegible]	0.0[illegible]
2.63	11.[illegible]7	0.580	0.[illegible]	0.05[illegible]
3.63	12.317	0.[illegible]0	0.6535	0.0771
5.13	14.[illegible]	1.131	0.7274	0.10[illegible]
6.63	15.[illegible]	1.462	0.7697	0.[illegible]34
8.13	15.035	1.792	0.7975	0.1636
9.63	15.[illegible]4	2.123	0.8127	0.1939
11.13	16.[illegible]6	2.454	0.8271	0.2240
12.63	16.[illegible]3	2.784	0.8364	0.2[illegible]
14.63	16.724	3.225	0.8537	0.2944
17.63	17.[illegible]73	3.887	0.8759	0.3544
21.63	17.569	4.764	0.8953	0.4353
26.63	18.[illegible]7	5.871	0.9235	0.5360
32.63	18.[illegible]7	7.193	0.9450	0.6567
38.63	1[illegible].[illegible]0	8.516	0.9696	0.7775
44.63	1[illegible].[illegible]	9.839	0.9861	0.89[illegible]

DEL= 49.69 MM DSTR= 6.37 MM THETA= [illegible].54 MM
RDEL= 0.527[illegible]E+05 RDSTR= [illegible].676[illegible]E+04 RTTA= 0.4815E+04

STATION 3

UINF= 20.[illegible] M/S
REX= 0.24[illegible]E+07 X= 2.272
T= 23.27 DEG.C RHO= 0.9787 KG/CU.M
MU= 0.1829E-04 KG/MS NU= 0.18[illegible]E-04 M*M/S

Y(MM)	U (M/S)	Y/TTA	U/UE	Y/DEL
0.62	5.[illegible]	0.[illegible]	0.2[illegible]	0.01[illegible]
0.82	[illegible]	0.17[illegible]	0.3445	0.0150
1.82	[illegible]	0.[illegible]	0.4257	0.035[illegible]
2.82	[illegible]	0.60[illegible]	0.4[illegible]	0.0[illegible]45
3.82	10.[illegible]0	0.815	0.5[illegible]	0.07[illegible]
5.32	12.[illegible]	1.130	0.[illegible]	0.10[illegible]
6.82	13.[illegible]	1.45[illegible]	0.6[illegible]	0.1[illegible]
8.32	14.[illegible]	1.77[illegible]	0.7[illegible]	0.1[illegible]
[illegible].82	15.[illegible]	2.0[illegible]	0.7[illegible]7	0.1[illegible]
11.32	16.[illegible]	2.41[illegible]	0.[illegible]40	0.2[illegible]
12.82	16.[illegible]	2.737	0.8[illegible]	0.24[illegible]
14.32	17.[illegible]	3.057	0.8563	0.2[illegible]
15.62	17.[illegible]	3.377	0.8713	0.30[illegible]
17.32	17.[illegible]	3.697	0.8823	0.3[illegible]
19.32	17.[illegible]71	4.124	0.8940	0.3[illegible]
2[illegible].32	18.[illegible]27	4.765	0.9[illegible]7	0.4[illegible]
27.32	18.7[illegible]0	5.832	0.9317	0.52[illegible]
32.32	19.[illegible]	6.900	0.9494	0.[illegible]
34.32	19.[illegible]31	8.180	0.96[illegible]	0.7412
44.32	1[illegible].732	9.461	0.[illegible]	0.8573

DEL= 51.70 MM DSTR= 7.[illegible] MM THETA= 4.68 MM
RDEL= 0.50[illegible]E+05 RDSTR= 0.776[illegible]E+04 RTTA= 0.50[illegible]E+04

STATION 4

UINF= 21.091 M/S
REX= 0.2674E+07 X= 2.372
T= 23.40 DEG.C RHO= 0.9780 KG/CU.M
MU= 0.1830E-04 KG/MS NU= 0.1871E-04 M*M/S

Y(MM)	U (M/S)	Y/TTA	U/UE	Y/DEL
0.62	5.[illegible]	0.124	0.2535	0.0118
1.[illegible]	[illegible].[illegible]59	0.269	0.[illegible]	0.0255
2.34	[illegible]	0.468	0.3[illegible]	0.04[illegible]
3.34	[illegible].[illegible]7	0.668	0.4[illegible]	0.06[illegible]
[illegible]	10.[illegible]15	0.8[illegible]7	0.4918	0.08[illegible]
[illegible]	11.[illegible]	1.167	0.5610	0.11[illegible]
7.34	12.[illegible]	1.467	0.6178	0.1395
8.84	13.[illegible]	1.767	0.[illegible]77	0.16[illegible]
10.34	14.133	2.067	0.71[illegible]	0.1[illegible]
11.84	15.[illegible]14	2.366	0.75[illegible]	0.225[illegible]
13.34	16.[illegible]2	2.66[illegible]	0.7870	0.25[illegible]
14.84	17.[illegible]5	2.966	0.8137	0.2[illegible]
16.34	17.[illegible]	3.266	0.8[illegible]	0.31[illegible]
18.34	18.[illegible]	3.666	0.8[illegible]77	0.34[illegible]
20.34	18.[illegible]13	4.065	0.[illegible]	0.3[illegible]
22.34	19.[illegible]	4.465	0.9165	0.4[illegible]
25.34	19.393	5.065	0.9248	0.4816
30.34	19.710	6.064	0.9440	0.5767
35.34	20.[illegible]	7.063	0.9[illegible]	0.6717
40.34	20.[illegible]	8.063	0.9725	0.7667
45.34	20.[illegible]40	9.062	0.9837	0.8618

DEL= 52.61 MM DSTR= [illegible] MM THETA= 5.[illegible] MM
RDEL= 0.5331E+05 RDSTR= 0.[illegible]271E+04 RTTA= 0.56[illegible]E+04

E-17 0-17

2853

CURVE 1 FIT: LOG(FN)= 0.1777E+01*LOG(Y/D)+ 0.7639E+01

UINF= 18.455 M/S
REX= 0.1984E+07　　X= 1.928
T= 18.46 DEG.C　　RHO= 0.9849 KG/CU.M
MU= 0.1805E-04 KG/MS　　NU= 0.1815E-04 M*M/S

Y(MM)	U (M/S)	Y/TTA	U/UE	Y/DEL
0.62	[illegible]	0.157	0.5180	0.0123
1.37	12.936	0.335	0.6795	0.0293
[illegible]	[illegible]	0.710	0.7417	[illegible]
4.82	[illegible]	1.223	0.7806	[illegible]
6.82	[illegible]	1.730	0.8182	[illegible]
9.82	[illegible]	2.401	[illegible]	[illegible]
12.82	[illegible]	3.252	0.8644	[illegible]
15.82	[illegible]	[illegible]	0.8727	0.3181
19.82	[illegible]	[illegible]	0.9012	[illegible]
24.82	[illegible]	4.236	0.9252	[illegible]
29.82	[illegible]	[illegible]	[illegible]	0.5963
34.82	[illegible]	[illegible]	0.9615	0.6086
39.82	[illegible]	10.131	0.9760	0.7072
44.82	[illegible]	11.373	0.9890	0.8378

DEL= 40.88 MM　　DSTR= 5.28 MM　　THETA= 3.56 MM
RDEL= [illegible]　　RDSTR= [illegible]　　RTTA= [illegible]
SHAPE FACTOR,H= 1.28

****
STATION 2
****

UINF= 18.315 M/S
REX= 0.2237E+07　　X= 2.002
T= 18.31 DEG.C　　RHO= [illegible] KG/CU.M
MU= [illegible] KG/MS　　NU= [illegible] M*M/S

Y(MM)	U (M/S)	Y/TTA	U/UE	Y/DEL
0.62	[illegible]	0.141	0.3310	0.0125
0.76	[illegible]	0.172	0.3548	[illegible]
[illegible]	[illegible]	0.229	[illegible]	[illegible]
[illegible]	[illegible]	[illegible]	[illegible]	[illegible]
[illegible]	[illegible]	0.456	[illegible]	[illegible]
[illegible]	10.127	[illegible]	[illegible]	[illegible]
[illegible]	11.465	0.730	0.5669	0.0667
[illegible]	12.231	[illegible]	[illegible]	[illegible]
[illegible]	13.155	1.193	0.7251	[illegible]
[illegible]	13.773	1.410	0.7565	[illegible]
[illegible]	[illegible]	1.873	[illegible]	[illegible]
11.26	[illegible]	[illegible]	[illegible]	[illegible]
[illegible]	[illegible]	3.233	[illegible]	[illegible]
19.26	[illegible]	4.183	[illegible]	0.3775
22.26	16.675	5.047	[illegible]	0.4521
27.26	[illegible]	[illegible]	0.9297	[illegible]
32.26	17.272	7.316	0.9480	[illegible]
[illegible]	17.627	8.675	[illegible]	0.7771
44.26	17.941	10.035	0.9157	0.8993

DEL= 49.27 MM　　DSTR= 5.32 MM　　THETA= 4.41 MM
RDEL= 0.4974E+05　　RDSTR= [illegible]　　RTTA= [illegible]

****
STATION 3
****

UINF= 18.445 M/S
REX= 0.2125E+07　　X= 2.091
T= 18.91 DEG.C　　RHO= 0.9933 KG/CU.M
MU= [illegible] KG/MS　　NU= 0.1820E-04 M*M/S

Y(MM)	U (M/S)	Y/TTA	U/UE	Y/DEL
0.62	4.934	0.133	0.2671	0.0132
0.77	4.968	0.166	0.2770	0.0161
1.27	[illegible]	0.273	0.3221	0.0265
1.77	6.653	0.381	0.3642	0.0370
2.27	7.317	0.490	0.4004	0.0474
3.27	8.381	0.733	0.4540	0.0543
4.27	9.203	0.919	0.5038	0.0892
6.27	10.835	1.349	0.5987	0.1310
8.27	12.375	1.779	0.6776	0.1733
11.27	14.221	2.434	0.7786	0.2365
14.27	15.326	3.070	0.8392	0.2982
18.27	16.168	3.930	0.8853	0.3819
23.27	16.755	5.006	0.9176	0.4863
28.27	17.193	6.081	0.9413	0.5919
33.27	17.553	7.157	0.9610	0.6952
38.27	17.856	8.380	0.9776	0.8102
44.27	18.107	9.523	0.9912	0.9251

DEL= 47.85 MM　　DSTR= 7.65 MM　　THETA= 4.55 MM
RDEL= 0.4841E+05　　RDSTR= 0.7770E+04　　RTTA= 0.4713E+04

****
STATION 4
****

UINF= 18.231 M/S
REX= 0.2345E+07　　X= 2.191
T= 18.75 DEG.C　　RHO= 0.9938 KG/CU.M
MU= 0.1807E-04 KG/MS　　NU= 0.1818E-04 M*M/S

Y(MM)	U (M/S)	Y/TTA	U/UE	Y/DEL
0.62	3.978	0.113	0.2135	0.0121
0.82	4.520	0.141	0.2491	0.0167
1.32	5.962	0.228	0.3233	0.0254
2.32	6.610	0.475	0.3546	0.0451
2.82	7.026	0.570	0.3810	0.0549
3.82	7.950	0.680	0.4332	0.0743
5.82	9.467	1.050	0.5133	0.1132
8.82	11.386	1.591	0.6173	0.1716
11.82	12.532	2.132	0.7012	0.2330
16.82	15.029	3.033	0.8149	0.3272
21.82	16.310	3.935	0.8843	0.4245
26.82	16.915	4.837	0.9171	0.5219
31.82	17.232	5.739	0.9391	0.6191
41.82	17.888	7.542	0.9697	0.8136

DEL= 51.40 MM　　DSTR= 9.47 MM　　THETA= 5.55 MM
RDEL= 0.5266E+05　　RDSTR= 0.9720E+04　　RTTA= 0.5680E+04

STATION 1

CURVE FIT: [illegible] 0.1069E+00*LOG(Y/D)+-0.6750E-02

E-643-13

0302

UINF= 15.1[illegible] M/S
REX= 0.15[illegible]E+07 X= 1.929
T= 23.71 DEG.C RHO= 0.9773 KG/CU.M
MU= 0.18[illegible]E-04 KG/MS NU= 0.18[illegible]E-04 M*M/S

Y(MM)	U (M/S)	Y/TTA	U/UE	Y/DEL
[illegible]	[illegible]	0.150	0.[illegible]6	0.0129
[illegible]	[illegible]	0.222	0.[illegible]790	0.[illegible]
[illegible]	[illegible]	0.4[illegible]	0.[illegible]12	0.[illegible]
[illegible]	[illegible]	0.[illegible]47	0.[illegible]	0.0[illegible]
5.[illegible]2	[illegible]3	1.[illegible]	0.7018	0.1227
[illegible]	[illegible]	[illegible]	0.12[illegible]8	0.1849
11.[illegible]2	[illegible]3	[illegible]	0.[illegible]	0.24[illegible]
14.9[illegible]	[illegible]	3.0[illegible]	0.865[illegible]	0.3[illegible]
[illegible]92	[illegible]	[illegible]	0.[illegible]981	0.39[illegible]
2[illegible].92	[illegible]	[illegible]	0.9[illegible]6	0.47[illegible]
2[illegible].92	[illegible]	[illegible]	0.926[illegible]	0.5[illegible]
31.92	[illegible]2	7.[illegible]	0.946[illegible]	0.661[illegible]
37.[illegible]2	[illegible]35	9.[illegible]	0.[illegible]670	0.78[illegible]
43.92	[illegible]	1[illegible]	0.[illegible]2	0.910[illegible]

DEL= 42.52 MM DSTR= 5.2[illegible] MM THETA= 4.[illegible]4 MM
RDEL= 0.34[illegible]E+05 RDSTR= 0.4284E+04 RTTA= 0.3355E+04
SHAPE FACTOR,H= 1.29
POWER LAW, N= 7.22

STATION 2

UINF= 15.[illegible]17 M/S
REX= 0.1602E+07 X= 2.005
T= 23.51 DEG.C RHO= 0.9779 KG/CU.M
MU= 0.1830E-04 KG/MS NU= 0.1871E-04 M*M/S

Y(MM)	U (M/S)	Y/TTA	U/UE	Y/DEL
0.62	7.159	0.133	0.[illegible]	0.0117
1.05	[illegible]02	0.225	0.[illegible]	0.0199
1.75	[illegible]13	0.375	0.[illegible]	0.0[illegible]
2.75	[illegible]79	0.589	0.[illegible]	0.05[illegible]
3.75	[illegible]	0.803	0.[illegible]	0.07[illegible]
4.75	[illegible]	1.018	0.[illegible]	0.0900
5.75	[illegible]	1.232	0.[illegible]	0.1[illegible]
7.2[illegible]	[illegible]	1.549	0.[illegible]	0.1[illegible]
8.75	[illegible]	1.875	0.[illegible]	0.1[illegible]
10.25	[illegible]	2.196	0.[illegible]	0.1[illegible]
11.75	[illegible]	2.518	0.[illegible]	0.2[illegible]
13.25	[illegible]	2.839	0.[illegible]	0.2[illegible]
14.75	[illegible]	3.160	0.[illegible]	0.2[illegible]
16.75	[illegible]	3.589	0.[illegible]	0.3[illegible]
18.75	[illegible]	4.017	0.[illegible]	0.3[illegible]
2[illegible]	[illegible]	4.446	0.[illegible]	0.3[illegible]
22.75	[illegible]	4.874	0.[illegible]	0.4[illegible]
24.75	[illegible]	5.303	0.[illegible]	0.4[illegible]
27.[illegible]	[illegible]	5.946	0.[illegible]	0.5[illegible]
31.75	[illegible]	6.803	0.[illegible]	0.6[illegible]
37.[illegible]	[illegible]	8.088	0.[illegible]	0.7[illegible]
43.7[illegible]	[illegible]	9.374	0.[illegible]	0.8[illegible]

DEL= 52.79 MM DSTR= 6.16 MM THETA= 4.67 MM
RDEL= 0.437[illegible]E+05 RDSTR= 0.5[illegible]E+04 RTTA= 0.3870E+04

STATION 3

UINF= 15.944 M/S
REX= 0.1782E+07 X= 2.094
T= 23.74 DEG.C RHO= 0.9772 KG/CU.M
MU= 0.183[illegible]E-04 KG/MS NU= 0.1874E-04 M*M/S

Y(MM)	U (M/S)	Y/TTA	U/UE	Y/DEL
0.62	6.753	0.127	0.4278	0.0123
1.30	8.[illegible]	0.[illegible]7	0.5126	0.0[illegible]59
2.30	9.[illegible]37	0.473	0.5851	0.0458
3.30	10.[illegible]24	0.678	0.6413	0.0657
4.30	10.773	0.884	0.6825	0.0856
5.30	11.233	1.089	0.7110	0.1056
6.80	11.[illegible]43	1.398	0.7503	0.1354
8.30	12.302	1.706	0.7793	0.1653
9.80	12.677	2.014	0.8031	0.1952
11.30	12.946	2.323	0.8202	0.2251
12.80	13.174	2.631	0.8346	0.2550
14.30	13.399	2.939	0.8488	0.2848
16.30	13.678	3.351	0.8652	0.3247
19.30	13.812	3.967	0.8752	0.3844
22.30	14.094	4.584	0.8929	0.4442
27.30	14.450	5.612	0.9154	0.5438
32.30	14.739	6.639	0.9337	0.6434
38.30	15.085	7.873	0.9557	0.7629
44.30	15.438	9.106	0.97[illegible]0	0.8824

DEL= 50.21 MM DSTR= 6.65 MM THETA= 4.86 MM
RDEL= 0.4272E+05 RDSTR= 0.5870E+04 RTTA= 0.4140E+04

E-9.69-13

0402

CURVE [illegible] [illegible]E-12

UINF= 15.[illegible] M/S
REX= 0.10 [illegible]E+07 X= 2.[illegible]
T= 23.[illegible] DEG.C RHO= 0.[illegible] KG/CU.M
MU= 0.1[illegible]E-04 KG/MS NU= 0.1[illegible]E-04 M*M/S

Y(MM)	U (M/S)	Y/TTA	U/UE	Y/DEL
[illegible]	[illegible]	[illegible]	[illegible]	[illegible]

DEL= [illegible] MM DSTR= [illegible] MM THETA= 4.[illegible] MM
RDEL= [illegible] RDSTR= [illegible] RTTA= 0.[illegible]
SHAPE FACTOR [illegible]

STATION 2

UINF= 15.[illegible] M/S
REX= 0.177[illegible]E+07 X= 2.[illegible]
T= 23.[illegible] DEG.C RHO= [illegible] KG/CU.M
MU= [illegible]E-04 KG/MS NU= 0.[illegible]E-04 M*M/S

Y(MM)	U (M/S)	Y/TTA	U/UE	Y/DEL
0.62	[illegible]	0.4557	0.3124	[illegible]
[illegible]	[illegible]	[illegible]	[illegible]	[illegible]
[illegible]	[illegible]	0.8114	0.2[illegible]	[illegible]
[illegible]	[illegible]	0.9239	0.2651	[illegible]
[illegible]	[illegible]	[illegible]	[illegible]	[illegible]

DEL= [illegible] MM DSTR= [illegible] MM THETA= 4.62 MM
RDEL= 0.[illegible] RDSTR= 0.5[illegible]E+05 RTTA= 0.[illegible]

STATION 3

UINF= 15.7[illegible] M/S
REX= 0.1[illegible]E+07 X= 2.221
T= 23.89 DEG.C RHO= 0.9757 KG/CU.M
MU= 0.1832E-04 KG/MS NU= 0.1875E-04 M*M/S

Y(MM)	U (M/S)	Y/TTA	U/UE	Y/DEL
0.62	6.[illegible]	0.[illegible]	0.3121	[illegible]
[illegible]	[illegible]	[illegible]	0.3134	[illegible]
1.43	[illegible]	[illegible]	[illegible]	[illegible]
2.43	[illegible]	[illegible]	[illegible]	[illegible]
3.43	[illegible]	0.5[illegible]	[illegible]	[illegible]
4.43	[illegible]	[illegible]	[illegible]	[illegible]
[illegible]	[illegible]	[illegible]	[illegible]	[illegible]
6.43	[illegible]	[illegible]	[illegible]	[illegible]
[illegible]	[illegible]	[illegible]	[illegible]	[illegible]
[illegible]	[illegible]	[illegible]	[illegible]	[illegible]
[illegible]	[illegible]	[illegible]	0.21[illegible]	[illegible]
[illegible]	[illegible]	[illegible]	[illegible]	[illegible]
[illegible]	[illegible]	[illegible]	[illegible]	[illegible]
[illegible]	[illegible]	[illegible]	[illegible]	[illegible]
[illegible]	[illegible]	[illegible]	[illegible]	[illegible]
[illegible]	[illegible]	[illegible]	[illegible]	[illegible]
[illegible]	[illegible]	[illegible]	[illegible]	[illegible]
[illegible]	[illegible]	[illegible]	[illegible]	[illegible]
[illegible]	[illegible]	[illegible]	[illegible]	[illegible]
[illegible]	[illegible]	[illegible]	[illegible]	[illegible]
[illegible]	[illegible]	[illegible]	[illegible]	[illegible]
[illegible]	[illegible]	[illegible]	0.7220	[illegible]
[illegible]	[illegible]	[illegible]	0.8218	[illegible]
[illegible]	[illegible]	[illegible]	0.8812	[illegible]

DEL= [illegible] MM DSTR= 7.[illegible] MM THETA= 4.96 MM
RDEL= 0.[illegible] RDSTR= 0.[illegible]E+04 RTTA= 0.4177E+04

STATION 4

UINF= 16.[illegible] M/S
REX= 0.[illegible] X= 2.321
T= 23.[illegible] DEG.C RHO= 0.9778 KG/CU.M
MU= 0.1832E-04 KG/MS NU= 0.1872E-04 M*M/S

Y(MM)	U (M/S)	Y/TTA	U/UE	Y/DEL
0.62	5.[illegible]	0.3584	0.31[illegible]	[illegible]
[illegible]	[illegible]	[illegible]	[illegible]	[illegible]
1.94	7.[illegible]	0.4218	[illegible]	[illegible]
[illegible]	[illegible]	[illegible]	[illegible]	[illegible]
[illegible]	[illegible]	[illegible]	[illegible]	[illegible]
[illegible]	[illegible]	[illegible]	[illegible]	[illegible]
[illegible]	[illegible]	0.6430	[illegible]	[illegible]
[illegible]	[illegible]	[illegible]	[illegible]	[illegible]
[illegible]	[illegible]	0.7293	0.1[illegible]	[illegible]
10.94	[illegible]	[illegible]	0.21[illegible]	[illegible]
[illegible]	2[illegible]	0.7552	[illegible]	[illegible]
[illegible]	[illegible]	0.8078	[illegible]	[illegible]
[illegible]	[illegible]	0.8323	[illegible]	[illegible]
[illegible]	[illegible]	0.8512	[illegible]	[illegible]
[illegible]	[illegible]	0.8706	[illegible]	[illegible]
[illegible]	[illegible]	0.8818	[illegible]	[illegible]
[illegible]	[illegible]	0.8936	[illegible]	[illegible]
[illegible]	[illegible]	[illegible]	0.5243	[illegible]
[illegible]	[illegible]	0.9305	0.6224	[illegible]
[illegible]	[illegible]	[illegible]	[illegible]	[illegible]
[illegible]	[illegible]	0.9725	0.8576	[illegible]

DEL= [illegible] MM DSTR= 8.01 MM THETA= 5.[illegible] MM
RDEL= [illegible] RDSTR= 0.[illegible]E+04 RTTA= 0.4676E+04

CURVE 1 FIT: LOG(FD)= 0.1142E+02*LOG(Y/D)+-0.5725E-02

E-11.59-13

0301

UINF= 15.242 M/S
REX= 0.1712E+07 X= 2.074
T= 21.50 DEG.C RHO= 0.9916 KG/CU.M
MU= 0.1827E-04 KG/MS NU= 0.1849E-04 M*M/S

Y(MM)	U (M/S)	Y/TTA	U/UE	Y/DEL
0.??	8.9	0.142	0.5905	0.0124
?.60	9.6	0.226	[illegible]	0.0194
1.60	10.2	0.340	0.6742	0.0298
?.?0	10.7	0.569	0.7142	[illegible]
3.?0	11.1	0.7?8	0.7338	[illegible]
?.?0	11.7	1.255	0.7747	0.1098
7.?0	12.0	1.7?2	0.7876	0.1432
?.?0	12.3	2.140	0.8160	0.1898
11.?0	12.5	2.625	0.8?19	0.2259
1?.?0	12.7	3.087	0.8410	0.2624
16.?5	13.0	3.749	0.8567	0.3?0?
20.?0	13.4	4.6?2	0.8865	0.4?9?
25.?0	13.7	5.825	0.9025	0.5195
30.?0	14.1	6.958	[illegible]	0.6?98
37.?0	14.5	8.567	0.9576	0.7695
45.?0	14.3	10.305	0.9403	[illegible]

DEL= 45.?5 MM DSTR= ?.64 MM THETA= 4.38 MM
RDEL= 0.??1?E+05 RDSTR= 0.???4E+04 RTTA= 0.?6??E+04
SHAPE FACTOR,H= 1.29

****
STATION 2
****

UINF= 15.1?? M/S
REX= 0.1761E+07 X= 2.??2
T= 2?.?? DEG.C RHO= ?.???? KG/CU.M
MU= 0.182?E-04 KG/MS NU= ?.?156E-04 M*M/S

Y(MM)	U (M/S)	Y/TTA	U/UE	Y/DEL
0.??	5.5	0.1?0	0.3771	0.0119
1.1?	7.1	0.2??	[illegible]	[illegible]
1.9?	8.3	0.3?6	0.5657	[illegible]
2.??	9.4	0.4?5	0.6?15	0.0??7
3.9?	10.2	0.8?3	0.6971	0.0749
4.9?	10.9	[illegible]	0.7?7?	[illegible]
5.9?	11.3	1.2??	0.7?33	0.11?3
7.90	11.8	1.?41	0.7?7?	0.1419
8.90	12.0	1.856	0.8?43	0.1709
10.4?	12.2	2.159	0.8?49	0.1?27
11.9?	12.4	2.??	0.8?13	0.2?15
13.4?	12.6	2.756	0.8?13	0.257?
14.9?	12.7	3.167	0.8512	0.2841
16.9?	13.?	3.?2?	0.8?60	0.3245
18.9?	13.1	3.941	0.87??	0.3?29
2?.9?	13.2	4.?8?	0.89??	0.4113
22.9?	13.4	4.775	0.9054	0.4307
25.9?	13.6	5.4??	0.9?66	0.4974
29.9?	13.9	6.?35	0.9?7?	0.5762
34.9?	14.1	7.?77	0.9442	0.67?2
39.90	14.4	8.320	0.9638	0.7652
44.90	14.7	9.353	0.9?37	0.8522

DEL= 52.?? MM DSTR= ?.54 MM THETA= ?.?? MM
RDEL= 0.4260E+05 RDSTR= 0.?35?E+04 RTTA= 0.352?E+0?

****
STATION 3
****

UINF= 15.550 M/S
REX= 0.1874E+07 X= ?.241
T= 22.45 DEG.C RHO= 0.9814 KG/CU.M
MU= 0.1825E-04 KG/MS NU= 0.1859E-04 M*M/S

Y(MM)	U (M/S)	Y/TTA	U/UE	Y/DEL
[illegible]	5.?	0.119	0.3394	0.0130
[illegible]	?.?	0.175	0.?706	0.0199
[illegible]	7.1	0.?67	0.4528	0.0?20
[illegible]	8.?	0.558	0.5??4	0.0?29
[illegible]	8.?	0.759	0.5682	0.0418
[illegible]	9.?	0.962	0.6135	0.1?27
[illegible]	10.2	1.?30	0.6551	0.1?41
[illegible]	10.9	1.519	0.7113	0.1655
[illegible]	11.6	1.906	0.7555	0.1969
[illegible]	12.?	2.?64	0.7954	0.2293
[illegible]	12.4	2.381	0.8074	0.2597
[illegible]	12.7	2.640	0.8273	0.?91?
[illegible]	12.9	3.061	0.8404	0.3228
[illegible]	13.1	3.245	0.85??	0.35?8
[illegible]	13.2	3.629	0.8672	0.3957
[illegible]	13.?	4.204	0.8834	0.458?
[illegible]	13.8	6.072	0.930?	0.5421
[illegible]	14.1	?.931	0.9214	0.5?67
[illegible]	14.5	?.891	0.9441	0.7514
[illegible]	14.9	?.?4?	0.9723	0.8769

DEL= 4?.79 MM DSTR= 7.09 MM THETA= 5.21 MM
RDEL= 0.?95?E+05 RDSTR= 0.6423E+04 RTTA= 0.4358E+04

****
STATION 4
****

UINF= 16.?PE M/S
REX= 0.2036E+07 X= 2.341
T= 22.50 DEG.C RHO= 0.9809 KG/CU.M
MU= 0.1825E-04 KG/MS NU= 0.1861E-04 M*M/S

Y(MM)	U (M/S)	Y/TTA	U/UE	Y/DEL
0.62	5.?	0.116	0.3124	0.0119
1.05	5.8	0.195	0.3622	0.0202
2.05	6.9	0.383	0.4?72	0.0394
3.05	7.6	0.57?	0.4764	0.0585
4.05	8.3	0.757	0.5109	0.0778
5.05	9.0	0.944	0.5518	0.0971
6.52	9.8	1.219	0.6147	0.1253
8.05	10.7	1.5?5	0.6739	0.1547
9.55	11.3	1.786	0.7106	0.1835
11.05	12.0	2.066	0.7515	0.2124
12.55	12.6	2.346	0.7854	0.2412
14.05	13.0	2.627	0.8149	0.2700
16.05	13.4	3.001	0.8307	0.3085
18.05	13.8	3.375	0.8672	0.3450
20.05	14.0	3.749	0.8762	0.3853
22.05	14.2	4.123	0.8903	0.4238
24.05	14.4	4.496	0.8994	0.4622
27.05	14.?	5.057	0.9143	0.5199
32.05	15.0	5.992	0.9369	0.6160
38.05	15.2	7.114	0.9533	0.7313
44.05	15.5	8.236	0.9732	0.8456

DEL= 52.03 MM DSTR= 8.23 MM THETA= 5.35 MM
RDEL= 0.4526E+05 RDSTR= 0.7163E+04 RTTA= 0.4653E+04

E-12.79-13

0401

CURVE 1 FIT: LOGIFMIX [illegible]

UINF= 15.150 M/S
REX= [illegible]
T= 20.31 DEG.C
MU= 0.1814E-04 KG/MS

X= 1.994
RHO= [illegible] KG/CU.M
NU= [illegible] M*M/S

Y(MM)	U (M/S)	Y/TTA	U/UE	Y/DEL
[illegible]	3.168	0.146	0.4176	0.0122
1.?0	10.035	0.378	[illegible]	[illegible]
2.60	10.373	[illegible]	[illegible]	0.0572
3.60	[illegible]	[illegible]	[illegible]	0.0774
4.60	[illegible]	[illegible]	[illegible]	0.0941
6.?0	[illegible]	[illegible]	[illegible]	[illegible]
8.60	[illegible]	[illegible]	[illegible]	0.1750
11.60	[illegible]	[illegible]	[illegible]	[illegible]
13.60	[illegible]	[illegible]	[illegible]	[illegible]
17.60	[illegible]	[illegible]	[illegible]	[illegible]
20.60	[illegible]	[illegible]	[illegible]	[illegible]
24.60	[illegible]	[illegible]	[illegible]	[illegible]
31.60	[illegible]	[illegible]	[illegible]	[illegible]
37.60	[illegible]	[illegible]	[illegible]	[illegible]
44.60	[illegible]	[illegible]	0.9180	[illegible]

DEL= 47.62 MM
RDEL= [illegible]

DSTR= [illegible]
RDSTR= [illegible]

THETA= [illegible]
RTTA= [illegible]

STATION 2

UINF= [illegible]
REX= [illegible]
T= 21.30 DEG.C
MU= [illegible] KG/MS

X= [illegible]
RHO= [illegible] KG/CU.M
NU= [illegible] M*M/S

Y(MM)	U (M/S)	Y/TTA	U/UE	Y/DEL
0.62	5.023	[illegible]	0.3081	[illegible]
1.25	[illegible]	[illegible]	[illegible]	[illegible]
2.25	[illegible]	[illegible]	[illegible]	[illegible]
3.25	[illegible]	[illegible]	[illegible]	[illegible]
4.25	[illegible]	[illegible]	[illegible]	[illegible]
[illegible]	[illegible]	[illegible]	[illegible]	[illegible]
[illegible]	[illegible]	[illegible]	[illegible]	[illegible]
8.25	[illegible]	[illegible]	[illegible]	[illegible]
9.75	[illegible]	[illegible]	[illegible]	[illegible]
11.25	[illegible]	[illegible]	[illegible]	[illegible]
12.75	[illegible]	[illegible]	[illegible]	[illegible]
14.25	[illegible]	[illegible]	0.8517	[illegible]
16.25	[illegible]	[illegible]	[illegible]	[illegible]
18.25	[illegible]	[illegible]	[illegible]	[illegible]
21.25	[illegible]	[illegible]	[illegible]	0.4554
24.25	[illegible]	[illegible]	[illegible]	[illegible]
28.25	[illegible]	[illegible]	[illegible]	[illegible]
32.25	[illegible]	[illegible]	[illegible]	[illegible]
37.25	[illegible]	[illegible]	[illegible]	[illegible]
[illegible]	[illegible]	[illegible]	[illegible]	[illegible]
44.25	[illegible]	[illegible]	[illegible]	[illegible]

DEL= 52.7? MM
RDEL= [illegible]

DSTR= 6.40 MM
RDSTR= 0.5379E+04

THETA= [illegible] MM
RTTA= [illegible]

STATION 3

UINF= 15.670 M/S
REX= 0.1834E+07
T= 22.15 DEG.C
MU= [illegible] KG/MS

X= 2.150
RHO= [illegible] KG/CU.M
NU= [illegible] M*M/S

Y(MM)	U (M/S)	Y/TTA	U/UE	Y/DEL
[illegible]	[illegible]	[illegible]	0.3090	[illegible]
1.21	[illegible]	[illegible]	[illegible]	[illegible]
2.21	7.621	[illegible]	[illegible]	[illegible]
3.21	[illegible]	[illegible]	[illegible]	[illegible]
4.21	[illegible]	[illegible]	[illegible]	[illegible]
[illegible]	[illegible]	[illegible]	[illegible]	[illegible]
[illegible]	[illegible]	[illegible]	[illegible]	[illegible]
[illegible]	[illegible]	[illegible]	[illegible]	[illegible]
[illegible]	11.724	[illegible]	[illegible]	[illegible]
11.21	[illegible]	[illegible]	[illegible]	[illegible]
12.71	[illegible]	[illegible]	[illegible]	[illegible]
[illegible]	[illegible]	[illegible]	[illegible]	[illegible]
[illegible]	[illegible]	[illegible]	[illegible]	[illegible]
[illegible]	[illegible]	[illegible]	[illegible]	[illegible]
[illegible]	[illegible]	[illegible]	[illegible]	[illegible]
[illegible]	[illegible]	[illegible]	[illegible]	[illegible]
[illegible]	[illegible]	[illegible]	[illegible]	[illegible]
[illegible]	[illegible]	[illegible]	[illegible]	[illegible]
[illegible]	[illegible]	[illegible]	[illegible]	[illegible]
43.21	[illegible]	[illegible]	[illegible]	[illegible]

DEL= 50.27 MM
RDEL= [illegible]

DSTR= [illegible] MM
RDSTR= 0.6545E+04

THETA= [illegible] MM
RTTA= [illegible]

STATION 4

UINF= 15.090 M/S
REX= [illegible]
T= 23.08 DEG.C
MU= [illegible] KG/MS

X= 2.259
RHO= [illegible] KG/CU.M
NU= [illegible] M*M/S

Y(MM)	U (M/S)	Y/TTA	U/UE	Y/DEL
[illegible]	[illegible]	[illegible]	[illegible]	[illegible]
[illegible]	[illegible]	0.233	[illegible]	[illegible]
[illegible]	[illegible]	0.415	[illegible]	[illegible]
[illegible]	[illegible]	[illegible]	[illegible]	[illegible]
[illegible]	[illegible]	[illegible]	[illegible]	[illegible]
[illegible]	[illegible]	[illegible]	[illegible]	[illegible]
[illegible]	[illegible]	[illegible]	0.6069	[illegible]
[illegible]	[illegible]	[illegible]	[illegible]	0.1450
9.78	[illegible]	1.770	[illegible]	[illegible]
11.28	[illegible]	2.051	0.7314	[illegible]
12.78	[illegible]	2.324	0.7617	[illegible]
[illegible]	[illegible]	2.596	0.7908	0.3137
[illegible]	[illegible]	[illegible]	[illegible]	[illegible]
18.28	[illegible]	[illegible]	[illegible]	0.4016
20.78	[illegible]	3.647	[illegible]	0.4455
[illegible]	[illegible]	4.233	[illegible]	[illegible]
[illegible]	[illegible]	4.778	[illegible]	[illegible]
[illegible]	[illegible]	[illegible]	[illegible]	[illegible]
[illegible]	[illegible]	[illegible]	0.9495	[illegible]
[illegible]	[illegible]	8.231	0.9977	[illegible]

DEL= 45.52 MM
RDEL= [illegible]

DSTR= [illegible] MM
RDSTR= [illegible]

THETA= [illegible]
RTTA= [illegible]

E-14,13-13

D501

STATION 1

CURVE 1 FIT: LOG(FD)= 0.1146E+00*LOG(Y/D)+-0.4671E-02

UINF= 15.0[illegible] M/S
REX= 0.18[illegible]E+07
T= 23.98 DEG.C
MU= 0.1832E-04 KG/MS

X= 2.234
RHO= 0.97[illegible] KG/CU.M
NU= 0.1877E-04 M*M/S

Y(MM)	U (M/S)	Y/TTA	U/UE	Y/DEL
[illegible]	9.291	0.135	0.5872	0.0117
1.00	10.000	0.233	0.64[illegible]	0.0[illegible]
2.00	[illegible]	0.449	0.59[illegible]	0.0388
3.00	11.462	0.669	0.7[illegible]57	0.0577
4.00	11.870	0.997	0.7565	0.0865
6.00	12.282	1.326	0.7762	0.1144
7.00	12.549	1.651	0.7931	0.1424
9.00	12.[illegible]2	1.9[illegible]	0.80[illegible]8	0.1742
[illegible]	13.[illegible]56	2.[illegible]2	0.[illegible]2	0.[illegible]
13.00	13.204	2.[illegible]	0.[illegible]	0.2469
[illegible]	13.[illegible]	3.2[illegible]	0.[illegible]	0.28[illegible]
[illegible]	13.791	3.[illegible]57	0.[illegible]	0.[illegible]
21.00	14.[illegible]	4.6[illegible]	0.[illegible]2	0.[illegible]
25.00	14.282	5.4[illegible]	0.9[illegible]	0.[illegible]79
30.0	14.719	[illegible]87	0.93[illegible]2	0.[illegible]85
35.00	15.026	7.[illegible]83	0.94[illegible]	0.[illegible]70
40.00	15.[illegible]79	8.[illegible]	0.9693	0.7576
45.00	15.[illegible]77	9.[illegible]	0.9[illegible]13	0.85[illegible]

DEL= 46.[illegible] MM
RDEL= 0.4[illegible]E+05
SHAPE FACTOR,H= 1.2[illegible]
POWER LAW, N= 6.9[illegible]

DSTR= [illegible] MM
RDSTR= 0.5[illegible]E+04

THETA= 4.56 MM
RTTA= 0.38[illegible]E+04

STATION 2

UINF= 15.067 M/S
REX= [illegible]E+07
T= [illegible] DEG.C
MU= [illegible]E-04 KG/MS

X= 2.280
RHO= 0.974[illegible] KG/CU.M
NU= 0.188[illegible]E-04 M*M/S

Y(MM)	U (M/S)	Y/TTA	U/UE	Y/DEL
[illegible]	5.937	0.132	[illegible]	0.0124
1.24	[illegible]	0.265	[illegible]	0.0249
2.24	[illegible]22	0.479	[illegible]33	0.0449
3.24	[illegible]65	0.691	0.6243	0.0648
4.23	[illegible]	0.905	0.6351	0.0847
[illegible]	11.[illegible]	1.118	0.7270	0.1047
6.24	11.[illegible]75	1.332	0.[illegible]	0.1247
7.24	11.312	[illegible]	0.7711	0.1447
9.74	12.645	1.865	0.8020	0.1747
11.24	12.[illegible]	2.[illegible]	0.[illegible]	0.2047
12.24	12.[illegible]	2.612	0.8328	0.2446
14.24	[illegible]	3.039	0.8440	0.2845
16.74	[illegible]	3.573	0.8678	0.3346
20.24	14.0[illegible]	4.323	0.8803	0.4045
24.24	14.234	5.173	0.9007	0.4845
29.24	14.652	6.240	0.9271	0.5844
34.24	14.947	7.308	0.9457	0.6843
39.24	15.265	8.375	0.9660	0.7843
43.24	15.465	9.223	0.9786	0.8642

DEL= 50.[illegible] MM
RDEL= 0.4[illegible]E+05

DSTR= 6.52 MM
RDSTR= 0.5524E+04

THETA= [illegible].69 MM
RTTA= 0.[illegible]E+04

STATION 3

UINF= 16.144 M/S
REX= 0.20[illegible]E+07
T= 24.80 DEG.C
MU= 0.1836E-04 KG/MS

X= 2.369
RHO= 0.9737 KG/CU.M
NU= 0.1886E-04 M*M/S

Y(MM)	U (M/S)	Y/TTA	U/UE	Y/DEL
0.62	4.637	0.116	0.2901	0.0119
1.22	5.074	0.277	0.3730	0.0234
2.22	7.063	0.414	0.4417	0.0426
3.22	8.089	0.6[illegible]	0.5060	0.0618
4.[illegible]	8.258	0.737	0.5542	0.0810
5.22	8.463	0.973	0.5921	0.1002
6.22	10.210	1.159	0.6334	0.1194
7.22	11.059	1.439	0.6833	0.1412
9.22	11.668	1.719	0.7263	0.1770
10.72	12.296	1.998	0.7694	0.2050
12.22	12.757	2.273	0.7983	0.2346
[illegible]	13.064	2.558	0.8176	0.2634
[illegible]	13.327	2.837	0.8335	0.2922
17.22	13.589	3.210	0.8502	0.3306
20.22	13.949	3.709	0.8[illegible]8	0.3882
[illegible]	14.222	4.[illegible]	0.8848	0.445[illegible]
27.22	14.569	5.074	0.91[illegible]	0.[illegible]
32.22	14.865	6.[illegible]6	0.93[illegible]1	0.61[illegible]
38.22	15.199	7.125	0.9510	0.733[illegible]
45.22	15.594	8.429	0.97[illegible]7	0.8681

DEL= 52.0[illegible] MM
RDEL= 0.4[illegible]E+05
SHAPE FACTOR,H= 1.5[illegible]
POWER LAW, N= 3.9[illegible]

DSTR= 8.11 MM
RDSTR= 0.6941E+04

THETA= 5.36 MM
RTTA= 0.[illegible]593E+04

STATION 4

UINF= 16.[illegible]4 M/S
REX= 0.21[illegible]E+07
T= 25.2[illegible] DEG.C
MU= 0.183[illegible]E-04 KG/MS

X= 2.469
RHO= 0.97[illegible]2 KG/CU.M
NU= 0.189[illegible]E-04 M*M/S

Y(MM)	U (M/S)	Y/TTA	U/UE	Y/DEL
0.62	[illegible]21	0.106	0.2667	0.0113
1.21	5.52[illegible]	0.[illegible]7	0.34[illegible]7	0.0221
2.21	6.563	0.378	0.4039	0.0403
3.21	7.[illegible]05	0.549	0.45[illegible]	0.0596
4.21	7.[illegible]9	0.720	0.[illegible]534	0.0[illegible]
5.21	8.577	0.891	0.5292	0.0951
6.69	9.523	1.[illegible]	0.5873	0.1221
8.21	10.172	1.405	0.6277	0.1499
9.71	10.887	1.661	0.6721	0.1772
11.21	11.473	1.918	0.7[illegible]2	0.2046
12.71	12.017	2.175	0.7[illegible]8	0.2310
14.21	12.[illegible]45	2.431	0.77[illegible]	0.2593
16.21	13.[illegible]69	2.773	0.8[illegible]	0.2959
18.21	13.558	3.115	0.8375	0.3323
20.21	13.9[illegible]8	3.458	0.8590	0.3688
23.21	14.301	3.971	0.882[illegible]	0.4235
27.21	14.720	4.655	0.9074	0.4965
32.21	15.016	5.511	0.9269	0.5878
38.21	15.373	6.537	0.9489	0.6973
44.21	15.672	7.504	0.9674	0.8068

DEL= 54.80 MM
RDEL= 0.4742E+05

DSTR= 9.27 MM
RDSTR= 0.8024E+04

THETA= 5.84 MM
RTTA= 0.5058E+04

E-7,74-9

0701

CURVE | FIT: LOG(FD)= 0.1190E+00*LOG(Y/D)+-0.1099E-01

UINF= 11.1?? M/S
REX= 0.1367E+07 X= 2.323
T= 24.87 DEG.C RHO= 0.9734 KG/CU.M
MU= [illegible]1836E-04 KG/MS NU= 0.1287E-04 M*M/S

Y(MM)	U (M/S)	Y/TTA	U/UF	Y/DEL
[illegible]	6.178	[illegible]191	[illegible]	0.[illegible]117
1.19	[illegible]	[illegible]	[illegible]	0.[illegible]
2.19	7.640	[illegible]	[illegible]	0.0413
3.19	7.925	[illegible]	0.7[illegible]8	0.0[illegible]
4.19	8.27[illegible]	[illegible]	[illegible]	0.0825
6.19	8.472	[illegible]	[illegible]	0.[illegible]
8.19	8.7[illegible]	[illegible]	0.[illegible]831	0.[illegible]565
10.19	8.891	[illegible]	[illegible]	0.[illegible]923
12.19	9.075	[illegible]	[illegible]	0.[illegible]
14.19	9.107	[illegible]	[illegible]164	0.[illegible]679
[illegible]	9.321	[illegible]	[illegible]	0.[illegible]244
[illegible]	9.4[illegible]	[illegible]	[illegible]	0.[illegible]
[illegible]	[illegible]	[illegible]642	[illegible]	0.4753
[illegible]	[illegible]	[illegible]	0.[illegible]932	0.5697
36.19	10.252	[illegible]	[illegible]	0.[illegible]829
43.19	10.586	[illegible]	[illegible]27	0.[illegible]150

DEL= 52.73 MM DSTR= [illegible] MM THETA= 5.12 MM
RDEL= [illegible] RDSTR= [illegible] RTTA= 0.3015E+04
SHAPE FACTOR,H= 1.29

STATION 2

UINF= 10.9[illegible] M/S
REX= [illegible] X= 2.39[illegible]
T= 25.56 DEG.C RHO= [illegible] KG/CU.M
MU= 0.1840E-04 KG/MS NU= [illegible] M*M/S

Y(MM)	U (M/S)	Y/TTA	U/UF	Y/DEL
[illegible]	[illegible]	[illegible]	[illegible]	0.0[illegible]2
[illegible].12	[illegible]	[illegible]	[illegible]	[illegible]
[illegible]	[illegible]	[illegible]	[illegible]	0.[illegible]
2.[illegible]	[illegible]	[illegible]	[illegible]524	[illegible]
3.[illegible]	[illegible]	0.606	0.6[illegible]	0.0[illegible]5
[illegible]	[illegible]	0.8[illegible]	0.70[illegible]5	0.0836
5.[illegible]	[illegible]	[illegible]	0.7344	0.1[illegible]7
[illegible]	[illegible]	[illegible]	[illegible]	0.1[illegible]
[illegible]	[illegible]274	[illegible]	0.7778	0.14[illegible]
[illegible]	[illegible]	[illegible]	[illegible]	[illegible]1741
11.[illegible]	[illegible]	[illegible]	[illegible]	[illegible]
[illegible]	[illegible]	[illegible]	[illegible]	[illegible]284
[illegible]	[illegible]	[illegible]	[illegible]	0.2646
[illegible]	[illegible]	3.1[illegible]	[illegible]	[illegible]
[illegible]	[illegible]	[illegible]	0.8673	[illegible]
[illegible]	[illegible]	[illegible]	0.[illegible]717	[illegible]
[illegible]	[illegible]	[illegible]	0.8830	[illegible]
[illegible]	[illegible]	[illegible]123	[illegible]9021	0.4810
[illegible]	[illegible]	[illegible]	[illegible]	0.57[illegible]
[illegible]	[illegible]	[illegible]	0.9417	0.6629
[illegible]	10.361	[illegible]	0.9574	0.75[illegible]4
45.62	10.456	8.775	0.96[illegible]9	0.8258

DEL= 55.24 MM DSTR= [illegible] MM THETA= 5.20 MM
RDEL= 0.[illegible]E+05 RDSTR= [illegible] RTTA= 0.3000E+04

STATION 3

UINF= 10.966 M/S
REX= 0.1439E+07 X= 2.488
T= 25.50 DEG.C RHO= 0.9699 KG/CU.M
MU= 0.1842E-04 KG/MS NU= 0.1899E-04 M*M/S

Y(MM)	U (M/S)	Y/TTA	U/UF	Y/DEL
[illegible]	[illegible]	0.1[illegible]	[illegible]	0.0[illegible]
1.24	[illegible]	[illegible]	[illegible]	0.0[illegible]
1.74	[illegible]	[illegible]	[illegible]	0.0[illegible]
2.74	[illegible]	[illegible]	[illegible]	0.0[illegible]
3.74	[illegible]	[illegible]	[illegible]	0.0[illegible]
4.74	[illegible]	[illegible]	0.[illegible]742	0.0[illegible]
[illegible]	[illegible]	[illegible]	[illegible]	[illegible]
[illegible]	[illegible]	1.2[illegible]	[illegible]	0.11[illegible]
[illegible]	[illegible]	[illegible]	[illegible]	[illegible]
[illegible]	[illegible]	1.7[illegible]	[illegible]	[illegible]
[illegible]	[illegible]	[illegible]	[illegible]	[illegible]
[illegible]	[illegible]	[illegible]	[illegible]	[illegible]
[illegible]	[illegible]	2.[illegible]	[illegible]	[illegible]
[illegible]	[illegible]	2.[illegible]	[illegible]	[illegible]
[illegible]	[illegible]	2.[illegible]	[illegible]	[illegible]
[illegible]	[illegible]	3.[illegible]	0.[illegible]613	[illegible]
[illegible]	[illegible]	3.[illegible]	[illegible]	[illegible]
[illegible]	[illegible]	3.5[illegible]	[illegible]	[illegible]
[illegible]	[illegible]	4.[illegible]	[illegible]	[illegible]
[illegible]	[illegible]	[illegible]	[illegible]	[illegible]
[illegible]	[illegible]	[illegible]	[illegible]	[illegible]
[illegible]	[illegible]	[illegible]	[illegible]	[illegible]
[illegible]	[illegible]	[illegible]	[illegible]	[illegible]
[illegible]	[illegible]	7.[illegible]	[illegible]9541	0.7145

DEL= [illegible] MM DSTR= 7.82 MM THETA= 5.79 MM
RDEL= [illegible] RDSTR= [illegible]52[illegible]E+04 RTTA= 0.335[illegible]E+04

STATION 4

UINF= 10.5[illegible] M/S
REX= [illegible] X= 2.583
T= [illegible] DEG.C RHO= 0.9686 KG/CU.M
MU= [illegible] KG/MS NU= 0.1503E-04 M*M/S

Y(MM)	U (M/S)	Y/TTA	U/UF	Y/DEL
[illegible]	[illegible]	[illegible]	0.4[illegible]	0.0[illegible]
[illegible]	[illegible]	[illegible]	0.4[illegible]18	0.0181
2.[illegible]	[illegible]	[illegible]	0.5[illegible]	0.0330
[illegible]	[illegible]210	[illegible]	0.5705	0.0407
4.[illegible]	[illegible]	[illegible]	0.6185	0.0655
5.[illegible]	[illegible]	[illegible]	0.6586	0.0891
7.[illegible]	[illegible]	[illegible]	0.6[illegible]51	0.[illegible]129
[illegible]	[illegible]	[illegible]	0.7[illegible]	0.14[illegible]
[illegible]	[illegible]	[illegible]	0.7666	0.1759
13.[illegible]	[illegible]	[illegible]	0.80[illegible]	0.[illegible]074
[illegible]	[illegible]	2.[illegible]	0.8241	0.2[illegible]
17.[illegible]	[illegible]	2.76[illegible]	0.8[illegible]	0.27[illegible]5
[illegible]	[illegible]	3.[illegible]	0.[illegible]	0.3[illegible]
[illegible]	[illegible]	[illegible]	0.8652	0.3[illegible]
[illegible]	[illegible]	4.0[illegible]	0.[illegible]774	0.3[illegible]
[illegible]	[illegible]018	5.1[illegible]	0.91[illegible]	0.5071
30.15	10.154	6.3[illegible]	0.9325	0.6176
44.15	10.30[illegible]	7.12[illegible]	0.9464	0.6964

DEL= 63.39 MM DSTR= [illegible] MM THETA= [illegible] MM
RDEL= 0.2663E+05 RDSTR= 0.[illegible]E+04 RTTA= 0.3579E+04

CURVE 1 FIT: [illegible] = [illegible]*LOG(Y/D)+[illegible]

E-12.03-9

0501

UINF= [illegible] M/S
RTX= [illegible] X= [illegible]
T= [illegible] RHO= [illegible] KG/CU.M
MU= [illegible] KG/MS NU= [illegible] M*M/S

Y(MM)	U (M/S)	Y/TTA	U/UE	Y/DEL
[illegible]	[illegible]	[illegible]	0.5462	[illegible]
1.75	7.421	[illegible]	[illegible]	[illegible]
2.75	[illegible]	[illegible]	[illegible]	[illegible]
3.75	7.313	[illegible]	0.7248	[illegible]
5.75	[illegible]	[illegible]	[illegible]	[illegible]
7.75	[illegible]	1.4[illegible]	0.7[illegible]	[illegible]
9.75	[illegible]	[illegible]	0.79[illegible]	[illegible]
11.75	[illegible]	[illegible]	0.8192	[illegible]
13.75	[illegible]	[illegible]	[illegible]	[illegible]
15.75	[illegible]	[illegible]	[illegible]	[illegible]
18.75	[illegible]	[illegible]	[illegible]	[illegible]
21.75	[illegible]	[illegible]	[illegible]	[illegible]
25.75	[illegible]	4.9[illegible]	[illegible]	0.45[illegible]
30.75	[illegible]	5.7[illegible]	0.9036	[illegible]
35.75	[illegible]	6.7[illegible]	[illegible]	0.67[illegible]
40.75	[illegible]	7.6[illegible]	[illegible]	0.7141
45.75	[illegible]	8.0[illegible]	[illegible]	0.8019

DEL= [illegible] MM DSTR= [illegible] MM THETA= [illegible] MM
RDEL= [illegible] RDSTR= [illegible] RTTA= [illegible]
SHAPE FACTOR, H= [illegible]

STATION 2

UINF= 12.[illegible] M/S
RTX= 0.[illegible]E+07 X= 2.[illegible]
T= [illegible] RHO= [illegible] KG/CU.M
MU= [illegible] KG/MS NU= [illegible] M*M/S

Y(MM)	U (M/S)	Y/TTA	U/UE	Y/DEL
[illegible]	[illegible]	[illegible]	[illegible]	[illegible]
1.47	[illegible]	[illegible]	[illegible]	[illegible]
2.47	[illegible]	[illegible]	[illegible]	[illegible]
3.47	[illegible]	[illegible]	[illegible]	[illegible]
[illegible]	[illegible]	[illegible]	[illegible]	[illegible]
[illegible]	[illegible]	[illegible]	[illegible]	[illegible]
[illegible]	[illegible]	[illegible]	[illegible]	[illegible]
[illegible]	[illegible]	[illegible]	0.7762	[illegible]
[illegible]	[illegible]	[illegible]	[illegible]	[illegible]
[illegible]	[illegible]	[illegible]	[illegible]	[illegible]
[illegible]	[illegible]	[illegible]	[illegible]	[illegible]
[illegible]	[illegible]	[illegible]	[illegible]	[illegible]
[illegible]	[illegible]	[illegible]	[illegible]	[illegible]
[illegible]	[illegible]	[illegible]	[illegible]	[illegible]
[illegible]	[illegible]	[illegible]	[illegible]	[illegible]
[illegible]	[illegible]	[illegible]	[illegible]	[illegible]
[illegible]	[illegible]	4.[illegible]	[illegible]	[illegible]
[illegible]	[illegible]	4.602	0.8974	[illegible]
[illegible]	[illegible]	5.566	0.9290	0.56[illegible]
[illegible]	[illegible]	[illegible]	[illegible]	[illegible]
41.47	[illegible]	[illegible]	[illegible]	[illegible]
45.47	[illegible]	8.042	[illegible]	[illegible]

DEL= [illegible] MM DSTR= 7.[illegible] MM THETA= [illegible] MM
RDEL= 0.32[illegible]E+05 RDSTR= 0.[illegible]E+04 RTTA= [illegible]
SHAPE FACTOR, H= [illegible]

STATION 3

UINF= 11.[illegible] M/S
RTX= 0.[illegible]E+07 X= [illegible]
T= [illegible] RHO= [illegible] KG/CU.M
MU= [illegible] KG/MS NU= [illegible] M*M/S

Y(MM)	U (M/S)	Y/TTA	U/UE	Y/DEL
[illegible]	[illegible]	0.132	[illegible]	[illegible]
[illegible]	[illegible]	[illegible]	[illegible]	[illegible]
[illegible]	[illegible]	0.346	[illegible]	[illegible]
[illegible]	[illegible]	0.510	0.5435	[illegible]
[illegible]	[illegible]	0.674	[illegible]	[illegible]
[illegible]	[illegible]	[illegible]	[illegible]	[illegible]
[illegible]	[illegible]	[illegible]	[illegible]	[illegible]
[illegible]	7.719	[illegible]	[illegible]	[illegible]
[illegible]	[illegible]	[illegible]	[illegible]	[illegible]
[illegible]	[illegible]	[illegible]	0.7597	[illegible]
[illegible]	[illegible]	[illegible]	[illegible]	[illegible]
[illegible]	[illegible]	2.313	[illegible]	[illegible]
[illegible]	[illegible]	[illegible]	[illegible]	[illegible]
[illegible]	[illegible]	[illegible]	0.8426	[illegible]
[illegible]	[illegible]	[illegible]	[illegible]	[illegible]
[illegible]	[illegible]	[illegible]	[illegible]	[illegible]
[illegible]	[illegible]	[illegible]	[illegible]	[illegible]
[illegible]	[illegible]	[illegible]	[illegible]	[illegible]
[illegible]	[illegible]	[illegible]	[illegible]	[illegible]
[illegible]	[illegible]	[illegible]	[illegible]	[illegible]
[illegible]	[illegible]	[illegible]	[illegible]	[illegible]

DEL= 57.22 MM DSTR= 8.73 MM THETA= [illegible] MM
RDEL= [illegible]E+05 RDSTR= 0.50[illegible]E+04 RTTA= [illegible]
SHAPE FACTOR, H= [illegible]

STATION 4

UINF= 11.[illegible] M/S
RTX= [illegible] X= 2.674
T= 27.0[illegible] RHO= [illegible] KG/CU.M
MU= [illegible] KG/MS NU= [illegible] M*M/S

Y(MM)	U (M/S)	Y/TTA	U/UE	Y/DEL
0.62	[illegible]	[illegible]	[illegible]	[illegible]
[illegible]	[illegible]	[illegible]	[illegible]	[illegible]
[illegible]	[illegible]	[illegible]	[illegible]	[illegible]
[illegible]	[illegible]	[illegible]	[illegible]	[illegible]
[illegible]	[illegible]	[illegible]	[illegible]	[illegible]
[illegible]	[illegible]	[illegible]	[illegible]	[illegible]
[illegible]	[illegible]	[illegible]	[illegible]	[illegible]
[illegible]	[illegible]	[illegible]	[illegible]	[illegible]
[illegible]	[illegible]	[illegible]	[illegible]	[illegible]
11.52	[illegible]	[illegible]	[illegible]	[illegible]
[illegible]	[illegible]	2.110	[illegible]	[illegible]
[illegible]	[illegible]	[illegible]	[illegible]	[illegible]
[illegible]	[illegible]	[illegible]	[illegible]	[illegible]
[illegible]	[illegible]	[illegible]	[illegible]	[illegible]
[illegible]	[illegible]	[illegible]	[illegible]	[illegible]
[illegible]	[illegible]	[illegible]	[illegible]	[illegible]
[illegible]	[illegible]	5.252	[illegible]	[illegible]
[illegible]	[illegible]	6.036	[illegible]	[illegible]
[illegible]	[illegible]	6.976	0.9506	0.7514

DEL= 59.25 MM DSTR= [illegible] MM THETA= 6.39 MM
RDEL= 0.3[illegible]E+05 RDSTR= 0.5418E+04 RTTA= 0.38[illegible]E+04

C-7.07-17

09N1

[illegible]

T(HR)	Q (M3/S)	ZATTA	U/US	Y/DEL
[illegible]	[illegible]	[illegible]	[illegible]	[illegible]

[illegible]

STATION [illegible]

[illegible]

T(HR)	Q (M3/S)	ZATTA	U/US	Y/DEL
[illegible]	[illegible]	[illegible]	[illegible]	[illegible]

[illegible]

STATION 1

[illegible]

T(HR)	Q (M3/S)	ZATTA	U/US	Y/DEL
[illegible]	[illegible]	[illegible]	[illegible]	[illegible]
[illegible]	[illegible]	[illegible]	[illegible]	[illegible]
[illegible]	[illegible]	[illegible]	[illegible]	[illegible]
[illegible]	[illegible]	[illegible]	[illegible]	[illegible]
[illegible]	[illegible]	[illegible]	[illegible]	[illegible]
[illegible]	[illegible]	[illegible]	[illegible]	[illegible]
[illegible]	[illegible]	[illegible]	[illegible]	[illegible]
[illegible]	[illegible]	[illegible]	[illegible]	[illegible]
[illegible]	[illegible]	[illegible]	[illegible]	[illegible]
[illegible]	[illegible]	[illegible]	[illegible]	[illegible]
[illegible]	[illegible]	[illegible]	[illegible]	[illegible]
[illegible]	[illegible]	[illegible]	[illegible]	[illegible]
[illegible]	[illegible]	[illegible]	[illegible]	[illegible]
[illegible]	[illegible]	[illegible]	[illegible]	[illegible]
[illegible]	15.441	[illegible]	[illegible]	[illegible]

DELS [illegible] DSTAR [illegible] THETA [illegible]

[illegible]

SHAPE FACTOR [illegible]

STATION 2

[illegible]

T(HR)	Q (M3/S)	ZATTA	U/US	Y/DEL
[illegible]	[illegible]	[illegible]	[illegible]	[illegible]
[illegible]	[illegible]	[illegible]	[illegible]	[illegible]
[illegible]	[illegible]	[illegible]	[illegible]	[illegible]
[illegible]	[illegible]	[illegible]	[illegible]	[illegible]
[illegible]	[illegible]	[illegible]	[illegible]	[illegible]
[illegible]	[illegible]	[illegible]	[illegible]	[illegible]
[illegible]	[illegible]	[illegible]	[illegible]	[illegible]
[illegible]	[illegible]	[illegible]	[illegible]	[illegible]
[illegible]	[illegible]	[illegible]	[illegible]	[illegible]
[illegible]	[illegible]	[illegible]	[illegible]	[illegible]
[illegible]	[illegible]	[illegible]	[illegible]	[illegible]
[illegible]	[illegible]	[illegible]	[illegible]	[illegible]
[illegible]	[illegible]	[illegible]	[illegible]	[illegible]
[illegible]	[illegible]	[illegible]	[illegible]	[illegible]
[illegible]	[illegible]	[illegible]	[illegible]	[illegible]

DELS [illegible] DSTAR [illegible] THETA [illegible]

[illegible]

CURVE 1 FIT: LOG(FO)= 0.1250F+05*LOG(/D)+-0.1342E-02

C-9.28-17

10N1

UINF= 16.374 M/S
REX= 0.1847E+07 X= 2.162
T= 27.55 DEG.C RHO= 0.9648 KG/CU.M
MU= 0.1848E-04 KG/MS NU= 0.1917E-04 M*M/S

Y(MM)	U (M/S)	Y/TTA	U/UE	Y/DEL
0.51	8.646	0.114	0.5374	0.0104
1.06	10.175	[illegible]	[illegible]	0.0217
1.16	11.617	[illegible]	[illegible]	[illegible]
2.86	11.824	[illegible]	[illegible]	[illegible]
[illegible]	12.114	0.971	0.7473	0.0851
5.86	12.524	[illegible]	0.7726	0.1104
7.35	12.705	[illegible]	0.7897	0.1504
[illegible]	13.079	[illegible]	0.8069	0.1811
[illegible]	13.427	2.410	0.8263	[illegible]
11.86	13.780	[illegible]	0.8501	[illegible]
14.86	14.009	3.256	0.8679	0.3446
19.86	14.220	4.424	0.8837	[illegible]
23.86	14.651	5.315	0.9044	0.4877
23.86	14.961	[illegible]	0.9207	0.5800
[illegible]	15.315	[illegible]	0.9431	0.5971
30.85	15.714	[illegible]	0.9694	[illegible]

DEL= 46.22 MM DSTR= 5.79 MM THETA= 4.49 MM
RDEL= 0.3343E+05 RDSTR= 0.4845E+04 RTTA= 0.3834E+04
SHAPE FACTOR,H= 1.30

STATION 2

UINF= 16.256 M/S
REX= 0.1865E+07 X= 2.235
T= 27.92 DEG.C RHO= 0.9639 KG/CU.M
MU= 0.1851E-04 KG/MS NU= 0.1921E-04 M*M/S

Y(MM)	U (M/S)	Y/TTA	U/UE	Y/DEL
0.51	5.349	0.112	0.3338	0.0105
[illegible]	7.000	[illegible]	0.4369	0.0217
1.52	8.472	[illegible]	[illegible]	0.0314
2.52	8.916	[illegible]	[illegible]	0.0417
3.52	10.443	[illegible]	[illegible]	0.0523
[illegible]	11.092	[illegible]	0.6830	0.0829
5.52	11.863	1.210	0.7444	0.1130
7.52	12.331	[illegible]	0.7787	0.1449
9.52	12.779	[illegible]	0.8064	0.1861
11.52	13.449	2.416	0.8298	0.2276
[illegible]	13.674	2.454	0.8435	0.2684
[illegible]	13.970	3.233	0.8623	0.3000
17.52	14.194	3.721	0.8750	0.3512
20.52	14.273	4.389	0.8860	0.4131
24.52	14.476	5.266	0.9055	0.4956
29.52	14.924	6.362	0.9273	0.5989
34.52	15.353	7.458	0.9477	0.7019
39.52	15.644	8.554	0.9658	0.8051

DEL= 48.47 MM DSTR= 6.31 MM THETA= 4.54 MM
RDEL= 0.3124E+05 RDSTR= 0.5344E+04 RTTA= 0.3847E+04
SHAPE FACTOR,H= 1.38

STATION 3

UINF= 16.328 M/S
REX= 0.1971E+07 X= 2.327
T= 24.31 DEG.C RHO= 0.9653 KG/CU.M
MU= 0.1853E-04 KG/MS NU= 0.1925E-04 M*M/S

Y(MM)	U (M/S)	Y/TTA	U/UE	Y/DEL
0.53	4.739	0.109	0.2966	0.0106
0.99	5.601	0.180	0.3501	0.0191
1.34	6.276	0.291	0.4251	0.0282
1.49	7.431	0.305	0.4633	0.0354
2.49	8.441	0.604	0.5220	0.0507
3.49	9.813	0.811	[illegible]	0.0791
4.99	10.001	1.02	0.6194	0.0994
5.99	11.006	1.336	[illegible]	0.1259
7.99	11.430	1.649	0.7390	0.1633
9.99	12.217	2.067	0.7833	0.2012
11.99	13.205	2.488	0.8180	0.2416
13.99	13.625	2.953	0.8430	0.2893
16.89	14.037	3.575	0.8676	0.3473
20.99	14.432	4.367	0.8840	0.4245
25.89	14.684	5.225	0.9005	0.5059
29.89	15.031	6.248	0.9372	0.6075
34.89	15.445	7.291	0.9556	0.7091
38.89	15.640	8.129	0.9698	0.7909

DEL= 49.21 MM DSTR= 7.09 MM THETA= 4.78 MM
RDEL= 0.4106E+05 RDSTR= 0.6002E+04 RTTA= 0.4305E+04
SHAPE FACTOR,H= 1.49

STATION 4

UINF= 16.308 M/S
REX= 0.2072E+07 X= 2.427
T= 28.75 DEG.C RHO= 0.9609 KG/CU.M
MU= 0.1855E-04 KG/MS NU= 0.1930E-04 M*M/S

Y(MM)	U (M/S)	Y/TTA	U/UE	Y/DEL
0.53	4.433	0.101	0.2712	0.0110
0.99	5.559	0.190	0.3403	0.0206
1.49	6.009	0.285	0.3940	0.0310
1.99	7.005	0.381	0.4280	0.0414
2.49	7.435	0.477	0.4550	0.0515
3.49	8.537	0.668	0.5256	[illegible]
4.49	9.045	0.860	0.5534	[illegible]
5.49	9.639	1.051	0.5809	[illegible]
6.99	10.311	1.338	0.6309	[illegible]
8.49	11.135	1.625	0.6811	[illegible]
10.49	11.687	2.008	0.7273	0.2195
12.49	12.651	2.391	0.7741	0.2601
14.49	13.320	2.774	0.8150	0.3019
17.49	13.953	3.349	0.8544	0.3642
21.49	14.498	4.114	0.8871	0.4475
26.49	14.957	5.072	0.9152	0.5517
32.49	15.346	6.220	0.9390	0.6766
38.49	15.731	7.369	0.9626	0.8016

DEL= 48.02 MM DSTR= 8.10 MM THETA= 5.22 MM
RDEL= 0.4107E+05 RDSTR= 0.6930E+04 RTTA= 0.4467E+04
SHAPE FACTOR,H= 1.55

CURVE 1 FIT: LOG(F(R)) = 0.1205E+00*LOG(Y/D.)+-7.3278E-02

C-12.02-17

10N2

UINF= 17.009 M/S
REX= 0.1721E+07   X= 1.902
T= 30.00 DEG.C   RHO= 0.9567 KG/CU.M
MU= 0.1901E-04 KG/MS   NU= 0.1945E-04 M*M/S

Y(MM)	U (M/S)	Y/TTA	U/UE	Y/DEL
0.51	9.197	0.123	0.5421	0.0111
1.24	10.765	[illegible]	0.6426	0.0274
1.54	11.324	[illegible]	0.6761	0.0335
[illegible]	11.638	[illegible]	0.6937	0.0447
[illegible]	12.203	[illegible]	0.7236	0.0563
[illegible]	12.643	[illegible]	0.7531	0.0878
5.54	[illegible]	1.327	0.7779	0.1234
7.54	13.571	1.817	[illegible]	[illegible]
[illegible]	[illegible]	[illegible]	0.8123	0.1855
10.54	[illegible]	[illegible]	[illegible]	[illegible]
13.54	[illegible]	3.244	[illegible]	0.2912
16.54	[illegible]	[illegible]	[illegible]	[illegible]
[illegible]	14.592	[illegible]	0.8760	[illegible]
[illegible]	[illegible]	[illegible]	[illegible]	0.5137
29.54	[illegible]	7.073	[illegible]	[illegible]
[illegible]	[illegible]	[illegible]	[illegible]	[illegible]
39.54	[illegible]	9.474	0.9772	0.8590

DEL= 42.48 MM   DSTR= 5.37 MM   THETA= 4.17 MM
RDEL= 0.[illegible]E+05   RDSTR= [illegible]   RTTA= 0.3623E+04
SHAPE FACTOR,H= 1.29

STATION 2

UINF= 16.900 M/S
REX= 0.1710E+07   X= 2.030
T= 30.00 DEG.C   RHO= 0.9551 KG/CU.M
MU= 0.1862E-04 KG/MS   NU= 0.1950E-04 M*M/S

Y(MM)	U (M/S)	Y/TTA	U/UE	Y/DEL
0.51	5.551	0.123	0.3393	[illegible]
[illegible]	6.712	[illegible]	0.4115	0.0139
[illegible]	[illegible]	[illegible]	0.5117	0.0348
[illegible]	9.572	[illegible]	0.5878	0.0259
[illegible]	10.982	0.861	0.6530	[illegible]
[illegible]	12.283	1.222	0.7315	[illegible]
[illegible]	13.123	1.583	0.7813	[illegible]
[illegible]	[illegible]	[illegible]	[illegible]	0.1727
[illegible]	[illegible]	2.435	0.8325	0.2167
[illegible]	[illegible]	[illegible]	[illegible]	0.2507
[illegible]	[illegible]	[illegible]	[illegible]	0.3282
[illegible]	[illegible]	[illegible]	0.9060	0.3887
[illegible]	15.313	[illegible]	0.9118	[illegible]
[illegible]	15.653	6.514	0.9341	0.5822
[illegible]	16.075	7.557	0.9563	0.7112
33.00	[illegible]	9.400	0.9789	0.8402

DEL= 48.55 MM   DSTR= 5.85 MM   THETA= 4.16 MM
RDEL= 0.4244E+05   RDSTR= [illegible]   RTTA= 0.3615E+04
SHAPE FACTOR,H= 1.41

STATION 3

UINF= 17.451 M/S
REX= 0.1925E+07   X= 2.147
T= 30.22 DEG.C   RHO= 0.9563 KG/CU.M
MU= 0.1867E-04 KG/MS   NU= 0.1947E-04 M*M/S

Y(MM)	U (M/S)	Y/TTA	U/UE	Y/DEL
[illegible]	[illegible]	0.124	0.2505	[illegible]
[illegible]	[illegible]	[illegible]	0.3301	0.0102
1.04	[illegible]	[illegible]	0.3933	0.0255
1.54	[illegible]	[illegible]	0.4242	0.0257
[illegible]	[illegible]	[illegible]	0.4605	0.0356
[illegible]	[illegible]	0.722	0.524	0.0725
[illegible]	[illegible]	0.976	0.5723	0.0920
5.54	[illegible]	1.132	0.6133	0.1134
7.54	[illegible]	1.635	0.6775	0.1541
9.54	[illegible]	1.741	0.7271	0.1748
[illegible]	13.504	2.119	0.7851	0.2153
12.54	14.445	2.557	0.8153	0.2557
14.54	[illegible]	2.705	0.8441	0.2977
16.54	[illegible]	[illegible]	0.8647	0.3700
[illegible]	[illegible]	3.084	0.8802	0.4003
[illegible]	15.259	4.596	0.9023	0.4414
27.54	[illegible]	5.015	0.9210	0.5674
32.54	16.806	6.035	0.9427	0.6662
[illegible]	[illegible]	7.858	0.9633	0.7890

DEL= 48.89 MM   DSTR= 7.49 MM   THETA= 4.07 MM
RDEL= 0.4779E+05   RDSTR= 0.6715E+04   RTTA= 0.4396E+04
SHAPE FACTOR,H= 1.53

STATION 4

UINF= 17.749 M/S
REX= 0.2082E+07   X= 2.247
T= 30.34 DEG.C   RHO= 0.9559 KG/CU.M
MU= 0.1861E-04 KG/MS   NU= 0.1948E-04 M* /S

Y(MM)	U (M/S)	Y/TTA	U/UE	Y/DEL
0.51	[illegible]	0.092	0.22[illegible]4	0.0079
0.81	[illegible]	0.145	0.28[illegible]	0.0155
1.41	[illegible]	[illegible]	0.34[illegible]	0.0272
2.11	5.909	0.390	0.3953	0.0476
2.81	7.572	[illegible]	0.4307	0.0581
[illegible]	8.441	0.616	0.4434	0.0774
[illegible]	9.139	0.866	0.5207	0.0926
5.81	9.778	1.016	0.5554	0.1110
7.81	10.561	1.290	0.5975	0.1360
8.81	11.179	1.550	0.6410	0.1659
10.81	12.057	1.820	0.6802	0.1947
12.81	12.930	2.193	0.7351	0.2373
[illegible]	13.503	2.041	0.7773	0.2713
[illegible]	14.348	2.901	0.8137	0.3103
[illegible]	15.047	3.441	0.8557	0.3591
23.11	15.655	4.163	0.8912	0.4451
28.11	16.160	5.201	0.9197	0.5814
33.11	16.518	5.951	0.9401	0.6377
[illegible]	16.728	6.862	0.9560	0.7741

DEL= 51.72 MM   DSTR= 9.93 MM   THETA= 2.55 MM
RDEL= 0.4730E+05   RDSTR= 0.5136E+04   RTTA= 0.5065E+04
SHAPE FACTOR,H= 1.61

CURVE 1 FIT: LOG(FC)= 0.1283E+02*LOG(Y/D)+-0.1175E-02

C-539-13

11N1

UINF= 12.35 M/S
REX= 0.1281E+07 X= 1.954
T= 26.01 DEG.C RHO= 0.9698 KG/CU.M
MU= 0.1842E-04 KG/MS NU= 0.1899E-04 M*M/S

Y(MM)	U (M/S)	Y/TTA	U/UE	Y/DEL
0.51	6.[illegible]	0.117	0.5142	[illegible]
0.99	7.[illegible]	0.234	0.6121	[illegible]
1.48	8.[illegible]	0.339	0.6711	[illegible]
1.98	[illegible]	0.453	0.6418	[illegible]
2.58	[illegible]17	0.590	0.7045	[illegible]
3.38	8.[illegible]3	0.773	0.[illegible]53	[illegible]
4.38	[illegible]	1.002	[illegible]	[illegible]
5.58	[illegible]	1.277	0.[illegible]715	[illegible]
7.08	[illegible]23	1.620	0.[illegible]71	[illegible]
8.58	[illegible]	1.9[illegible]	[illegible]	[illegible]
10.58	[illegible]	2.420	[illegible]	[illegible]
[illegible]	[illegible]	2.876	0.8364	[illegible]
15.58	[illegible]	3.574	0.8548	[illegible]
[illegible]	[illegible]34	4.2[illegible]1	0.[illegible]75	[illegible]
22.58	[illegible]37	5.166	0.8[illegible]3	[illegible]
28.58	[illegible]	6.5[illegible]	0.9[illegible]1	[illegible]
32.58	[illegible]	7.5[illegible]2	0.[illegible]5[illegible]	[illegible]
39.58	[illegible]17	9.0[illegible]	0.9742	[illegible]

DEL= [illegible] MM DSTR= 5.6[illegible] MM THETA= 4.[illegible] MM
RDEL= 0.2727E+05 RDSTR= 0.[illegible]E+04 RTTA= 0.2843E+04
SHAPE FACTOR,H= 1.[illegible]

STATION 2

UINF= 12.3[illegible] M/S
REX= 0.[illegible]E+07 X= 2.[illegible]
T= 26.33 DEG.C RHO= 0.9[illegible] KG/CU.M
MU= 0.18[illegible]E-04 KG/MS NU= 0.[illegible]E-04 M*M/S

Y(MM)	U (M/S)	Y/TTA	U/UE	Y/DEL
0.51	[illegible]06	0.11[illegible]	0.3370	0.011[illegible]
0.99	[illegible]2	[illegible]	[illegible]	[illegible]
1.[illegible]	[illegible]	0.3[illegible]	[illegible]	[illegible]
2.00	[illegible]	0.45[illegible]	0.[illegible]521	0.[illegible]46
2.75	7.[illegible]	[illegible]	0.6[illegible]3	[illegible]
3.55	[illegible]34	[illegible]	[illegible]	0.07[illegible]
[illegible]	[illegible]06	[illegible]	0.7[illegible]	[illegible]
5.55	[illegible]2	1.[illegible]	[illegible]	0.1200
[illegible]	[illegible]	1.5[illegible]	0.7702	0.153[illegible]
8.55	9.[illegible]37	1.[illegible]27	0.79[illegible]	0.18[illegible]
10.55	10.[illegible]7	2.377	0.8[illegible]	0.2298
12.55	10.[illegible]14	2.828	0.8[illegible]	0.2734
15.55	10.[illegible]	3.504	0.85[illegible]4	0.3367
18.55	[illegible]	4.180	0.8777	0.4041
21.55	[illegible]	4.856	0.8973	0.4694
25.55	11.159	5.759	0.9163	0.5566
31.55	11.[illegible]46	7.110	0.9472	0.6873
37.55	11.[illegible]5	8.462	0.9693	0.8180

DEL= 45.91 MM DSTR= [illegible] MM THETA= 4.4[illegible] MM
RDEL= 0.2[illegible]E+05 RDSTR= 0.[illegible]E+04 RTTA= 0.2[illegible]E+04
SHAPE FACTOR,H= 1.39

STATION 3

UINF= 12.33 M/S
REX= 0.1373E+07 X= 2.119
T= 26.70 DEG.C RHO= 0.9675 KG/CU.M
MU= 0.1845E-04 KG/MS NU= 0.1907E-04 M*M/S

Y(MM)	U (M/S)	Y/TTA	U/UE	Y/DEL
0.5[illegible]	[illegible]99	0.1[illegible]	0.2[illegible]	0.[illegible]
1.0[illegible]	[illegible]727	[illegible]	0.[illegible]72	0.[illegible]
1.57	[illegible]	[illegible]	0.[illegible]510	[illegible]
2.37	[illegible]0	[illegible]	[illegible]	[illegible]
3.37	[illegible]16	[illegible]	0.[illegible]5[illegible]	[illegible]75
4.37	[illegible]6	[illegible]	0.[illegible]	[illegible]45
5.37	7.377	1.[illegible]	0.[illegible]52	[illegible]
6.37	[illegible]35	1.[illegible]	0.[illegible]27	[illegible]
7.37	[illegible]	1.[illegible]	0.712[illegible]	[illegible]
8.3[illegible]	[illegible]	1.[illegible]	0.73[illegible]	0.[illegible]27
9.3[illegible]	[illegible]	1.[illegible]	0.7572	[illegible]
10.87	[illegible]	[illegible]	0.7707	[illegible]
12.[illegible]	[illegible]	2.411	0.8127	[illegible]
[illegible]	[illegible].70	2.801	0.8330	[illegible]
[illegible]	10.[illegible]	3.190	0.8[illegible]	[illegible]
19.37	10.[illegible]75	3.775	0.87[illegible]	[illegible]
[illegible]	[illegible]9	4.555	0.9050	[illegible]86
[illegible]	11.[illegible]27	5.529	0.9279	[illegible]
[illegible]	11.[illegible]4	6.5[illegible]4	0.9[illegible]	0.[illegible]
[illegible]	11.733	7.6[illegible]3	0.9610	0.[illegible]14

DEL= 58.[illegible] MM DSTR= 7.4[illegible] MM THETA= 5.13 MM
RDEL= 0.[illegible]E+05 RDSTR= 0.4931E+04 RTTA= 0.3318E+04
SHAPE FACTOR,H= 1.45

STATION 4

UINF= 12.42 M/S
REX= 0.1[illegible]E+07 X= 2.219
T= 27.16 DEG.C RHO= 0.9660 KG/CU.M
MU= 0.1847E-04 KG/MS NU= 0.1912E-04 M*M/S

Y(MM)	U (M/S)	Y/TTA	U/UE	Y/DEL
0.51	3.[illegible]35	0.09[illegible]	0.2791	0.00[illegible]
0.99	[illegible]07	0.180	0.3605	0.0[illegible]
[illegible]9	5.167	0.271	0.[illegible]217	0.02[illegible]
[illegible]	[illegible]78	0.3[illegible]2	0.45[illegible]	0.[illegible]
2.69	[illegible]57	0.489	0.4[illegible]25	0.05[illegible]
3.09	[illegible]77	0.671	0.5[illegible]	0.0[illegible]
4.69	[illegible]7	0.852	0.56[illegible]	0.[illegible]
5.[illegible]	[illegible]12	1.034	0.6027	0.[illegible]
6.[illegible]9	[illegible]	1.2[illegible]6	0.[illegible]07	0.[illegible]
7.69	[illegible]	1.[illegible]7	0.66[illegible]	0.[illegible]
8.69	[illegible]	1.579	0.[illegible]913	0.[illegible]30
10.19	[illegible]3	1.852	0.7271	0.[illegible]
[illegible]	[illegible]5	2.124	0.76[illegible]	0.21[illegible]
13.69	[illegible]	2.4[illegible]	0.7[illegible]	0.[illegible]
15.69	[illegible]3	2.8[illegible]	0.8283	0.[illegible]
18.69	[illegible]2	3.396	0.8533	0.[illegible]06
22.69	10.[illegible]4	4.123	0.8[illegible]57	0.[illegible]256
27.69	11.2[illegible]	5.032	0.9132	0.51[illegible]
32.69	11.[illegible]3	5.940	0.930[illegible]	0.6132
38.69	11.7[illegible]	7.031	0.9552	0.7258

DEL= 53.31 MM DSTR= 8.28 MM THETA= 5.50 MM
RDEL= 0.34[illegible]E+05 RDSTR= 0.5381E+04 RTTA= 0.3575E+04
SHAPE FACTOR,H= 1.51

C-12.22-13

11N2

[illegible]

STATION 7

[illegible]

[illegible]	U [illegible]	[illegible]	[illegible]	[illegible]
[illegible]	[illegible]	[illegible]	[illegible]	[illegible]

THETA= [illegible] MM

[illegible]

STATION [illegible]

[illegible]

[illegible]	U [illegible]	[illegible]	[illegible]	[illegible]
[illegible]	[illegible]	[illegible]	[illegible]	[illegible]

DELS= 47.04 MM   DSTR= [illegible].90 MM   THETA= [illegible].40 MM

[illegible]

SHAPE FACTOR [illegible]

A-7.55-17

16N1

UINF= [illegible] (M/S) AT X= [illegible] (M)

VIRTUAL ORIGIN =[illegible] (M)

DATA SET [illegible]

T= [illegible] RHO= [illegible]
MU= [illegible] NU= [illegible]

Y (MM)	U (M/S)
[illegible]	0.107772E+01
[illegible]	[illegible]
[illegible]	[illegible]
[illegible]	[illegible]
[illegible]	[illegible]
[illegible]	[illegible]
[illegible]	[illegible]
[illegible]	[illegible]
[illegible]	[illegible]
[illegible]	[illegible]
[illegible]	[illegible]
[illegible]	[illegible]
[illegible]	[illegible]
[illegible]	[illegible]
[illegible]	[illegible]
[illegible]	[illegible]
[illegible]	[illegible]
[illegible]	[illegible]
[illegible]	[illegible]
[illegible]	[illegible]

DELTA= [illegible] (MM) DSTR= [illegible] MM THETA= [illegible] MM

RX= [illegible] RDEL= [illegible] RDSTR= [illegible]
RTHETA= [illegible]

SHAPE FACTOR (DSTR/TTA) = [illegible]

UINF= [illegible] (M/S) AT X= [illegible] (M)

VIRTUAL ORIGIN =[illegible] (M)

DATA SET [illegible]

T= [illegible] RHO= [illegible]
MU= [illegible] NU= [illegible]

Y (MM)	U (M/S)
[illegible]	[illegible]
[illegible]	[illegible]
[illegible]	[illegible]
[illegible]	[illegible]
[illegible]	[illegible]
[illegible]	[illegible]
[illegible]	[illegible]
[illegible]	[illegible]
[illegible]	[illegible]
[illegible]	[illegible]
[illegible]	[illegible]
[illegible]	[illegible]
[illegible]	[illegible]
[illegible]	[illegible]
[illegible]	[illegible]
[illegible]	[illegible]
[illegible]	[illegible]
[illegible]	[illegible]
[illegible]	[illegible]
[illegible]	[illegible]

DELTA= 0.490042E+02 (MM) DSTR= [illegible] MM THETA= [illegible] MM

RX= [illegible] RDEL= [illegible] RDSTR= [illegible]
RTHETA= [illegible]

SHAPE FACTOR (DSTR/TTA) = [illegible]

UINF= [illegible] (M/S) AT X= [illegible] (M)

VIRTUAL ORIGIN =[illegible] (M)

DATA SET [illegible]

T= [illegible] RHO= [illegible]+00
MU= [illegible] NU= [illegible]-04

Y (MM)	U (M/S)
[illegible]	[illegible]
[illegible]	[illegible]
[illegible]	[illegible]
[illegible]	[illegible]
[illegible]	[illegible]
[illegible]	[illegible]
[illegible]	[illegible]
[illegible]	[illegible]
[illegible]	[illegible]
[illegible]	[illegible]
[illegible]	[illegible]
[illegible]	[illegible]
[illegible]	[illegible]
[illegible]	[illegible]
[illegible]	[illegible]
[illegible]	[illegible]
[illegible]	[illegible]
[illegible]	[illegible]
[illegible]	[illegible]
[illegible]	[illegible]
[illegible]	[illegible]

DELTA= [illegible] (MM) DSTR= [illegible] MM THETA= 0.46524[illegible]E+01 MM

RX= [illegible] RDEL= [illegible]E+05 RDSTR= [illegible]

SHAPE FACTOR (DSTR/TTA) = [illegible]

UINF= [illegible] (M/S) AT X= [illegible] (M)

VIRTUAL ORIGIN =[illegible] (M)

DATA SET [illegible]

T= [illegible] RHO= [illegible]
MU= [illegible] NU= 0.194487E-04

Y (MM)	U (M/S)
[illegible]	[illegible]
[illegible]	[illegible]
[illegible]	[illegible]
[illegible]	[illegible]
[illegible]	[illegible]
[illegible]	[illegible]
[illegible]	[illegible]
[illegible]	[illegible]
[illegible]	[illegible]
[illegible]	[illegible]
[illegible]	[illegible]
[illegible]	[illegible]
[illegible]	[illegible]
[illegible]	[illegible]
[illegible]	[illegible]
[illegible]	[illegible]
[illegible]	[illegible]
[illegible]	[illegible]
[illegible]	[illegible]
[illegible]	[illegible]
[illegible]	[illegible]

DELTA= [illegible] (MM) DSTR= 0.736996E+01 MM THETA= 0.522957E+01 MM

RX= [illegible]E+06 RDEL= 0.452457E+05 RDSTR= 0.642327E+04
RTHETA= 0.443735E+04

SHAPE FACTOR (DSTR/TTA) = 0.144753E+01

CURVE 1 FIT: LOG(FD)= 0.1192E+00*LOG(Y/D)+-0.9503E-02

E-7.27-17

23N1

50% Blocked

UINF= 16.695 M/S
REX= 0.2155E+07 X= 2.424
T= 24.73 DEG.C RHO= 0.9752 KG/CU.M
MU= 0.1832E-04 KG/MS NU= 0.1877E-04 M*M/S

Y(MM)	U (M/S)	Y/TTA	U/UE	Y/DEL
0.50	9.277	0.102	0.5613	0.0095
1.00	10.431	0.205	0.6205	0.0191
1.50	10.932	0.307	0.6518	0.0285
2.00	11.248	0.410	0.6831	0.0382
3.00	11.73	0.615	0.7089	0.0573
4.00	12.172	0.820	0.7345	0.0764
5.00	12.413	1.025	0.7513	0.0955
6.00	12.656	1.230	0.7662	0.1145
7.50	12.958	1.537	0.7844	0.1432
9.00	13.107	1.844	0.7993	0.1719
11.00	13.436	2.254	0.8131	0.2101
13.00	13.717	2.664	0.8313	0.2483
15.00	13.997	3.074	0.8482	0.2865
18.00	14.236	3.689	0.8618	0.3438
22.00	14.638	4.508	0.8861	0.4202
27.00	15.022	5.533	0.9093	0.5157
32.00	15.292	6.558	0.9317	0.6112
38.00	15.724	7.787	0.9518	0.7258

DEL= 52.34 MM DSTR= 6.26 MM THETA= 4.88 MM
RDEL= 0.4655E+05 RDSTR= 0.5564E+04 RTTA= 0.43[illegible]E+04
SHAPE FACTOR,H= 1.28
POWER LAW. N= 7.[illegible]8

STATION 2

UINF= 16.647 M/S
REX= 0.2212E+07 X= 2.500
T= 24.83 DEG.C RHO= 0.9740 KG/CU.M
MU= 0.1834E-04 KG/MS NU= 0.1892E-04 M*M/S

Y(MM)	U (M/S)	Y/TTA	U/UE	Y/DEL
0.50	7.030	0.105	0.4266	0.0102
0.82	7.896	0.172	0.4797	0.0167
1.22	8.708	0.256	0.5284	0.0249
1.72	9.417	0.362	0.5714	0.0351
2.32	10.135	0.488	0.6153	0.0473
3.32	11.179	0.698	0.6793	0.0677
4.32	11.901	0.908	0.7221	0.0881
5.32	12.364	1.119	0.7512	0.1085
6.32	12.726	1.329	0.7722	0.1289
7.32	12.964	1.539	0.7865	0.1493
8.82	13.272	1.854	0.8053	0.1799
10.32	13.487	2.170	0.8183	0.2105
12.32	13.779	2.590	0.8337	0.2513
14.32	13.996	3.010	0.8492	0.2921
16.82	14.212	3.538	0.8623	0.3431
19.32	14.448	4.062	0.8766	0.3941
22.32	14.717	4.692	0.8923	0.4553
27.32	15.037	5.743	0.9124	0.5572
33.32	15.423	7.005	0.9358	0.6796
39.32	15.827	8.266	0.9603	0.8020

DEL= 49.03 MM DSTR= 6.35 MM THETA= 4.76 MM
RDEL= 0.4338E+05 RDSTR= 0.5615E+04 RTTA= 0.4209E+04
SHAPE FACTOR,H= 1.33

STATION 3

UINF= 16.962 M/S
REX= 0.2327E+07 X= 2.589
T= 24.73 DEG.C RHO= 0.9739 KG/CU.M
MU= 0.1836E-04 KG/MS NU= 0.1885E-04 M*M/S

Y(MM)	U (M/S)	Y/TTA	U/UE	Y/DEL
0.50	5.993	0.095	0.3573	0.0095
0.79	6.778	0.151	0.4042	0.0150
1.19	7.350	0.227	0.4383	0.0226
1.79	8.112	0.341	0.4835	0.0340
2.39	8.722	0.456	0.5200	0.0454
3.09	9.406	0.589	0.5602	0.0587
4.09	10.240	0.780	0.6111	0.0777
5.09	10.917	0.971	0.6509	0.0967
6.09	11.525	1.161	0.6872	0.1157
7.09	12.296	1.352	0.7331	0.1347
8.59	12.761	1.639	0.7603	0.1631
10.09	13.175	1.924	0.7855	0.1916
12.09	13.629	2.305	0.8126	0.2296
14.09	13.997	2.687	0.8345	0.2676
17.09	14.35	3.259	0.8555	0.3246
21.09	14.753	4.022	0.8796	0.4005
26.09	15.138	4.975	0.9026	0.4955
32.09	15.573	6.119	0.9285	0.6095
38.09	15.923	7.263	0.9494	0.7234

DEL= 52.65 MM DSTR= 7.42 MM THETA= 5.24 MM
RDEL= 0.4732E+05 RDSTR= 0.6672E+04 RTTA= 0.4713E+04
SHAPE FACTOR,H= 1.42
POWER LAW. N= 6.81

STATION 4

UINF= 17.356 M/S
REX= 0.2473E+07 X= 2.690
T= 24.95 DEG.C RHO= 0.9732 KG/CU.M
MU= 0.1837E-04 KG/MS NU= 0.1887E-04 M*M/S

Y(MM)	U (M/S)	Y/TTA	U/UE	Y/DEL
0.50	5.444	0.090	0.3169	0.0098
0.89	6.406	0.161	0.3728	0.0174
1.29	7.043	0.233	0.4099	0.0252
1.69	7.495	0.305	0.4362	0.0330
2.19	7.992	0.396	0.4651	0.0427
2.89	8.655	0.522	0.5037	0.0564
3.69	9.299	0.667	0.5412	0.0720
4.69	9.945	0.847	0.5793	0.0915
5.69	10.502	1.028	0.6112	0.1110
6.69	11.104	1.208	0.6463	0.1306
7.69	11.665	1.389	0.6789	0.1501
9.19	12.341	1.659	0.7182	0.1793
10.69	12.856	1.931	0.7482	0.2086
12.69	13.479	2.292	0.7845	0.2477
14.69	14.001	2.653	0.8149	0.2867
16.69	14.429	3.015	0.8396	0.3257
19.69	14.847	3.556	0.8641	0.3843
23.69	15.304	4.279	0.8907	0.4623
28.69	15.666	5.182	0.9117	0.5599
33.69	15.994	6.085	0.9309	0.6575
38.69	16.332	6.988	0.9505	0.7551

DEL= 51.24 MM DSTR= 8.22 MM THETA= 5.54 MM
RDEL= 0.4712E+05 RDSTR= 0.7558E+04 RTTA= 0.5091E+04
SHAPE FACTOR,H= 1.48

E-12 0-1"

23N2

50% Blocked

CURVE 1 FIT: LOG(FD)= 0.1264E+00*LOG(Y/D)--0.1358E-01

UINF= 16.6[illegible] M/S X= 2.359
REX= 0.2[illegible]E+07 RHO= 0.9733 KG/CU.M
T= 25.[illegible] DEG.C NU= 0.1888E-04 M*M/S
MU= 0.1837E-04 KG/MS

Y(MM)	U (M/S)	Y/TTA	U/UE	Y/DEL
0.50	8.[illegible]	0.134	0.5[illegible]	0.0105
0.81	9.7[illegible]	0.160	[illegible]	0.0170
1.31	10.[illegible]	0.273	0.6[illegible]	0.0276
1.81	10.87[illegible]	0.387	0.6[illegible]	0.0381
2.31	11.21[illegible]	0.491	0.6[illegible]	0.0486
3.31	11.73[illegible]	0.610	0.71[illegible]	0.0696
4.31	12.[illegible]	0.858	0.73[illegible]	0.0907
5.31	12.29[illegible]	1.177	0.74[illegible]	0.1117
6.31	12.5[illegible]	1.315	0.76[illegible]	0.1328
7.81	12.77[illegible]	1.878	0.77[illegible]	0.1643
9.81	13.1[illegible]	2.064	0.79[illegible]	0.2064
11.81	13.4[illegible]	2.661	0.81[illegible]	0.2485
14.81	13.7[illegible]	3.306	0.83[illegible]	0.3116
17.81	14.0[illegible]	3.911	0.85[illegible]	0.3749
20.81	14.30[illegible]	4.527	0.87[illegible]	0.4379
24.81	14.60[illegible]	5.159	0.89[illegible]	0.5218
29.81	15.20[illegible]	6.712	0.93[illegible]	0.6273
34.81	15.58[illegible]	7.254	0.94[illegible]	0.7325
40.81	15.92[illegible]	9.306	0.96[illegible]	0.8377

DEL= 4[illegible].41 MM DSTR= 6.[illegible]4 MM THETA= [illegible] MM
RDEL= 0.4347E+05 RDSTR= 0.5491E+04 RTTA= 0.4[illegible]22E+04
SHAPE FACTOR,H= 1.7[illegible]
POWER LAW. N= 6.05

STATION 2

UINF= 16.85[illegible] M/S X= 2.4[illegible]
REX= 0.21[illegible]E+07 RHO= 0.97[illegible] KG/CU.M
T= 25.51 DEG.C NU= 0.1894E-04 M*M/S
MU= 0.1845E-04 KG/MS

Y(MM)	U (M/S)	Y/TTA	U/UE	Y/DEL
0.40	5.312	[illegible]	0.3223	0.0077
0.74	6.[illegible]3	[illegible]	0.3642	0.0147
1.01	6.689	0.2[illegible]6	0.4059	0.0201
1.51	7.618	0.3[illegible]8	0.4622	0.0300
2.01	8.6[illegible]	0.410	0.5[illegible]5	0.0400
2.51	9.[illegible]3	0.512	0.5513	0.0499
3.01	9.[illegible]83	0.614	0.5874	0.0598
3.51	10.208	0.716	0.6229	0.0698
4.01	10.70[illegible]	0.817	0.6515	0.0797
5.01	11.512	1.021	0.7044	0.0996
6.00	12.127	1.223	0.7357	0.1193
7.01	12.56[illegible]	1.429	0.7623	0.1393
8.01	12.864	1.633	0.7804	0.1592
9.01	13.[illegible]63	1.837	0.7924	0.1791
10.51	13.409	2.143	0.8135	0.2089
12.01	13.656	2.448	0.8295	0.2387
14.01	14.015	2.856	0.8502	0.2785
16.01	14.158	3.264	0.8587	0.3182
18.01	14.[illegible]87	3.672	0.8655	0.3580
21.01	14.510	4.283	0.8802	0.4176
26.01	14.975	5.300	0.9084	0.5169
31.01	15.258	6.322	0.9255	0.6164
36.01	15.6[illegible]	7.341	0.9476	0.7157
41.01	15.922	8.360	0.9659	0.8151

DEL= 50.31 MM DSTR= 6.87 MM THETA= 4.91 MM
RDEL= 0.44[illegible]E+05 RDSTR= 0.6041E+04 RTTA= 0.4313E+04
SHAPE FACTOR,H= 1.40

STATION 3

UINF= 17.180 M/S X= 2.533
REX= 0.2296E+07 RHO= 0.9711 KG/CU.M
T= 25.59 DEG.C NU= 0.1895E-04 M*M/S
MU= 0.1840E-04 KG/MS

Y(MM)	U (M/S)	Y/TTA	U/UE	Y/DEL
0.50	3.985	0.089	0.2367	0.0098
0.82	4.9[illegible]	0.145	0.2875	0.0161
1.32	5.7[illegible]	0.233	0.3356	0.0259
1.82	6.[illegible]	0.322	0.3729	0.0357
2.32	6.8[illegible]	0.410	0.4016	0.0456
2.82	7.3[illegible]	0.498	0.4327	0.0554
3.62	8.[illegible]	0.646	0.4792	0.0711
4.62	8.9[illegible]7	0.817	0.5271	0.0907
5.62	9.[illegible]	0.993	0.5744	0.1104
6.62	10.[illegible]	1.170	0.6061	0.1300
7.62	11.[illegible]	1.347	0.6522	0.1496
9.12	11.9[illegible]	1.612	0.7041	0.1791
10.62	12.695	1.877	0.7464	0.2086
12.62	13.307	2.231	0.7871	0.2478
14.62	13.6[illegible]	2.597	0.8154	0.2881
16.62	14.167	2.938	0.8332	0.3264
19.62	14.5[illegible]	3.468	0.8538	0.3853
22.62	14.781	3.998	0.8691	0.4442
27.62	15.287	4.882	0.8989	0.5424
33.62	15.760	5.943	0.9272	0.6603
39.62	16.195	7.003	0.9524	0.7781

DEL= 57.92 MM DSTR= 8.82 MM THETA= 5.66 MM
RDEL= 0.5417E+05 RDSTR= 0.8002E+04 RTTA= 0.5130E+04
SHAPE FACTOR,H= 1.5[illegible]
POWER LAW. N= 3.57

STATION 4

UINF= 17.40[illegible] M/S X= 2.633
REX= 0.240[illegible]E+07 RHO= 0.9631 KG/CU.M
T= 26.20 DEG.C NU= 0.1902E-04 M*M/S
MU= 0.1843E-04 KG/MS

Y(MM)	U (M/S)	Y/TTA	U/UE	Y/DEL
0.51	3.451	0.086	0.2073	0.0096
0.78	4.103	0.128	0.2382	0.0143
1.16	4.887	0.196	0.2837	0.0219
1.66	5.557	0.280	0.3225	0.0313
2.16	6.122	0.364	0.3495	0.0407
2.66	6.593	0.448	0.3787	0.0502
3.66	7.735	0.617	0.4258	0.0690
4.66	8.[illegible]95	0.784	0.4699	0.0877
5.66	8.719	0.954	0.5061	0.1067
6.66	9.234	1.123	0.5363	0.1256
7.66	9.894	1.291	0.5743	0.1445
9.16	10.768	1.544	0.6250	0.1728
10.66	11.553	1.797	0.6705	0.2010
12.16	12.192	2.050	0.7077	0.2293
14.16	12.994	2.387	0.7543	0.2671
16.66	13.886	2.809	0.8061	0.3142
19.66	14.640	3.315	0.8499	0.3708
23.66	15.[illegible]27	3.989	0.8838	0.4462
28.66	15.657	4.832	0.9093	0.5405
33.66	16.[illegible]15	5.675	0.9296	0.6348
39.66	16.[illegible]91	6.687	0.9514	0.7480

DEL= 53.02 MM DSTR= 9.87 MM THETA= 5.93 MM
RDEL= 0.4852E+05 RDSTR= 0.9028E+04 RTTA= 0.5428E+04
SHAPE FACTOR,H= 1.66

CURVE 1 FIT: LOG(FD)= 0.1135E+00*LOG(Y/D)+-0.3739E-02

E-14.51-17

24N1

50% Blocked

UINF= 15.573 M/S
REX= 0.1684E+07
T= 26.74 DEG.C
MU= 0.1846E-04 KG/MS

X= 2.062
RHO= 0.9574 KG/CU.M
NU= 0.1908E-04 M*M/S

Y(MM)	U (M/S)	Y/TTA	U/UE	Y/DEL
0.5[illegible]	8.[illegible]06	0.[illegible]19	0.5710	0.0106
[illegible].8[illegible]	9.[illegible]65	0.197	0.6267	0.0175
1.36	10.[illegible]	0.312	0.6693	0.0277
1.86	10.753	0.427	0.6972	0.0379
2.35	10.989	0.5[illegible]9	0.7125	0.0479
2.86	11.2[illegible]1	0.656	0.7[illegible]15	0.0583
3.36	11.536	0.770	0.7462	0.0685
4.36	11.836	1.000	0.7574	0.0889
5.36	12.[illegible]7[illegible]	1.2[illegible]	0.7823	0.1093
6.36	12.283	1.453	0.79[illegible]4	0.1296
7.86	12.530	1.802	0.8125	0.1602
9.36	12.[illegible]22	2.146	0.8249	0.1908
11.36	12.955	2.605	0.8400	0.2316
14.36	13.222	3.293	0.8574	0.2927
17.36	13.476	3.981	0.873[illegible]	0.3539
21.36	13.[illegible]13	4.[illegible]08	0.8955	0.4354
26.36	14.132	6.044	0.9163	0.5373
32.36	14.516	7.420	0.9412	0.6596
40.36	14.[illegible]50	9.255	0.9694	0.[illegible]227

DEL= 44.0[illegible] MM DSTR= 5.54 MM THETA= 4.36 MM
RDEL= 0.76[illegible]E+05 RDSTR= 0.4529E+04 RTTA= 0.3561E+04
SHAPE FACTOR,H= 1.27
POWER LAW. N= 7.37

STATION 2

UINF= 15.13[illegible] M/S
REX= 0.169[illegible]E+07
T= 26.89 DEG.C
MU= 0.1846E-04 KG/MS

X= 2.133
RHO= 0.9659 KG/CU.M
NU= 0.1909E-04 M*M/S

Y(MM)	U (M/S)	Y/TTA	U/UE	Y/DEL
0.52	4.628	0.[illegible]02	0.3090	0.0101
0.79	5.369	0.154	0.3584	0.0153
1.09	5.985	0.213	0.3995	0.0211
1.59	6.[illegible]01	0.[illegible]1	0.4540	0.0307
[illegible].09	7.525	0.409	0.5024	0.0404
2.69	8.276	0.525	0.5525	0.0520
3.29	9.00[illegible]	0.643	0.60[illegible]	0.0636
4.29	9.994	0.838	0.6672	0.0830
5.29	10.733	1.033	0.7165	0.1023
6.29	11.198	1.229	0.7475	0.1216
7.29	11.547	1.424	0.77[illegible]	0.1410
8.[illegible]9	11.755	1.619	0.7849	0.1603
9.79	11.964	1.912	0.7987	0.1893
11.29	12.163	2.205	0.8120	0.2183
13.29	12.391	2.596	0.8272	0.2570
16.29	12.695	3.182	0.8475	0.3150
19.29	12.972	3.768	0.8660	0.3730
22.29	13.215	4.354	0.8823	0.4310
28.29	13.605	5.526	0.9083	0.5470
34.29	14.032	6.698	0.9368	0.6631
[illegible].29	1[illegible].356	7.870	0.9585	0.7791

DEL= 51.71 MM DSTR= 7.20 MM THETA= 5.12 MM
RDEL= 0.40[illegible]E+05 RDSTR= 0.5705E+04 RTTA= 0.4056E+04
SHAPE FACTOR,H= 1.41
POWER LAW. N= 4.92

STATION 3

UINF= 15.404 M/S
REX= 0.1795E+07
T= 27.01 DEG.C
MU= 0.1847E-04 KG/MS

X= 2.227
RHO= 0.9655 KG/CU.M
NU= 0.1911E-04 M*M/S

Y(MM)	U (M/S)	Y/TTA	U/UE	Y/DEL
0.52	2.562	0.[illegible]	0.1680	0.0099
0.88	3.462	0.155	0.2270	0.0167
1.38	4.330	0.243	0.2839	0.0262
1.88	4.97[illegible]	0.332	0.3260	0.0357
2.38	5.49[illegible]	0.420	0.3601	0.0452
3.18	6.2[illegible]3	0.561	0.4053	0.0605
4.18	7.023	0.737	0.4605	0.0795
5.18	7.810	0.914	0.5121	0.0985
6.18	8.563	1.090	0.5615	0.1175
7.18	9.234	1.267	0.6055	0.1365
8.18	9.844	1.443	0.6455	0.1555
9.18	10.438	1.619	0.6844	0.1745
10.18	10.[illegible]	1.796	0.7144	0.1935
11.18	11.396	1.972	0.7473	0.2125
12.68	11.949	2.237	0.7835	0.2411
14.18	12.336	2.501	0.8089	0.2696
16.18	12.750	2.854	0.8361	0.3076
19.18	13.182	3.383	0.8644	0.3646
23.18	13.432	4.089	0.8809	0.4407
28.18	13.7[illegible]	4.971	0.9019	0.5357
33.18	14.058	5.853	0.9219	0.6308
39.18	14.426	6.9[illegible]	0.9460	0.7448

DEL= 52.60 MM DSTR= 9.[illegible] MM THETA= 5.67 MM
RDEL= 0.4240E+05 RDSTR= 0.7465E+04 RTTA= 0.4570E+04
SHAPE FACTOR,H= 1.63
POWER LAW. N= 3.16

STATION 1

UINF= 1[illegible].123 M/S
REX= 0.1951E+07
T= 27.24 DEG.C
MU= 0.1848E-04 KG/MS

X= 2.327
RHO= 0.9553 KG CU.M
NU= 0.1913E-04 M*M/S

Y(MM)	U (M/S)	Y/TTA	U/UE	Y/DEL
0.51	2.735	0.082	0.1714	0.0097
0.78	3.299	0.126	0.2067	0.0149
1.28	4.104	0.207	0.2571	0.0244
1.88	4.745	0.304	0.2973	0.0359
2.68	5.433	0.433	0.3404	0.0511
3.68	6.1[illegible]6	0.595	0.3831	0.0702
4.68	6.797	0.757	0.4259	0.0893
5.68	7.423	0.918	0.4651	0.1084
6.68	7.966	1.0[illegible]	0.4990	0.1275
8.18	8.801	1.323	0.5514	0.1561
9.68	9.420	1.565	0.5902	0.1847
11.68	10.425	1.888	0.6531	0.2229
13.68	11.224	2.212	0.7032	0.2611
15.68	1[illegible].046	2.535	0.7547	0.2992
18.68	12.933	3.020	0.8103	0.3565
21.68	13.506	3.505	0.8461	0.4138
24.68	14.044	3.990	0.8799	0.4710
29.68	14.492	4.799	0.9079	0.5664
34.68	14.840	5.6[illegible]7	0.9297	0.6619
39.68	15.156	6.415	0.9495	0.7573

DEL= 52.40 MM DSTR= 10.79 MM THETA= 6.19 MM
RDEL= 0.4415E+05 RDSTR= 0.9093E+04 RTTA= 0.5212E+04
SHAPE FACTOR,H= 1.74

E-904-17

28N1

57% Blocked

CURVE 1 FIT: LOG(FD)= 0.1224E+02*LOG(Y/D)+-0.6742E-02

UINF= 16.[illegible] M/S
REX= 0.1[illegible]E+07 X= 2.129
T= 27.[illegible] DEG.C RHO= 0.9667 KG/CU.M
MU= 0.1847E-04 KG/MS NU= 0.1912E-04 M*M/S

Y(MM)	U (M/S)	Y/ITA	U/UF	Y/DEL
[illegible]	6.[illegible]	0.[illegible]	0.5562	0.0117
0.75	[illegible]	0.[illegible]	0.6073	0.0166
[illegible].25	10.575	0.[illegible]	0.[illegible]	0.0272
1.75	[illegible]	0.4[illegible]5	0.6772	0.0377
2.25	11.[illegible]67	0.[illegible]	0.6965	0.0482
3.25	[illegible]	0.764	0.7232	0.[illegible]
4.25	12.[illegible]1	[illegible].572	0.7666	0.[illegible]
5.75	12.641	1.[illegible]	0.7727	0.12[illegible]
7.25	12.[illegible]	1.[illegible]	0.7[illegible]	0.1536
8.75	[illegible]	1.5[illegible]7	0.8[illegible]	0.1[illegible]52
10.25	13.41[illegible]	2.[illegible]7	0.8102	0.2169
12.25	13.[illegible]2	2.776	0.8[illegible]	0.2[illegible]
14.25	[illegible]	3.[illegible]	0.8[illegible]4	0.[illegible]
17.25	14.[illegible]	3.[illegible]	0.[illegible]	0.3[illegible]
20.25	14.[illegible]	4.[illegible]	0.8849	0.[illegible]5
23.25	[illegible]	[illegible]	0.[illegible]	0.4[illegible]7
28.25	[illegible]	6.[illegible]	0.[illegible]	0.[illegible]
34.75	15.[illegible]	7.[illegible]	0.95[illegible]	0.72[illegible]
41.25	[illegible]	9.[illegible]	0.9[illegible]	0.[illegible]

DEL= [illegible] MM DSTR= [illegible].71 MM THETA= [illegible] MM
RDEL= 0.[illegible] RDSTR= 0.4[illegible]E+04 RTTA= 0.3825E+04
SHAPE FACTOR,H= [illegible]
POWER LAW, N= [illegible]

STATION 2

UINF= 16.[illegible] M/S
REX= 0.1[illegible]E+07 X= 2.255
T= 27.[illegible] DEG.C RHO= [illegible].966 KG/CU.M
MU= 0.1845E-04 KG/MS NU= 0.1916E-04 M*M/S

Y(MM)	U (M/S)	Y/ITA	U/UF	Y/DEL
[illegible]	[illegible]	0.[illegible]7	0.[illegible]49	0.[illegible]
[illegible]	7.[illegible]2	0.[illegible]7	0.4261	0.[illegible]
1.41	[illegible]	0.[illegible]	0.4870	[illegible]
1.91	[illegible]	0.[illegible]3	0.5[illegible]	[illegible]
2.41	[illegible]	0.577	0.55[illegible]	[illegible]
3.61	10.[illegible]	0.71[illegible]	0.65[illegible]	0.0[illegible]
4.61	11.[illegible]	0.[illegible]	0.70[illegible]	0.[illegible]
5.61	12.1[illegible]	1.1[illegible]	0.7[illegible]	0.[illegible]
6.61	12.[illegible]6	1.[illegible]	0.7617	0.[illegible]
8.11	12.[illegible]	1.[illegible]	0.7801	0.16[illegible]
[illegible]	[illegible]	1.[illegible]	0.8[illegible]	0.1[illegible]7
11.61	[illegible]	[illegible]	0.8[illegible]	0.2[illegible]
13.61	[illegible]	2.[illegible]	0.8[illegible]5	0.2[illegible]
15.61	14.[illegible]	[illegible]	0.8571	0.[illegible]
[illegible]	14.[illegible]	[illegible]	0.[illegible]	0.3[illegible]
[illegible]	14.[illegible]	[illegible]	0.[illegible]	0.4[illegible]
25.61	14.[illegible]	5.[illegible]	0.[illegible]	0.5[illegible]
[illegible]	[illegible]	6.[illegible]	0.9[illegible]	0.61[illegible]
[illegible]	[illegible]	7.[illegible]3	0.9478	0.7[illegible]
41.61	[illegible]	[illegible]	0.9[illegible]	0.[illegible]

DEL= [illegible] MM DSTR= 6.73 MM THETA= 4.[illegible] MM
RDEL= [illegible] RDSTR= 0.5[illegible]E+04 RTTA= 0.4[illegible]E+04
SHAPE FACTOR,H= [illegible]
POWER LAW, N= [illegible]

STATION 3

UINF= 16.638 M/S
REX= 0.1[illegible]E+07 X= 2.[illegible]94
T= 27.5[illegible] DEG.C RHO= 0.9648 KG/CU.M
MU= 0.1840E-04 KG/MS NU= 0.1917E-04 M*M/S

Y(MM)	U (M/S)	Y/ITA	U/UF	Y/DEL
[illegible]	[illegible]	0.1[illegible]	0.[illegible]	0.0107
0.75	[illegible]	0.132	0.[illegible]	0.0152
1.25	[illegible]	0.2[illegible]	0.4123	0.[illegible]
1.75	7.4[illegible]	0.[illegible]	0.4514	0.[illegible]44
2.25	[illegible]	0.470	0.[illegible]	0.[illegible]
3.25	[illegible].877	0.[illegible]	0.5[illegible]	0.[illegible]32
4.25	9.[illegible]	0.[illegible]	0.[illegible]	0.[illegible]24
5.25	10.4[illegible]	1.[illegible]	0.[illegible]	0.1017
6.25	11.[illegible]	1.[illegible]	0.6[illegible]	0.1[illegible]
7.25	11.[illegible]	1.4[illegible]	0.7[illegible]	0.1[illegible]
8.25	12.055	1.[illegible]	0.7[illegible]	0.1[illegible]
[illegible]	12.711	1.[illegible]3	0.7717	0.1[illegible]
11.25	[illegible]	2.172	0.7[illegible]	0.21[illegible]
13.25	[illegible]	2.557	0.[illegible]7	0.[illegible]54
[illegible]	[illegible]	2.[illegible]	0.[illegible]72	0.[illegible]
17.25	[illegible]	[illegible]	0.[illegible]	0.[illegible]22
[illegible]	14.[illegible]	3.711	0.[illegible]	0.[illegible]7
[illegible]	[illegible]	4.[illegible]	0.[illegible]	0.4[illegible]
[illegible]	14.91[illegible]	5.[illegible]	0.[illegible]7	0.5[illegible]
[illegible]	15.[illegible]	6.[illegible]	0.[illegible]	0.6013
[illegible]	15.[illegible]	6.[illegible]	0.94[illegible]	0.6[illegible]
41.25	[illegible]	7.[illegible]	0.[illegible]647	0.7[illegible]

DEL= [illegible] MM DSTR= 7.59 MM THETA= 5.2[illegible] MM
RDEL= 0.4[illegible]E+05 RDSTR= 0.6588E+04 RTTA= 0.4512E+04
SHAPE FACTOR,H= 1.46
POWER LAW, N= [illegible]

STATION 4

UINF= 17.077 M/S
REX= 0.2125E+07 X= 2.394
T= [illegible] DEG.C RHO= 0.9639 KG/CU.M
MU= 0.[illegible]E-04 KG/MS NU= 0.192[illegible]E-04 M*M/S

Y(MM)	U (M/S)	Y/ITA	U/UF	Y/DEL
0.52	4.[illegible]	0.[illegible]	0.2[illegible]	0.0[illegible]
0.92	5.[illegible]	0.15[illegible]	0.3423	0.0175
1.42	6.[illegible]	0.2[illegible]	0.3[illegible]	0.0270
1.92	7.[illegible]	0.[illegible]	0.4232	0.0365
2.42	7.71[illegible]	0.4[illegible]	0.4561	0.[illegible]07
3.42	[illegible]	0.[illegible]	0.4[illegible]	0.[illegible]49
4.42	[illegible]	0.[illegible]	0.5[illegible]	0.[illegible]
5.42	[illegible]	0.[illegible]	0.5738	0.1[illegible]
6.42	10.[illegible]	1.[illegible]	0.6[illegible]	0.1[illegible]
7.42	10.77[illegible]	1.[illegible]	0.6[illegible]	0.1[illegible]
8.92	11.4[illegible]	1.[illegible]	0.6776	0.1[illegible]
[illegible]	12.[illegible]	1.[illegible]	0.71[illegible]	0.1[illegible]
12.42	12.[illegible]	2.[illegible]	0.75[illegible]	0.[illegible]
14.42	[illegible]	2.475	0.7[illegible]	0.[illegible]
[illegible]	[illegible]	2.[illegible]	0.[illegible]	0.[illegible]
[illegible]	14.[illegible]	[illegible].161	0.8[illegible]	0.[illegible]
[illegible]	14.[illegible]	[illegible]	0.8[illegible]	0.[illegible]
[illegible]	14.[illegible]	4.[illegible]	0.87[illegible]	0.[illegible]
[illegible]	[illegible]	4.[illegible]	0.[illegible]	0.[illegible]
[illegible]	15.7[illegible]	5.[illegible]	0.[illegible]	0.[illegible]
[illegible]	16.[illegible]	6.[illegible]	0.9536	0.7[illegible]

DEL= [illegible] MM DSTR= [illegible] MM THETA= [illegible] MM
RDEL= [illegible] RDSTR= 0.7[illegible]E+04 RTTA= 0.[illegible]E+04
SHAPE FACTOR,H= 1.53
POWER LAW, N= [illegible]

CURVE 1 FIT: LOG(FD)= 0.1200E+00*LOG(Y/D)--0.5621E-02

E-11,77-17

29N1

67% Blocked

UINF= 16.590 M/S
REX= 0.1893E+07
T= 25.90 DEG.C
MU= 0.1842E-04 KG/MS

X= 2.154
RHO= 0.9699 KG/CU.M
NU= 0.1899E-04 M*M/S

Y(MM)	U (M/S)	Y/TTA	U/UE	Y/DEL
0.50	9.175	0.112	0.5587	0.0103
[illegible]	9.925	0.193	0.6179	0.0165
[illegible]	10.721	0.262	0.6527	0.0268
1.80	11.143	0.434	0.6784	0.0371
2.30	11.418	0.516	0.6952	0.0474
3.00	11.807	0.673	0.7140	0.0618
3.80	12.066	0.853	0.7333	0.0792
4.80	12.443	1.077	0.7576	0.0988
5.80	12.724	1.302	0.7747	0.1194
7.30	13.085	1.639	0.7955	0.1503
8.80	13.275	1.975	0.8082	0.1812
10.80	13.579	2.424	0.8267	0.2224
12.80	13.821	2.873	0.8415	0.2635
15.80	14.123	3.547	0.8599	0.3253
[illegible]	14.442	4.220	0.8793	0.3871
21.80	14.630	4.893	0.8911	0.4488
25.80	14.977	5.791	0.9119	0.5312
30.80	15.288	6.914	0.9309	0.6342
35.80	15.713	8.036	0.9567	0.7371
41.80	16.047	9.383	0.9770	0.8607

DEL= [illegible] MM   DSTR= 5.72 MM   THETA= 4.46 MM
RDEL= 0.4327E+05   RDSTR= 0.4997E+04   RTTA= 0.3892E+04
SHAPE FACTOR.H= 1.28
POWER LAW. N= 7.05

STATION 2

UINF= 16.758 M/S
REX= 0.1047E+07
T= 20.13 DEG.C
MU= 0.1847E-04 KG/MS

X= 2.240
RHO= 0.9654 KG/CU.M
NU= 0.1901E-04 M*M/S

Y(MM)	U (M/S)	Y/TTA	U/UE	Y/DEL
0.50	5.546	0.100	0.3375	0.0101
0.90	6.572	0.183	0.3975	0.0134
1.20	7.345	0.257	0.4470	0.0234
1.70	8.228	0.378	0.5007	0.0335
2.40	9.206	0.522	0.5602	0.0487
3.40	10.166	0.735	0.6192	0.0695
4.40	11.201	0.947	0.6855	0.0901
5.40	11.571	1.150	0.7255	0.1132
6.40	12.450	1.371	0.7577	0.1304
7.40	12.739	1.524	0.7763	0.1506
8.90	13.133	1.932	0.7992	0.1809
10.40	13.474	2.221	0.8170	0.2112
12.40	13.765	2.645	0.8341	0.2516
15.40	14.062	3.282	0.8558	0.3122
18.40	14.350	3.919	0.8733	0.3727
22.40	14.729	4.768	0.8964	0.4535
26.40	15.012	5.617	0.9135	0.5343
31.40	15.295	6.679	0.9309	0.6352
36.40	15.716	7.740	0.9564	0.7362
41.40	15.990	8.802	0.9731	0.8371

DEL= 49.5[illegible] MM   DSTR= 6.58 MM   THETA= 4.71 MM
RDEL= 0.4255E+05   RDSTR= 0.5749E+04   RTTA= 0.4112E+04
SHAPE FACTOR.H= 1.40
POWER LAW. N= 5.03

STATION 3

UINF= 17.131 M/S
REX= 0.2085E+07
T= 26.18 DEG.C
MU= 0.1843E-04 KG/MS

X= 2.319
RHO= 0.9692 KG/CU.M
NU= 0.1901E-04 M*M/S

Y(MM)	U (M/S)	Y/TTA	U/UE	Y/DEL
0.50	4.189	0.080	0.2470	0.0091
0.82	5.017	0.147	0.2958	0.0150
1.22	5.740	0.219	0.3385	0.0223
1.72	6.481	0.309	0.3821	0.0314
2.22	7.153	0.399	0.4188	0.0406
2.72	7.752	0.525	0.4571	0.0534
3.72	8.464	0.658	0.4992	0.0680
4.72	9.256	0.848	0.5457	0.0863
5.72	9.959	1.028	0.5872	0.1046
6.72	10.620	1.207	0.6207	0.1229
7.72	11.229	1.387	0.6620	0.1411
9.22	[illegible]	1.656	0.7126	0.1685
11.22	12.918	2.016	0.7617	0.2051
13.22	13.656	2.375	0.7993	0.2416
15.22	14.021	2.734	0.8267	0.2782
17.22	14.351	3.094	0.8462	0.3148
20.22	14.735	3.633	0.8688	0.3696
24.22	15.161	4.351	0.8943	0.4427
29.22	[illegible]	5.249	0.9157	0.5341
35.22	15.935	6.327	0.9356	0.6438
41.22	[illegible]	7.405	0.9582	0.7534

DEL= 54.7[illegible] MM   DSTR= 8.57 MM   THETA= [illegible].57 MM
RDEL= 0.4920E+05   RDSTR= 0.7722E+04   RTTA= 0.5015E+04
SHAPE FACTOR.H= 1.54
POWER LAW. N= 3.71

STATION 4

UINF= 17.493 M/S
REX= .2217E+07
T= 25.82 DEG.C
MU= 0.1846E-04 KG/MS

X= 2.419
RHO= 0.9671 KG/CU.M
NU= 0.1909E-04 M*M/S

Y(MM)	U (M/S)	Y/TTA	U/UE	Y/DEL
0.50	4.188	0.085	0.2418	0.0095
0.70	4.866	0.128	0.2810	0.0144
[illegible]	5.628	0.213	0.3250	0.0239
[illegible]	6.509	0.331	0.3759	0.0371
[illegible]	7.172	0.467	0.4141	0.0523
3.70	8.067	0.630	0.4658	0.0712
[illegible]	8.659	0.805	0.5023	0.0901
6.20	9.644	1.058	0.5569	0.1165
[illegible]	10.488	1.312	0.6056	0.1469
9.20	11.174	1.565	0.6453	0.1752
11.20	12.131	1.903	0.7005	0.2132
14.20	13.257	2.411	0.7655	0.2700
17.20	14.154	2.918	0.8173	0.3268
20.20	14.759	3.425	0.8523	0.3836
25.20	15.438	4.270	0.8915	0.4782
30.20	15.661	5.115	0.9159	0.5729
35.20	16.223	5.961	0.9374	0.6675
40.20	16.542	6.806	0.9552	0.7622

DEL= 52.82 MM   DSTR= 9.51 MM   THETA= 5.92 MM
RDEL= 0.4841E+05   RDSTR= 0.8713E+04   RTTA= 0.5422E+04
SHAPE FACTOR.H= 1.61
POWER LAW. N= 3.30

E-8.56-17

30°

80% Blocked

[illegible]

Y(MM)	U(M/S)	Y/THA	U/UE	Y/DEL
[illegible]	[illegible]	[illegible]	[illegible]	[illegible]

STATION 3

[illegible]

Y(MM)	U(M/S)	Y/THA	U/UE	Y/DEL
[illegible]	[illegible]	[illegible]	[illegible]	[illegible]

STATION 4

[illegible]

Y(MM)	U(M/S)	Y/THA	U/UE	Y/DEL
[illegible]	[illegible]	[illegible]	[illegible]	[illegible]

E-11.66-17

0101

80% Blocked

[illegible] Y/DEL

SHAPE FACTOR,H= 1.39

POWER LAW, N= 6.26

STATION 2

STATION 3

UINF= 18.532 M/S

REX= [illegible] 7

T= 22.14 DEG.C

MU= [illegible] KG/MS

K= [illegible]

RHO= [illegible].9791 KG/CU.M

NU= [illegible] M**2/S

Y(MM)	U (M/S)	Y/TTA	U/UE	Y/DEL
0.53	5.1[illegible]	[illegible]	[illegible]	[illegible]
[illegible]	5.917	[illegible].147	[illegible]	[illegible]
[illegible]	6.744	[illegible]	[illegible]	[illegible]
[illegible]	7.[illegible]	[illegible]	[illegible]	[illegible]
2.83	[illegible]	[illegible]	[illegible]	[illegible]
[illegible]	[illegible]	[illegible]	[illegible]	[illegible].725
[illegible]	[illegible]	[illegible]55	[illegible]	[illegible]
[illegible]	[illegible]	[illegible]	[illegible]	[illegible]
[illegible]	[illegible]	[illegible]	[illegible]	[illegible]
7.83	[illegible]	1.335	[illegible]	[illegible]
[illegible]	[illegible]	1.631	[illegible]	[illegible].1757
11.33	[illegible].147	[illegible]	[illegible]	[illegible]
[illegible]	[illegible]	2.447	[illegible]	[illegible]
[illegible]	[illegible]	[illegible]	[illegible]	[illegible]
[illegible]	[illegible]	[illegible]	[illegible]	[illegible]
[illegible]	[illegible]	4.216	[illegible]	[illegible]
28.83	16.762	[illegible]	[illegible]	0.5459
[illegible]	17.172	[illegible]	[illegible]	0.5505
[illegible]	17.597	7.[illegible]	0.9540	0.7731

DEL= [illegible] MM DSTR= [illegible] MM THETA= 5.[illegible] MM

RDEL= 0.52[illegible] RDSTR= 0.8562E+04 RTTA= 0.564[illegible]

SHAPE FACTOR,H= 1.5[illegible]

POWER LAW, N= [illegible]

STATION 4

UINF= 18.903 M/S

REX= 0.2746E+ 7

T= 23.34 DEG.C

MU= [illegible]-04 KG/MS

K= [illegible].714

RHO= 0.9788 KG/CU.M

NU= 0.[illegible]-04 M**2/S

Y(MM)	U (M/S)	Y/TTA	U/UE	Y/DEL
[illegible]	[illegible]	[illegible]	[illegible]	[illegible]
[illegible]	4.927	[illegible]	[illegible]	[illegible]
1.[illegible]	5.[illegible]	[illegible]	[illegible]	[illegible]
[illegible]	[illegible]	[illegible]	[illegible]	[illegible]
[illegible]	[illegible]	[illegible]	[illegible]	[illegible]
[illegible]	[illegible]	[illegible]	[illegible]	[illegible]
4.55	[illegible]	[illegible]	[illegible]	[illegible]
5.55	[illegible]	[illegible]	[illegible]	[illegible]
[illegible]	[illegible]	[illegible]	[illegible]	[illegible]
7.55	[illegible]	[illegible]	[illegible]	[illegible]
[illegible]	[illegible]	1.472	[illegible]	[illegible]
[illegible]	12.567	1.717	0.6715	[illegible]
[illegible]	13.416	[illegible]	[illegible]	[illegible]
14.55	[illegible]	2.357	[illegible]	[illegible]
17.55	[illegible]	[illegible]	[illegible]	[illegible]
[illegible]	[illegible]	3.[illegible]	[illegible]	[illegible]
[illegible]	[illegible]	[illegible]	[illegible]	[illegible]
[illegible]	[illegible]	[illegible]	[illegible]	[illegible]
34.[illegible]	[illegible]	5.[illegible]	[illegible]	0.6179
[illegible]	17.76[illegible]	[illegible]	0.9495	0.7252

DEL= 55.02 MM DSTR= [illegible] MM THETA= 5.15 MM

RDEL= 0.5659E+05 RDSTR= 0.[illegible]E+05 RTTA= 0.6219E+04

SHAPE FACTOR,H= 1.62

POWER LAW, N= 3.22

APPENDIX E

E1 Accuracy of Experimental Equipment

Table E1.1 lists the equipment used, and the errors involved.

TABLE E1.1

INSTRUMENT, MAKE & MODEL	ACCURACY OR ERROR
Cambridge potentiometer, type 44228	± 0,01 millivolt
Doric DVM, type DS-100	± 0,001 volt
Riken Denshi X-Y Recorder, type F-3D	Within ± 0,3%
Positioning of hot-wire	± 0,5 mm
Water U-tubes	± 0,4 mm H_2O
Van Essen manometer, model 6750	± 0,002" H_2O
Fortin barometer	± 0,001 mm Hg
Disa anemometer, type 55D01	Output read on DVM
Disa lineariser, type 55D10	Output read on DVM
Disa RMS voltmeter type 55D35	Output read on DVM
Disa Auxilliary [illegible]t, type 55D25	Output read on DVM
Hewlett-Packard Spectrum analyser, type 3580 A	Output plotted by the X-Y recorder

TABLE E1.1 (cont.)

INSTRUMENT, MAKE & MODEL	ACCURACY OR ERROR
Hewlett-Packard Log Voltmeter/ Converter, type 7562	Output plotted by the X-Y recorder
Tektronix oscilloscope model with Polaroid camera	-

The values presented in Table E1.1 are the maximum errors expected.

When using the Van Essen manometer with the nozzle unit of the hot-wire calibration rig, the error in velocity may be estimated from :-

$$\frac{dV}{V} = \frac{1}{2}\left(\frac{dh}{h} - \frac{\delta\rho}{\rho}\right) \qquad \text{....... [E1.1]}$$

Assuming no error in ρ,

V(m/s)	h("H_2O)	% error
2,2	0,01	10
5,0	0,05	2
16,0	0,50	0,2

Clearly, the expected error at low velocities is very large. A linear regression analysis was used to fit a curve to the calibration values, and an error of 0,1 m/s was typical.

The error in measuring the transpiration flow rate was estimated as follows (using an ordinary water manometer) :-

Basic error for orifice plate : 2,3% (BS 1042)

$$\frac{dQ}{Q} = \tfrac{1}{2}\left[\frac{dh}{h} + \frac{dp_1}{p_1} + \frac{dT}{T}\right] + 2\frac{dd}{d} \qquad \text{....... [E1.2]}$$

$$\frac{dQ}{Q} = \tfrac{1}{2}\left[\frac{0,5}{20} + \frac{0,5}{8534} + (0,01 + 0,004)\right] + 2\frac{0,01}{38}$$

$$\frac{dQ}{Q} = 2\% + \text{basic error}$$

$$\frac{dQ}{Q} = 4,3\%$$

As v_w was directly proportional to Q,

$$\frac{dv_w}{v_w} = 4,3\%$$

This could be even greater if an error had been made in calculating the surface area of the porous plate, However, as h increased, the large term, dh/h, in E1.2 decreased.

In measuring the power spectrum, the emphasis was on the shape of the curve, and the occurrence of any peaks. The exact frequency and power of these peaks was not required to be known, and therefore an error analysis was not attempted for these measurements.

The main stream velocities measured with the anemometer did not drop below 5 m/s, which was within 2% and considered acceptable.

APPENDIX F

F1 Some Details Pertaining to the Programme

F1.1 The pressure gradient term

A pressure gradient would clearly alter the main stream velocity, and therefore u_e, β and p^+. It would, however, also affect the ξ grid spacing, even if constant x spacing was used in the physical plane. As a preliminary test, a constant pressure gradient was assumed. It was thought that the small increase in U_∞ caused by the growth of the boundary layer in an enclosed flow situation could be fitted with a straight line.

Then $du_e/dx = c$ .... [F1.1]

This changes the x-axis transformation :

$$\int_0^{\xi} d\xi = \mu\rho\int_0^{x}(xc + u_{e_o})dx$$ .... [F1.2]

For condition [F1.1],

$$\beta = 1 - \left(\frac{u_{e_o}}{u_e}\right)^2$$ .... [F1.3]

where $u_{e_o} = 0{,}99 \times U_\infty$

With injection, assumption [F1.1] proved inadequate.

F1.2 Numerical Integration

Certain quantities were obtained by integrating. δ^* was obtained as follows.

$$\delta^* = -\left(\frac{2\xi}{\rho u_e}\right)^{\frac{1}{2}}\int_0^{\eta_\infty} \phi'(\xi,\eta)d\eta$$

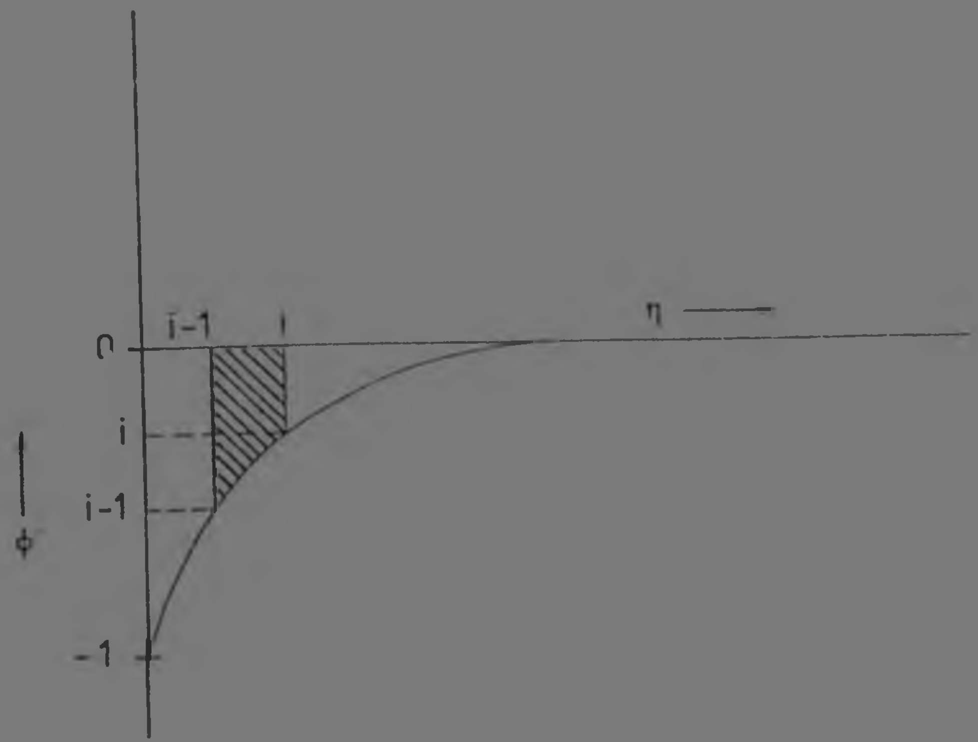

FIG F1.1 : SKETCH SHOWING TRAPEZOIDAL RULE

$$\text{Integral} = \sum_{i=2}^{N} (\phi'_i + \phi'_{i-1}) \times (\eta_i - \eta_{i-1}) \times \tfrac{1}{2} \quad \ldots \text{[F1.4]}$$

F2 <u>Initial Computer Runs</u>

A few trial runs were attempted without transpiration. A laminar profile was generated near the point of transition, assumed to occur at $Re_x = 3{,}2 \times 10^5$. From this point $\varepsilon^+ \neq 0$, and the programme marched into the transition region. The result obtained is shown in Fig F2.1. The uninjected laminar boundary layer with a small, linear pressure gradient ($du/dx = 10^{1/s}$) was attempted next. The profiles, shown in Fig F2.2, varied slightly from the first profile in Fig F2.1 (laminar, zero pressure gradient). Finally, a series of turbulent profiles were generated by the programme, starting at $Re_x = 3{,}24 \times 10^5$ with fully turbulent profiles. Values of c_f were not in satisfactory agreement with theory, thus the forward difference equation for ϕ_w'' was altered.

TABLE F2.1 Results of Initial Computer Runs

x(m)	ξ x 10^4	A^+	Re_xx10^{-5}	Re_θ	θ(mm)	H	δ(mm)	c_fx10^3
MHKTRANS L-0-10 (x_{trip} = 0,591 m)								
0,588	1,0578	26,0	3,185	330	0,609	2,56	5,04	1,41
0,597	1,0740	26,0	3,233	328	0,606	2,15	5,08	2,35
0,606	1,0902	26,0	3,282	333	0,616	1,90	5,23	4,18
0,615	1,1064	26,0	3,331	343	0,633	1,81	5,63	4,46
MHKDUX10 L-0-10								
0,076	0,1420	28,99	0,443	125	0,214	2,48	1,85	4,23
0,085	0,1595	29,27	0,500	132	0,224	2,47	1,96	4,01
0,094	0,1771	29,43	0,557	138	0,233	2,47	2,05	3,87
0,103	0,1949	29,55	0,616	144	0,242	2,45	2,13	3,75
MHKFLOW1 T-0-10								
0,598	1,0758	26,0	3,239	881	1,627	1,41	18,20	5,06
0,607	1,0920	26,0	3,287	893	1,649	1,41	18,70	5,16
0,616	1,1082	26,0	3,336	905	1,670	1,41	19,21	5,15
0,625	1,1244	26,0	3,385	916	1,691	1,41	19,35	5,11

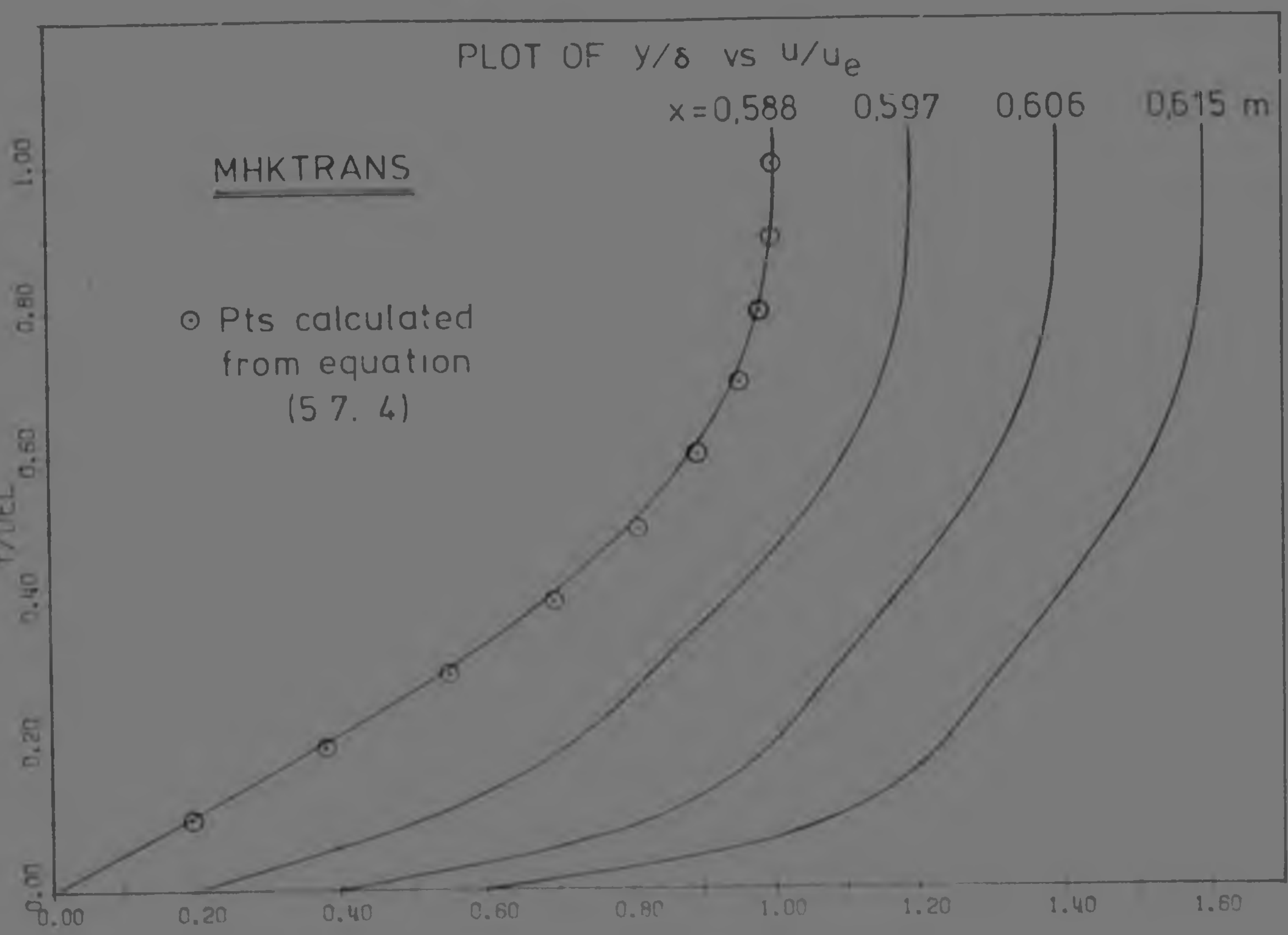

FIG F2.1 : LAMINAR PROFILES BEFORE AND DURING TRANSITION

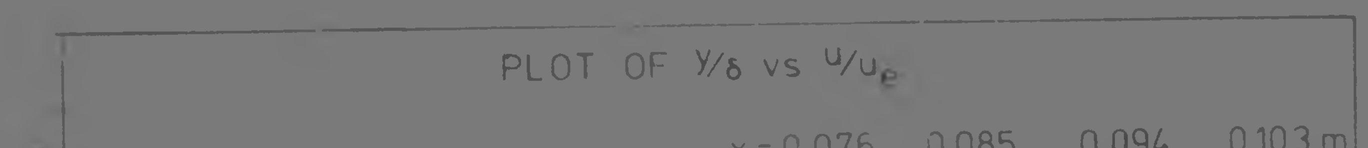

FIG F2.2 : LAMINAR PROFILES WITH PRESSURE GRADIENT

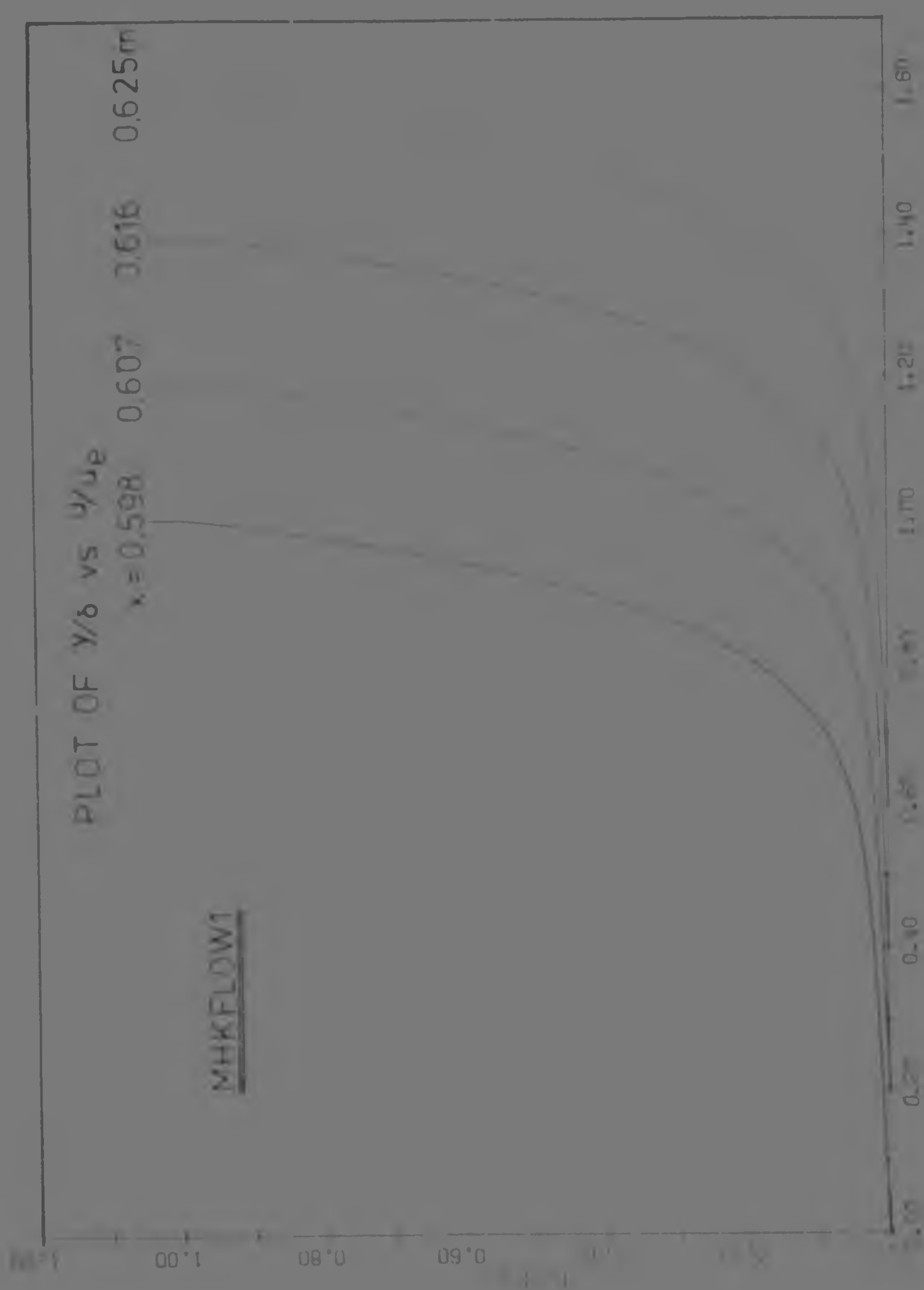

FIG F2.3 : TURBULENT INPUT PROFILES

F3 Results of Main Computer Runs

TABLE F3.1

Station	A^+	Re_θ	t (mm)	H	δ (mm)	$c_f \times 10^3$
MHKIJ001 T-1-17						
3	26,00	1812	1,97	1,33	23,14	4,085
10	23,11	1894	2,06	1,34	25,01	5,120
20	23,03	2019	2,19	1,36	26,48	4,818
30	22,95	2139	2,32	1,38	27,23	4,560
40	22,89	2257	2,45	1,39	28,74	4,357
50	22,83	2372	2,58	1,39	29,47	4,190
60	22,78	2486	2,70	1,40	31,03	4,049
MHKIJ002 T-2-17						
3	26,00	1812	1,97	1,33	23,14	4,085
10	20,93	1910	2,07	1,34	25,01	6,054
20	20,76	2065	2,24	1,37	26,48	5,580
30	20,59	2216	2,41	1,39	27,99	5,197
40	20,44	2364	2,57	1,41	28,74	4,896
50	20,31	2509	2,72	1,42	30,30	4,648
60	20,19	2652	2,88	1,43	31,89	4,438
MHKIJ003 T-3-17						
3	26,00	1811	1,97	1,33	23,53	4,088
10	19,15	1925	2,09	1,35	24,73	6,845
20	18,89	2109	2,29	1,38	26,92	6,229
30	18,64	2288	2,49	1,41	28,46	5,743
40	18,42	2465	2,68	1,43	29,22	5,361
50	18,22	2639	2,87	1,44	30,80	5,046
60	18,05	2812	3,05	1,45	32,42	4,779

Station	A^+	Re_θ	θ(mm)	H	δ(mm)	$c_f \times 10^3$
MHKIJ005 T-5-17						
3	26,00	1811	1,97	1,33	23,53	4,088
10	16,47	1953	2,12	1,35	24,73	8,507
20	16,09	2189	2,38	1,40	26,92	7,652
30	15,72	2421	2,63	1,43	28,46	6,980
40	15,40	2653	2,88	1,46	30,04	6,446
50	15,11	2883	3,13	1,48	31,66	6,003
60	14,84	3114	3,38	1,50	33,33	5,626
MHKIJ007 T-7-17						
3	26,00	1811	1,97	1,33	23,25	4,091
10	14,38	1978	2,15	1,36	25,13	9,909
20	13,94	2260	2,45	1,41	27,37	8,897
30	13,52	2542	2,76	1,46	28,93	8,085
40	13,14	28 25	3,07	1,49	31,39	7,432
50	12,79	3109	3,38	1,52	33,08	6,886
60	12,47	3394	3,69	1,54	34,84	6,420
MHKIJ009 T-9-17						
3	26,00	1811	1,97	1,33	23,25	4,091
10	12,81	2000	2,17	1,36	25,13	11,501
20	12,39	2322	2,52	1,42	27,37	10,390
30	11,94	2646	2,87	1,47	29,74	9,450
40	11,55	2975	3,23	1,51	32,27	8,683
50	11,18	3307	3,59	1,54	34,00	8,034
60	10,84	3643	3,96	1,57	36,77	7,476
MHKIJ010 T-10-17						
3	26,00	1811	1,97	1,33	23,15	4,095
10	11,97	2010	2,18	1,36	25,74	11,853
20	11,56	2353	2,56	1,43	28,03	10,727
30	11,11	2700	2,93	1,48	29,63	9,761
40	10,70	3052	3,31	1,52	32,15	8,969
50	10,33	3409	3,70	1,56	34,82	8,298
60	9,98	3771	4,10	1,58	36,65	7,719

Station	A^+	Re_θ	θ (mm)	H	δ (mm)	$c_f \times 10^3$
MHKIJ012 T-12-17						
3	26,00	1811	1,97	1,33	23,33	4,096
10	10,78	2029	2,20	1,36	25,23	13,279
20	10,42	2403	2,61	1,43	28,25	12,142
30	9,98	2786	3,03	1,48	30,70	11,092
40	9,58	3177	3,45	1,53	33,30	10,216
50	9,22	3576	3,88	1,56	35,09	9,467
60	8,88	3982	4,32	1,60	37,96	8,817
MHKIJ015 T-15-17						
3	26,00	1810	1,97	1,33	23,70	4,098
10	9,34	2051	2,23	1,35	25,62	15,419
20	9,07	2461	2,67	1,42	27,90	14,318
30	8,66	2886	3,13	1,47	31,18	13,155
40	8,29	3325	3,61	1,52	33,82	12,162
50	7,94	3776	4,10	1,56	36,63	11,301
60	7,61	4239	4,60	1,59	39,61	10.547
MHKIJ017 T-17-17						
3	26,00	1810	1,97	1,33	23.22	4,100
10	9,27	2052	2.23	1,35	25,82	15,201
20	8,99	2464	2,68	1,42	28,12	14,105
30	8,59	2891	3,14	1,47	30,56	12,957
40	8,21	3332	3,62	1,52	34,08	11,977
50	7,87	3785	4,11	1,56	36,91	11,129
60	7,54	4249	4,61	1,59	39,92	10,386

TABLE F3.2 Turbulent Shear Layer with Injection and Pressure Gradient

Test run MHKDUX003, du/dx = 10 1/s, F = 0,003, XTR = 0,8 m

x(m)	$Re_x \times 10^{-6}$	δ(mm)	θ(mm)	Re_θ	H	$p^+ \times 10^5$	A^+	$c_f \times 10^3$
0,790	1,069	22,05	1,78	2406	1,31	3,49	26,55	3,842
0,825	1,132	22,32	1,80	2464	1,31	1,81	21,03	6,003
0,875	1,224	23,30	1,84	2578	,33	1,89	21,00	5,584
0,925	1,320	23,63	1,88	2685	1,34	2,00	20,95	5,250
0,975	1,418	24,61	1,92	2788	1,35	2,09	20,93	4,979
1,025	1,518	24,91	1,95	2888	1,36	2,16	20,91	4,759
1,075	1,622	25,19	1,98	2986	1,36	2,21	20,91	4,573

TABLE F3.3 Computer runs with XTR small, U_∞ = 17 m/s, du/dx = 0 1/s

x(m)	$Re_x \times 10^{-5}$	δ(mm)	θ [illegible]	Re_θ	H	A^+	$c_f \times 10^3$
MHKLONG3 T-3[illegible] XTR = 0,312 m							
0,254	2,325	8,27	0,73	665	1,46	26,00	5,001
0,359	3,286	10,79	1,02	934	1,40	21,97	22,759
0,509	4,659	14,52	1,45	1328	1,43	21,23	15,222
0,659	6,032	18,08	1,92	1755	1,46	20,52	11,231
0,809	7,405	21,89	2,40	2200	1,47	19,94	8,978
0,959	8,778	26,02	2,89	2644	1,48	19,45	7,542
1,109	10,151	30,52	3,38	3095	1,4[illegible]	[illegible]	6,550
MHKLONG5 T-4,765-17 XTR = 0,312 m							
0,254	3,325	8,27	0,73	665	1,46	26,00	5,001
0,359	3,286	10,80	1,01	925	1,35	20,72	31,735
0,509	4,659	14,53	1,43	1313	1,37	19,75	20,820
0,659	6,032	18,65	1,95	1786	1,42	18,78	14,980
0,809	7,405	23,26	2,51	2300	1,45	17,97	11,685
0,959	8,778	27,64	3,10	2841	1,48	17,29	9,594
1,109	10,151	32,41	3,71	3398	1,49	16,70	8,156

F4 Input Data for the Programme

NX, the number of $\xi(x)$ stations, including the first two

DX, the ξ step length $\Delta\xi$, for equal steps (as noted before, these steps need not be equal)

X(1), the value of x at the first ξ station, in m

XTR, the value of x at the start of the porous section for injected flow

IY, the number of η grid points

K, the ratio of adjacent η step lengths. If K = 1, equal step length results

H, the first η step length

UINF, mainstream velocity, in m/s

DUDX, a pressure gradient term, in s^{-1}

PSTAT, static pressure, in Pa

T, temperature of mainstream, in ^{0}C

VW, injection velocity, in m/s

IJOB, 0 - no plot output
1 - plot velocity profile } For IJOB = 1, the JCL had to set up another job

EQUIVALENT NOTATION USED IN PROGRAMME

ROMAN

$A+$	AP	U_{CL}	UCL
c_f	CF	u_e	UE
du_e/dx	DUDX	u_w^*, u_τ	USTR
f''	FDD	$u+$	UP
h	H	U_∞	UINF
H	H12	v_w	VW, VW1
K	K	v_w^+	VWP
$p+$	PP	x	X
Re_x	REX	y	Y
$Re_{\delta*}$	RDSTR	$y+$	YP
Re_θ	RTTA	y/θ	YOTTA
u	U	y/δ	YODEL

GREEK

β	BETA	μ	MU
δ	DEL	ν	NU
$\delta*$	DSTR	ξ	XI
$\varepsilon+$	EP	ρ	RHO
ε_i+	EPI	τ	[illegible]
η	ETA	ϕ	P
θ	TTA	ϕ'	PD
κ	KL	ϕ''	PDD

```
*************************************************************************************************************************

EVEL 2.2 (SEPT 76)                         OS/360  FORTRAN H EXTENDED              DATE 78.027/16.00.41       PAGE   1
QUESTED OPTIONS:
TIONS IN EFFECT: NAME(MAIN) OPTIMIZE(1) LINECOUNT(60) SIZE(MAX) AUTODBL(NONE)
                 SOURCE EBCDIC NOLIST NODECK OBJECT NOMAP NOFORMAT NOGOSTMT NOXREF NOALC NOANSF TERM FLAG(I)
                 C       PROGRAMME TO SOLVE THE MOMENTUM EQUATION FOR
                 C       INCOMPRESSIBLE,LAMINAR OR TURBULENT BOUNDARY
                 C       LAYER FLOW,WITH SUCTION OR INJECTION AT THE
                 C       WALL,AND PRESSURE GRADIENT.
                 C
                 C       AN EDDY-VISCOSITY FORMULATION IS USED FOR THE
                 C       REYNOLDS STRESS
                 C
 ISN 0002                REAL*8 KL,EX,FAI,DTAMP,KPI,FWR,H12
 ISN 0003                REAL*8 A(96,5),B(96,1)
 ISN 0004                REAL*8 Y(100),ETA(100),YDEL(100),YETTA(100)
 ISN 0005                REAL*8 P(4,100),PD(4,100),PDD(4,100),UV(100),FD(100)
 ISN 0006                REAL*8 EP(100)
 ISN 0007                REAL*8 X(60),XI(60)
 ISN 0008                REAL*8 K,H,DX,FXI,MU,RHO
 ISN 0009                REAL*8 DSTR(4)
 ISN 0010                REAL*8 DEL,FDEL,CF,USTR,UE,UEO,UINF,TAU,PP,AP
 ISN 0011                REAL*8 PET,DUDX,ETA,RA,DDEL,RETA,PSTAT
 ISN 0012                REAL*8 T,VW,VWU,VW1,VWP,FDD
 ISN 0013                REAL*8 DIMS1,DIMS2
 ISN 0014                REAL*8 A1,B1,C1,D1,E1,F1,G1,H1,I1,J1,K1,J2,K2
 ISN 0015                REAL*8 X1,X2,X3,X4,X5,X6,XITR,XTR
                 C       DATA
 ISN 0016                XTR=2.29700
 ISN 0017                IY=100
 ISN 0018                NX=3
 ISN 0019                DX=0.0100
 ISN 0020                H=0.06500
 ISN 0021                X(1)= 0.9000
 ISN 0022                K=1.03000
 ISN 0023                UINF=17.0000
 ISN 0024                DUDX=0.000
 ISN 0025                T=22.200
 ISN 0026                PSTAT=5.000
 ISN 0027                VW1=0.12900
 ISN 0028                KL=0.400
 ISN 0029                NC=1
 ISN 0030                ICOU=0
 ISN 0031                JOBP=0
                 C       IF JOBP=0 PLOT IS SUPPRESSED, JOBP=1 ALLOWS PLOT
                 C
 ISN 0032                VWU=VW1/UINF
 ISN 0033                UEO=UINF*0.9900
                 C
 ISN 0034                WRITE(6,1000) UINF,DUDX,VWU
 ISN 0035        1000    FORMAT(/////T10,'UINF =',D13.5,'  M/S',//T10,'DU/DX=',D13.6,'  1/S'
                        *,//T10,'VW/UINF=',D13.6)
 ISN 0036                T=T+273.1600
 ISN 0037                RHO=(PSTAT+3513.600)*9.80900/(287.100*T)
                 C
                 C       CALCULATE MU
                 C
 ISN 0038                MU=(((T-275.0)/25.)*0.121+1.725)*1.0D-5


EVEL 2.2 (SEPT 76)             MAIN        OS/360  FORTRAN H EXTENDED              DATE 78.027/16.00.41       PAGE   2
                 C
                 C       CALCULATE TAU
                 C
 ISN 0039                TAU=TAUF(RHO,MU,X,DUDX,UEO,NC)
                 C
 ISN 0040                WRITE(6,911) TAU,RHO,MU
 ISN 0041         911    FORMAT(/T5,'TAU=',D13.6,5X,'RHO=',D13.5,6X,'MU=',D13.5)
                 C
                 C       DEFINE PARAMETERS FOR SUBROUTINE LEQT1B
 ISN 0042                N=IY-4
                 C
                 C
 ISN 0043                DO 1 I=2,NX
 ISN 0044                X(I)=X(I-1)+DX
 ISN 0045           1    CONTINUE
 ISN 0046                DO 2 J=1,NX
 ISN 0047                XI(J)=MU*RHO*X(J)*(X(J)*DUDX/2.000+UEO)
 ISN 0048           2    CONTINUE
 ISN 0049                XITR=MU*RHO*XTR*(XTR*DUDX/2.0+UEO)
                 C       GENERATE ETA POINTS
 ISN 0050                CALL MK001(H,K,IY,ETA)
                 C
                 C       CALCULATE CONSTANTS FOR MATRIX A
 ISN 0051                CALL MK002(H,K,A1,B1,C1,D1,E1,F1,X1,X2,X3,X4,X5,X6)
                 C
 ISN 0052                NC=1
 ISN 0053          85    CALL MK003(X,DUDX,UEO,UE,ETA,NC,PP,AP,TAU,RHO,MU,VW1,USTR,VWP,VW)
 ISN 0054                IF(X(NC) .LT. 0.0390) GO TO 3000
 ISN 0055                IF(NC .EQ. 1) GO TO 18
 ISN 0056                GO TO 19
 ISN 0057          18    FDD=TAU*(2.000*XI(NC))**0.5/(RHO*UE*UE*MU)
 ISN 0060          19    CONTINUE
                 C
 ISN 0061                CALL MK004(ETA,TAU,XI,MU,RHO,P,PD,IY,DUDX,VW,NC,FDD,NDEL,UE,PP,
                        *AP,XI,USTR,DSTR,FDEL,DEL)
                 C
 ISN 0062                CALL MK005(P,RHO,K,H,IY,NC,ETA)
 ISN 0063                IF(NC .EQ. 2) GO TO 82
 ISN 0065                NC=NC+1
 ISN 0066                TAU=TAUF(RHO,MU,X,DUDX,UEO,NC)
 ISN 0067                FDD=TAU*DSQRT(2.0*XI(NC))/(RHO*UE*UE*MU)
 ISN 0068                GO TO 85
 ISN 0069        3000    CONTINUE
 ISN 0070                CALL MK011(ETA,X,XI,NC,IY,MU,RHO,P,PD,PDD,DUDX,DEL,UE,UINF,K
                        *,H,XITR,NC11)
 ISN 0071                IF(NC .EQ. 2) GO TO 82
 ISN 0073                NC=NC+1
 ISN 0074                TAU=TAUF(RHO,MU,X,DUDX,UEO,NC)
 ISN 0075                GO TO 85
 ISN 0076          82    CONTINUE
                 C
                 C
                 C       SET UP DO LOOP IN X DIRECTION
 ISN 0077                IN=IY-4
 ISN 0078                GP=0
 ISN 0079                NAT=NX+1
 ISN 0080          95    NITER=0
 ISN 0081                NC=NC+1
```

```
ISN 0092            IF(NC .EQ. NXI) STOP
ISN 0094            NCA=NC-3*GR
ISN 0095            NXI=[illegible]-NCA
ISN 0096            IF(NXI[illegible]) 3,4,5
ISN 0097       3    NCA1=2
ISN 0098            NCA[illegible]=1
ISN [illegible]     GO TO 6
ISN [illegible]  4  NCA1=1
ISN [illegible]     NCA2=3
ISN [illegible]     GO TO 6
ISN [illegible]  5  NCA1=3
ISN [illegible]     NCA2=2
ISN [illegible]  6  CONTINUE
ISN [illegible]     IF(NCA .NE. 3) GO TO 17
ISN [illegible]     GR=GR+1
ISN 0099      17    CONTINUE
              C     CALCULATE UE,BETA,P* AND A*
              C
              C     CALCULATE TAU FOR NEW X STATION
              C
ISN 0100            FX1=2.0D0*XI(NC)
ISN 0101            FX=DSQRT(FX1)
ISN 0102            NAT=NCA
ISN 0103            IF(NITER .EQ. 0) NAT=NCA1
ISN 0105            TAU=[illegible]*RHO*UE*UE*PDD(NAT,1)/FX
              C
ISN 0106            CALL MK003(X,DUDX,UEO,UE,BETA,NC,PP,AP,TAU,RHO,MU,VW1,USTR,VWP,VW)
              C
              C     CALCULATE BOUNDARY CONDITIONS
ISN 0107            P(4,1)=[illegible]
ISN 0108            KP1=[illegible]+1.0
ISN 0109            PTAWP=P(4,1)*K*(KP1+1.0)*P(NCA1,3)-K*H*KP1
ISN 0110            [illegible]
ISN 0111            WRITE(6,9391) [illegible]
ISN 0112    9391    FORMAT([illegible])
              C     CALCULATE EPSI
ISN 0113      90    CALL MK006(XI,ETA,PDD,RHO,MU,AP,DEL,EP,NC,NCA,DSTR,KL,NCA1,NCA2,
                   *UE,NITER,IY,K)
ISN 0114     910    FORMAT(/T5,'NITER=',I3,3X,'NCA=',I3,3X,'NCA1=',I3,3X,'NCA2=',I3)
ISN 0115            IF(NITER .GT. 10) GO TO 8
              C
              C     CALCULATE EPSI DASH
              C
              C     GENERATE A
ISN 0117            CALL MK00[illegible](A,A1,B1,C1,[illegible],X6,XI,NC,K,IY,P,
                   *PD,PDD,NCA,NCA1,[illegible])
              C     GENERATE B
ISN 0118            CALL MK009(XI,P,PD,PDD,NCA,NCA1,NCA2,NC,IY,NITER,B)
              C
              C     MODIFY A AND B
ISN 0119            B(1,1)=B(1,1)-A(1,1)*P(4,1)-A(1,2)*P(4,2)
ISN 0120            B(2,1)=B(2,1)-A(2,1)*P(4,2)
ISN 0121            A(IE-1,4)=[illegible]
ISN 0122            A(IE,3)=[illegible]
ISN 0123            A(1,1)=0.0D0
ISN 0124            A(2,1)=0.0D0
ISN 0125            A(1,2)=0.0D0
ISN 0126            A(IE,4)=0.0D0
```



```
ISN 0127            A(IE-1,5)=0.0D0
ISN 0128            A(IE,5)=0.0D0
ISN 0129            CALL [illegible]
              C     CONVERT B TO [illegible]
ISN 0130            CALL MK0[illegible]
ISN 0131            CALL MK0[illegible]
ISN 0132            CALL MK0[illegible]
ISN 0133            IF(ITER .EQ. [illegible]) GO TO [illegible]
              C
              C     ESTABLISH EDGE OF BOUNDARY LAYER
ISN 0135            CALL MK013(PD,NDEL,ETA, EDEL,IY)
              C     CALCULATE DEL STAR
ISN 0136            CALL MK014(PD,XI,RHO,UE,NDEL,K,H,DSTR,NC,ETA)
              C
              C     TEST FOR CONVERGENCE
ISN 0137            NTI=NCA
ISN 0138            IF(NITER .EQ. 0) NTI=NCA1
              C
              C
ISN 0140      51    DIFS1=PDD(4,1)-PDD(NTI,1)
ISN 0141            DIFS2=DSTR(4)-DSTR(NTI)
ISN 0142            DIFS1=DABS(DIFS1)
ISN 0143       7    DIFS2=DABS(DIFS2)
ISN 0144            CALL [illegible]
ISN 0145            WRITE(6,[illegible]) DIFS1,DIFS2,NITER
ISN 0146    [illegible] FORMAT([illegible]'DIFS1=',[illegible]  'DIFS2=',[illegible]
                   *[illegible])
ISN 0147            IF(DIFS1 .LT. 0.05D0 .AND. DIFS2 .LT. 0.01D0) GO TO 8
ISN 0149            NITER = NITER+1
ISN 0150            GO TO 90
ISN 01[illegible] 8 CONTINUE
              C
              C     THE SOLUTION HAS NOW CONVERGED
              C
              C     CALCULATE THETA
ISN 0152            CALL [illegible]
              C     SUBROUTINE TO CALCULATE THE VARIABLES REQUIRED FOR PRINTING
ISN 0153            CALL [illegible]
                   *[illegible]
ISN 0154            H12=DSTR(NCA)/TTA
ISN 0155            REWIND[illegible]
ISN 0156            WRITE(6,1001) NC
ISN 0157    1001    FORMAT(1H1,///T10,'STATION',I4,/T10,11('*'),/)
ISN 0158            WRITE(6,1010) X(NC)
ISN 0159    1010    FORMAT([illegible])
ISN 0160            WRITE([illegible])
ISN 0161    1011    FORMAT([illegible])
ISN 0162            WRITE([illegible])
ISN 0163    1012    FORMAT([illegible])
ISN 0164            WRITE(6,1002) [illegible]
ISN 0165    1002    FORMAT([illegible],'DELSTR=',
                   *[illegible])
ISN 0166            WRITE(6,1003) [illegible]
ISN 0167    1003    FORMAT([illegible])
                   *[illegible]
ISN 0168            WRITE(6,1004) [illegible]
ISN 0169    1004    FORMAT([illegible],'DETECT=',
                   *[illegible])
```

```
LEVEL 2.2  (SEPT 76)           MAIN           OS/360  FORTRAN H EXTENDED           DATE 78.027/16.00.41        PAGE  5

ISN 0170                WRITE(6,1005) [illegible]
ISN 0171        1005    FORMAT(//////1 ,'[illegible]',D13.6,'  N/S')
ISN 0172        1006    FORMAT(1H1,///1[illegible],'Y(N)',T24,'[illegible]',T40,'PD',T55,'PDD',T69,'U/UL',
                       *T84,'Y/TTA',T99,'[illegible]'./)
ISN 0173        1007    FORMAT(7(3X,D13.6))
                C
                C
                C
ISN 0174                IF([illegible] .EQ. 0) GO TO 2003
ISN 0176                IF(NC .EQ. 3) GO TO 1505
ISN 0178                [illegible]
ISN 0179                IF([illegible] .EQ. 0) GO TO 2002
ISN 0181                GO TO 2003
ISN 0182        2002    CONTINUE
ISN 0183                ICOU=ICOU+1
ISN 0184                WRITE(6,1006)
ISN 0185                DO 1250 I=1,10
ISN 0186                WRITE(6,1007)Y(I),P(NCA,I),PD(NCA,I),PDD(NCA,I),
                       *FD(I),YOTTA(I),[illegible](I))
ISN 0187        1250    CONTINUE
ISN 0188                DO 1251 I=[illegible],NN,5
ISN 0189                WRITE(6,1007)Y(I),P(NCA,I),PD(NCA,I),PDD(NCA,I),
                       *FD(I),YOTTA(I),EP(I)
ISN 0190        1251    CONTINUE
ISN 0191                DO 1243 I=1,NP
ISN 0192                IF([illegible]) .LT. [illegible].0) WRITE(6,1501)
ISN 0194                [illegible] .LT. 0.0) STOP
ISN 0196                IF(FD( [illegible] .GT. 1.2) WRITE(5,1502)
ISN 0198                IF(FD(I) .GT. 1.2) STOP
ISN 0200                WRITE(10,10400) YOTTA(I),FD(I)
ISN 0201        1243    CONTINUE
ISN 0202                DO 1252 I=11,[illegible]
ISN 0203                WRITE(10,10400) YOTTA(I),FD(I)
ISN 0204        1252    CONTINUE
ISN 0205                DO 1253 I=50,NN,5
ISN 0206                WRITE(10,10400) YOTTA(I),FD(I)
ISN 0207        1253    CONTINUE
ISN 0208                IF(NC .EQ. 3) WRITE(10,10500)
ISN 0210                IF(NC .GT. 3) WRITE(10,10501)
ISN 0212                IF(NC .EQ. 3) WRITE(10,10000)
ISN 0214                IF(NC .EQ. 10)WRITE(10,10001)
ISN 0216                IF(NC .EQ. 20)WRITE(10,10002)
ISN 0218                IF(NC .EQ. 30)WRITE(10,10003)
ISN 0220                IF(NC .EQ. 40)WRITE(10,10004)
ISN 0222                IF(NC .EQ. 50)WRITE(10,10005)
ISN 0224                IF(NC .EQ. 60)WRITE(10,10006)
ISN 0226                WRITE(10,10600)
ISN 0227                WRITE(10,10700)
ISN 0228                IF(NC .EQ. NX) GO TO 1505
ISN 0230                GO TO 2003
ISN 0231        1505    DO 1245 I=1,NN[illegible]
ISN 0232                WRITE(10,10800) YOTTA(I),EP(I)
ISN 0233        1245    CONTINUE
ISN 0234                WRITE(10,10900)
ISN 0235                WRITE(10,10901)
ISN 0236                WRITE(10,11000)
ISN 0237                WRITE(10,12000)
ISN 0238                IF(ICOU .GT. 6) GO TO 2003

LEVEL 2.2  (SEPT 76)           MAIN           OS/360  FORTRAN H EXTENDED           DATE 78.027/16.00.41        PAGE  6

ISN 0240                IF(NC .EQ. NX) GO TO 2003
ISN 0242                GO TO 2002
ISN 0243        1501    FORMAT(/////[illegible],'PROGRAMME STOPPED BECAUSE [illegible]')
ISN 0244        1502    FORMAT(/////[illegible],'PROGRAMME STOPPED BECAUSE FD GT 1.2'[illegible])
ISN 0245        10400   FORMAT(F8.4,F7.4)
ISN 0246        10500   FORMAT(' [illegible] '' TITLE=''U/UE VS Y/TTA'' XTITLE=
                       *[illegible]')
ISN 0247        10501   FORMAT('[illegible]')
ISN 0248        10600   FORMAT('[illegible]')
ISN 0249        10700   FORMAT('[illegible]')
ISN 0250        10800   FORMAT(F8.4,F8.4)
ISN 0251        10900   FORMAT('[illegible]')
ISN 0252        10901   FORMAT('[illegible]')
ISN 0253        11000   FORMAT('[illegible]')
ISN 0254        12000   FORMAT('[illegible]')
ISN 0255        10000   FORMAT('LABEL=''0''')
ISN 0256        10001   FORMAT('LABEL=''1''')
ISN 0257        10002   FORMAT('LABEL=''2''')
ISN 0258        10003   FORMAT('LABEL=''3''')
ISN 0259        10004   FORMAT('LABEL=''4''')
ISN 0260        10005   FORMAT('LABEL=''5''')
ISN 0261        10006   FORMAT('LABEL=''6''')
                C       STEP TO NEXT X STATION
                C
ISN 0262        2003    CONTINUE
ISN 0263                GO TO 95
ISN 0264        2000    WRITE(6,2001)
ISN 0265        2001    FORMAT(//T[illegible],'PROGRAMME STOPPED BECAUSE IER=[illegible]')
ISN 0266                STOP
ISN 0267                END
OPTIONS IN EFFECT*NAME(MAIN) OPTIMIZE(1) LINECOUNT(60) SIZE(MAX) AUTODBL(NONE)
OPTIONS IN EFFECT*SOURCE EBCDIC NOLIST NODECK OBJECT NOMAP NOFORMAT NOGOSTMT NOXREF NOALC NOANSF TERM FLAG(I)
STATISTICS*     SOURCE STATEMENTS =     [illegible], PROGRAM SIZE =     [illegible], SUBPROGRAM NAME = MAIN
STATISTICS*  NO DIAGNOSTICS GENERATED
**** END OF COMPILATION ******                                  [illegible]K BYTES OF CORE NOT USED
```

```
[illegible]VEL 2.2 (SEPT 76)                    OS/360  FORTRAN H EXTENDED              DATE 78.0[illegible]/16.01.21       PAGE   1
[illegible]UESTED OPTIONS:
[illegible]IONS IN EFFECT: [illegible]
                   SOURCE EBCDIC NOLIST NODECK OBJECT NOMAP NOFORMAT NOGOSTMT NOXREF NOALC NOANSF TERM FLAG(I)

                     C     ************************************************
                     C     SUBROUTINE [illegible],PO,[illegible],DEL,UE,UINF,
 ISN 0002                 [illegible]
                     C     ************************************************
                     C     PROGRAMME TO CALCULATE INITIAL PROFILES FOR LAMINAR FLOW.
                     C     DEL IS DETERMINED FROM AN EQUATION AND FROM THE PROFILE
                     C     AN ITERATIVE PROCESS IS USED
                     C
                     C
 ISN 0003                 REAL*8 [illegible](100),F(100),FDD(100),[illegible](100)
 ISN 0004                 REAL*8 ETA(100),P(4,100),PD(4,100),PDD(4,100),FD(100)
 ISN 0005                 REAL*8 [illegible]
 ISN 0006                 REAL*8 [illegible],ET2
 ISN 0007                 REAL*8 [illegible]
 ISN 0008                 REAL*8 [illegible],FA,GA,E2
 ISN 0009                 REAL*8 [illegible],DIFS2,A1,A2,A3,[illegible]
 ISN 0010                 REAL*4 DSTR(4)
                     C
 ISN 0011            11   AF=2.0D0*[illegible]
 ISN 0012                 NITER=0
 ISN 0013                 FXI=DSQRT(AF)
                     C
 ISN 0014                 DEL2=[illegible]
 ISN 0015                 DEL=DSQRT(DEL2)
 ISN 0016            6    LAM=[illegible]
 ISN 0017                 DF=[illegible]*DEL)
 ISN 0018                 DO 1 J=1,IY
 ISN 0019                 ETD(J)=ETA(J)*DF
 ISN 0020            1    CONTINUE
 ISN 0021                 NITER=NITER+1
 ISN 0022                 WRITE(6,103) NITER,NC,DEL
 ISN 0023            103  FORMAT(/T5,'NITER=',I4,6X,'NC=',I4,5X,'DEL=',D13.6,/)
                     C
 ISN 0024                 DO 2 I=1,IY
 ISN 0025                 E2=ETD(I)*ETD(I)
 ISN 0026                 E3=E2*ETD(I)
 ISN 0027                 FA=[illegible]
 ISN 0028                 GA=[illegible]
 ISN 0029                 FD(I)=[illegible]
 ISN 0030            2    CONTINUE
                     C
                     C    DETERMINE EDGE OF B.L.
 ISN 0031                 NDEL=0
 ISN 0032            4    NDEL=NDEL+1
 ISN 0033                 DIFS1=1.0D0-FD(NDEL)
 ISN 0034                 DIFS1=DABS(DIFS1)
 ISN 0035                 IF(DIFS1 .LT. 0.001D0) GO TO 3
 ISN 0037                 IF(NDEL .EQ. IY) GO TO 3
 ISN 0039                 GO TO 4
 ISN 0040            3    EDEL=ETA(NDEL)
 ISN 0041                 DEL1=FX1*EDEL/(RHO*UE)
 ISN 0042                 DIFS2=DEL-DEL1


[illegible]VEL 2.2 (SEPT 76)          MK00IL          OS/360  FORTRAN H EXTENDED              DATE 78.027/16.01.21       PAGE   2

 ISN 0043                 DIFS2=DABS(DIFS2)
 ISN 0044                 DEL=DEL1
 ISN 0045                 DEL=[illegible]
 ISN 0046                 IF(DIFS2 .LT. [illegible]) GO TO 5
 ISN 0048                 IF(NITER .GT. [illegible]) GO TO [illegible]
 ISN 0050                 GO TO 6
                     C
 ISN 0051            5    CONTINUE
 ISN 0052                 DO 14 J=NDEL,IY
 ISN 0053                 FD(J)=1.0D0
 ISN 0054            14   CONTINUE
 ISN 0055                 [illegible]*DEL)
 ISN 0056                 DO 15 I=1,IY
 ISN 0057                 [illegible]*ETA(I)
 ISN 0058            15   CONTINUE
 ISN 0059                 F(1)=0.0D0
 ISN 0060                 DO 7 I=2,IY
 ISN 0061                 J=I-1
 ISN 0062                 F(I)=(FD(I)+FD(J))*(ETA(I)-ETA(J))/2.0D0+F(J)
 ISN 0063            7    CONTINUE
 ISN 0064                 A1=-K*3.0D0/(H*(1.0D0+K))
 ISN 0065                 A2=(K-1.0D0)*K/H
 ISN 0066                 A3=K/(H*(1.0D0+K))
 ISN 0067                 IYM1=IY-1
 ISN 0068                 DO 8 I=2,IYM1
 ISN 0069                 [illegible]
 ISN 0070            8    CONTINUE
 ISN 0071                 [illegible]
 ISN 0072                 [illegible]
 ISN 0073                 [illegible]
 ISN 0074                 [illegible]
 ISN 0075                 IYM2=IY-2
 ISN 0076                 KF=[illegible]
 ISN 0077                 FDD(IY)=(FD(IY)-FD(IYM1))/(KF*H)
 ISN 0078                 DO 9 I=1,IY
 ISN 0079                 P(NC,I)=F(I)-ETA(I)
 ISN 0080                 PD(NC,I)=FD(I)-1.0D0
 ISN 0081                 PDD(NC,I)=FDD(I)
 ISN 0082            9    CONTINUE
 ISN 0083                 VW=0.0D0
                     C
 ISN 0084                 [illegible]
 ISN 0085                 TE=0.0D0
 ISN 0086                 DO 11 J=2,[illegible]
 ISN 0087                 JJ=J-1
 ISN 0088                 TE=TE+(PD(1,J)+PD(1,JJ))*(ETA(J)-ETA(JJ))/2.0D0
 ISN 0089            11   CONTINUE
 ISN 0090                 DSTR(1)=[illegible]
 ISN 0091                 RETURN
 ISN 0092                 END
[illegible]IONS IN EFFECT*NAME(MAIN) OPTIMIZE(1) LINECOUNT(60) SIZE(MAX) AUTODBL(NONE)
[illegible]IONS IN EFFECT*SOURCE EBCDIC NOLIST NODECK OBJECT NOMAP NOFORMAT NOGOSTMT NOXREF NOALC NOANSF TERM FLAG(I)
[illegible]ATISTICS*   SOURCE STATEMENTS =     91, PROGRAM SIZE =    [illegible], SUBPROGRAM NAME =MK00IL
[illegible]ATISTICS*  NO DIAGNOSTICS GENERATED
```

```
VEL 2.2  (SEPT 76)                    OS/360  FORTRAN H EXTENDED              DATE 78.027/16.01.18        PAGE   1
UESTED OPTIONS:
IONS IN EFFECT:  NAME(MAIN) OPTIMIZE(1) LINECOUNT(60) SIZE(MAX) AUTODBL(NONE)
                 SOURCE EBCDIC NOLIST NODECK OBJECT NOMAP NOFORMAT NOGOSTMT NOXREF NOALC NOANSF TERM FLAG(I)

                 C
                 C      ****************************************************
                 C        FUNCTION TO CALCULATE TAU FOR MAIN
                 C      ****************************************************
ISN 0002                FUNCTION TAUF(RHO,NU,X,DUDX,UEO,NC)
ISN 0003                REAL*8 UE,UEO,RHO,NU,X(60),DUDX,RX,TAUF
ISN 0004                UE=X(NC)*DUDX*UEO
ISN 0005                RX=RHO*UE*X(NC)/NU
ISN 0006                RX=RX**0.2D0
ISN 0007                TAUF=0.0296D0*RHO*UE*UE/RX
ISN 0008                RETURN
ISN 0009                END
VEL 2.2  (SEPT 76)                    OS/360  FORTRAN H EXTENDED              DATE 78.027/16.01.30        PAGE   1
UESTED OPTIONS:
IONS IN EFFECT:  NAME(MAIN) OPTIMIZE(1) LINECOUNT(60) SIZE(MAX) AUTODBL(NONE)
                 SOURCE EBCDIC NOLIST NODECK OBJECT NOMAP NOFORMAT NOGOSTMT NOXREF NOALC NOANSF TERM FLAG(I)

                 C      ****************************************************
ISN 0002                SUBROUTINE MK001(H,K,IY,ETA)
                 C      ****************************************************
                 C      PROGRAMME TO CALCULATE ETA FOR MAIN
ISN 0003                REAL*8 H,K,KM1,KS
ISN 0004                REAL*8 ETA(100)
ISN 0005                KM1=K-1.0D0
ISN 0006                ETA(1)=0.0D0
ISN 0007                IF(K .EQ. 1.0D0) GO TO 20
ISN 0009                DO 1 I=2,IY
ISN 0010                J=I-1
ISN 0011                KS=K**J-1.0D0
ISN 0012                ETA(I)=H*KS/KM1
ISN 0013         1      CONTINUE
ISN 0014                GO TO 30
ISN 0015         20     DO 40 I=2,IY
ISN 0016                J=I-1
ISN 0017                ETA(I)=ETA(J)+H
ISN 0018         40     CONTINUE
ISN 0019         30     CONTINUE
ISN 0020                RETURN
ISN 0021                END
VEL 2.2  (SEPT 76)                    OS/360  FORTRAN H EXTENDED              DATE 78.027/16.01.35        PAGE   1
UESTED OPTIONS:
IONS IN EFFECT:  NAME(MAIN) OPTIMIZE(1) LINECOUNT(60) SIZE(MAX) AUTODBL(NONE)
                 SOURCE EBCDIC NOLIST NODECK OBJECT NOMAP NOFORMAT NOGOSTMT NOXREF NOALC NOANSF TERM FLAG(I)

ISN 0002                SUBROUTINE MK002(H,K,A1,B1,C1,D1,E1,F1,X1,X2,X3,X4,X5,X6)
                 C      PROGRAMME TO CALCULATE THE CONSTANTS REQUIRED IN SETTING UP
                 C      THE MATRIX A
ISN 0003                REAL*8 H,K,A1,B1,C1,D1,E1,F1,G1,H1,I1,J1,K1,K1M,KP1,K2,H2,H3
ISN 0004                REAL*8 X1,X2,X3,X4,X5,X6
                 C
ISN 0005                K1M=1.0D0-K
ISN 0006                KP1=1.0D0+K
ISN 0007                K2=KP1**2.0D0
ISN 0008                H2=H**2.0D0
ISN 0009                H3=H**3.0D0
                 C
ISN 0010                A1=-K**3.0D0/(H*KP1)
ISN 0011                B1=-K1M*K/H
ISN 0012                C1=K/(H*KP1)
                 C
ISN 0013                D1=2.0D0*(K**4.0D0)/(H2*KP1)
ISN 0014                E1=-2.0D0*(K**3.0D0)/H2
ISN 0015                F1=2.0D0*(K**3.0D0)/(H2*KP1)
                 C
ISN 0016                G1=-2.0D0*K**6.0D0/(H3*K2)
ISN 0017                H1=2.0D0*(K**3.0D0*K-1.0D0)*K**5.0D0/(H3*KP1)
ISN 0018                I1=-K**6.0D0/K2*K*(1M*1.0D0/K2
ISN 0019                I1=2.0D0(K*1)*K**3.0D0/H3
ISN 0020                J1=2.0D0*(-K1M*K**2.0D0-1.0D0)*K**2.0D0/(H3*KP1)
ISN 0021                K1=2.0D0*K**2.0D0/(H3*K2)
ISN 0022                X1=2.0D0*K**6.0D0/(H2*KP1)
ISN 0023                X2=-2.0D0*K**5.0D0/H2
ISN 0024                X3=2.0D0*K**5.0D0/(H2*KP1)
ISN 0025                X4=2.0D0*K**/(H2*KP1)
ISN 0026                X5=-2.0D0*K/H2
ISN 0027                X6=2.0D0*K/(H2*KP1)
ISN 0028                RETURN
ISN 0029                END
VEL 2.2  (SEPT 76)                    OS/360  FORTRAN H EXTENDED              DATE 78.027/16.01.44        PAGE   1
UESTED OPTIONS:
IONS IN EFFECT:  NAME(MAIN) OPTIMIZE(1) LINECOUNT(60) SIZE(MAX) AUTODBL(NONE)
                 SOURCE EBCDIC NOLIST NODECK OBJECT NOMAP NOFORMAT NOGOSTMT NOXREF NOALC NOANSF TERM FLAG(I)

ISN 0002                SUBROUTINE MK003(X,DUDX,UEO,U ,BETA,NC,PP,AP,TAU,RHO,NU,VW1,USTR,
                       *VWP,VW)
                 C      PROGRAMME TO CALCULATE UE,BETA,VW,P*,A*,USTR,AND VWP
                 C
ISN 0003                REAL*8 DUDX,UEO,UE,BETA,PP,AP,TAU,RHO,NU,VW1,VW,USTR,NU,USTR3,
                       *VWP,PFW
ISN 0004                REAL*8 X(60)
ISN 0005                REAL*8 AP1,AP2
ISN 0006                UE=X(NC)*DUDX*UEO
ISN 0007                BETA=1.0D0-(U /UE)**2
ISN 0008                USTR=(TAU/RHO)**0.5D0
ISN 0009                PP=UE*DUDX*NU/(USTR**3)
ISN 0010                IF(X(NC) .GE. 2.297D0 .AND. X(NC) .LT. 2.70D0) GO TO 1
ISN 0012                VW=0.0D0
ISN 0013                AP1 1.0D0-11.8D0*PP
ISN 0014                AP=26.0D0/DSQRT(AP1)
ISN 0015                WRITE(6,100) NC,PP,AP,USTR,UE
ISN 0016         100    FORMAT(/I5,'AT',I4,2X,'P*=',D13.6,2X,'AP=',D13.6,2X,'USTR=',
                       *D13.6,2X,'UE=',D13.6,/I5,'FROM MK003',/)
ISN 0017                GO TO 2
ISN 0018         1      VW=VW1
ISN 0019                VWP=VW/USTR
ISN 0020                PFW=DEXP(11.8D0*VWP)
ISN 0021                AP2=-PP*(PFW-1.0D0)/VWP+PFW
ISN 0022                AP=26.0D0/DSQRT(AP2)
ISN 0023         2      RETURN
ISN 0024                END
```

```
[illegible]IONS IN EFFECT: NAME(MAIN) OPTIMIZE(1) LINECOUNT(60) SIZE(MAX) AUTODBL(NONE)
                       SOURCE EBCDIC NOLIST NODECK OBJECT NOMAP NOFORMAT NOGOSTMT NOXREF NOALC NOANSF TERM FLAG(I)

ISN 0002          SUBROUTINE VAPDA( TA,TAU,XL,RI,RHO,P,PD,IY,DUDX,VW,NC,FDD,NDEL,
                 *UE,PP,AP,XI,U,TR,DSTR,EDEL,DEL)
           C
           C      PROGRAMME TO GENERATE INITIAL VELOCITY PROFILES.
           C
ISN 0003          REAL*4 SR4
ISN 0004          REAL*8 TAU,XL,MU,RHO,DUDX,VW,USTR,UE,PP,AP,NU,EXI,AEXI,SR2,SR1,
                 *SR3,USE,[illegible],DSTR(4),DIF[illegible],MU,EDEL
ISN 0005          REAL*8 ETA(100),YP(100),UP(100),FD(100),P(4,100),PD(4,100),
                 *G(100),F(100)
ISN 0006          REAL*8 X(100)
ISN 0007          REAL*8 PEW
ISN 0008          REAL*8 DEL
           C
ISN 0009          USTR=MU*FDD*UE*UE*0.5D0*(2.0D0/X(NC))**0.5D0
ISN 0010          USTR=USTR**0.[illegible]D0
ISN 0011          NU=MU/RHO
ISN 0012          EXI=(2.0D0*X(NC))**0.5D0
ISN 0013          AEXI=EXI*USTR/(NU*UE)
ISN 0014          DO 1 I=1,IY
ISN 0015          YP(I)=AEXI*ETA(I)
ISN 0016     1    CONTINUE
           C
ISN 0017          G(1)=1.0D0
ISN 0018          DO 2 I=2,IY
ISN 0019          SR2=YP(I)/AP
ISN 0020          IF(SR2 .LT. 0.01D0) GO TO 300
ISN 0022            PEW=0.0D0
ISN 0023            IF(SR2 .LT. 100) PEW=1.0D0/DEXP(SR2)
ISN 0025          SR4=1.0D0-PEW
ISN 0026          GO TO 301
ISN 0027   300    SR4=0.0D0
ISN 0028   301    SR1=2.0D0*XL*YP(I)*SR4
ISN 0029          SR3=SR1**2.0D0
ISN 0030          G(I)=2.0D0/(1.0D0+DSQRT(1.0D0+SR3))
ISN 0031     2    CONTINUE
           C
           C      INTEGRATION
ISN 0032          UP(1)=0.0D0
ISN 0033          DO 3 I=2,IY
ISN 0034          J=I-1
ISN 0035          UP(I)=(G(I)+G(J))*(YP(I)-YP(J))/2.0D0+UP(J)
ISN 0036     3    CONTINUE
ISN 0037          USE=USTR/UE
ISN 0038          DO 4 I=1,IY
ISN 0039          FD(I)=UP(I)*USE
ISN 0040     4    CONTINUE
           C      DETERMINE EDGE OF BOUNDARY LAYER
ISN 0041          NDEL=0
ISN 0042     8    NDEL=NDEL + 1
ISN 0043          DIFS=1.0D0-FD(NDEL)
ISN 0044          IF(DIFS .LT. 0.0001D0) GO TO 9
ISN 0046          IF(NDEL .EQ. IY) GO TO 9
```

```
[illegible]EVEL 2.2 (SEPT 76)          [illegible]          OS/360  FORTRAN H EXTENDED          DATE 78.027/16.01.49          PAGE   2

ISN 0048          GO TO 8
ISN 0049     9    NO2=NDEL
ISN 0050           DO 41 I=NO2,IY
ISN 0051          FD(I)=1.0D0
ISN 0052    41    CONTINUE
           C
           C      INTEGRATE TO OBTAIN F
ISN 0053          F(1)=0.0D0
ISN 0054          DO 5 I=2,IY
ISN 0055          J=I-1
ISN 0056          F(I)=(FD(I)+FD(J))*(ETA(I)-ETA(J))/2.0D0+F(J)
ISN 0057     5    CONTINUE
           C
           C      GENERATE P AND PD
ISN 0058          DO 6 I=1,IY
ISN 0059          P(NC,I)=F(I)-ETA(I)
ISN 0060     6    CONTINUE
ISN 0061          DO 7 I=1,IY
ISN 0062          PD(NC,I)=FD(I)-1.0D0
ISN 0063     7    CONTINUE
           C
           C      CALCULATE DSTR
ISN 0064          TEMP=0.0D0
ISN 0065          DO 10 I=2,NDEL
ISN 0066          J=I-1
ISN 0067          TEMP=TEMP+(PD(NC,I)+PD(NC,J))*(ETA(I)-ETA(J))/2.[illegible]0
ISN 0068    10    CONTINUE
ISN 0069          DSTR(NC)=-EXI*TEMP/([illegible])
ISN 0070          EDEL=ETA(NDEL)
ISN 0071          DEL=EXI*EDEL/(RHO*UE)
ISN 0072          RETURN
ISN 0073          END
```

```
[illegible]IONS IN EFFECT: NAME(MAIN) OPTIMIZE(1) LINECOUNT(60) SIZE(MAX) AUTODBL(NONE)
                       SOURCE EBCDIC NOLIST [illegible] OBJECT [illegible] [illegible] [illegible] NOXREF NOALC NOANSF TERM FLAG(I)

ISN 0002          SUBROUTINE MFOD5(G,GD,K,H,IY,NC,ETA)
           C      GENERAL DIFFERENTIATING PROGRAMME
ISN 0003          REAL*8 G(4,100),GD(4,100),K
ISN 0004          REAL*8 ETA(100)
ISN 0005          REAL*8 H,K1M,KP1,AS,BS,CS
           C
ISN 0006          NI=NC
ISN 0007          K1M=1.0D0-K
ISN 0008          KP1=K+1.0D0
ISN 0009          IYM1=IY-1
ISN 0010          AS=-K**[illegible]1.0D0/(H*KP1)
ISN 0011          BS=-K1M*K/H
ISN 0012          CS=K/(H*KP1)
           C
ISN 0013          DO 1 I=2,IYM1
ISN 0014          GD(NI,I)=(AS*G(NI,I-1)+BS*G(NI,I)+CS*G(NI,I+1))/[illegible]
ISN 0015     1    CONTINUE
           C      TO OBTAIN GD(NI,1) AND GD(NI,IY), A FIRST ORDER POLYNOMIAL [illegible]
           C      IS USED
           C
ISN 0016          GD(NI,1)=-G(NI,1)*K*(K+2.0)+G(NI,2)*KP1*KP1-G(NI,3)
ISN 0017          GD(NI,1)=GD(NI,1)/(H*K*KP1)
           C
ISN 0018          IYM2=IY-2
ISN 0019          GD(NI,IY)=KP1*GD(NI,IYM1)-K*GD(NI,IYM2)
           C
ISN 0020          RETURN
ISN 0021          END
```

```
IONS IN EFFECT: [illegible] NOALC NOANSF TERM FLAG(I)
ISN 0002          SUBROUTINE MK30B(A,A1,B1,C1,D1,E1,F1,X1,X2,X3,X4,X5,X6,XI,NC,K,
                 *IY,PDD,PED,NCA,NCA1,NITER,BETA,ETA,EP)
             C
             C    PROGRAMME TO CALCULATE THE COEFFICIENT MATRIX A
ISN 0003          REAL*8 XI(60)
ISN 0004          REAL*8 A1,B1,C1,D1,E1,F1,X1,X2,X3,X4,X5,X6
ISN 0005          REAL*8 A(60,5),P(4,100),PD(4,100),PDD(4,100),EP(100)
ISN 0006          REAL*8 NN,DH1,DH2
ISN 0007          REAL*8 K
ISN 0008          REAL*8 Z1,Z2,Z3,Z4,Z5,Z6,Z7
ISN 0009          REAL*8 ETA(100)
ISN 0010          REAL*8 BETA
             C
             C
ISN 0011          DH1=XI(NC-1)-XI(NC-2)
ISN 0012          DH2=XI(NC)-XI(NC-1)
ISN 0013          NN=(DH1+.0D0*DH2)/(DH2*(DH1+DH2))
ISN 0014          NT=NCA
ISN 0015          IF(NITER .GT. 0) GO TO 10
ISN 0017          NT=NCA1
ISN 0018     10   IE=IY-4
ISN 0019          DO 1 J=1,IE
ISN 0020          I=J+2
ISN 0021          I3=J+1
ISN 0022          A(J,1)=A1*X1*(1.0D0+EP(I-1))/K**13
ISN 0023     1    CONTINUE
ISN 0024          DO 2 J=1,IE
ISN 0025          I=J+2
ISN 0026          I3=J+1
ISN 0027          I2=J+1
ISN 0028          Z1=A1*X2*(1.0D0+EP(I-1))/K**13
ISN 0029          Z2=B1*D1*(1.0D0+EP(I))/K**13
ISN 0030          Z3=D1*(P(NT,I)*ETA(I))/K**12
ISN 0031          Z4=BETA*A1*(PD(NT,I)+2.0D0)/K**1
ISN 0032          Z5=2.0D0*XI(NC)*NN*E1*(PD(NT,I)+1.0D0)/K**1
ISN 0033          A(J,2)=Z1+Z2+Z3-Z4-Z5
ISN 0034     2    CONTINUE
ISN 0035          DO 3 J=1,IE
ISN 0036          I=J+2
ISN 0037          I3=J+1
ISN 0038          I2=J+1
ISN 0039          Z1=A1*X3*(1.0D0+EP(I-1))/K**13
ISN 0040          Z2=B1*E1*(1.0D0+EP(I))/K**13
ISN 0041          Z3=C1*X4*(1.0D0+EP(I+1))/K**13
ISN 0042          Z4=E1*(P(NT,I)*ETA(I))/K**12
ISN 0043          Z5=BETA*B1*(PD(NT,I)+2.0D0)/K**1
ISN 0044          Z6=2.0D0*XI(NC)*(PD(NT,I)+1.0D0)*NN*D1/K**1
ISN 0045          Z7=2.0D0*XI(NC)*PDD(NT,I)*NN
ISN 0046          A(J,3)=Z1+Z2+Z3+Z4-Z5-Z6+Z7
ISN 0047     3    CONTINUE
ISN 0048          DO 4 J=1,IE
ISN 0049          I=J+2
ISN 0050          I3=J+1
```

```
VCL 2.2 (SEPT 76)          MKOCA          OS/360  FORTRAN H EXTENDED          DATE 79.027/16.02.05          PAGE 2
```

```
ISN 0051          I2=J+1
ISN 0052          Z1=B1*F1*(1.0D0+EP(I))/K**13
ISN 0053          Z2=C1*X5*(1.0D0+EP(I+1))/K**13
ISN 0054          Z3=F1*(P(NT,I)*ETA(I))/K**12
ISN 0055          Z4=BETA*C1*(PD(NT,I)+2.0D0)/K**1
ISN 0056          Z5=2.0D0*XI(NC)*C1*NN*(PD(NT,I)+1.0D0)/K**1
ISN 0057          A(J,4)=Z1+Z2+Z3-Z4-Z5
ISN 0058     4    CONTINUE
ISN 0059          DO 5 J=1,IE
ISN 0060          I=J+2
ISN 0061          I3=J+1
ISN 0062          A(J,5)=C1*X6*(1.0D0+EP(I+1))/K**13
ISN 0063     5    CONTINUE
ISN 0064          RETURN
ISN 0065          END
IONS IN EFFECT: NAME(MAIN) OPTIMIZE(1) LINECOUNT(60) SIZE(MAX) AUTODBL(NONE)
                SOURCE EBCDIC NOLIST NODECK OBJECT NOMAP NOFORMAT NOGOSTMT NOXREF NOALC NOANSF TERM FLAG(I)
ISN 0002          SUBROUTINE MK006(XI,ETA,PDD,RHO,MU,AP,DEL,FF,NC,NCA,DSTR,KL,NCA1,
                 *NCA2,IT,NITER,IY,X)
             C    PROGRAMME TO CALCULATE EPSI THROUGHOUT ETA RANGE
             C
ISN 0003          REAL*8 KL
ISN 0004          REAL*8 X(60)
ISN 0005          REAL*8 UFXI
ISN 0006          REAL*8 EOPL
ISN 0007          REAL*8 XI(60)
ISN 0008          REAL*8 ETA(100),PDD(4,100),EPI(100),EP(100)
ISN 0009          REAL*8 RHO,MU,AP,DEL,DSTR(4),UF,T1,DIFSI,FXI,T2
ISN 0010          NT=NCA
ISN 0011          FXI=(2.0D0*XI(NC))**0.5D0
ISN 0012          IF(NITER .GT. 0) GO TO 1
ISN 0014          NT=NCA1
ISN 0015     1      EOPL=RHO*UF*DEL/FXI
ISN 0016          IF(X(NC) .LT. 0.0C9D0) GO TO 300
ISN 0018          DO 2 I=1,IY
ISN 0019          IF(ETA(I) .LE. 0.0C0001D0) GO TO 400
ISN 0021          T1=1.0D0+5.5D0*(ETA(I)/[illegible])**6
ISN 0022          GO TO 401
ISN 0023     400    T1=1.0D0
ISN 0024     401  EP(I)=((0.0168D0*UF*DSTR(NT))/T1)*(RHO[illegible])
ISN 0025     2    CONTINUE
ISN 0026          EPI(1)=0.0D0
ISN 0027          UFXI=((FXI*PDD(NT,1)/MU)**0.5D0)/AP
ISN 0028          I=1
ISN 0029     3    I=I+1
ISN 0030          T1=-ETA(I)*UFXI
ISN 0031            T2=1.0D0
ISN 0032            IF(T1 .GT. -50.0D0) T2=1.0D0-DEXP(T1)
ISN 0034          EPI(I)=(KL*ETA(I)*T2)**2*FXI*PDD(NT,I)/MU
ISN 0035          DIFSI=EP(I)-EPI(I)
ISN 0036          IF(DIFSI .LT. 0.0D0) GO TO 4
ISN 0038          IF(I .EQ. IY) GO TO 4
ISN 0040          GO TO 3
ISN 0041     4    DO 5 J=1,I
ISN 0042          EP(J)=EPI(J)
ISN 0043     5    CONTINUE
ISN 0044          WRITE(6,10000) I
ISN 0045   10000  FORMAT(///1X,'THE MATCHING POINT FOR EPSI WAS AT ',I4,//)
ISN 0046          GO TO 301
ISN 0047     300  DO 6 I=1,IY
ISN 0048          EP(I)=0.0D0
ISN 0049     6    CONTINUE
ISN 0050     301    CONTINUE
ISN 0051          RETURN
ISN 0052          END
```

```
EVEL 2.2  (SEPT 76)                OS/360  FORTRAN H EXTENDED           DATE 78.027/16.02.10      PAGE   1
QUESTED OPTIONS:
TIONS IN EFFECT: NAME(MAIN) OPTIMIZE(1) LINECOUNT(60) SIZE(MAX) AUTODBL(NONE)
                 SOURCE EBCDIC NOLIST NODECK OBJECT NOMAP NOFORMAT NOGOSTMT NOXREF NOALC NOANSF TERM FLAG(I)

  ISN 0002            SUBROUTINE MK009(XI,P,PD,PDD,NCA,NCA1,NCA2,NC,IY,NITER,B)
                C     PROGRAMME TO CALCULATE VECTOR B
                C
  ISN 0003            REAL*8 LL,MM,DH1,DH2,T1,T2,T3,FX,T4
  ISN 0004            REAL*8 XI(70)
  ISN 0005            REAL*8 P(4,100),PD(4,100),PDD(4,100),B(96,1)
  ISN 0006            FX=2.0D0*XI(NC)
  ISN 0007            NT=NCA
  ISN 0008            IF(NITER .GT. 0) GO TO 10
  ISN 0010            NT=NCA1
  ISN 0011      10    IE=IY-4
  ISN 0012            DH1=XI(NC-1)-XI(NC-2)
  ISN 0013            DH2=XI(NC)-XI(NC-1)
  ISN 0014            LL=DH2/(DH1*(DH1+DH2))
  ISN 0015            MM=-(DH1+DH2)/(DH1*DH2)
  ISN 0016            DO 1 J=1,IE
  ISN 0017            I=J+2
  ISN 0018            T1=LL*PD(NCA2,I)+MM*PD(NCA1,I)
  ISN 0019            T2=(PD(NT,I)+1.0D0)*T1
  ISN 0020            T3=LL*P(NCA2,I)+MM*P(NCA1,I)
  ISN 0021            T4=PDD(NT,I)*T3
  ISN 0022            B(J,1)=FX*(T2-T4)
  ISN 0023       1    CONTINUE
  ISN 0024            RETURN
  ISN 0025            END
```

```
EVEL 2.2  (SEPT 76)                OS/360  FORTRAN H EXTENDED           DATE 78.027/16.02.14      PAGE   1
QUESTED OPTIONS:
TIONS IN EFFECT: NAME(MAIN) OPTIMIZE(1) LINECOUNT(60) SIZE(MAX) AUTODBL(NONE)
                 SOURCE EBCDIC NOLIST NODECK OBJECT NOMAP NOFORMAT NOGOSTMT NOXREF NOALC NOANSF TERM FLAG(I)

  ISN 0002            SUBROUTINE MK010(B,P,IY)
                C     PROGRAMME TO WRITE B AS P
  ISN 0003            REAL*8 B(96,1),P(4,100)
  ISN 0004            IE=IY-4
  ISN 0005            DO 1 J=1,IE
  ISN 0006            I=J+2
  ISN 0007             P(4,I)=B(J,1)
  ISN 0008       1    CONTINUE
                C
                C     FIND P(4,IY-1) AND P(4,IY)
  ISN 0009            P(4,IY-1)=P(4,IY-2)
  ISN 0010            P(4,IY)=P(4,IY-2)
                C
  ISN 0011             RETURN
  ISN 0012            END
```

```
EVEL 2.2  (SEPT 76)                OS/360  FORTRAN H EXTENDED           DATE 78.027/16.02.19      PAGE   1
QUESTED OPTIONS:
TIONS IN EFFECT: NAME(MAIN) OPTIMIZE(1) LINECOUNT(60) SIZE(MAX) AUTODBL(NONE)
                 SOURCE EBCDIC NOLIST NODECK OBJECT NOMAP NOFORMAT NOGOSTMT NOXREF NOALC NOANSF TERM FLAG(I)

  ISN 0002             SUBROUTINE MK011(P,PD,K,H,IY)
                C     PROGRAMME TO CALCULATE PD, WITH BOUNDARY CONDITIONS
  ISN 0003            REAL*8 P(4,100),PD(4,100)
  ISN 0004            REAL*8 K,H,TA,TB,TC,K1,KP1,K1M
  ISN 0005            PD(4,1)= 1.0D0
  ISN 0006            KP1=K+1.0D0
  ISN 0007            K1M=1.0D0-K
  ISN 0008            IYM1=IY-1
  ISN 0009            TA=-K**3.0D0/(H*KP1)
  ISN 0010            TB=-K1M*K/H
  ISN 0011            TC=K/(H*KP1)
  ISN 0012            DO 1 I=2,IYM1
  ISN 0013            K1=K**I
  ISN 0014            PD(4,I)=P(4,I-1)*TA/K1+P(4,I)*TB/K1+P(4,I+1)*TC/K1
  ISN 0015       1    CONTINUE
  ISN 0016            PD(4,IY)=0.0D0
  ISN 0017            RETURN
  ISN 0018            END
```

```
EVEL 2.2  (SEPT 76)                OS/360  FORTRAN H EXTENDED           DATE 78.027/16.02.24      PAGE   1
QUESTED OPTIONS:
TIONS IN EFFECT: NAME(MAIN) OPTIMIZE(1) LINECOUNT(60) SIZE(MAX) AUTODBL(NONE)
                 SOURCE EBCDIC NOLIST NODECK OBJECT NOMAP NOFORMAT NOGOSTMT NOXREF NOALC NOANSF TERM FLAG(I)

  ISN 0002            SUBROUTINE MK012(P,ETA,PD,PDD,K,H,IY)
                C     PROGRAMME TO CALCULATE PDD FROM P
                C
  ISN 0003            REAL*8 P(4,100),H[illegible]
  ISN 0004            REAL*8 PD(4,100),PDD(4,100),ETA(100),K
  ISN 0005            REAL*8 H,T1A,T2A,T3A,K1,KF
  ISN 0006            REAL*8 KP1,K1M
  ISN 0007            IYM1=IY-1
  ISN 0008            KP1=K+1.0D0
  ISN 0009            K1M=1.0D0-K
  ISN 0010            T1A=-K**3.0D0/(H*KP1)
  ISN 0011            T2A=-K1M*K/H
  ISN 0012            T3A=K/(H*KP1)
  ISN 0013            DO 1 I=2,IYM1
  ISN 0014            K1=K**I
  ISN 0015            PDD(4,I)=(PD(4,I-1)*T1A+PD(4,I)*T2A+PD(4,I+1)*T3A)/K1
  ISN 0016       1    CONTINUE
  ISN 0017            D1=(PD(4,1)-PD(4,2))/(ETA(1)-ETA(2))
  ISN 0018            D2=(PD(4,2)-PD(4,3))/(ETA(2)-ETA(3))
  ISN 0019            D3=(D1-D2)/(ETA(1)-ETA(3))
  ISN 0020            PDD(4,1)=D1+D3*(ETA(1)-ETA(2))
  ISN 0021            IYM2=IY-2
  ISN 0022            KF=K**IYM1
  ISN 0023            PDD(4,IY)=(PD(4,IY)-PD(4,IYM1))/(KF*H)
  ISN 0024            RETURN
  ISN 0025            END
```

```
TIONS IN EFFECT: [illegible] NOALC NOANSF TERM FLAG(I)
                 [illegible]

 ISN 0002            SUBROUTINE MK01[illegible](PD,NDEL,[illegible]ETA,[illegible],IY)
               C     PROGRAMME TO [illegible] THE EDGE OF THE BOUNDARY LAYER.
                     REAL*8 PD(4,100),ETA(100)
 ISN 0003            REAL*8 [illegible],[illegible]DEL
 ISN 0004            NDEL=0
 ISN 0005            NDEL=NDEL+1
 ISN 0006       1    [illegible]
 ISN 0007            IF([illegible] .LT. 0.000100) GO TO 2
 ISN 0008            IF(NDEL .EQ. IY) GO TO 2
 ISN 0009            GO TO 1
 ISN 0010       2    EDEL=ETA(NDEL)
 ISN 0011            WRITE(6,100) EDEL,NDEL
 ISN 0012            FORMAT(/T[illegible],'FROM MK013, [illegible]',D13.6,'      AND NDEL=',I4,/)
 ISN 0013     100    RETURN
 ISN 0014            END
 ISN 0015
 ISN 0016
 ISN 0017
TIONS IN EFFECT: NAME(MAIN) OPTIMIZE(1) LINECOUNT(60) SIZE(MAX) [illegible]
                 SOURCE EBCDIC NOLIST NODECK OBJECT NOMAP NOFORMAT NOGOSTMT NOXREF NOALC NOANSF TERM FLAG(I)

 ISN 0002            SUBROUTINE [illegible](PD,[illegible],[illegible] JC,NDEL,K,H,DSTR,NC,ETA)
               C     PROGRAMME TO CALCULATE DEL STAR
 ISN 0003            REAL*8 PD(4,100),ETA(100)
 ISN 0004            REAL*8 [illegible],UC,K,H,DSTR(4),ATP,FXI
 ISN 0005            REAL*8 XI(60)
               C
 ISN 0006            ATP=0.000
 ISN 0007            DO 1 I=2,NDEL
 ISN 0008            J=I-1
 ISN 0009            ATP=ATP+(PD(4,I)+PD(4,J))*(ETA(I)-ETA(J))/2.000
 ISN 0010       1    CONTINUE
 ISN 0011            [illegible]
 ISN 0012            [illegible]
 ISN 0013            RETURN
 ISN 0014            END

EVEL 2.2  (SEPT 76)                OS/360  FORTRAN H EXTENDED            DATE 78.027/16.02.39       PAGE   1

QUESTED OPTIONS:

TIONS IN EFFECT: NAME(MAIN) OPTIMIZE(1) LINECOUNT(60) SIZE(MAX) AUTODBL(NONE)
                 SOURCE EBCDIC NOLIST NODECK OBJECT NOMAP NOFORMAT NOGOSTMT NOXREF NOALC NOANSF TERM FLAG(I)

 ISN 0002            SUBROUTINE MK01[illegible],PD,PDD,DSTR,NCA,IY)
               C      PROGRAMME TO WRITE THE PRESENT ITERATION INTO THE PRESENT STATION
               C
 ISN 0003            REAL*8 P(4,100),PD(4,100),PDD(4,100),DSTR(4)
 ISN 0004            DO 1 I=1,IY
 ISN 0005            P(NCA,I)=P(4,I)
 ISN 0006       1    CONTINUE
 ISN 0007            DO 2 I=1,IY
 ISN 0008            PD(NCA,I)=PD(4,I)
 ISN 0009       2    CONTINUE
 ISN 0010            DO 3 I=1,IY
 ISN 0011            PDD(NCA,I)=PDD(4,I)
 ISN 0012       3    CONTINUE
 ISN 0013            DSTR(NCA)=DSTR(4)
 ISN 0014            RETURN
 ISN 0015            END
TIONS IN EFFECT: NAME(MAIN) OPTIMIZE(1) LINECOUNT(60) SIZE(MAX) AUTODBL(NONE)
                 SOURCE EBCDIC NOLIST NODECK OBJECT NOMAP NOFORMAT NOGOSTMT NOXREF NOALC NOANSF TERM FLAG(I)

 ISN 0002            SUBROUTINE [illegible](PD,[illegible],NDEL,K,H,DS[illegible])
               C     PROGRAMME TO CALCULATE THETA.
               C
 ISN 0003            REAL*8 [illegible]
 ISN 0004            REAL*8 [illegible],K,H,DSTR(4),TTA,ATP,T1,T2,FXI
 ISN 0005            REAL*8 PD(4,100),ETA(100)
 ISN 0006            ATP=0.000
 ISN 0007            DO 1 I=2,NDEL
 ISN 0008            J=I-1
 ISN 0009            T1=PD(NCA,I)*(1.000+PD(NCA,I))
 ISN 0010            T2=PD(NCA,J)*(1.000+PD(NCA,J))
 ISN 0011            ATP=ATP+(T1+T2)*(ETA(I)-ETA(J))/2.000
 ISN 0012       1    CONTINUE
 ISN 0013            FXI=(XI(NC)*2.000)**0.500
 ISN 0014            TTA=-FXI*ATP/(R[illegible])
 ISN 0015            RETURN
 ISN 0016            END
TIONS IN EFFECT: NAME(MAIN) OPTIMIZE(1) LINECOUNT(60) SIZE(MAX) AUTODBL(NONE)
                 SOURCE EBCDIC NOLIST NODECK OBJECT NOMAP NOFORMAT NOGOSTMT NOXREF NOALC NOANSF TERM FLAG(I)

 ISN 0002            SUBROUTINE [illegible],PD,PDD,IY,NCA,[illegible],CF,UV,FC,USTR,UE,TAU,RX,
                    *[illegible]
               C     PROGRAMME TO CALCULATE VARIABLES PRIOR TO PRINTING
               C
 ISN 0003            REAL*8 P(4,100),PD(4,100),PDD(4,100),UV(100),Y(100),
                    *YDTTA(100),[illegible](100),XI([illegible]),X[illegible]
 ISN 0004            REAL*8 CF,USTR,DSTR(4),UE,TAU,RX,RTTA,RDEL,RHO,MU,EDEL,D,L,TTA,
                    *FXI
 ISN 0005            REAL*8 ETA(100),FD(100)
 ISN 0006            FXI=(XI(NC)*2.000)**0.500
 ISN 0007            CF=MU*(2.000/(XI(NC)))**0.500*PDD(NCA,1)
 ISN 0008            TAU=[illegible]*UE/2.000
 ISN 0009            U[illegible]=DABS(TAU)
 ISN 0010            USTR=(TAU/RHO)**0.500
 ISN 0011            DO 1 I=1,IY
 ISN 0012            Y(I)=FXI*ETA(I)/(RHO*UE)
 ISN 0013       1    CONTINUE
 ISN 0014            DEL=Y([illegible])
 ISN 0015            RX=RHO*UE*X(NC)/MU
 ISN 0016            RDEL=RHO*UE*DEL/MU
 ISN 0017            RTTA=RHO*UE*TTA/MU
               C
 ISN 0018            DO 2 I=1,IY
 ISN 0019            FD(I)=P(NCA,I)+1.0
 ISN 0020       2    CONTINUE
 ISN 0021            DO 3 I=1,IY
 ISN 0022            UV(I)=FD(I)*UE
 ISN 0023       3    CONTINUE
 ISN 0024            IF(DEL .LT. 0.1D-5) GO TO 6
 ISN 0026            DO 4 I=1,IY
 ISN 0027            YODEL(I)=Y(I)/DEL
 ISN 0028       4     CONTINUE
 ISN 0029       6    CONTINUE
 ISN 0030            DO 5 I=1,[illegible]
 ISN 0031            YDTTA(I)=Y(I)/TTA
 ISN 0032       5    CONTINUE
 ISN 0033            RETURN
 ISN 0034            END
```

```
EVEL 2.2  (SEPT 76)                         OS/360  FORTRAN H EXTENDED            DATE 78.027/16.02.54     PAGE  1
EQUESTED OPTIONS:
TIONS IN EFFECT: NAME(MAIN) OPTIMIZE(1) LINECOUNT(60) SIZE(MAX) AUTODBL(NONE)
                 SOURCE EBCDIC NOLIST NODECK OBJECT NOMAP NOFORMAT NOGOSTMT NOXREF NOALC NOANSF TERM FLAG(I)
  ISN 0002                 SUBROUTINE AAZM(AA,B,N)
  ISN 0003                  IMPLICIT REAL*8 (A-H,O-Z)
  ISN 0004                 DIMENSION A(96,97),X(96),AA(96,5),B(96,1)
  ISN 0005                 JJ1=N+1
  ISN 0006                 NP1=N+1
  ISN 0007                 DO 1 J=1,N
  ISN 0008                 DO 2 I=1,N
  ISN 0009                       A(I,J)=0.0D0
  ISN 0010               2 CONTINUE
  ISN 0011               1 CONTINUE
  ISN 0012                 J=3
  ISN 0013                 DO 1000 I=1,3
  ISN 0014                             A(I,1)=AA(I,J)
  ISN 0015                                 J=J-1
  ISN 0016         1000    CONTINUE
                   C
  ISN 0017                 J=4
  ISN 0018                 DO 1001 I=1,4
  ISN 0019                             A(I,2)=AA(I,J)
  ISN 0020                                 J=J-1
  ISN 0021         1001    CONTINUE
                   C
  ISN 0022                 NM4=N-4
  ISN 0023                 DO 1002 IS=1,NM4
  ISN 0024                              J=5
  ISN 0025                             JJ=IS+2
  ISN 0026                             IT=IS+4
  ISN 0027                             DO 1003 I=IS,IT
  ISN 0028                                       A(I,JJ)=AA(I,J)
  ISN 0029                                              J=J-1
  ISN 0030         1003    CONTINUE
  ISN 0031         1002    CONTINUE
                   C
  ISN 0032                 J=5
  ISN 0033                 NM3=N-3
  ISN 0034                 NM1=N-1
  ISN 0035                 DO 1004 I=NM3,N
  ISN 0036                             A(I,NM1)=AA(I,J)
  ISN 0037                                     J=J-1
  ISN 0038         1004    CONTINUE
  ISN 0039                 J=5
  ISN 0040                 NM2=N-2
  ISN 0041                 DO 1005 I=NM2,N
  ISN 0042                             A(I,N)=AA(I,J)
  ISN 0043                            J=J-1
  ISN 0044         1005    CONTINUE
  ISN 0045                 DO 1006 I=1,N
  ISN 0046                           A(I,NP1)=B(I,1)
  ISN 0047         1006    CONTINUE
  ISN 0048                 M7=1
  ISN 0049                 N=JJ1-1
  ISN 0050                 IF(N.LE.0)STOP
  ISN 0052                 DET=1.

EVEL 2.2  (SEPT 76)              AAZM          OS/360  FORTRAN H EXTENDED            DATE 78.027/16.02.54     PAGE  2
  ISN 0053                 L=N-1
  ISN 0054                 NP=N+1
  ISN 0055                 DO 36 K=1,L
  ISN 0056                 M=K+1
  ISN 0057                 ADD=DABS(A(K,K))
  ISN 0058                 IR=K
  ISN 0059                 DO 38 I=M,N
  ISN 0060                 ATT=DABS(A(I,K))
  ISN 0061                 IF(ADD-ATT)37,38,38
  ISN 0062          37     ADD=ATT
  ISN 0063                 IR=I
  ISN 0064          38     CONTINUE
  ISN 0065                 IF(IR-K)39,41,39
  ISN 0066          39     DET=-DET
  ISN 0067                 DO 40 J=K,NP
  ISN 0068                 S=A(IR,J)
  ISN 0069                 A(IR,J)=A(K,J)
  ISN 0070          40     A(K,J)=S
  ISN 0071          41     DO 36 I=M,N
  ISN 0072                 IF(A(I,K).EQ.0.0)GOTO 
  ISN 0074                 S=A(I,K)/A(K,K)
  ISN 0075                 DO 36 J=M,NP
  ISN 0076                 A(I,J)=A(I,J)-S*A(K,J)
  ISN 0077          36     CONTINUE
  ISN 0078                 X(N)=A(N,NP)/A(N,N)
  ISN 0079                 DO 43 I=1,L
  ISN 0080                 K=N-I
  ISN 0081                 M=K+1
  ISN 0082                 S=0.
  ISN 0083                 DO 42 J=M,N
  ISN 0084          42     S=S+A(K,J)*X(J)
  ISN 0085                 X(K)=(A(K,NP)-S)/A(K,K)
  ISN 0086          43     CONTINUE
  ISN 0087                 IF(M7.EQ.0)GOTO 30
  ISN 0089          30     CONTINUE
  ISN 0090                 DO 1007 I=1,N
  ISN 0091                           B(I,1)=X(I)
  ISN 0092         1007    CONTINUE
  ISN 0093                 RETURN
  ISN 0094                 END
PTIONS IN EFFECT*NAME(MAIN) OPTIMIZE(1) LINECOUNT(60) SIZE(MAX) AUTODBL(NONE)
PTIONS IN EFFECT*SOURCE EBCDIC NOLIST NODECK OBJECT NOMAP NOFORMAT NOGOSTMT NOXREF NOALC NOANSF TERM FLAG(I)
TATISTICS*     SOURCE STATEMENTS =      93, PROGRAM SIZE =    76..., SUBPROGRAM NAME =  AAZM
TATISTICS*  NO  DIAGNOSTICS GENERATED
**** END OF COMPILATION ******                                         375K BYTES OF CORE NOT USED
TATISTICS*  NO  DIAGNOSTICS THIS STEP
```

LIST OF REFERENCES

1 BALE B.A. *Mass Transfer Through a Porous Tube.* M.Sc. Thesis, University of the Witwatersrand, 1975.

2 BIRD R.B., STEWART W.E. and LIGHTFOOT E.N. *Transport Phenomena.* John Wiley and Sons Inc., New York, 1960.

3 BLACK T.J. and SARNECKI A.J. *The Turbulent Boundary Layer with Suction and Injection.* British Aeronautical Research Council, R & M, No 3387, London, 1958.

4 EBECI T. and SMITH A.M.O. *A Finite Difference Method for calculating Compressible Laminar and Turbulent Boundary Layers.* Journal of Basic Engineering. (Trans. ASME Series D), V.12,3 : pp 523-535, 1970 a.

5 CEBECI T. *Behaviour of Turbulent Flow near a porous Wall with Pressure Gradient.* AIAA Journal, V.8,12 : pp 2152 - 2156, 1970 b.

6 CEBECI T. and MOSINSKIS G.J. *Calculation of Incompressible Boundary Layers with Mass Transfer, including highly Acce ating Flows.* Journal of Heat Transfer, (Trans. ASME Series C), V.93,3 : pp 271-280, 1971.

7 CEBECI T. and SMITH A.M.O. *Analysis of Turbulent Boundary Layers.* Academic Press New York, 1974.

8 CEBECI T. and BRADSHAW P. *Momentum Transfer in Boundary Layers.* Hemisphere Publishing Co., Washington, 1977.

9 CHEERS B.A. *Note on Wind Tunnel Contractions.* British Aeronautical Research Council, R & M, No 2137, London, 1945.

10 DRYDEN H.L. *Air Flow in the Boundary layer near a Plate.* N.A.C.A. Report No 562, Washington, 1936.

11 DUWEZ P. and WHEELER H.L. *Experimental Study of Cooling by Injection of a Fluid Through a Porous Material.* Journal of the Aeronautical Sciences, V.15, pp 509-521, 1948.

12 FALKNER V.M. and SKAN S.W. *Some approximate solutions of the boundary layer equation.* Philosophical Magazine, V.12, pp 865-896, 1931.

13 GRIMSON J. *Fluid Dynamics and Heat Transfer.* McGraw-Hill Book Co., Maidenhead, 1971.

14 GROOTENHUIS P. *The Mechanism and Application of Effusion Cooling.* The Journal of the Royal Aeronautical Society, V.63, 578, pp 73-89, 1959.

15 HARTNETT J.P., BIRKEBAK R.C. and ECKERT E.R.G. *Velocity Distributions, Temperature Distributions, Effectiveness and Heat Transfer for Air Injected Through a Tangential Slot into a Turbulent Boundary Layer.* Journal of Heat Transfer (Trans. ASME Series C), V.83, 3, pp 293-306, 1961.

16 HILDEBRAND F.B. *Advanced Calculus for Applications.* Prentice-Hall Inc., Englewood Cliffs, New Jersey, 1962.

17 HORSLEY R.R. *An Experimental and Theoretical Analysis of transient demisting phenomena as applied to wall jet flows.* PhD thesis, University of the Witwatersrand, 1975.

18 KINNEY R.B. *Skin Friction Drag of a Constant Property Boundary Layer with Uniform Injection.* AIAA Journal, V.5, 4, pp 624-630, 1967.

19 KRIEG H.R.F. *Determination of velocity and temperature profiles, and the heat transfer characteristics in injection cooled porous pipes with turbulent axial flows.* B.Sc. thesis, University of the Witwatersrand, 1975.

20 LAUNDER B.E. and SPALDING D.B. *Mathematical Models of Turbulence.* Academic Press, London, 1972.

21 MAYHEW Y.R. and ROGERS G.F.C. *Thermodynamic and Transport Properties of Fluids (S.I. Units).* Blackwell and Mott, Oxford, 1970.

22 McQUAID J. *The Calculation of Turbulent Boundary Layers with Injection.* British Aeronautical Research Council, R & M, No 3542, London, 1967.

23 MICKLEY H.S. and DAVIS R.S. *Momentum Transfer for Flow over a Flat Plate with Blowing.* NACA TN 4017, 1956.

24 MILNE-THOMSON L.M. *The Calculus of Finite Differences.* MacMillan and Co., London, 1933.

25 MOFFAT R.J. and KAYS W.M. *The Turbulent Boundary Layer on a Porous Plate : Experimental Heat Transfer with Uniform Blowing and Suction.* International Journal of Heat and Mass Transfer, V.11, 10, pp 1547-1566, 1968.

26 PLETCHER R.H. *On a Finite Difference Solution for the constant Property Turbulent Layer.* AIAA Journal, V.7, 2, pp 305-311, 1969.

27 PLETCHER R.H. *Prediction of Transpired Turbulent Boundary Layers.* Journal of Heat Transfer (Trans. ASME Series C), V.96, 1, pp 89-94, 1974.

28 POPE A. *Wind Tunnel Testing.* John Wiley & Sons, Inc. New York, 1954.

29 SCHEIDEGGER A.E. *The Physics of Flow through Porous Media.* The MacMillan Company, New York, 1957.

30 SCHETZ J.A. and NERNEY B. *Turbulent Boundary Layers with Injection and Surface Roughness.* AIAA Journal, V. 15, 9, pp 1288-1294, 1977.

31 SCHLICHTING H. *Boundary Layer Theory.* McGraw-Hill Book Co., New York, 1968.

32 SIMPSON R.L., MOFFAT R.J. and KAYS W.M. *The Turbulent Boundary Layer on a Porous Plate : Experimental Skin Friction with Variable Injection and Suction.* International Journal of Heat and Mass Transfer, V.12, 7, pp 771-787, 1969.

33 SLATTERY J.C. *Momentum, Energy and Mass Transfer in Continua.* McGraw-Hill Book Co., New York, 1972.

34 SMITH A.M.O. and CEBECI T. *Solution of the Boundary Layer Equations for Incompressible Flow.* Stanford Heat and Mass Transfer Conference, 1968.

35 SUCIU S.N. *High Temperature Turbine Design Considerations.* AGARD conference (Propulsion and Energetics Division), ref no 15, 1970.

36 THOMPSON B.G.J. *A new two-parameter family of mean velocity profiles for incompressible turbulent boundary layers on smooth walls.* British Aeronautical Research Council, R & M, No. 3463, London, 1965.

37 VAN DRIEST E.R. *On Turbulent Flow near a Wall.* Journal of the Aerospaces Sciences, V.23, 11, pp 1007-1011, 1956.

38 WHITEKAR S. *Advances in Theory of Fluid Motion in Porous Media.* Industrial and Engineering Chemistry, V.61, 12, 1969.

39 *Instruction and Service Manual for Type 55D01 Anemometer.* DISA

40 *Instruction and Service Manual for Spectrum Analyser, Type 3590 A.* Hewlett-Packard.

41 *Flow Measurement.* British Standard Code, BS1042, 1943.

ADDENDUM

The ratio of displacement thickness to momentum thickness, H, numerically quantifies the shape of the boundary layer. The "fuller" the profile, the smaller H.

The following admittedly over-simplified analysis suggests the trend di[illegible]sed. A consideration of the following sketches indicates the typical values of H, and its relationship with other properti[illegible] of the boundary layer.

ie. as H increases, [illegible] dec[illegible]ases.

Thus $H = f(1/[illegible])$

From Reynolds Analogy, and experimental results for heat transfer,

$St = [illegible]/2$ (Bird, Stewart and Lightfoot, 1960)

And with injection :-

$St = [illegible]/2 \times 1{,}16$ F [illegible] $0{,}004$ (Moffat and Kays, 1968)

Thus $St = f(1/H)$

However, c_f decreases with injection ratio, as does St (see Moffat and Kays, 1968).

Thus, as H increases, St decreases. From Fig 7.13, it is clear that H increased with F, and for the restricted flow case, H was higher for a given x station and injection ratio, for fixed primary and secondary flow rates.

By definition, $St = \dfrac{h}{\rho c_p V_\infty}$ – h = heat transfer coefficient

Heat transfer, $Q = h(t_e - t_w)$

If St decreases, so does h, and for hypothetically constant Q and t_e, t_w must decrease. Hence a lower wall temperature results, which is the desired effect.

Considering the injection velocity profile with blockage shown in Fig 7.14, leads to comparing it with the turbulent velocity, varying in space rather than with time. Although the average injected momentum is unaltered for a fixed secondary flowrate, it may be more meaningful to use some form of root mean square value for v_s with blockage. The greater penetration of y momentum clearly has a greater decellerating effect on the boundary layer – it may also decrease the heat transfer coefficient. However, only extensive experimentation can conclusively verify this qualitative speculation.